B E R I C H T E

aus dem

INSTITUT FÜR MEERESKUNDE

an der

CHRISTIAN-ALBRECHTS-UNIVERSITÄT KIEL

Nr. 97

1982

CTD Measurements Made From F.S. POSEIDON During JASIN 1978

A Data Report

by

A. Hörch, P.J. Minnett and J.D. Woods

DOI 10.3289/IFM_BER_97

Copies of this report can be obtained from:

Dipl. Oz. A. Horch
Institut für Meereskunde an der Universität Kiel
Abteilung Regionale Ozeanographie
Düsternbrooker Weg 20
D 2300 Kiel 1
Federal Republic of Germany

ISSN 0341-8561

Die „Berichte aus dem Institut für Meereskunde" erscheinen in unregelmäßiger Folge und sind gedacht als Arbeitsunterlagen für den sich mit dem jeweiligen Thema befassenden Personenkreis. Die Hefte werden fortlaufend numeriert. Sie sind unredigierte Beiträge und geben allein die Meinung des Verfassers wieder.

D 2300 Kiel 1, Düsternbrooker Weg 20

Contents

Tables

Figures

Summary

This data report is a presentation of CTD-data collected from R/V "Poseidon" during the International JASIN Experiment in August and September 1978. There are two sorts of data sets:

1.) Yoyo's lasting 5 to 6 hours (1 long Yoyo lasting 18 hours) to 100 m depth. The interval between profiles was 5 minutes.

2.) Two CTD-Boxes in the FIA with a side length of 10 to 12 km and a spacing between stations of about 1 km. Depth of profiles: 500 m.

The Yoyo data is shown as contours of temperature, salinity and density in pressure-time sections, and of temperature and salinity in density-time sections. The data from the Boxes are shown similarly but as functions of distance.

A table with drogue measurements is included.

Zusammenfassung

Dieser Datenbericht umfaßt die Darstellung der auf F.S. "Poseidon" gesammelten CTD-Daten, die während dem internationalen JASIN (Joint Air-Sea Interaction)-Experiment in den Monaten August, September im Jahre 1978 gewonnen wurden. Es handelt sich um zwei Arten von Datensätzen:

1.) Yoyo-Daten, d.h. Zeitreihen bei quasi-ortsfestem Schiff von durchschnittlich 5-6 Stunden Länge (1 Reihe 18 Stunden lang) bis 100 m Tiefe. Abstand zwischen den Profilen: 5 Minuten.

2.) Zwei CTD-Boxes im FIA (Fixed Intensive Array) mit Seitenlängen von 10 bis 12 km und Stationsabständen von etwa 1 km. Tiefe der Profile: 500 m.

Die Yoyo-Daten wurden als Isoplethendiagramme von Temperatur, Salzgehalt und Dichte gegen Druck und von Temperatur und Salzgehalt gegen Dichte dargestellt. Die Seiten der CTD-Boxes wurden in analoger Weise als Schnitte dargestellt.

Eine Tabelle mit Driftbojenmessungen ist beigefügt.

Introduction

This report presents measurements of temperature, salinity and density in the upper ocean taken from F.S. Poseidon during Phase II of the Joint Air-Sea Interaction Project (JASIN) in 1978 (Pollard 1978).

The activities on Poseidon, and other vessels, have been summarized by Siedler and Zenk (1980) and a full account has been given in a cruise report (Institut für Meereskunde, Kiel, 1978). Details of the JASIN project are to be found in documents published by the Royal Society, London (1977, 1978, 1979).

Acknowledgements

Figures 1, 5 and 6 of this report are reprinted with permission from Siedler and Zenk: "JASIN 1978, Field activities on the research vessels 'Meteor', 'Planet', 'Poseidon' and the research aircraft D-CMET", published in "Meteor" Forschungsergebnisse, 1980

We thank Professor K. Bowden, University of Liverpool and the UK Natural Environment Research Council for the loan of the Neil Brown CTD used to collect the data reported here.

The contribution of Stefan Hesse in helping to process the data is gratefully acknowledged.

It is a pleasure to acknowledge the support for this contribution to the international JASIN project by the UK Institute of Oceanographic Sciences and in particular Dr. R.T. Pollard, JASIN scientific coordinator.

The planning and analysis phases of the JASIN project received support from the NATO Science Committee, Air-Sea Interaction Special Programme.

This authors' work was supported by the Deutsche Forschungsgemeinschaft, Bonn - Bad Godesberg. Contracts: Wo 254/2 and Wo 254/5 - Ocean Fronts; Wo 254/4, Wo 254/6, Wo 254/8 and Wo 254/9 - Meteor Auswertung.

1. CTD Data Sampling Scheme

The CTD data presented here can be divided into three parts: two surveys of profiles to 500 m forming closed boxes round the moorings of the Fixed Intensive Array (FIA) and a series of CTD yo-yo stations to 100 m made in synchronisation with those from other ships.

The "First Box" consisted of a survey round the FIA with stations separated by 0.5 nautical miles along sections of 4-5 nautical miles. The stations at the corners of the box were to 1000 m. The period covered is from 1600Z on 24 August (day 236) to 0930Z on 26 August (day 238). The stations began at the south-east corner of the box (see fig. 2) and are listed in table 1.

The "Second Box" began at 0830Z on 3 September (day 246) and continued to 1450Z on 5 September (day 248). The station separation was again 0.5 nautical miles (see fig. 3). With only one exception, which was a 1000 m comparison profile with the AKADEMIK VERNADSKY, the profiles were to 500 m (see table 2).

The CTD yo-yo stations were to 100 m made at 5 minute intervals in synchronisation with those from other ships in the period between the two Boxes (see table 3). The first yo-yo series was part of the First Multiship Experiment (see fig. 5) from 1155Z on 29 August (241) to 0610Z on 30 August (242) close to the drifting spar buoy P2. After the other ships dispersed, POSEIDON continued to make yo-yo measurements in the vicinity of P2 until 0300Z on 1 September (244). The Second Multiship Experiment took place close to the H2 mooring (see fig. 6) from 1000Z, 2 September (245) to 0600Z, 3 September (246), with Poseidon successively occupying three positions at the north-east corner of the fixed-position ship array.

The CTD stations were punctuated by radon measurements, which generally lasted three hours and by dye mixing experiments (see the cruise report). The results of near surface parachute drogue observations made in support of the other measurements are given in table 4.

2. Instrumentation and Data Acquisition

Data were collected using a Neil Brown Instrument Systems MK III Conductivity, Temperature and Depth (CTD) probe (Brown 1974, Brown and Morrison, 1978). The data were archived on magnetic tape using a Nova computer which also calculated salinity and density (σ_t). Plots of profiles and yo-yo sections were also drawn by the computer but those presented here have been subjected to an extensive correction and editing scheme (see section 4) as the parameters derived in real-time suffered from instrumental effects. The sampling program also recorded data from the shipboard meteorological instruments once every two minutes.

The NBIS CTD delivers a data cycle every 32 ms, and the sampling program stored a cycle generally every 96 ms. A program change on 3 September (246) enabled every second data cycle to be stored, and this version of the program was used during the Second Box. Data cycles were lost when the computer was occupied writing data blocks to magnetic tape (0.288s for blocks to MTØ, 0.416s for MT1) and when the meteorological data were sampled (0.192s when MTØ was on-line, 0.288s for MT1).

A new conductivity cell was fitted at the start of the cruise, on the manufacturer's recommendation, and a new thermistor was installed on 26 August (238) so the temperature data from the First Box were taken with only the platinum resistance thermometer.

The CTD was lowered with a nominal rate of 0.5 m/s, which gave a sampling interval of about 5 cm or 3 cm depending on the program speed. Only the descending parts of the profiles (including yo-yos) have been processed.

Throughout the periods of data acquisition, navigation fixes were taken at half-hourly intervals and at the start of individual stations of the box surveys. Generally the fixes were made using the Loran-C system, but when recepting was poor combinations of good Loran-C and Decca Navigator channels were found to produce consistent readings. Radar ranging using moorings and other ships were frequently made, especially during the multiship experiments, but, while they endorse the positions derived from the routine navigation procedure, they have not been used to derive the navigation information used in this report.

3. Calibration and Accuracy

The precision of the NBIS CTD is ultimately limited by the digitizing interval in each of the three channels. These limits are 0.0005K in temperature, 0.001 ms/cm in conductivity and 0.05 dbar in pressure. The electronics noise is stated to be smaller than these values (Brown 1974). Comparison between derived salinity and water bottle samples has shown that a precision of ± 0.0024 ppt over a range of salinity values is possible (Fofonoff, Hayes and Millard, 1974). In practice, these limits are rarely reached and the accuracies of the measurements are determined by other factors, such as the accuracy of the calibration procedure, calibration drift, contamination of the sensors (especially the conductivity cell) and, in the presence of gradients, by the speed of response of the sensors.

The CTD used from F.S. Poseidon during JASIN was loaned by the University of Liverpool, U.K., and had been calibrated at the Institute of Oceanographic Sciences (Wormley), U.K. The temperature channel was found to be accurate to ± 0.001K (Mathers 1978, private communcation). This pre-cruise temperature calibration, being an equilibrium calibration, is of the platinum resistance thermometer and is equally applicable to temperature data gathered with or without the additional thermistor. The post cruise calibration in Kiel showed a small correction of less than 0.005K in the temperature range met in the JASIN area. As this is not larger than the quoted accuracy of the reference thermometers which were available at the time, the pre-cruise temperature calibration is believed to have been applicable throughout JASIN. This is in accordance with the manufacturer's claim for the stability of the temperature channel of ± 0.001K per month (Brown 1974). Comparison with sea-surface temperatures taken with a bucket thermometer at the start and end of selected profiles revealed no appreciable bias.

The conductivity cell and its matched interface card were replaced at the start of the cruise. The value of the cell factor given by the manufacturer is 0.99993 ± 0.00001. Comparison with sea-surface salinity values determined with a Guildline "Autosal" thermostatic salinometer gave cell factors in the range 0.99948 to 1.00048. The variation with time was not systematic. In processing the data, a constant cell factor has been used for data from profiles forming a specific part of the cruise (e.g. for each of the Boxes, or for groups of yo-yo stations), which are shown in Table 5. The cell factors all lie within about ± 0.0005 of unity, and this deviation produces changes in the derived salinity of about ± 0.020 ppt in the range encountered in JASIN. Comparison with the surface salinities gives a scatter in the corrected derived salinities of 0.0073 ppt (standard deviation of 100 samples).

In addition to this limit on the accuracy of the salinity value, the "spiking" effect in the regions of rapidly changing temperature gradient produces a further local degradation of the salinity data. This effect has largely been removed in the data processing by a time constant correction to the temperature signal and a salinity spike rejection criterion (see Section 4 and Appendix A). However, it is likely that some of the small closed contours in the salinity sections are caused by bad data which were not correctable. Thus the accuracy of the derived salinity could be estimated at ± 0.010 ppt with possible local degradation to say ± 0.030 ppt in parts of the thermocline.

The temperature coefficient of the strain gauge pressure cell is believed to be one of the main sources of error in the pressure signal. The coefficient is given as 0.3 dbar/K. The characteristics of the heat transfer from the water to the cell are not known, but even if the full range of the temperature change reached the cell, an error of a few decibars at most would

have been caused. As only data from the descending profiles have been used, the relative accuracy in the pressure signal is believed to be better than $\pm$ 1 dbar. The effect of the pressure measurement error on the derived salinity is negligible: a 1 dbar error in pressure would introduce a salinity error of less than 0.0005 ppt.

The effects on the derived density (σ_t) of a measurement error of $\pm$ 0.005K in temperature and an error of $\pm$ 0.010 ppt in salinity are $\pm$ 0.001 and $\pm$ 0.008 respectively. Thus in the region of a badly corrected salinity spike a σ_t error of say 0.025 might be experienced, but elsewhere the accuracy of the derived σ_t values is about $\pm$ 0.010.

A selection of T-S curves drawn from the processed data were compared with similar diagrams of data from other ships when the stations were close by. Comparison with the processed data of ATLANTIS II, DISCOVERY, METEOR, PLANET and TYDEMAN failed to reveal any discrepancies which could not be attributed to oceanic variability.

4. Data Processing

The CTD data have been processed on the PDP 11/45 of the Institut für Meereskunde, Kiel, which necessitated translating the data tapes from Nova to PDP integer format. This stage introduced many errors into the data (see below) which could not be avoided as the Nova was again at sea during this time. The stages of the data processing are summarized in table 6 and are enlarged upon below.

Stage 1: Subdivision of yo-yo data

The yo-yo data had been archived in long magnetic tape files and before transfer to the PDP these were subdivided into data files consisting of only one profile each. This meant that both yo-yo data and conventional profiles could be treated identically.

Stage 2: Translation of tapes from Data General to PDP format.

During this operation a very large, but variable, number of parity errors were registered. A few files are without errors, while in others almost all blocks gave rise to error messages. In addition, the loss and insertion of bytes in the blocks caused severe disruption to the data cycle sequence.

Stage 3: Correction of parity errors and time base generation.

a) In many cases the sites of lost bytes, or the occurrence of extra bytes, were easily identifiable and can be corrected. Extra bytes were removed and null bytes inserted in the most significant place in words where errors had occurred. When ambiguous cases were found, the solution involving the removal or insertion of the least number of bytes was adopted. In a small number of cases whole data cycles were removed.

b) Meteorological data cycles were removed to leave files with CTD data only.

c) The channels recording data and time (to 1 second resolution) were found not to increase monotonically. The bad values appear to have been caused by one or more bits going low for one or more cycles, presumably as the result of loose contacts in the computer real-time clock. These bad values were identified and corrected.

d) As many data cycles were collected within any given second and therefore had exactly the same values for time, the time channels were augmented with another one holding parts of seconds, to millisecond resolution, to give each cycle a unique time and to enable time constant corrections to the raw data. The intervals between cycles were made such that they are as regular as possible (but remain multiples of 0.032s - the basic CTD cycling time), with allowances for time lost to meteorological data sampling and buffering to tape, with the criterion that time increases monotonically and that the millisecond value goes over 1000 at the change of whole seconds.

Stage 4: Time corrections and editing.

a) The measured variables (P,T,C) were scanned for spikes and these bad values were replaced by those linearly interpolated in time. Many spikes were due to confusion in the input channels (e.g. instead of a data cycle consisting of P,T,C some were P,P,C and others P,T,T/2), the cause of which has not been identified, and others due to misidentification of the position of extra or missing bytes in stage 3a. Spikes were first identified on a maximum acceptable first difference basis and then, after these

had been replaced, as points lying more than three standard deviations away from an estimate of the mean. As the block size is rather small (30 cycles), a biased estimate of the mean, using also the cycles from the previous, corrected block, was employed.

b) Conductivity cell calibration has been made using water bottle samples, worked up with an Autosal salinometer. The cell constant was found not to be constant and varied between groups of stations, with values from 0.99948 to 1.000252. The changes do not appear to be systematic.

c) Spikes in the derived variables could be classified into three groups:-

   i) Sharp spikes (i.e. only a few data points) to lower salinities, in descending profiles, associated with large dT/dP.

   ii) More extensive spikes (i.e. one to several decibars extent) to higher salinities, on descending profiles, occurring immediately after regions of large dT/dP, causing static instability.

   iii) Spikes, with many data points but with small vertical extent, to higher salinities, on descending profiles, associated with the roll of the ship.

   Type (i) spikes are the result of different time constants for the response of the conductivity signal and the temperature signal and spikes of type (ii) are thought to have been caused by a mismatch between time constants of the platinum thermometer and electronic integrator. By analysing a case where the CTD recorded its own passage from air to water this error could be modelled with time constants for the thermometer of 0.436s and integrator

of 0.530s (see Appendix A). The time response of the corrected temperature should be that of the thermistor and the best time constant was found to be 0.090s. Before correcting type (iii) spikes the raw data were smoothed with a three-point running average. Enforcing strict monotony in pressure did not remove the spikes of type (iii) as the salinity channel had, in most cases already reached a spike value before dP/dt changed sign. Because each spike contains many data points statistical editing techniques were ineffective (in several cases the ratio of good to bad data points is about 7:5). A minimum acceptable lowering rate criterion was tried, and, because the least resolvable non-zero lowering rate (0.78 dbar/s; least count in P = 0.05 dbar, cycle time = 0.064 s) was in excess of the mean lowering rate of about 0.5 dbar/s, many good data points are rejected, while some were accepted despite having bad values.

The final solution is: a) enforce a minimum lowering rate (defined by at least one increment in P per cycle)

b) if p' denotes a pressure where dP/dt < 0, reject all following data with P < P' + 1 dbar.

This removed all type (iii) spikes.

However, there remained a few residual spikes in salinity, some in excess of 50 ppm, occurring at sharp changes in dT/dt (generally only at the bottom of the mixed layer). These could not be consistently improved by changes in thermistor time constant estimates, and also by the introduction of a conductivity cell time constant (both positive and negative).

d) Derived variables were calculated from corrected variables using standard formulae (salinity from Fofonoff, Dec. 1974 version), and smoothed with a three-point running mean.

e) Statistical edit of all derived variables; acceptable values must lie within 3 standard deviations of a biased mean (as in 4 a).

Stage 5: Interpolation.

A linear interpolation scheme was used to reduce the data to values at pressure levels every 0.1 dbar. As the profiles had previously been monotonized in pressure, the problem of multiple encounters of an interpolation level was avoided.

Stage 6: Clipping of residual salinity spikes.

Despite the corrections applied during earlier stages of the data processing there were still obvious cases where the salinity profiles and consequently the density profiles, contained bad values. These may have been caused by transient blocking of the conductivity cell or, in the regions of sharp changes in the temperature gradient, by residual time constant effects (possibly introduced by errors in the generation of the millisecond time base, stage 3 d). Typical values in these spikes were 0.05 - 0.1 ppt over a pressure range of 1-3 dbar. These bad data were removed and replaced by linearly interpolated values after being identified on a maximum acceptable first difference basis (equivalent to a maximum acceptable vertical salinity gradient). The size of this threshold value was chosen subjectively (typically 0.08 ppt/dbar). The program scanned up to three tape blocks of data (i.e. data from a pressure range of 9 dbar) in search of the place where salinity returned to acceptable values. In only a very few cases was this procedure unsuccessful and correction of the data not feasible.

On some occasions offsets in the salinity profile were observed and are believed to have been caused by fouling of the conductivity cell. The lost data are not recoverable and these parts of the profiles, or rarely whole profiles, have been removed.

Stage 7: Filtering and interpolation.

The clean data from the previous stage were smoothed with a low-pass filter with half-power-wavenumber of 0.5 $dbar^{-1}$ and interpolated to values at $\Delta P = 0.5$ dbar or $\Delta\sigma_t = 0.005$. Only the first encounter of any given σ_t value in a profile has been used. The profiles generally start at 5 dbar pressure.

Stage 8: Translation to IfM format.

This stage was necessary to enable the use of existing programs from the IfM libraries. The data processing programs had used a special tape format which was more efficient for our purposes and allowed a larger number of variables per cycle than is usual.

5. Data Presentation

The CTD data presented here in figs 7 to 148 are shown as vertical sections. Data from the yo-yo stations are drawn as functions of time, with tick-marks on the top part of the figure frame showing the start time of each profile. Data from descending profiles only have been used. Data from the stations of the two "Box" surveys are displayed as functions of distance; the x-axis being the displacement from the corner station at the start of the section. The geographic orientation of each section is marked on each figure. The tick-marks at the top show start positions of the descending profiles.

The figures show isopleths of temperature, salinity and density (σ_t) against pressure, and of temperature and salinity against σ_t. In calculating the positions of the isopleths, linear interpolation between nearest points was used.

The yo-yo sections are shown with contour intervals:

Δ T = 0.2 K
Δ S = 0.01 ppt
$\Delta\sigma_t$ = 0.05

In addition there are sections drawn with higher resolution for some yo-yo stations of the Second Multiship Experiment (stations 60 and 61) in which a strong frontal signal was observed in the near surface layer.

The data from the "Boxes" are shown with two pressure scales: 0-100 dbar and 0-500 dbar. The contour intervals in the 100 dbar sections are the same as for the yo-yo data, whereas those in the 500 dbar sections are:

Δ T = 0.4 K
Δ S = 0.02 ppt
$\Delta\sigma_t$ = 0.06

The lower 500 dbar of the few stations that reached 1000 dbar are not shown.

One salient feature of the plots with σ_t-ordinate is the disordered nature of the isohalines compared with the smoothness of the isotherms. The main reason for this is the relatively small range of salinities and thus the small effect of salinity on σ_t compared with the stabilizing effect of temperature. These disordered structures often just show changes of about 0.01 ppt in salinity, which close to the measurement accuracy (see Section 3) and thus these structures may be noise.

Gaps in the isopleths are caused by parts of profiles which were irretrievably lost to the data processing scheme. The few cases of data being irretrievable but not rejected have given rise to easily identifiable non-physical structures in the sections, e.g. Figs. 76, 77, 92, 131. Figures 149 to 157 show profiles from a small selection of stations. These are the corner stations of the "Boxes". As it is not feasible to include profiles from all stations, these are presented to give a representation of some of the data in a conventional form.

APPENDIX A

TIME CONSTANT CORRECTION

In an attempt to achieve fast and accurate temperature measurements, the Neil Brown CTD uses two thermometers: a platinum resistance thermometer (manufactured by Rosemount) and a fast bead thermistor (Brown, 1974; Brown and Morrison, 1978). The outputs from both thermometers are combined electronically in the underwater unit to give the "temperature signal", which should have the speed of response of the thermistor combined with the accuracy and long-term stability of the platinum resistance thermometer. The success of this operation depends on the flow of heat from the water to the platinum resistance thermometer being characterized by a single time constant, which is accurately known and to which the electronics circuitry is correctly adjusted. In practice, the heat flow from the water is not adequately described by a single time constant, and it is very difficult to determine the value of the principal one.

A consequence of the mismatch between the principal time constant of the platinum resistance thermometer and that of the electronics is an overshoot or a bounce in the signal when the sensors pass from a region of high to low temperature gradient. Such a feature was apparent in these data. An overshoot in the temperature signal followed regions of high temperature gradient causing statically unstable salinity "spikes" which extended over several decibars. These erroneous data were different in nature from those of salinity spikes by differences in the responses of the thermometer and conductivity cell and did not respond to the conventional thermometer time constant correction (see section 4).

$$\varepsilon = \frac{1}{\tau_p \tau_E} \int_o^t \Delta T(\tau_p \exp(-\xi/\tau_E) - \tau_E \exp(-\xi/\tau_p))d\xi$$

$$= \Delta T (\exp(-t/\tau_E) - \exp(-t/\tau_p)) \qquad \text{(A10)}$$

The maximum error occurs when $d\varepsilon/dt = 0$ at $t = t^*$

$$\text{i.e.} \quad \frac{1}{\tau_E} \exp - t^*/\tau_E = \frac{1}{\tau_p} \exp - t^*/\tau_p$$

$$\text{i.e.} \quad t^* = \frac{\tau_E \tau_p}{\tau_p - \tau_E} \ln(\tau_p/\tau_E) \qquad \text{(A11)}$$

Thus τ_E and τ_p can be estimated from the size of and the elapsed time to the maximum overshoot in the data following a step change in temperature.

A suitable example of temperature change was found at the start of profile PJC092 where the data were logged as the CTD passed from the air through the sea surface and was held at a few metres depth for about a minute. The change from the air temperature of 13.642 °C to a water temperature of 12.732 °C caused an overshoot in the data followed by a slow recovery to the mixed layer temperature (see Fig. A1). The maximum overshoot was -0.065K after an elapsed time of 0.480 + 0.064s, assuming that the temperature change occured in less than the sampling interval of 0.064s, and that the increase in temperature from the overshoot was not caused by local heating of the water by the CTD itself. This latter assumption is supported by the fact that the measured temperature remained within about 10mK of 12.73 °C until the bottom of the mixed layer was reached at a depth of about 8 dbar.

Numerical solution of equations A10 and A11 gave $\tau_E = 0.530$s and $\tau_p = 0.436$s. A correction applied with these values improved the response but a slight bounce, amounting to ∿-2 %

Making the assumption that the heat flow to the platinum resistance thermometer can be characterized by a single time constant, τ_p seconds, the effect of a mismatched electronics time constant, τ_E seconds, can be described.

Let τ_T seconds be the time constant of the thermistor and F(t) °C be the fluid temperature, then, at $t \gg \tau_p, \tau_T$, the platinum resistance thermometer output is:

$$T_p(t) = \frac{1}{\tau_p} \int_o^t F(t-\xi) \exp(-\xi/\tau_p)\, d\xi \qquad (A1)$$

and the combined temperature signal would be:

$$T(t) = \frac{1}{\tau_T} \int_o^t F(t-\xi) \exp(-\xi/\tau_T)\, d\xi \qquad (A2)$$

The response of the electronic circuitry, when performing perfectly, would be $E(t) = T - T_p$

$$\text{i.e. } E(t) = \frac{1}{\tau_p \tau_T} \int_o^t F(t-\xi) (\tau_p \exp(-\xi/\tau_T) - \tau_T \exp - (\xi/\tau_p))d\xi \qquad (A3)$$

If the electronic circuitry is imperfectly adjusted, i.e. $\tau_E \neq \tau_p$ then the output, E* , is given by:

$$E^*(t) = \frac{1}{\tau_E \tau_T} \int_o^t F(t-\xi) (\tau_E \exp(-\xi/\tau_T) - \tau_T \exp(-\xi/\tau_p))d\xi \qquad (A4)$$

so the error in the temperature signal, $\varepsilon = E^* - E$, is:

$$\varepsilon(t) = \frac{1}{\tau_p \tau_E} \int_o^t F(t-\xi) (\tau_E \exp(-\xi/\tau_p) - \tau_p \exp(-\xi/\tau_E))d\xi \qquad (A5)$$

Thus, given values of τ_E and τ_p , and knowledge of F(t) , the error ε can be found and the measured temperature signal, $T_p + E^*$, could be corrected to give T, the correct measured temperature signal. This could then be corrected for the finite response-time of the thermistor if the value of τ_T

were known. Values of τ_p, τ_E and τ_T can be estimated from the data, but $F(t)$ is not known until the corrections have been applied. However, since the data exist as a discrete time-series, with interval δt, an approximate correction can be found.

The discrete form of the function $T_p(t)$ can be written as:

$$T_{p_i} = F_i - \sum_{n=o}^{i-1} \Delta F_n \exp((n-i)\delta t/\tau_p) \qquad (A6)$$

where $\Delta F_n = F_n - F_{n-1}$

Thus the correction, $-\varepsilon_i$, can be written:

$$\varepsilon_i = \sum_{n=o}^{i-1} \Delta F_n \left(\exp(n-i)\delta t/\tau_p) - \exp((n-i)\delta t/\tau_E)\right) \qquad (A7)$$

The correction scheme for the measured data point T'i is

$$T_i = T'_i + \sum_{n=o}^{i-1} \Delta F^*_n \left(\exp(n-i)\delta t/\tau_p) - \exp((n-i)\delta t/\tau_E)\right) \qquad (A8)$$

and $$F_i = T_i + \frac{\Delta T i}{\delta t} \cdot \tau_t \qquad (A9)$$

where F^*_i is the corrected measurement of the fluid temperature. In practice, the summation need not to be made from n=0, but from n=i-m where $m\delta t$ is sufficiently long for the exponential weights to make the contribution of earlier terms negligible. To remove the Nyquist frequency noise introduced by the first differencing operation, the resulting time series must be smoothed with a three-point running mean.

The values of τ_E and τ_p can be estimated from the response of the signal to a step change in the environmental temperature. Let a temperature change of Θ°C occure at t=0, then the error is given by:

of the step size after an elapsed time of about 1.5s, persisted. Tests with $\tau_p > 0.436$s and $\tau_E < 0.530$s produced curves with overshoot closer to the raw data, and those with $\tau_p < 0.436$s and $\tau_E > 0.530$s generated a bigger bounce.

The initial response to the temperature step could be well described by an exponential function with a time constant of 90 ± 5ms. This would be the time constant of the thermistor. After the correction described above, the value of τ_T which appeared to recover the best temperature step was 70 ± 5 ms (see Fig.A1). The correction with τ_T = 90 ms produced a very thin layer directly at the surface almost 0.1 K cooler than the mixed layer temperature.

However, in applying the fast time constant correction (e.g. A9) to data from the thermocline the value of τ_T = 90 ms was best in reducing salinity spikes. The cool surface layer apparently caused by the 90 ms time constant over-correcting the exponential response might thus have been real and possibly caused by evaporative or radiative cooling.

To summarize, the entire temperature data were corrected for the mismatch between the time constants of the platinum resistance thermometer using equations A8 and A9 with the following parameters:

$\tau_p = 0.436$ s
$\tau_E = 0.530$ s
$\tau_T = 0.090$ s

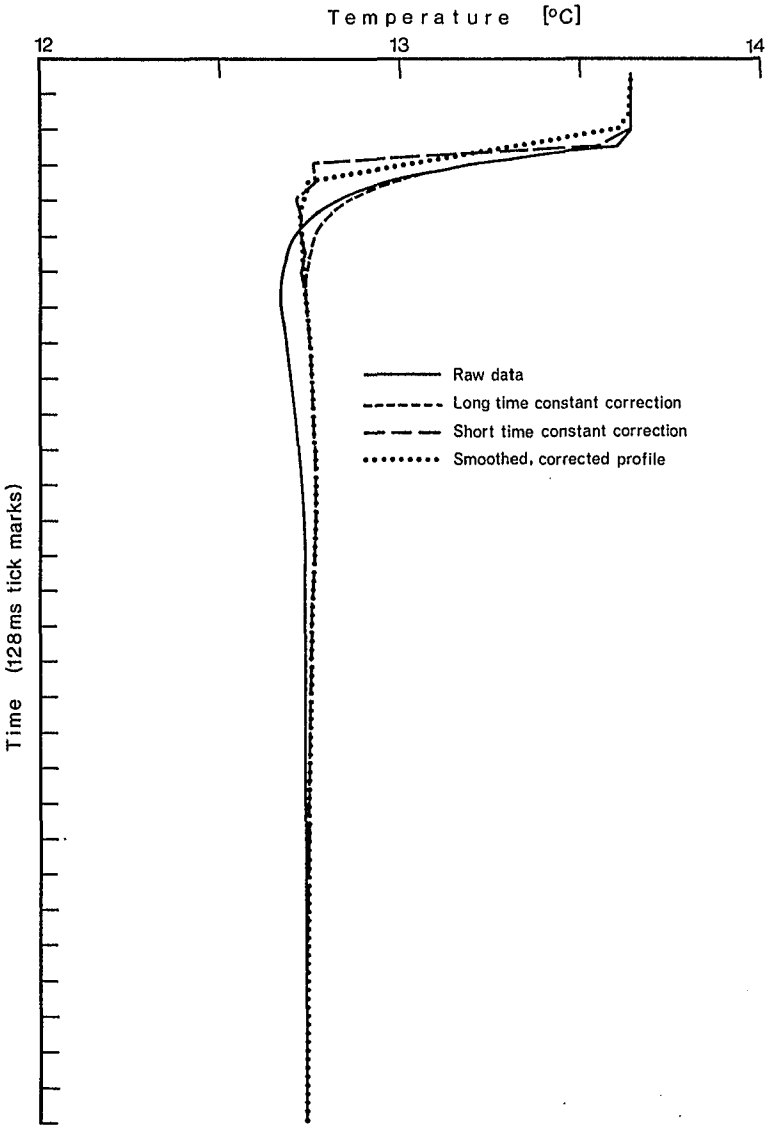

Fig. A1 Corrections to response to step change in temperature

Table 1 - CTD station list for Box 1

Station No.	Date 1978 Day/Month	Time (GMT) Start - End	Position at Beginning Lat. (N)	Long. (W)	
P1415	24/8	13.37 - 14.05	58°55.4'	12°37.8'	
P1416	24/8	15.54 - 16.25	58°55.4'	12°26.5'	
P1417	24/8	16.48 - 17.16	58°55.9'	12°26.8'	
P1418	24/8	17.32 - 18.01	58°56.4'	12°26.6'	
P1419	24/8	18.16 - 18.45	58°56.9'	12!26.6'	
P1420	24/8	18.59 - 19.29	58°57.3'	12°26.4'	
P1421	24/8	19.41 - 20.11	58°58.0'	12°26.4'	
P1422	24/8	20.24 - 20.51	58°58.5'	12°26.8'	
P1423	24/8	21.01 - 21.32	58°58.9'	12°26.5'	
P1424	24/8	21.46 - 22.16	58°59.4'	12°26.7'	
P1425	24/8	22.31 - 23.01	58°59.9'	12°26.5'	
P1426	24/8	23.22 - 23.50	59°00.8'	12°26.2'	
P1427	25/8	00.37 - 01.23	59°01.6'	12°25.7'	to 1000 m
P1428	25/8	03.18 - 03.52	59°02.9'	12°26.7'	
P1429	25/8	04.06 - 04.37	59°02.4'	12°26.5'	
P1430	25/8	04.52 - 05.23	59°02.4'	12°27.6'	
P1431	25/8	05.30 - 06.05	59°0.24'	12°28.5'	
P1432	25/8	06.21 - 06.49	59°02.4'	12°29.7'	
P1433	25/8	06.59 - 07.29	59°02.4'	12°31.4'	
P1434	25/8	07.38 - 08.08	59°02.5'	12°31.4'	
P1435	25/8	08.25 - 08.54	59°02.4'	12°32.4'	
P1436	25/8	09.26 - 09.55	59°02.5'	12°33.4'	
P1437	25/8	10.15 - 10.43	59°02.5'	12°34.1'	
P1438	25/8	11.05 - 11.34	59°02.5'	12°35.4'	
P1439	25/8	11.48 - 12.48	59°02.4'	12°36.3'	to 1000 m
P1440	25/8	13.05 - 13.35	59°01.9'	12°36.3'	
P1441	25/8	13.52 - 14.22	59°01.4'	12°36.3'	
P1442	25/8	14.38 - 15.07	59°00.9'	12°36.3'	
P1443	25/8	15.21 - 15.52	59°00.4'	12°36.4'	
P1444	25/8	16.08 - 16.39	58°59.9'	12°36.4'	
P1445	25/8	16.56 - 17.26	58°59.4'	12°36.4'	
P1446	25/8	17.43 - 18.11	58°58.9'	12°36.4'	
P1447	25/8	18.33 - 19.03	58°58.5'	12°36.4'	
P1448	25/8	19.19 - 19.47	58°57.9'	12°36.5'	
P1449	25/8	20.04 - 20.33	58°57.4'	12°36.2'	
P1450	25/8	20.58 - 21.28	58°56.9'	12°36.4'	
P1451	25/8	21.50 - 22.46	58°56.4'	12°36.3'	to 1000 m
P1452	25/8	23.05 - 23.34	58°56.2'	12°34.9'	
P1453	25/8	23.53 - 00.23	58°56.0'	12°34.3'	
P1454	26/8	00.40 - 01.11	58°55.8'	12°33.9'	
P1455	26/8	01.21 - 01.51	58°55.6'	12°32.5'	
P1456	26/8	02.07 - 02.38	58°55.4'	12°31.5'	
P1457	26/8	02.55 - 03.26	58°55.3'	12°30.6'	
P1458	26/8	03.42 - 04.13	58°55.1'	12°29.7'	
P1459	26/8	04.29 - 04.57	58°55.0'	12°28.9'	
P1460	26/8	05.17 - 05.46	58°54.8'	12°27.9'	
P1461	26/8	06.01 - 06.55	58°54.6'	12°26.9'	to 1000 m
P1462 *(P1416)	26/8	07.30 - 07.58	58°55.4'	12°26.5'	
P1463 *(P1417)	26/8	08.14 - 08.43	58°55.9'	12°26.5'	
P1464 *(P1418)	26/8	09.00 - 09.29	58°56.4'	12°26.6'	

*Repetition of a station

Table 2 - CTD station list for Box 2

Station No.	Date 1978 Day/Month	Time (GMT) Start - End	Position at Beginning Lat. (N)	Long. (W)
P1501	03/9	08.28 - 08.51	59°02.4'	12°24.1'
P1502	03/9	09.10 - 09.33	59°01.9'	12°24.1'
P1503	03/9	09.50 - 10.13	59°01.4'	12°24.1'
P1504	03/9	10.29 - 10.52	59°00.9'	12°24.0'
P1505	03/9	11.03 - 11.26	59°00.4'	12°24.1'
P1506	03/9	11.42 - 12.07	58°59.8'	12°24.0'
P1507	03/9	12.21 - 12.47	58°59.3'	12°24.1'
P1508	03/9	13.01 - 13.25	58°58.8'	12°24.0'
P1509	03/9	13.40 - 14.06	58°58.2'	12°24.0'
P1510	03/9	14.17 - 14.40	58°57.6'	12°24.1'
P1511	03/9	14.57 - 15.21	58°57.6'	12°25.0'
P1513	03/9	22.05 - 22.27	58°57.6'	12°25.0'
*(P1511)				
P1514	03/9	22.49 - 23.13	58°57.6'	12°25.9'
P1515	03/9	23.32 - 23.55	58°57.6'	12°26.9'
P1516	04/9	00.10 - 00.31	58°57.6'	12°27.9'
P1517	04/9	00.49 - 01.10	58°57.6'	12°28.9'
P1518	04/9	01.23 - 01.44	58°57.6'	12°29.8'
P1519	04/9	02.04 - 02.28	58°57.6'	12°30.8'
P1520	04/9	02.42 - 03.03	58°57.6'	12°31.8'
P1521	04/9	03.15 - 03.38	58°57.6'	12°32.7'
P1522	04/9	03.55 - 04.16	58°57.6'	12°33.7'
P1523	04/9	04.33 - 04.56	58°57.6'	12°34.7'
P1524	04/9	05.16 - 05.39	58°57.6'	12°35.7'
P1525	04/9	05.53 - 06.17	58°58.1'	12°35.8'
P1526	04/9	06.41 - 07.04	58°58.6'	12°35.8'
P1527	04/9	07.20 - 07.42	58°59.1'	12°35.8'
P1528	04/9	07.55 - 08.19	58°59.6'	12° 35.8'
P1529	04/9	08.38 - 09.00	59°00.2'	12°35.7'
P1530	04/9	09.19 - 09.43	59°00.6'	12°35.6'
P1531	04/9	10.03 - 10.25	59°01.2'	12°35.8'
P1532	04/9	10.44 - 11.06	59°01.6'	12°35.9'
P1533	04/9	11.28 - 11.52	59°02.4'	12°35.7'
P1534	04/9	12.13 - 12.35	59°02.3'	12°34.7'
P1535	04/9	12.58 - 13.19	59°02.4'	12°33.9'
P1536	04/9	13.40 - 14.03	59°02.4'	12°32.9'
P1537	04/9	14.27 - 14.50	59°02.4'	12°31.9'
P1538	04/9	15.11 - 15.32	59°02.4'	12°31.0'
P1539	04/9	16.06 - 16.29	59°02.4'	12°30.0'
P1540	04/9	16.45 - 17.07	59°02.4'	12°29.1'
P1541	04/9	17.21 - 17.44	59°02.4'	12°28.1'
P1542	04/9	18.07 - 18.30	59°02.4'	12°27.2'
P1543	04/9	18.46 - 19.40	59°02.4'	12°26.2'
P1544	04/9	12.21 - 19.44	59°02.4'	12°25.3'
P1545	04/9	19.56 - 20.20	59°02.4'	12°24.1'
*(P1501)				
P1547	05/9	00.38 - 01.02	59°02.4'	12°35.7'
*(P1533)				
P1548	05/9	01.29 - 01.53	59°02.4'	12°34.8'
*(P1534)				
P1549	05/9	02.09 - 02.27	59°02.4'	12°33.8'
*(P1535)				

Table 2 - CTD station list for Box 2 (continued)

Station No.	Date 1978 Day/Month	Time (GMT) Start - End	Position at Beginning Lat. (N)	Long. (W)	
P1550	05/9	02.49 - 03.12	59°02.4'	12°31.8'	
*(P1537)					
P1551	05/9	03.28 - 03.51	59°02.4'	12°30.8'	
*(P1538)					
P1552	05/9	04.02 - 04.25	59°02.4'	12°29.8'	
*(P1539)					
P1553	05/9	04.55 - 05.17	59°02.8'	12°28.8'	
P1554	05/9	05.35 - 05.59	59°02.4'	12°28.0'	
*(P1541)					
P1555	05/9	10.47 - 11.15	59°02.3'	12°27.4'	
*(P1542)					
P1556	05/9	11.37 - 12.19	59°02.4'	12°26.8'	to 1000 m
P1557	05/9	12.35 - 12.57	59°02.4'	12°25.9'	
*(P1543)					
P1558	05/9	13.10 - 13.33	59°02.3'	12°24.8'	
*(P1544)					
P1559	05/9	13.45 - 14.08	59°02.3'	12°24.1'	
*(P1501, P1545)					
P1560	05/9	14.24 - 14.47	59°02.3'	12°23.1'	

*Repetition of a station

Table 3 - CTD station list for YOYOs

Station No.	YOYO No.	Date 1978 Day/Month	Time (GMT) Start - End	Position at Beginning Lat. (N)	Long. (W)	Position at End Lat. (N)	Long. (W)
P1482	52	29/8	11.55 - 17.46	58°53.8'	12°20.4'	58°53.3'	12°20.1'
P1482	53	29/8	17.48 - 23.59	58°53.3'	12°20.1'	58°53.3'	12°22.2'
P1482	54	30/8	00.06 - 06.11	58°53.3'	12°22.3'	58°55.1'	12°22.6'
P1485	55	30/8	09.49 - 14.30	58°53.9'	12°20.7'	58°53.7'	12°18.7'
P1488	56	31/8	10.00 - 15.00	58°51.1'	12°11.6'	58°50.6'	12°07.8'
P1490	57	31/8	18.25 - 02.52	58°48.9'	12°05.7'	58°48.7'	12°07.7'
P1492	58	01/9	16.47 - 17.19	58°47.1'	12°04.0'	58°47.2'	12°04.0'
P1497	59	02/9	11.23 - 15.03	59°26.0'	12°27.5'	59°26.5'	12°27.8'
P1499	60	02/9	18.44 - 23.50	59°25.9'	12°26.2'	59°26.1'	12°27.6'
P1499	61	02/9	23.54 - 02.59	59°26.1'	12°27.6'	59°26.8'	12°28.6'

Table 4 - Drogue measurements

Date 1978 Day/Month	Time interval GMT	Drogue depth m	Position at Beginning Lat. (N)	Long. (W)	Drifting Speed km/h	Direction towards
21/8	13.00-15.55	40-42	58°57.7'	11°38.0'	0.30	110°
21/8	15.55-16.42	40-42			0.75	150°
21/8	16.42-20.48	40-42			0.40	135°
22/8	16.00-19.00	40	59°02.2'	11°50.0'	0.60	135°
23/8	09.34-10.23	40	59°01.2'	11°43.4'	0.84	330°
23/8	10.23-11.23	40			0.76	012°
23/8	11.23-13.50	40			0.69	045°
23/8	13.50-15.53	40			1.03	083°
23/8	15.53-16.37	40			0.64	130°
23/8	16.37-18.06	40			1.00	130°
26/8	14.00-16.02	40	58°53.2'	12°20.5'	0.74	148°
26/8	17.57-21.24	40			0.30	108°
26/8	21.24-23.10	40			0.49	108°
26-27/8	23.10-03.10	40			0.52	140°
27/8	05.02-10.53	40	58°51.5'	12°17.9'	0.65	107°
26/8	15.45-17.49	60			0.41	135°
26/8	17.49-21.36	60			0.415	118°
26/8	21.36-23.23	60			0.535	110°
26-27/8	23.23-03.25	60			0.46	140°
27/8	03.25-09.30	60			0.58	0.92°
27-28/8	16.08-06.05	20	58°56.9'	12°24.5'	0.27	165°
28/8	06.05-18.50	20			0.225	165°
01/9	06.20-10.00	26	58°47.1'	12°04.0'	0.425	210°
01/9	10.00-14.30	26			0.17	350°
01/9	14.30-16.30	26			0.525	070°
01/9	16.30-18.00	26			0.80	085°
01/9	06.35-16.00	42			0.18	125°
01/9	16.00-23.40	42			0.30	100°
01/9	18.00-23.40	42			0.175	110°
01/9	06.35-23.40	42			0.23	110°

Table 5 - Cell Constants used in Conductivity Calibration

Date 1978 Day/Month	Cell Constant	Stations	Data
24-28/8	1.00048	P1415-P1464	Box 1
29-30/8	0.999897	P1482-P1485	Yo-yos at first Multiship Experiment
31/8 - 1-2/9	1.0002525	P1488-P1499	Yo-yos at P2 and H2 (Second Multiship Exp.)
3-4/9	0.99948	P1501-P1560	Box 2

Table 6 - JASIN Data Processing

Stage	Program Name	Purpose
1	PNFL2	Division of yo-yo data into files containing one profile
2	POSRSX	Translation from Nova data files to PDP RSX11M ANSI files
3	PJ1Ø2	Translation read errors correction, introduction of a time base with milliseconds, removal of improbable measurements, block averaging
4	PJ2Ø4	Time constant correction, calibration correction, recalculate derived quantities, smooth variables with a three-point running mean and statistical editing, monotonization in pressure
5	PJ3Ø1	Interpolation to $\Delta P = 0.1$ dbar
6	PJCLIP	Remove effects of residual salinity spikes
7	PJ3Ø1	Filter and interpolate to $\Delta P = 0.5$ dbar and $\Delta\sigma_t = 0.005$. Only the first encounter of a given σ_t value in a profile is used.
7a	PLXYØ4*	Plot profiles and T-S diagrams
8	PJ4Ø1	Translation into IfM format
9	PLSECT	Plot isopleth diagrams and sections

* Plots of the profiles were made after most processing stages to assess improvements and to show where reprocessing was necessary with improved parameters.

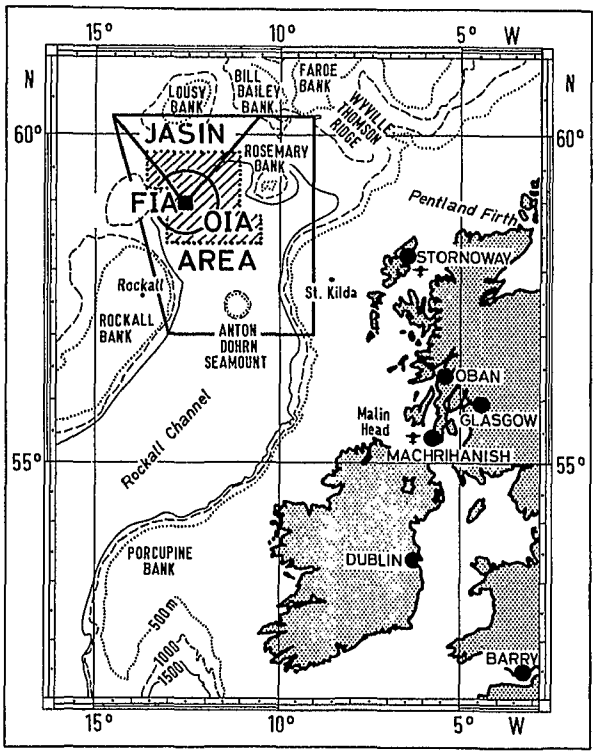

Fig. 1 The JASIN area. FIA = Fixed Intensive Array, OIA = Oceanographic Intensive Array. The Large Scale Array including the meteorological triangle is also plotted.

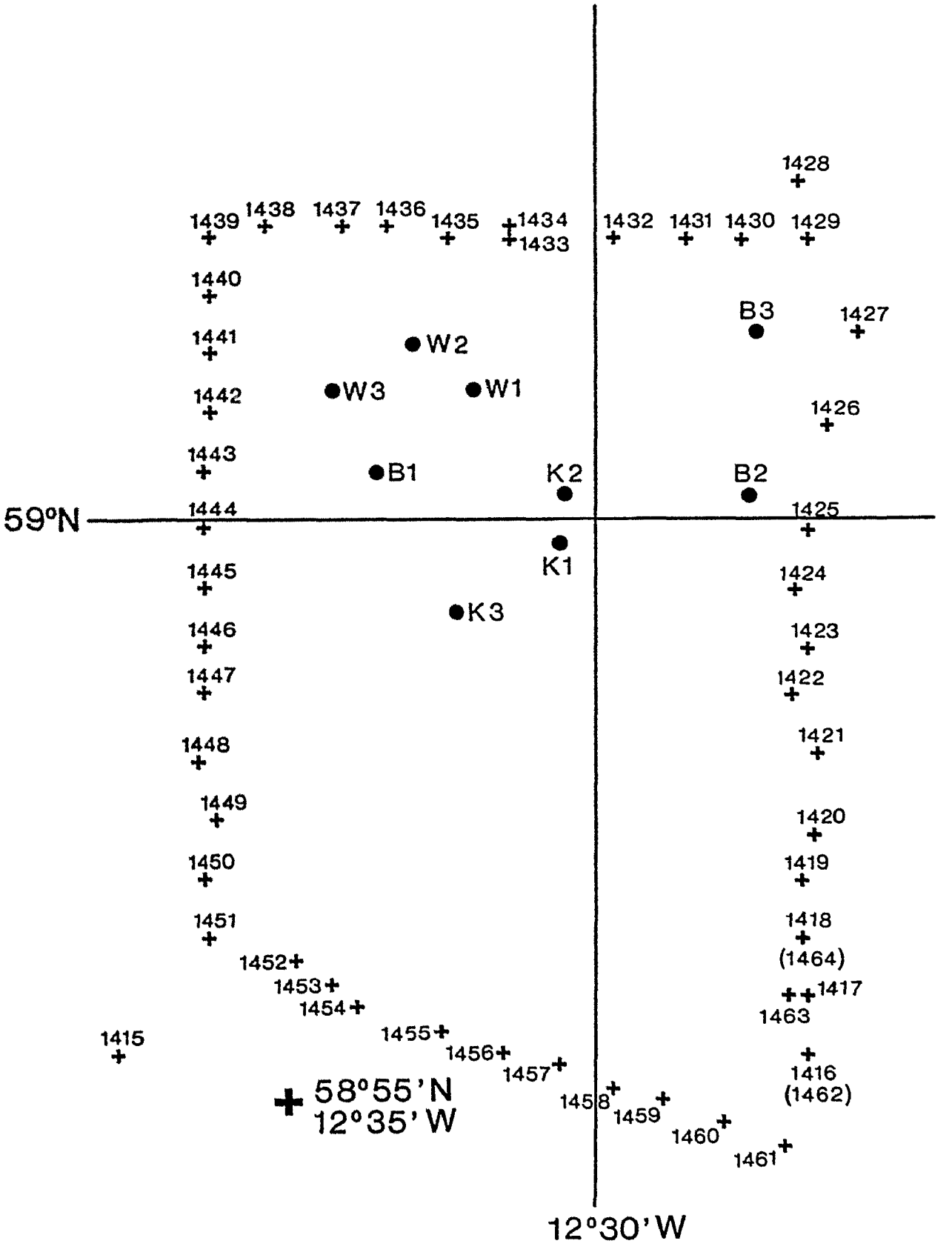

Fig. 2 CTD Box 1 24-26 August 1978
Station No. 1416-1461

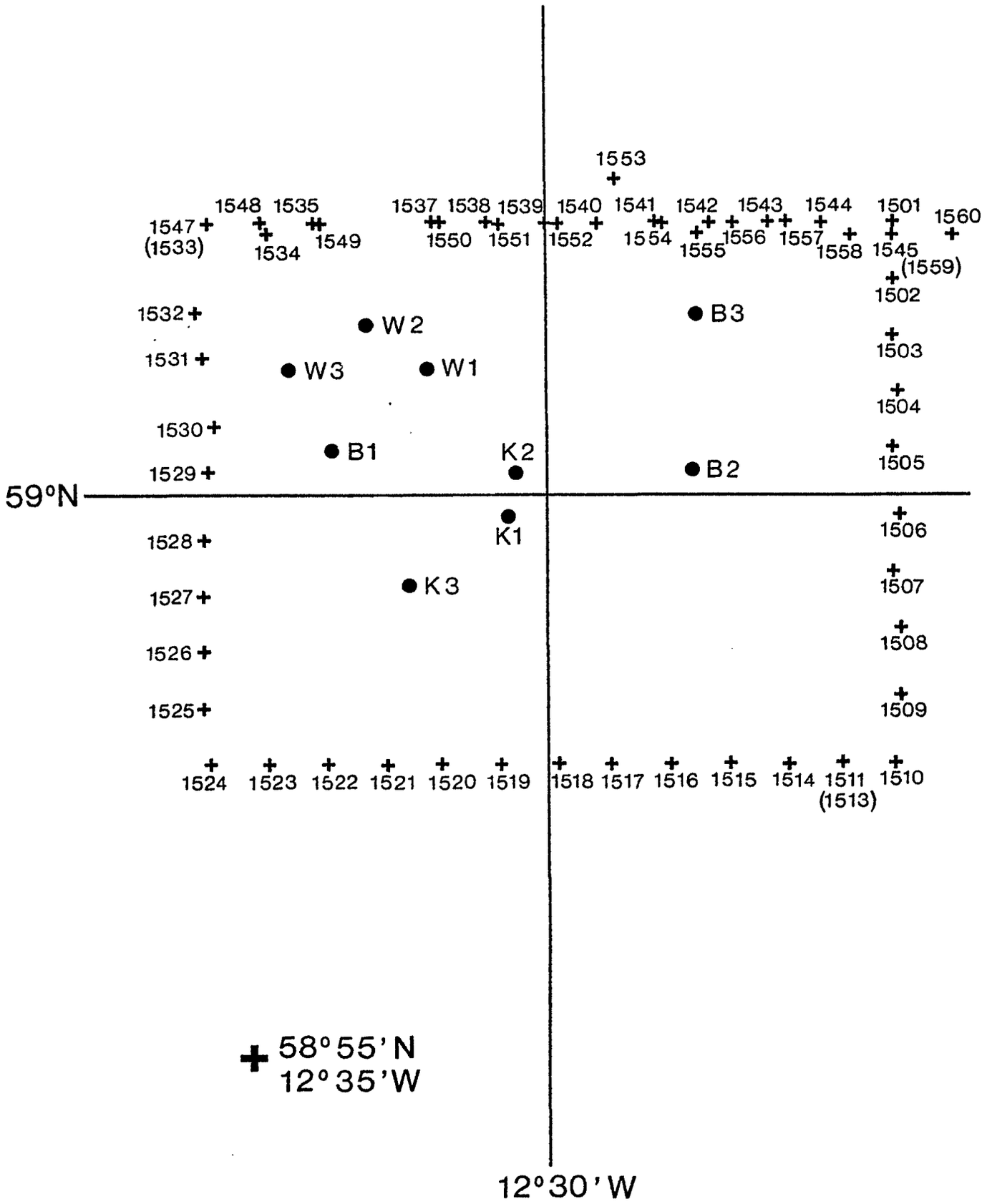

Fig. 3 CTD Box 2 3-5 September 1978
Station No. 1501-1560

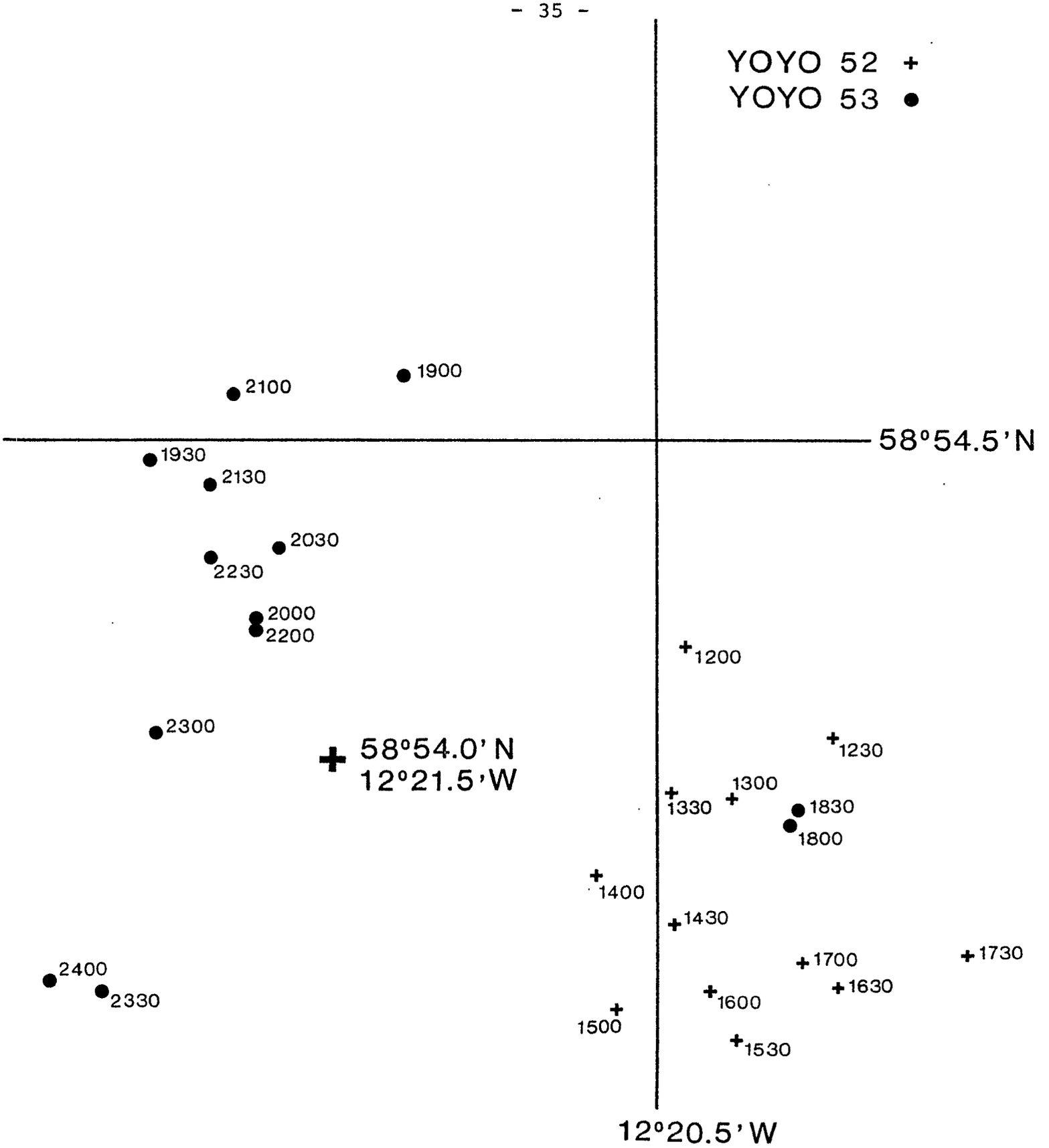

Fig. 4a YOYO Stations 52,53
First Multiship Experiment 29 August 1978

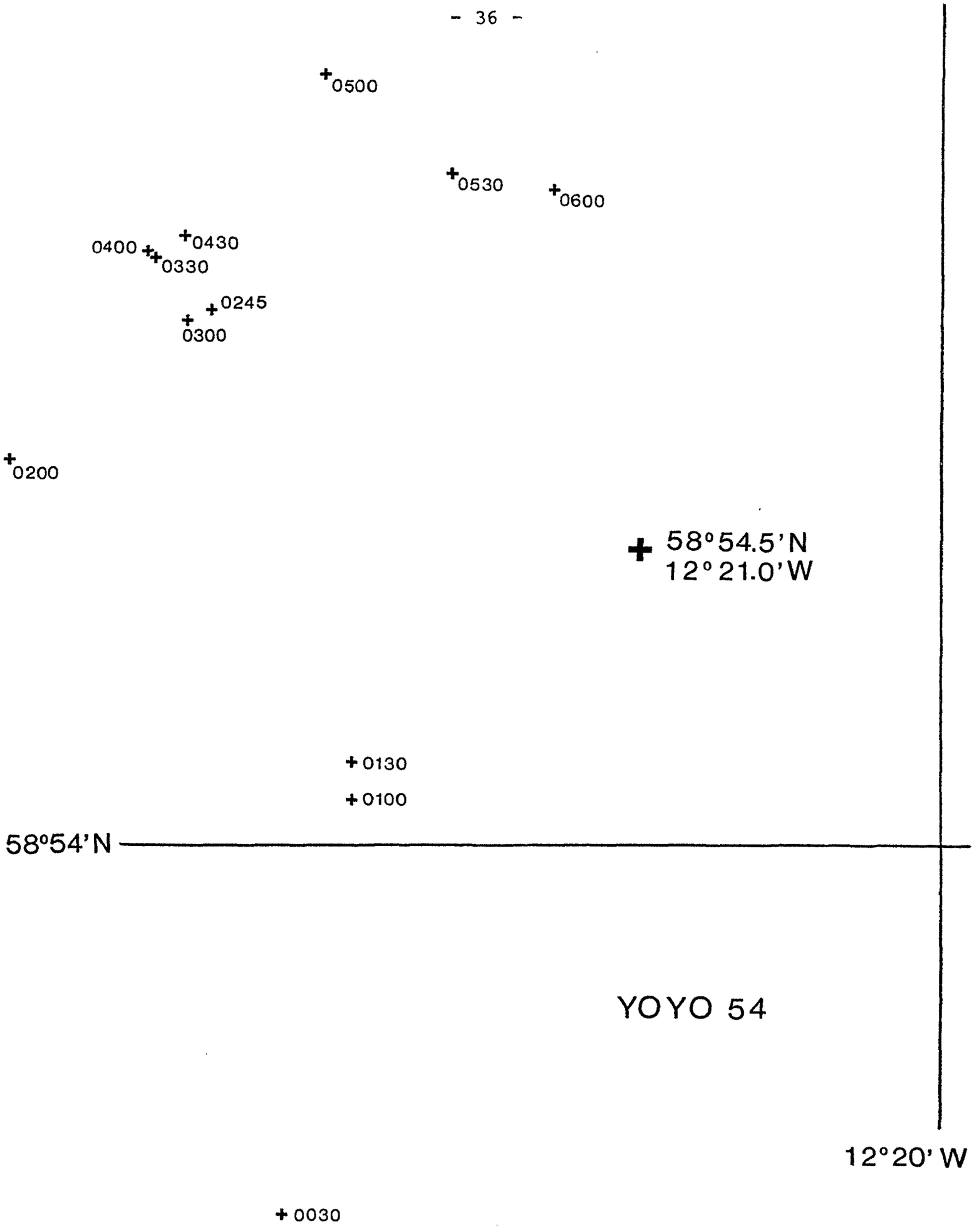

Fig. 4b YOYO Station 54
First Multiship Experiment 30 August 1978

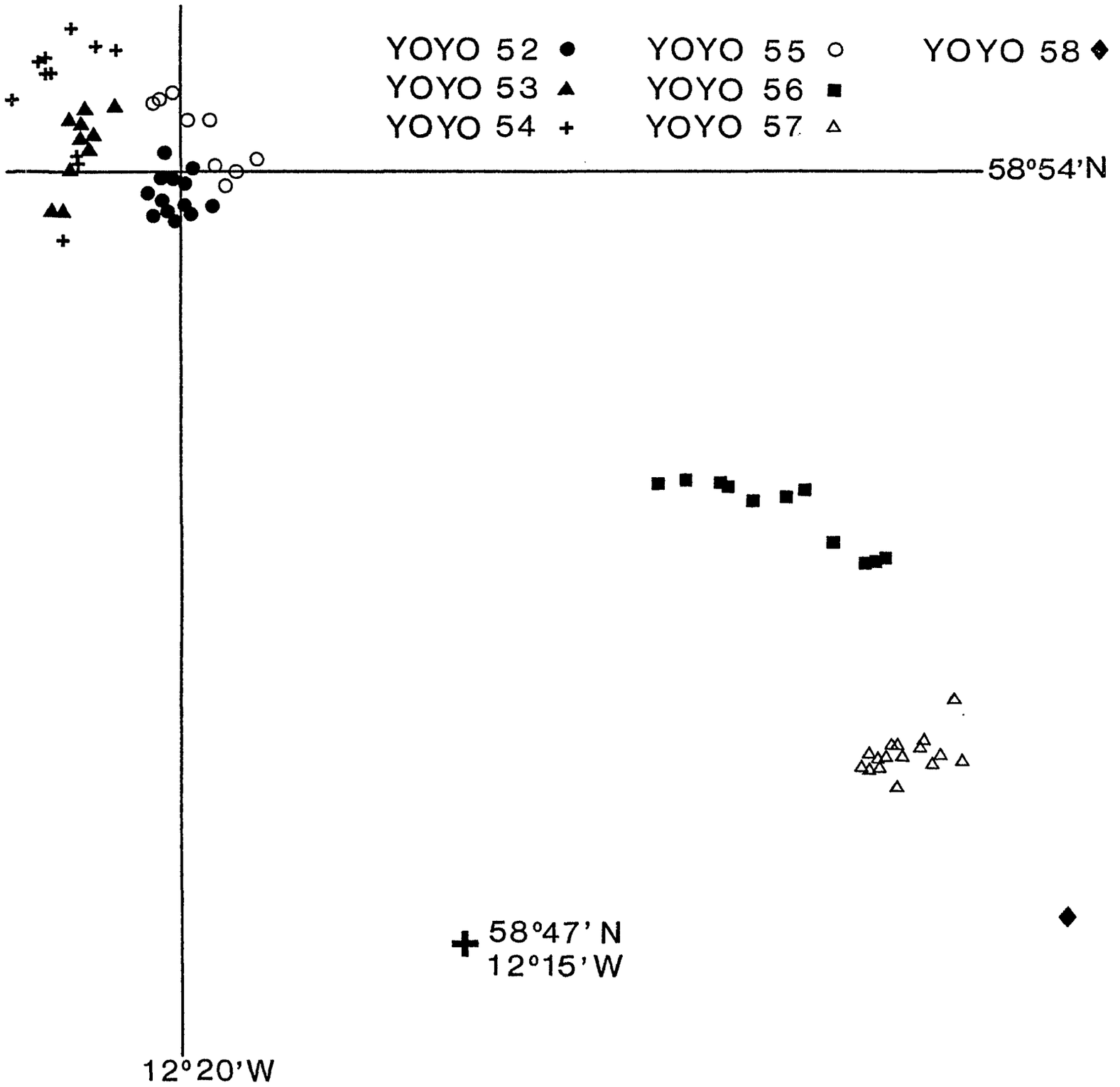

Fig. 4c YOYO Stations 52-58

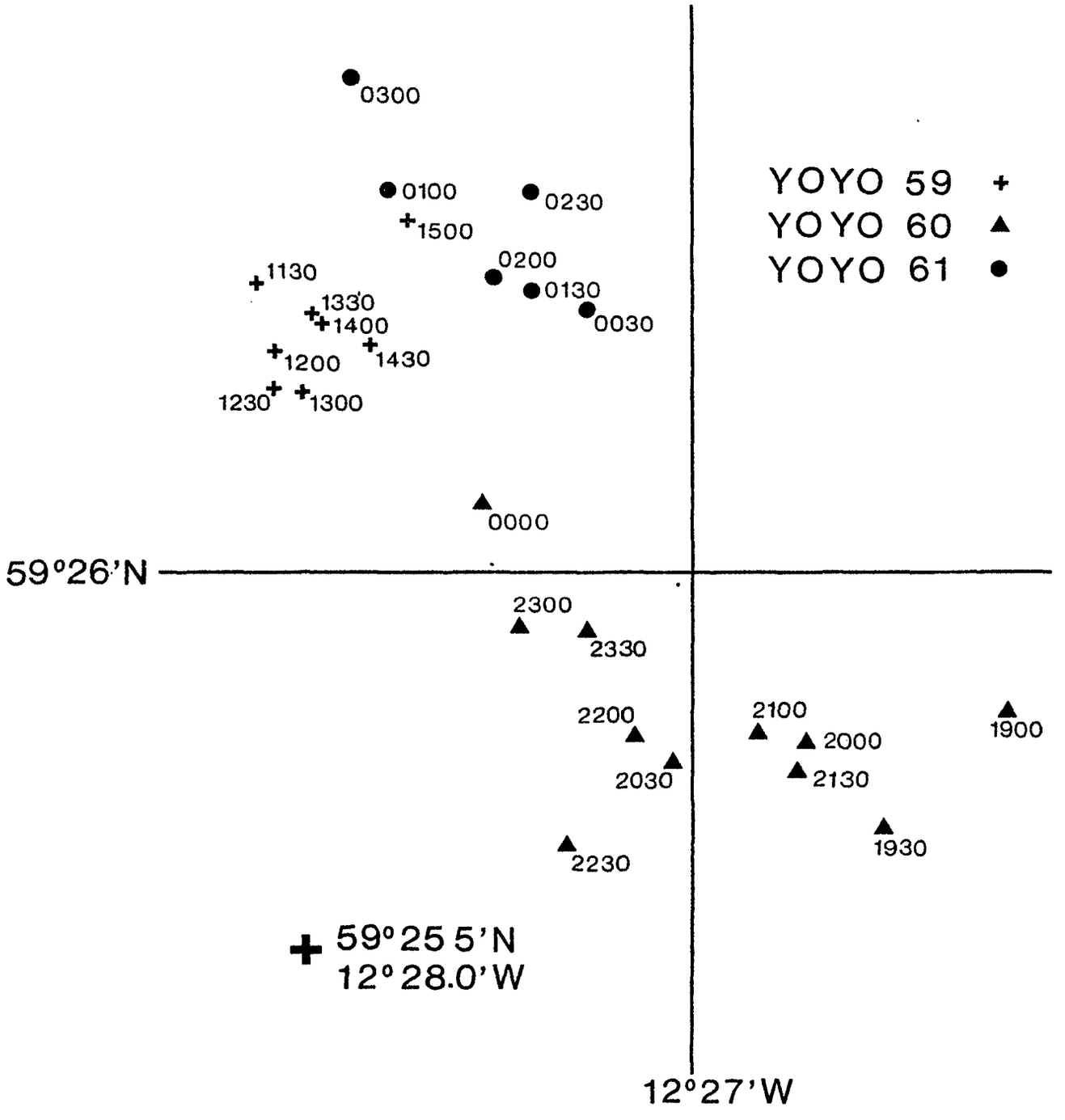

Fig. 4d YOYO Stations 59,60,61
Second Multiship Experiment 2-3 September 1978

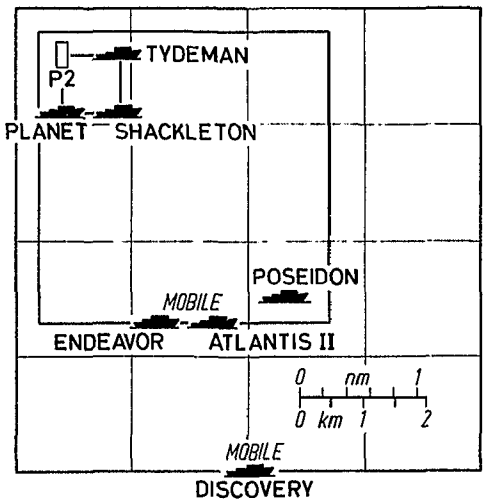

Fig. 5 Distribution of drifting and roving ships during the First Multiship Experiment (29/30 August 1978). The centre of the area shown was about 14 km south east of the FIA.

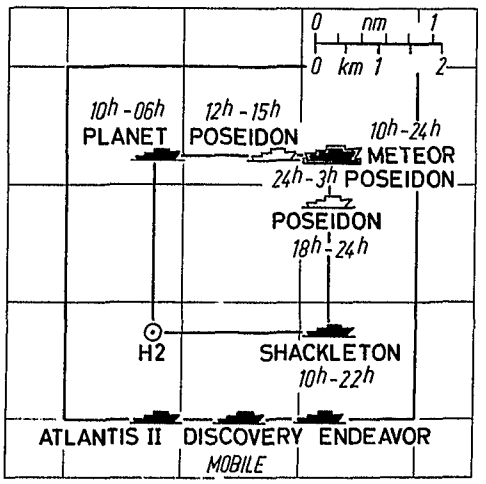

Fig. 6 Distribution of fixed position and roving ships during the Second Multiship Experiment (2/3 September 1978). Buoy H2 was moored at 59° 25' N, 12° 30' W about 47 km north of the FIA.

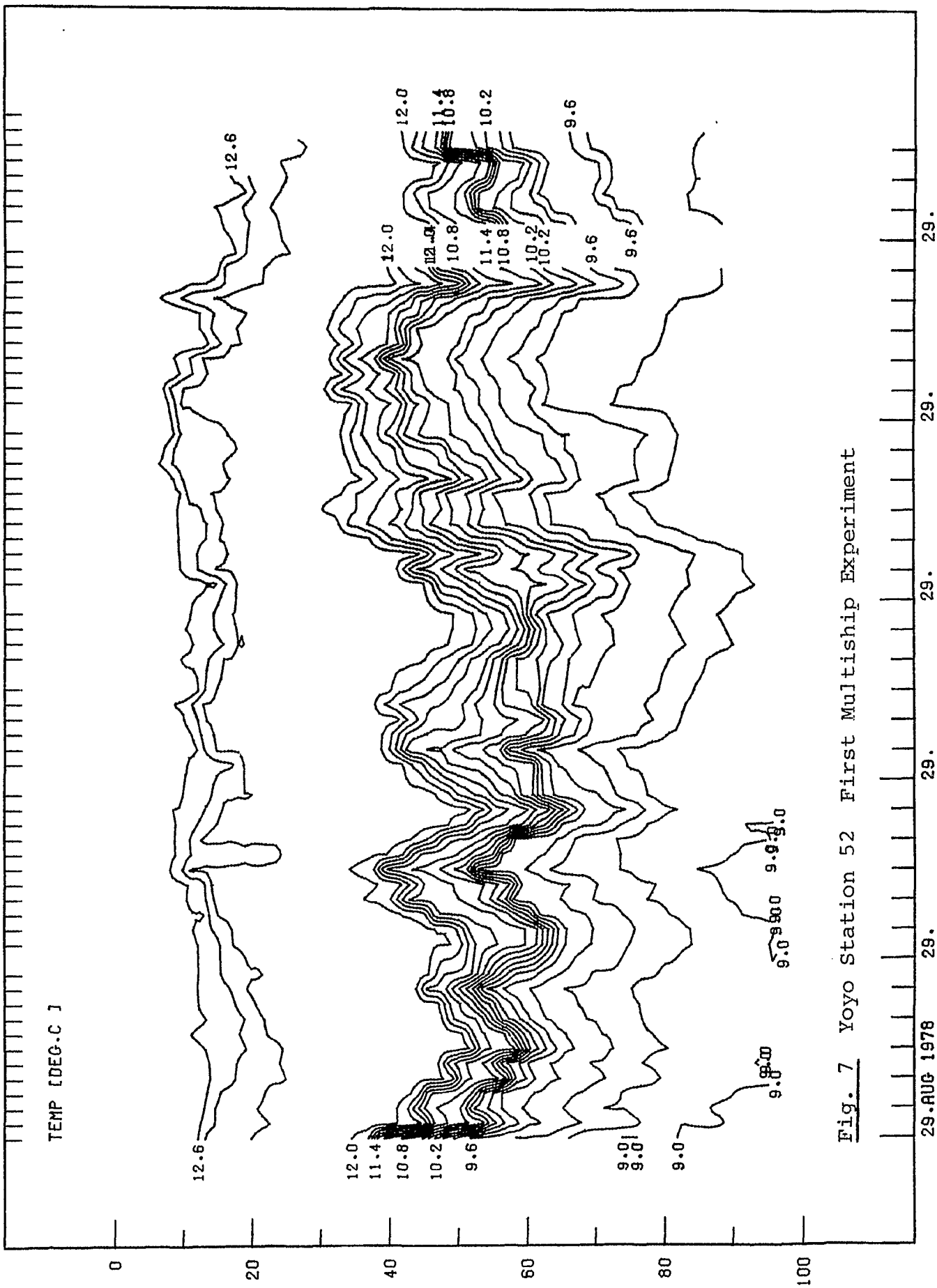

Fig. 7 Yoyo Station 52 First Multiship Experiment

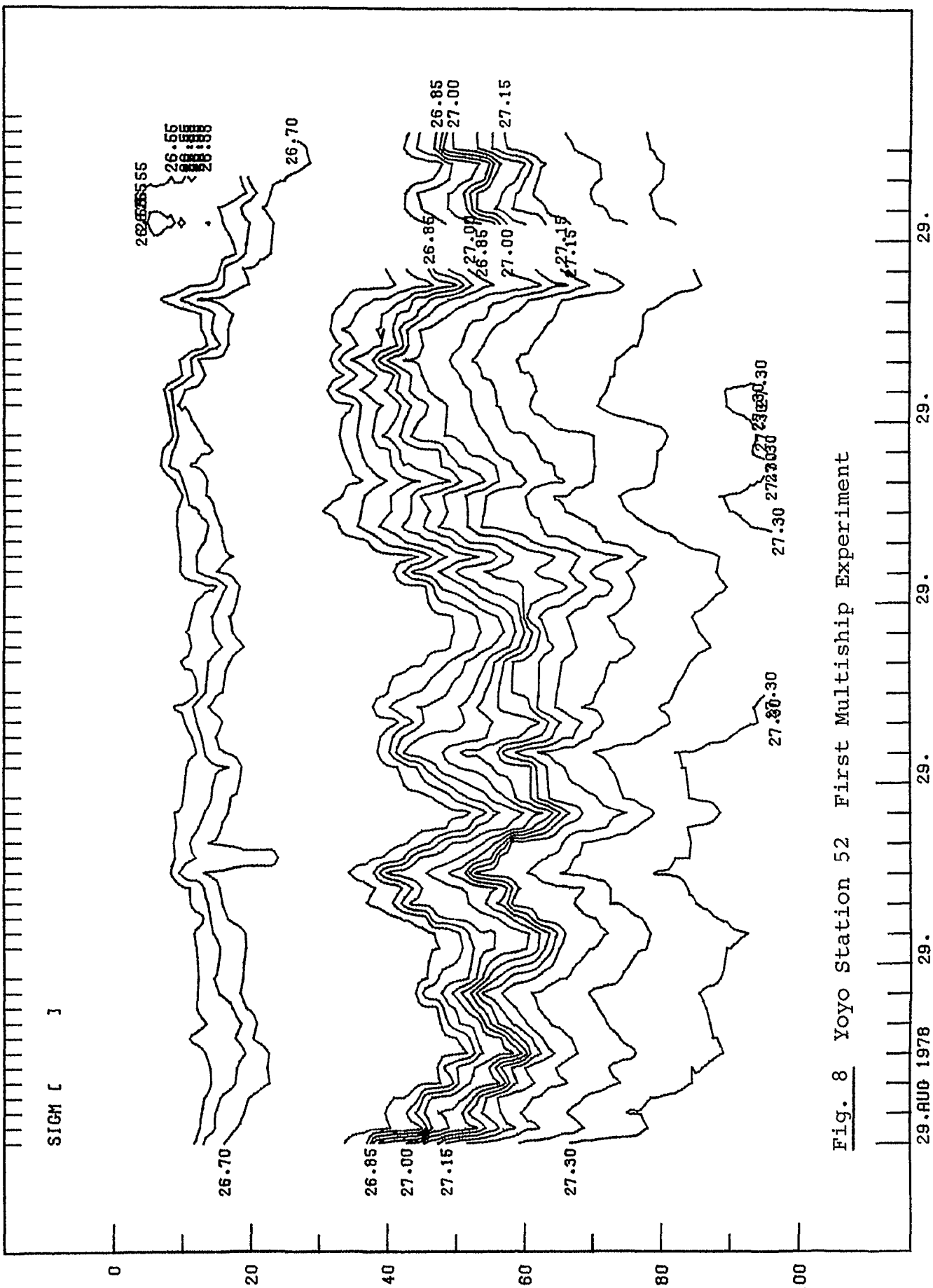

Fig. 8 Yoyo Station 52 First Multiship Experiment

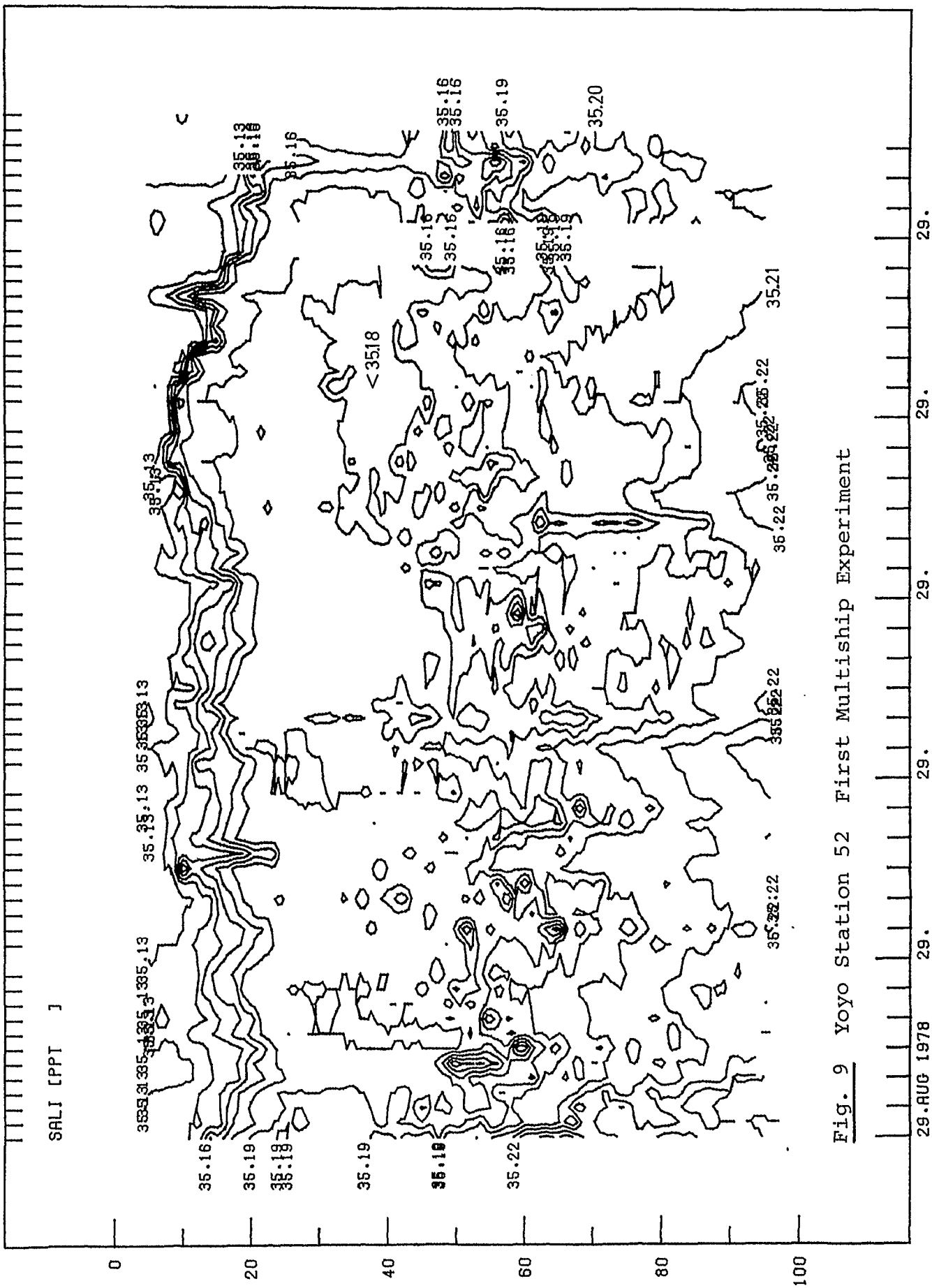

Fig. 9 Yoyo Station 52 First Multiship Experiment

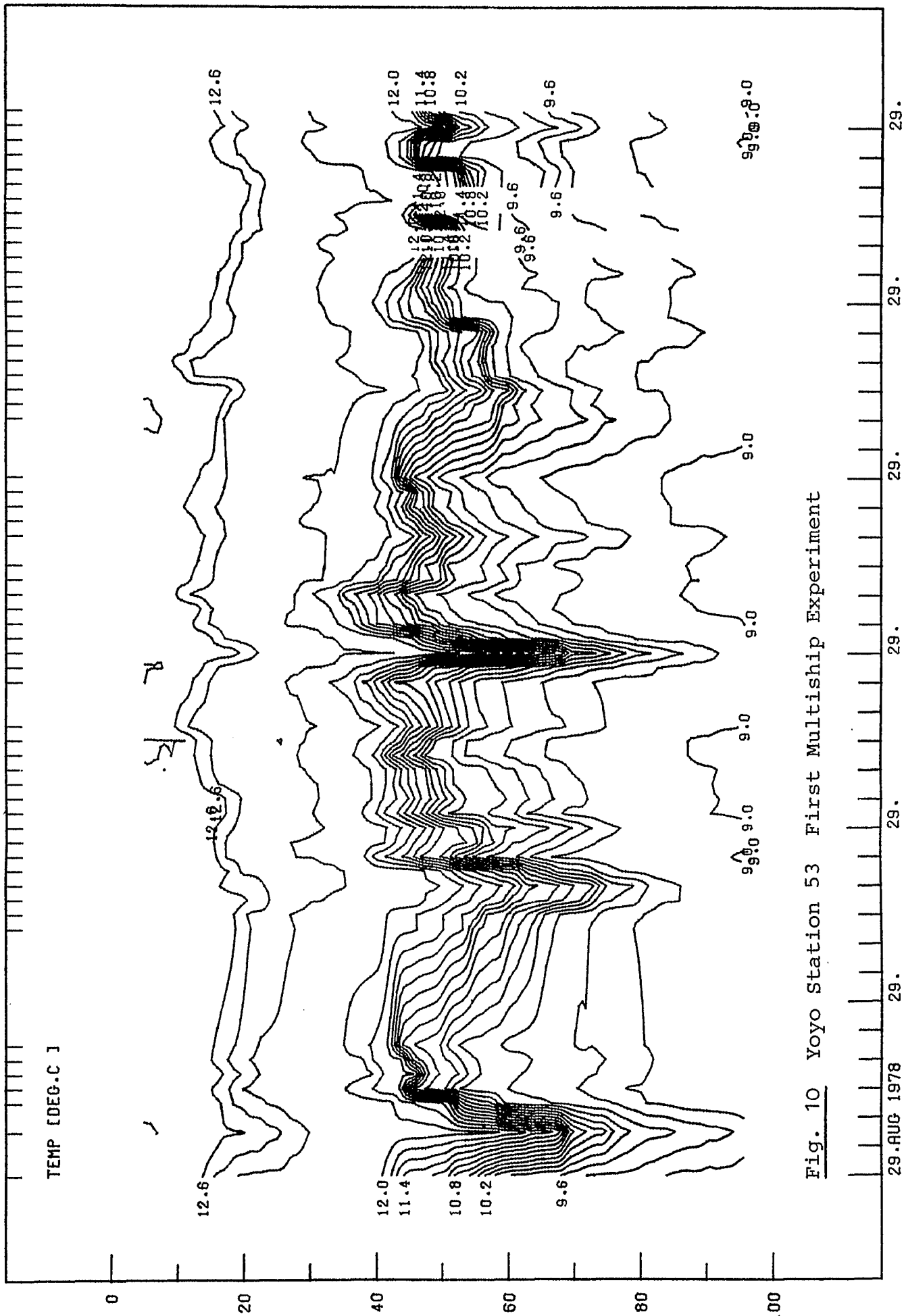

Fig. 10 Yoyo Station 53 First Multiship Experiment

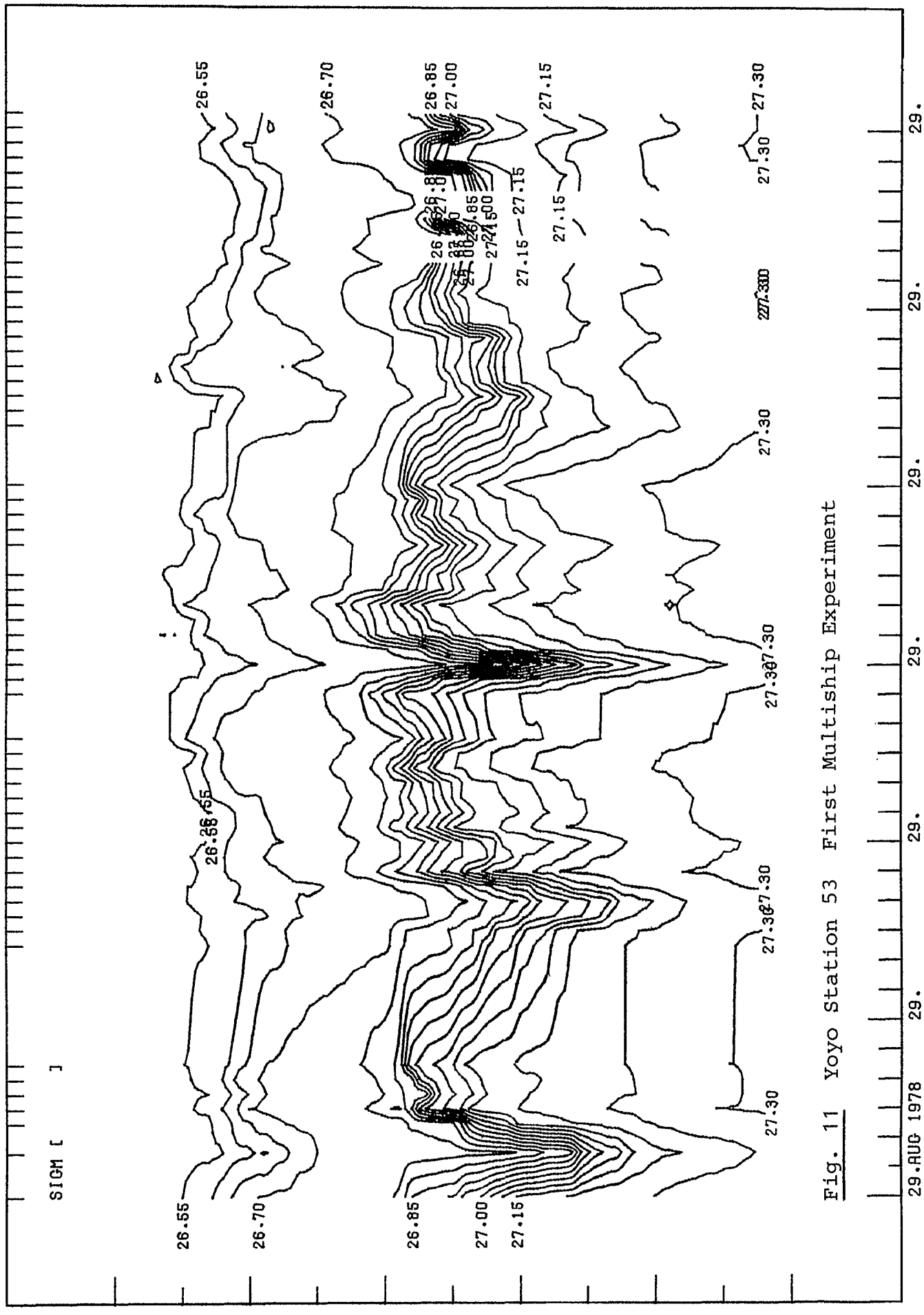

Fig. 11 Yoyo Station 53 First Multiship Experiment

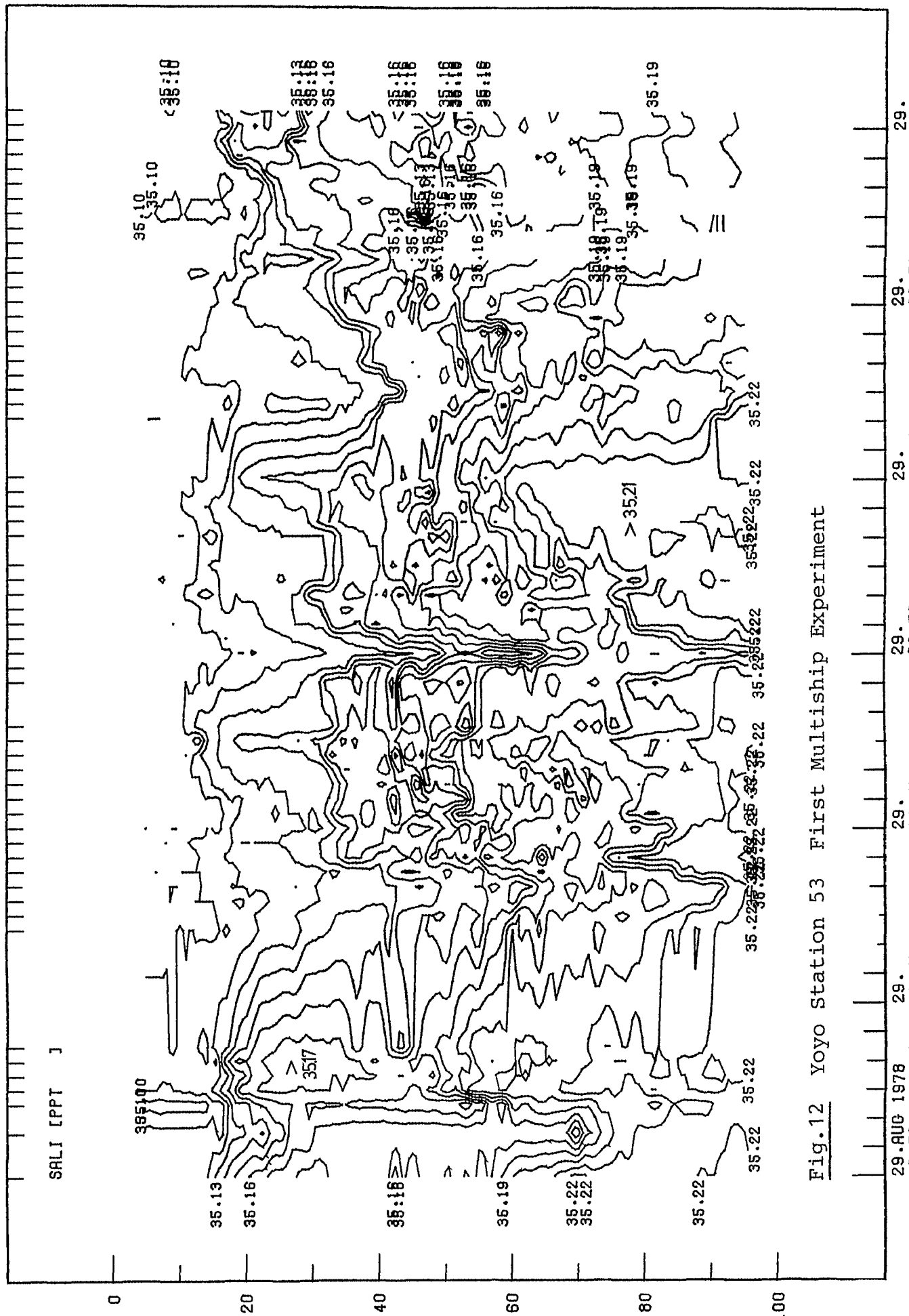

Fig.12 Yoyo Station 53 First Multiship Experiment

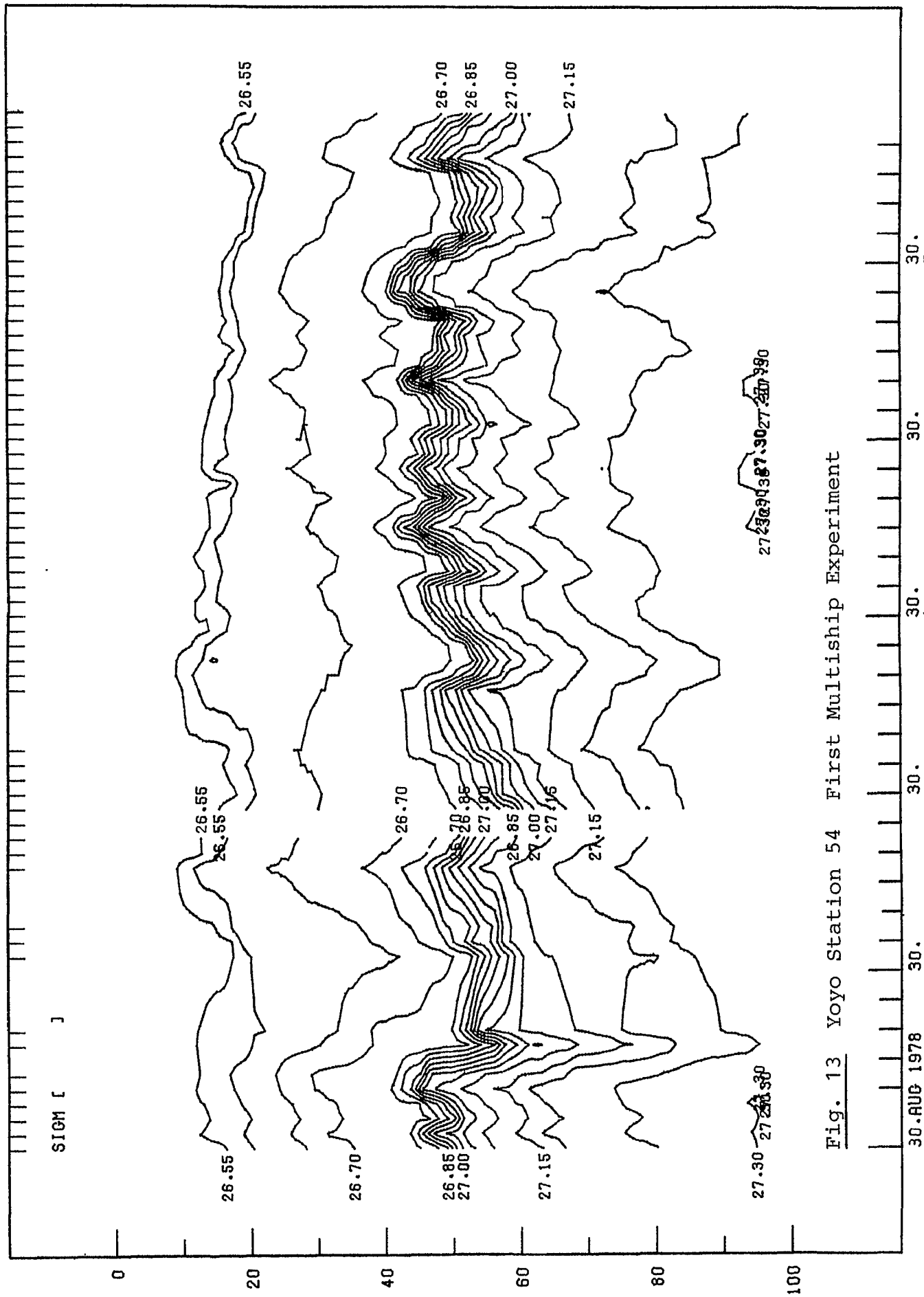

Fig. 13 Yoyo Station 54 First Multiship Experiment

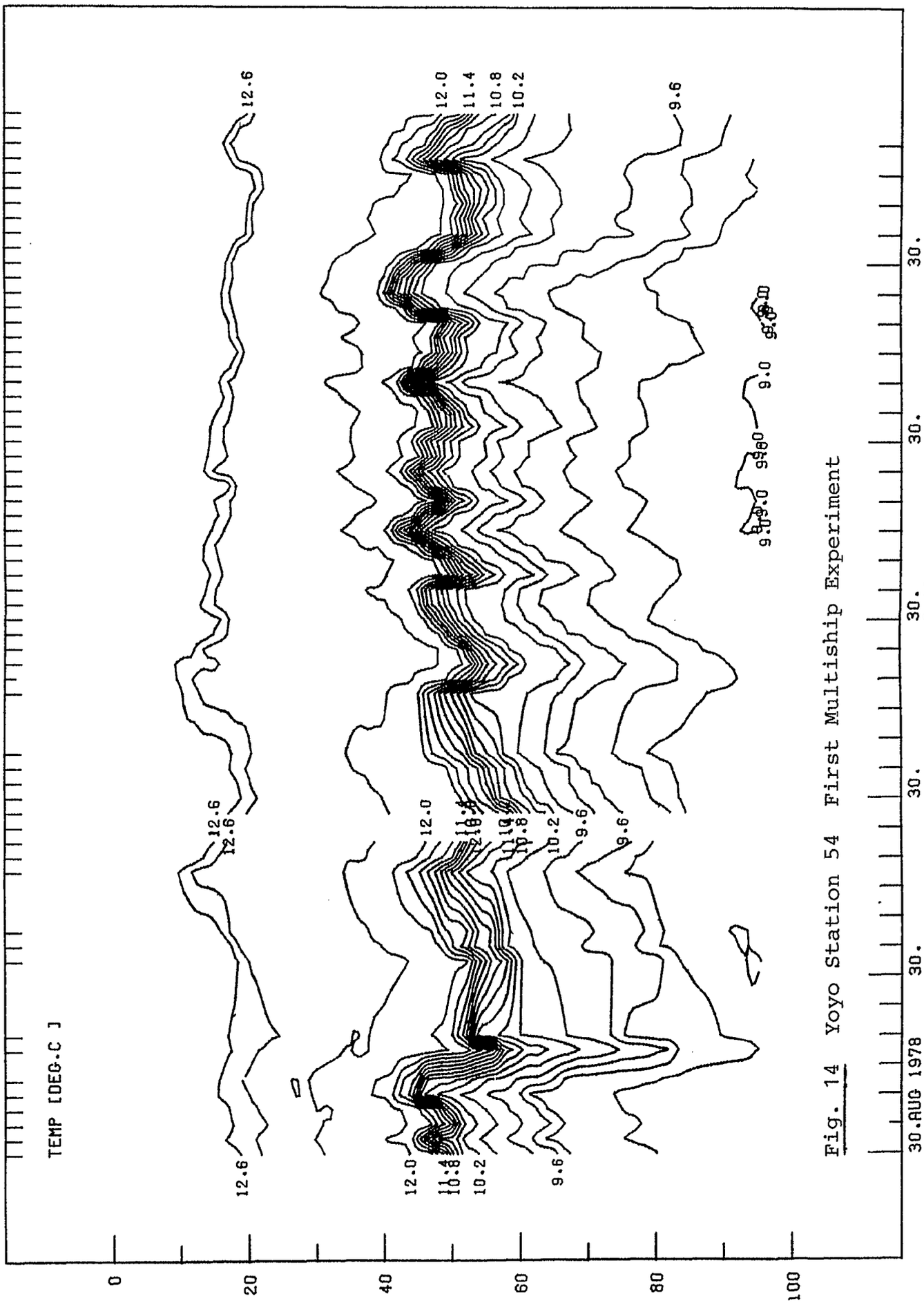

Fig. 14 Yoyo Station 54 First Multiship Experiment

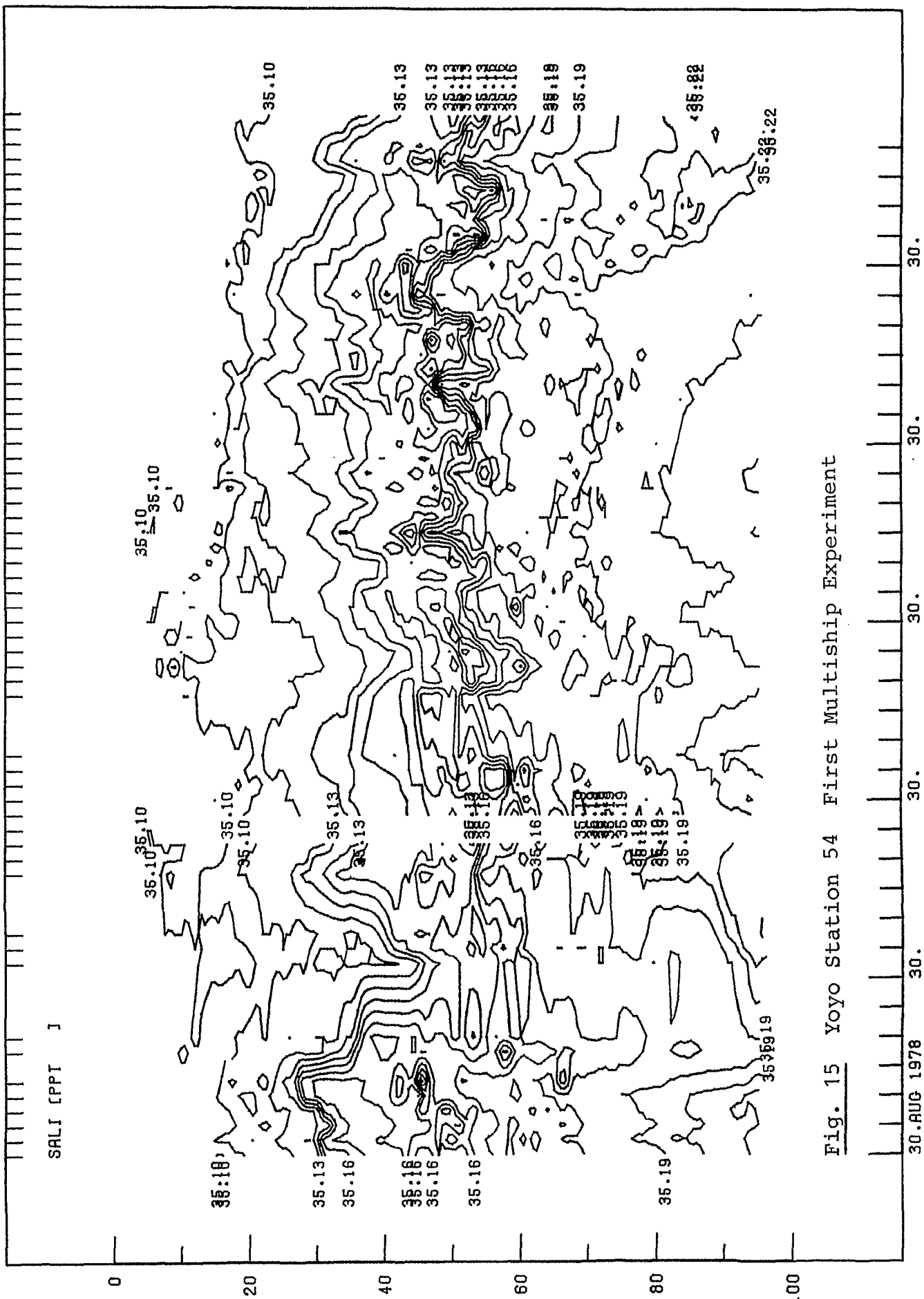

Fig. 15 Yoyo Station 54 First Multiship Experiment

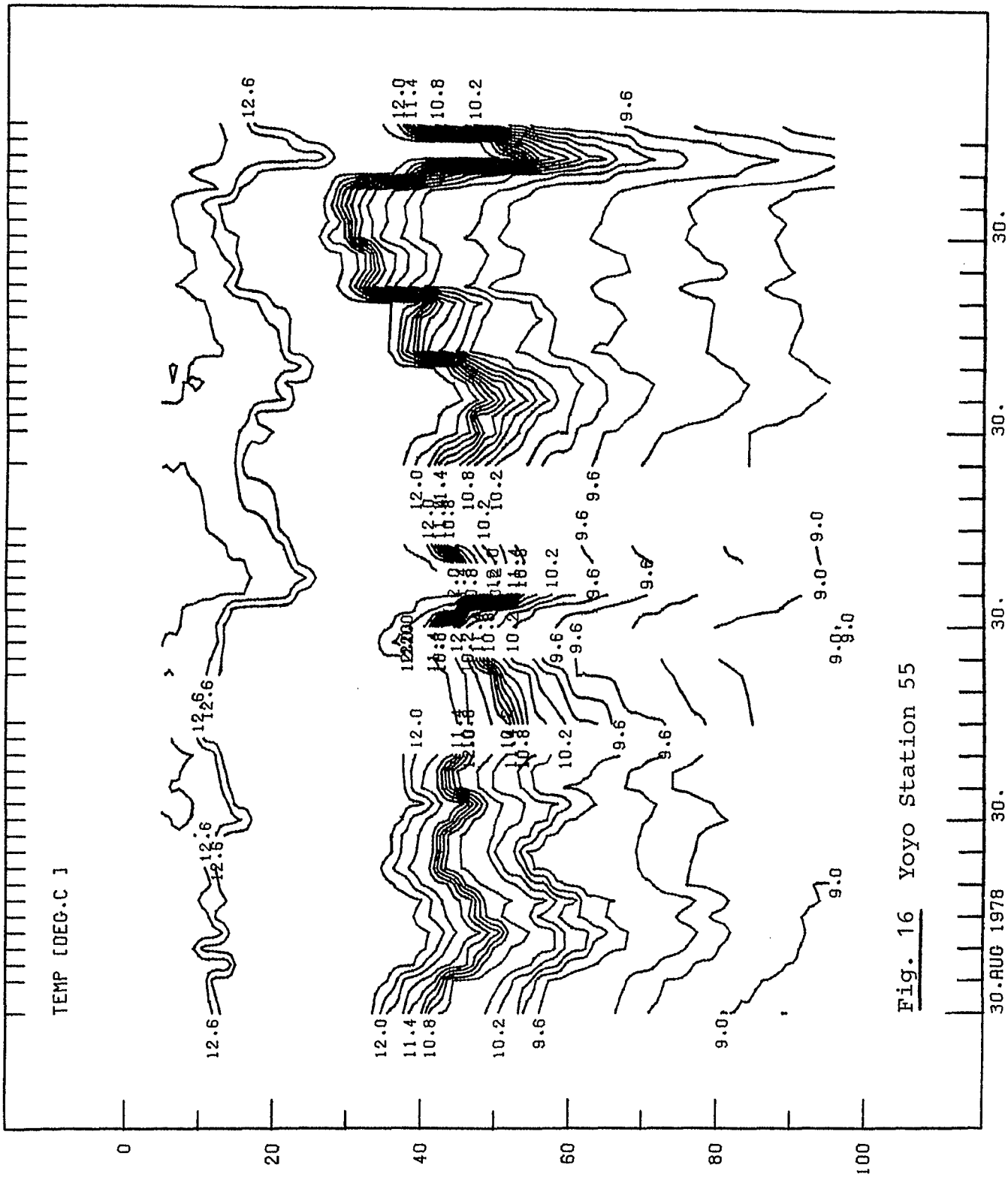

Fig. 16 Yoyo Station 55

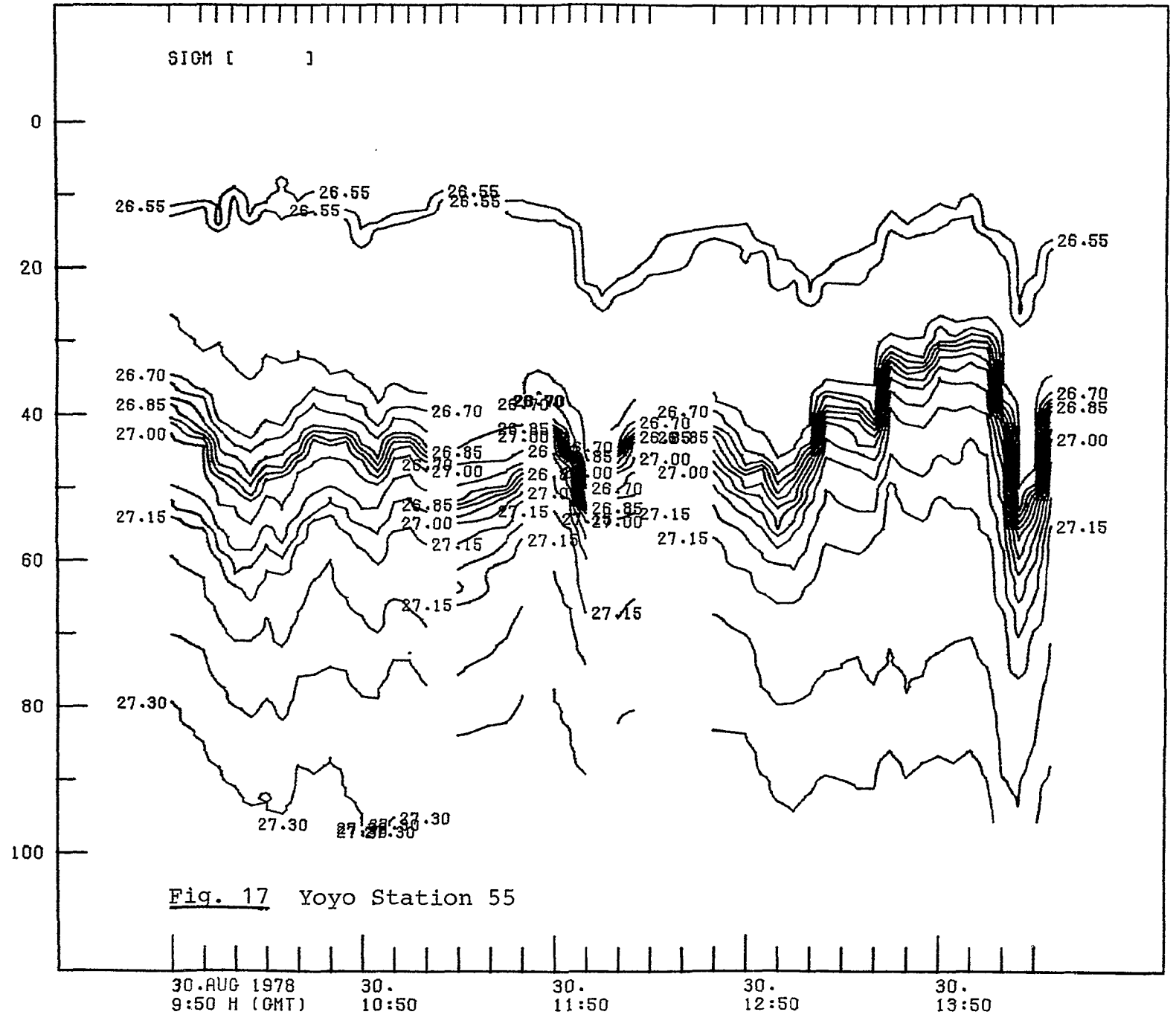

Fig. 17 Yoyo Station 55

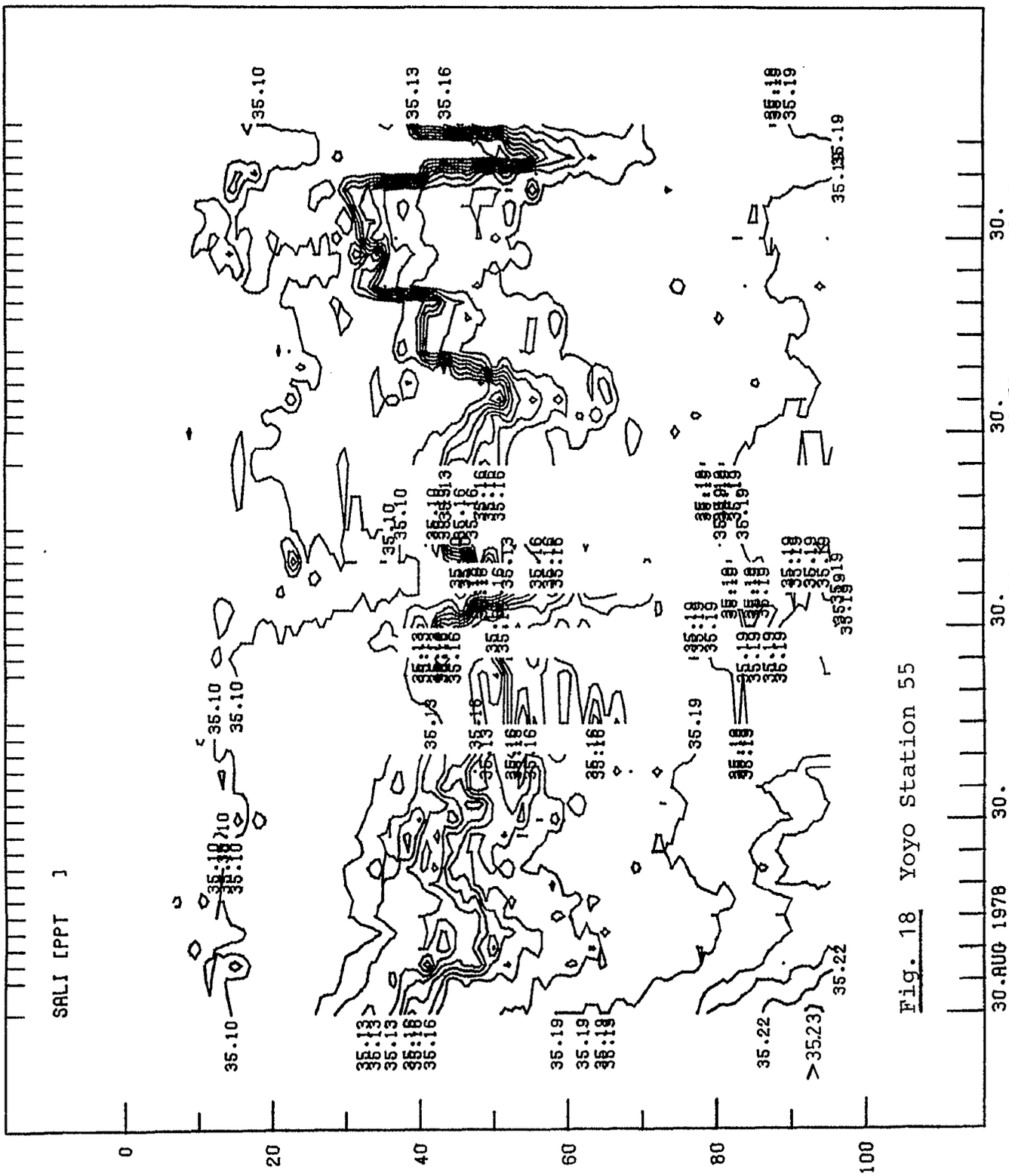

Fig. 18 Yoyo Station 55

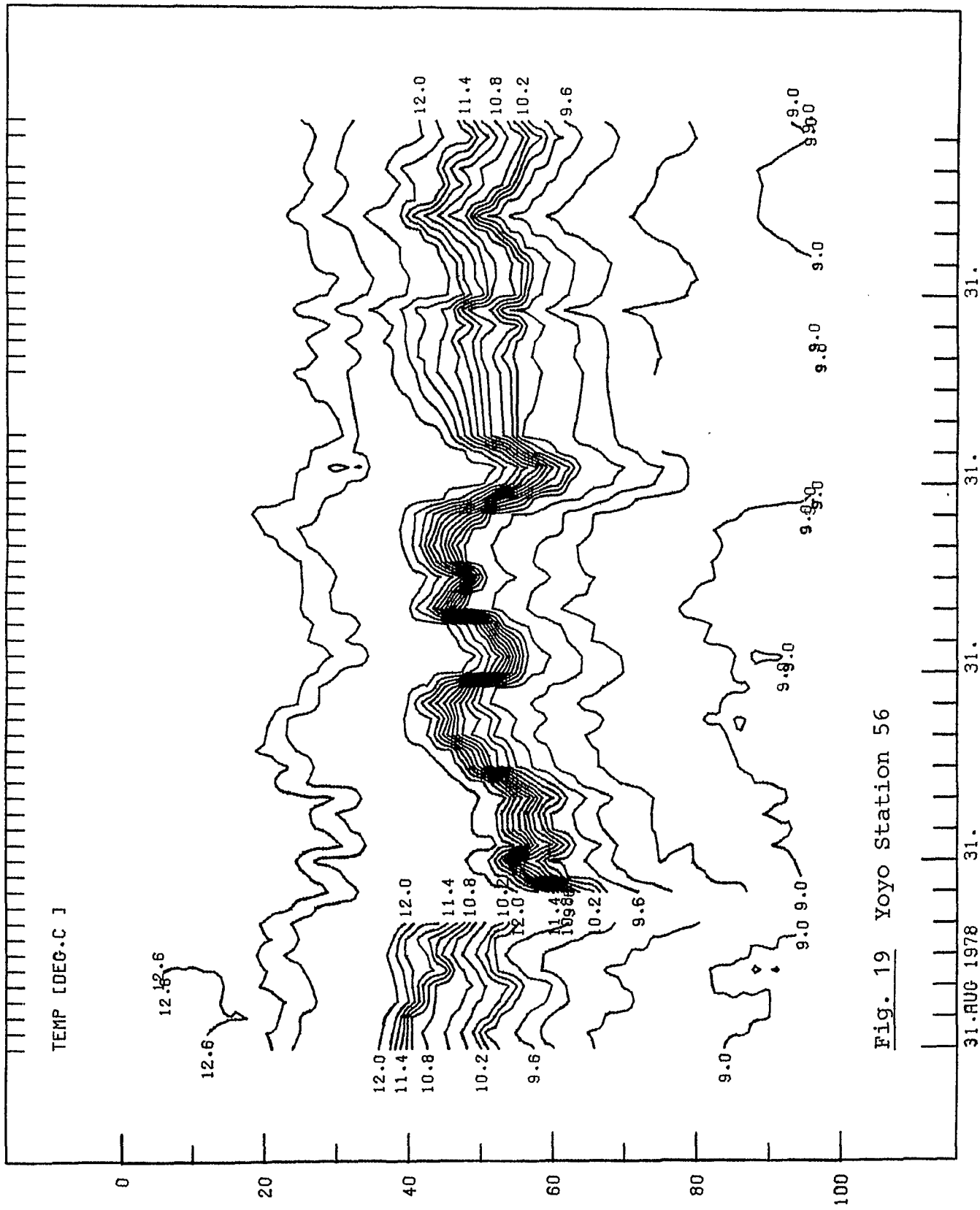

Fig. 19 Yoyo Station 56

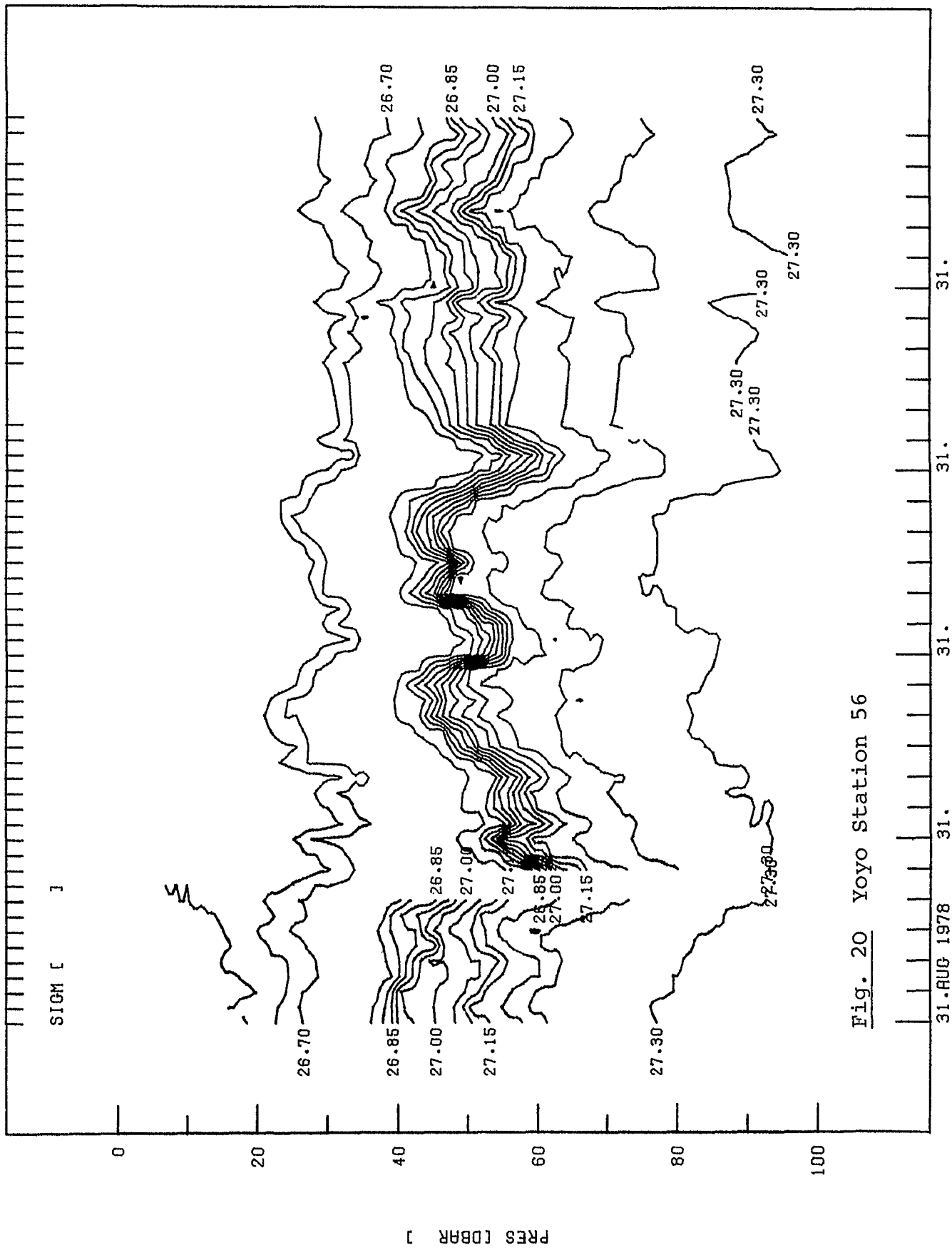

Fig. 20 Yoyo Station 56

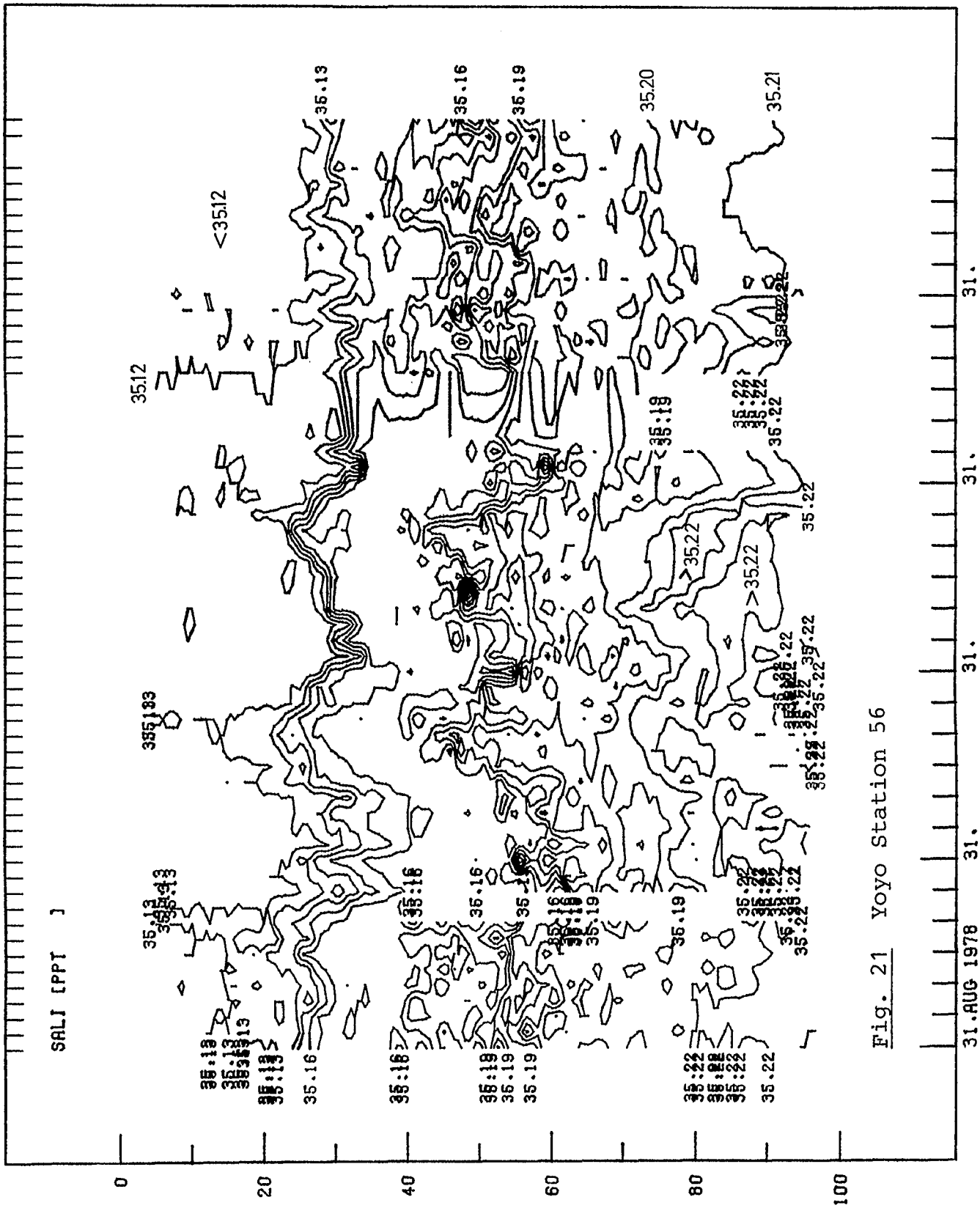

Fig. 21 Yoyo Station 56

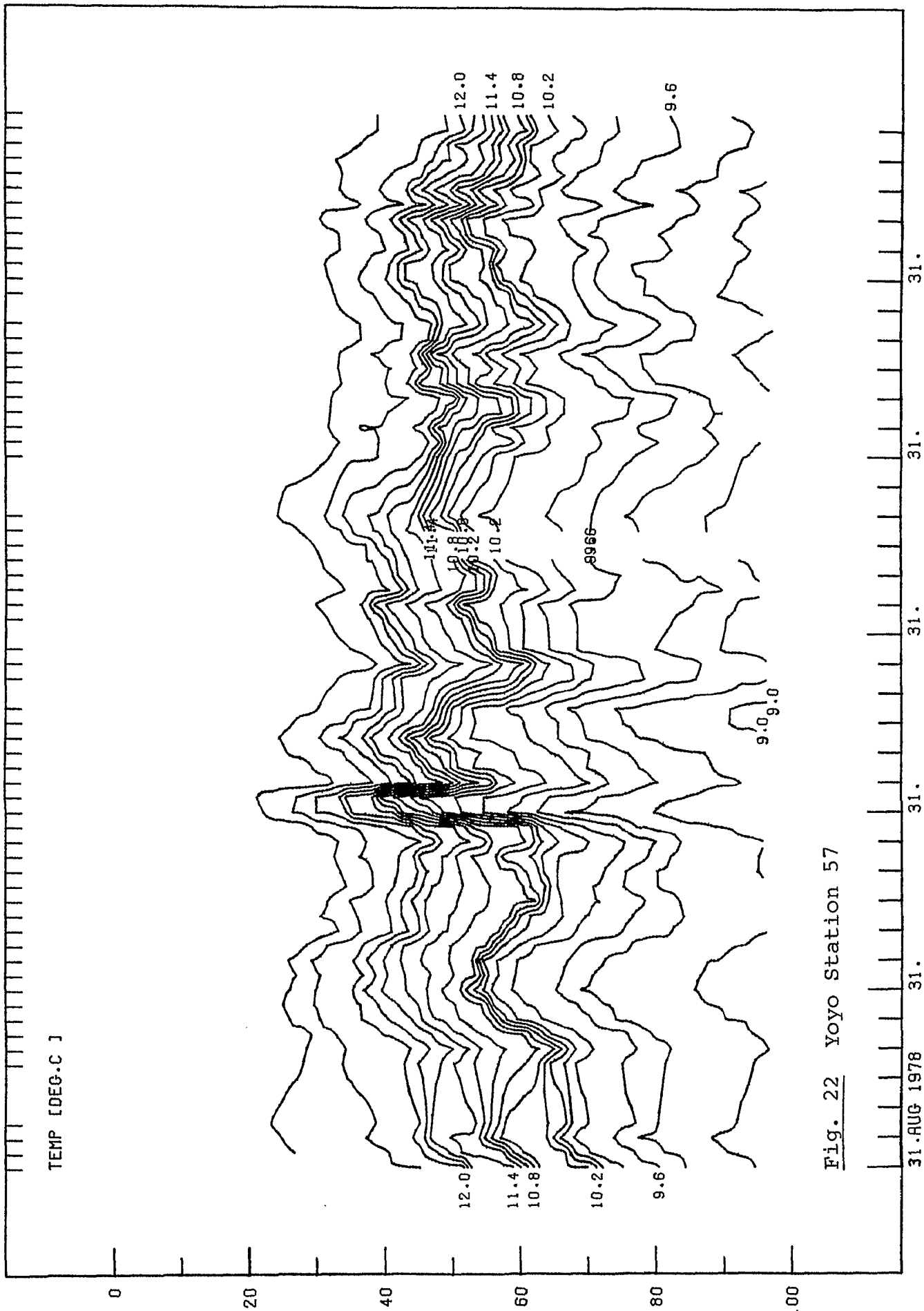

Fig. 22 Yoyo Station 57

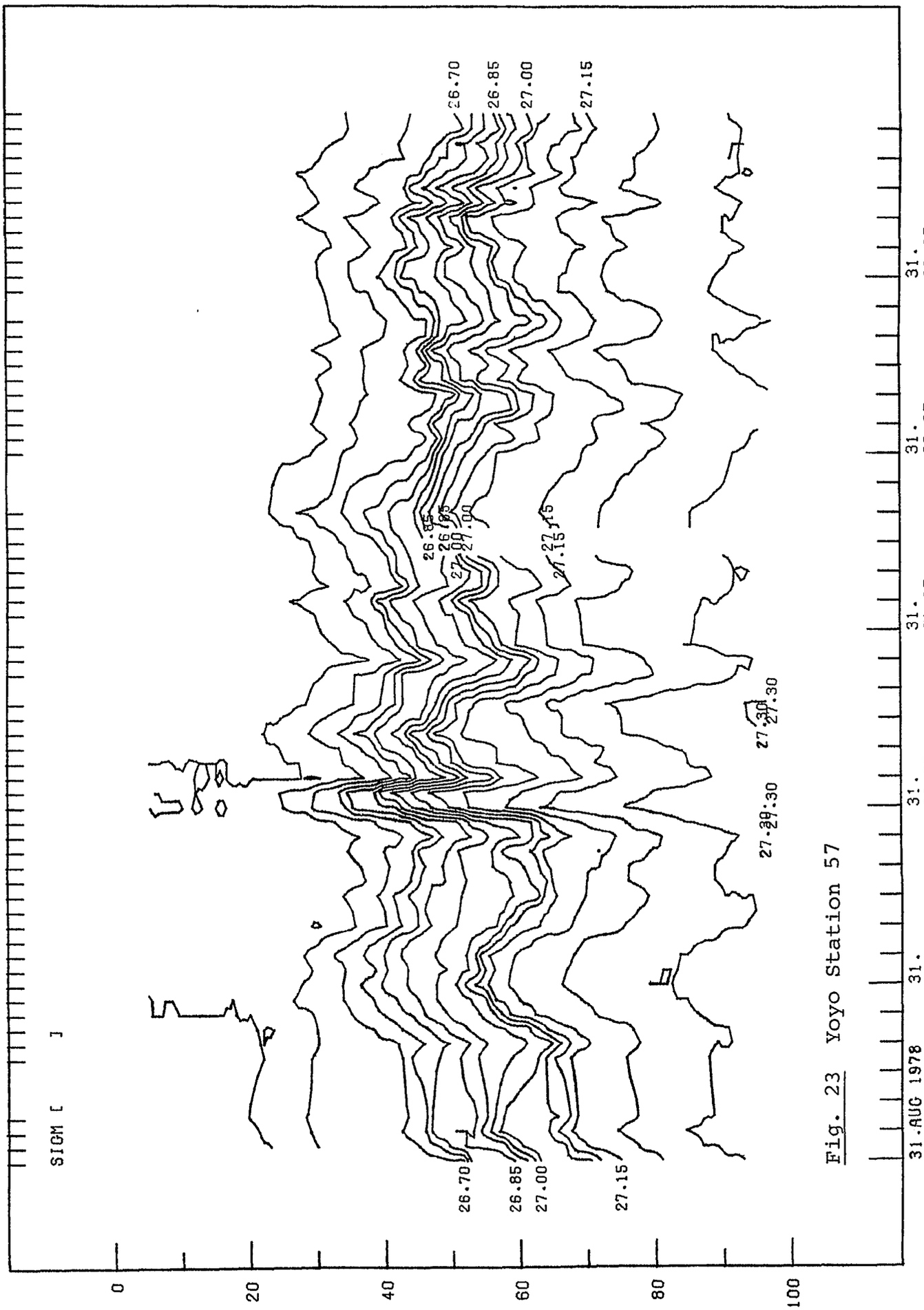

Fig. 23 Yoyo Station 57

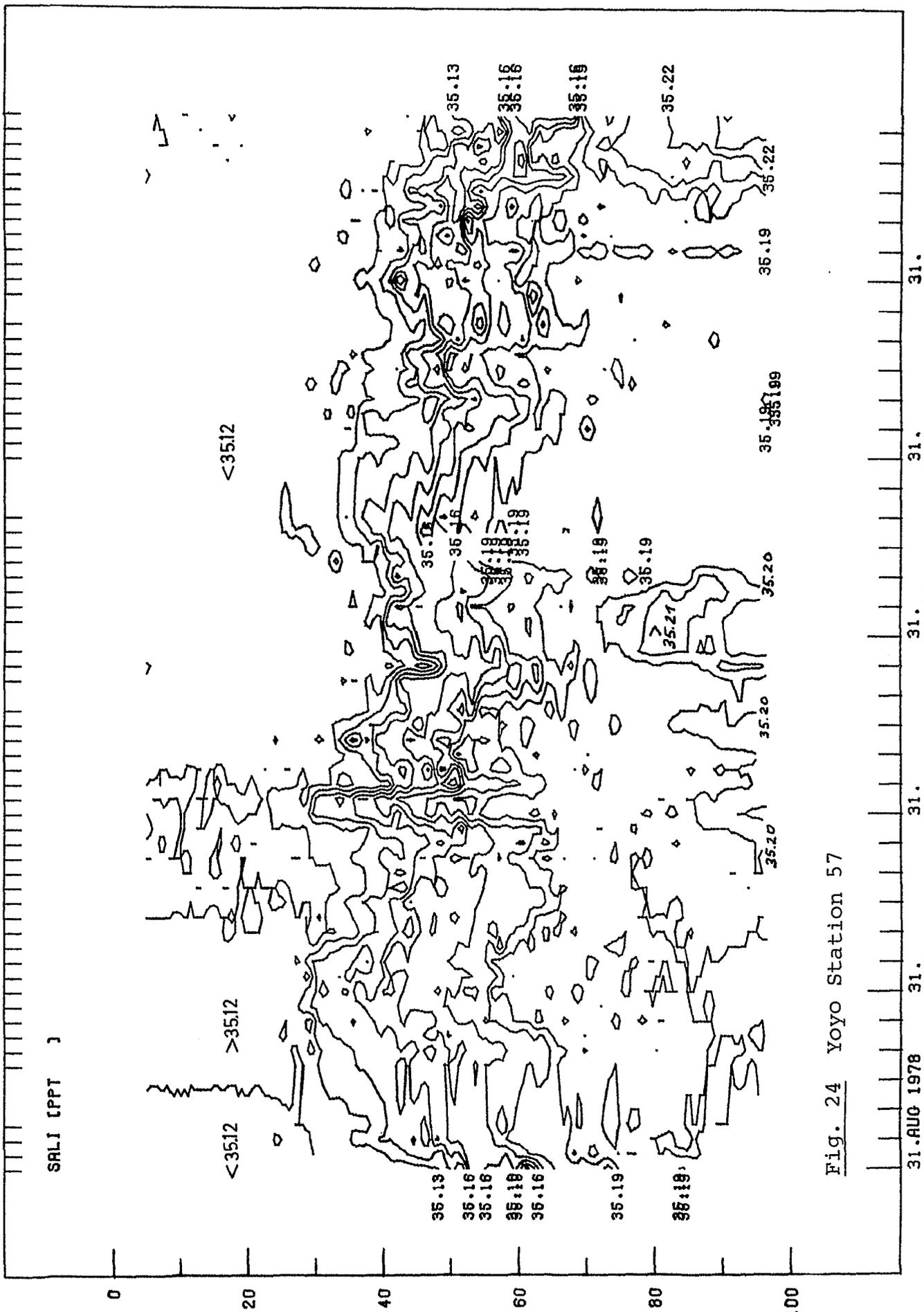

Fig. 24 Yoyo Station 57

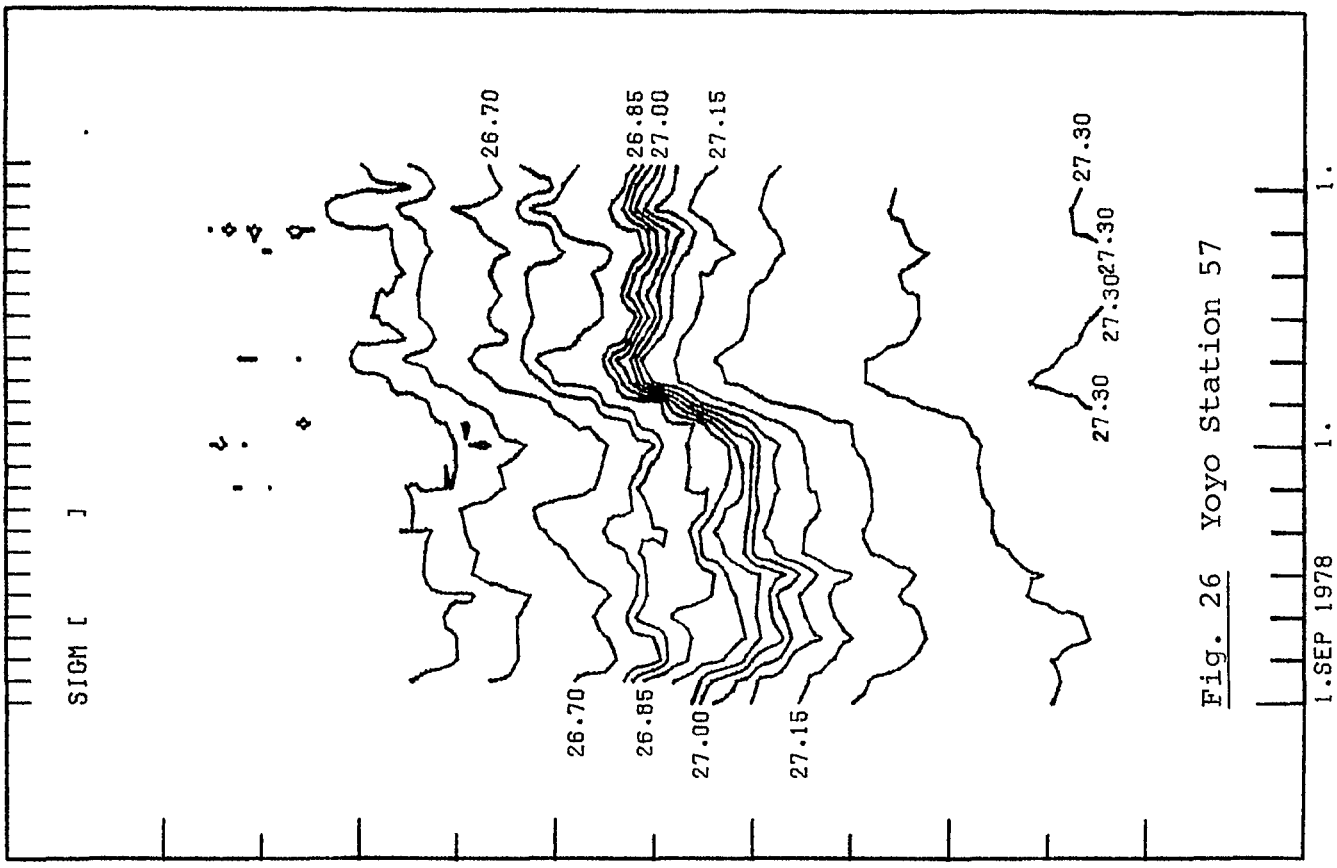

Fig. 26 Yoyo Station 57

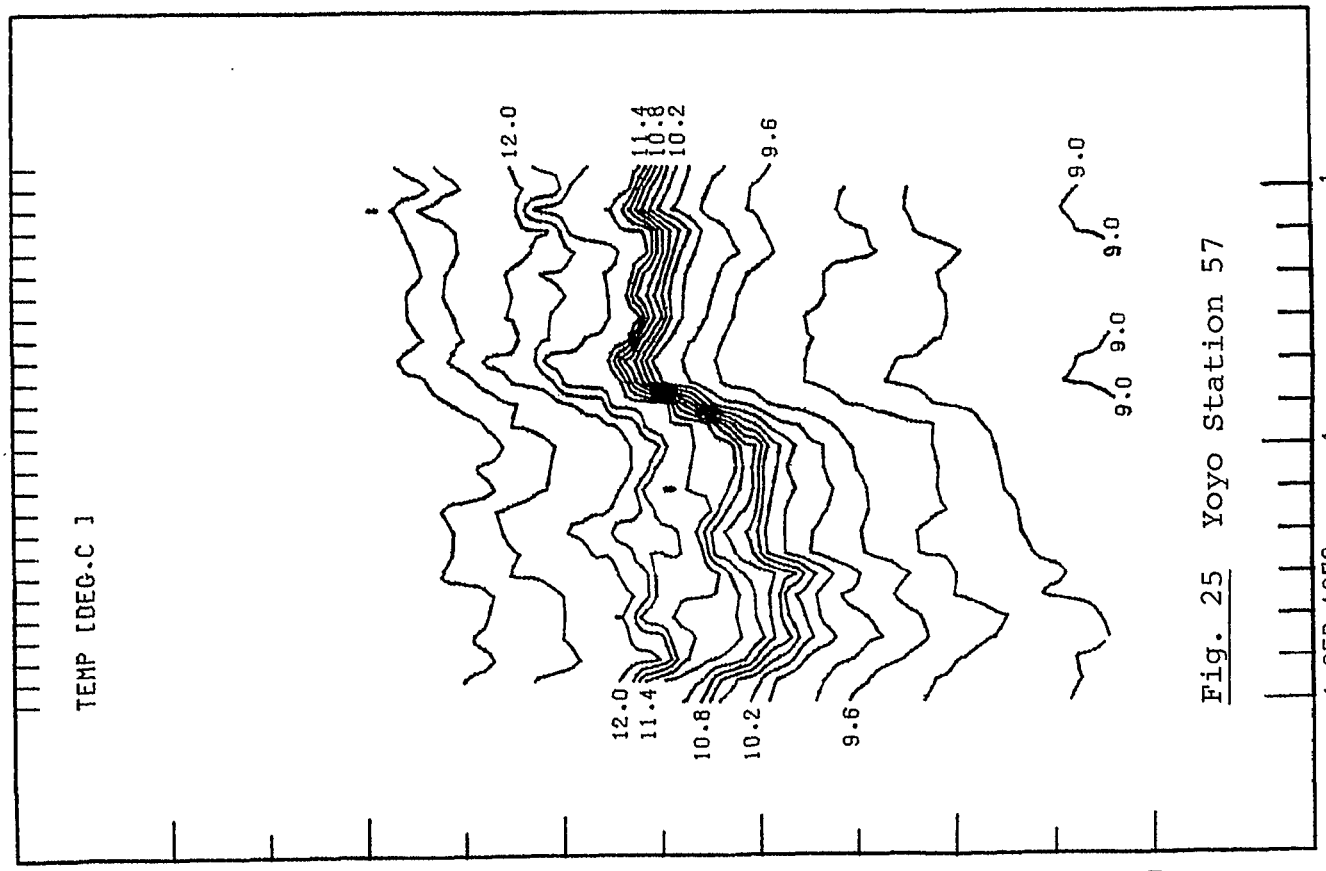

Fig. 25 Yoyo Station 57

PJCL570045

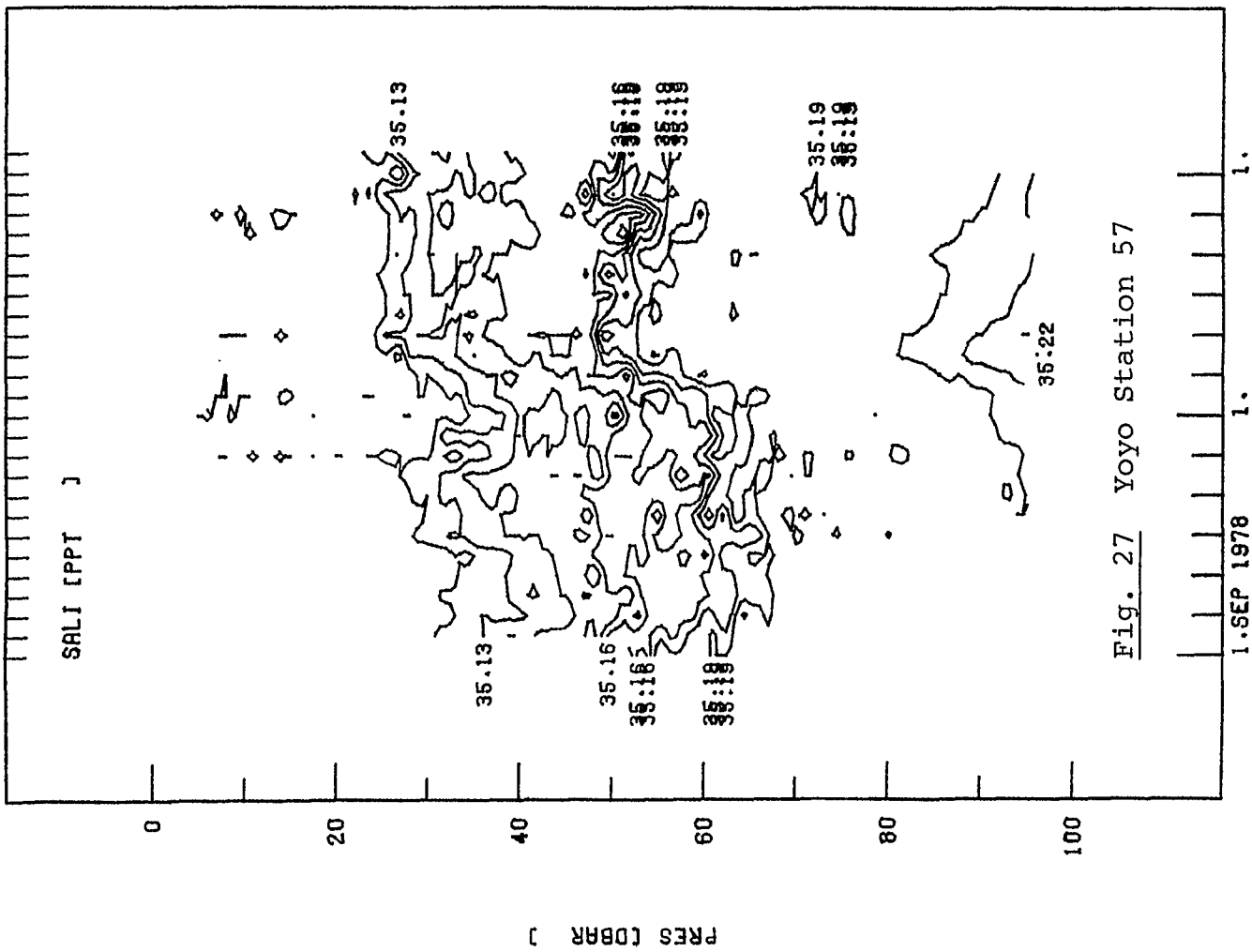

Fig. 27 Yoyo Station 57

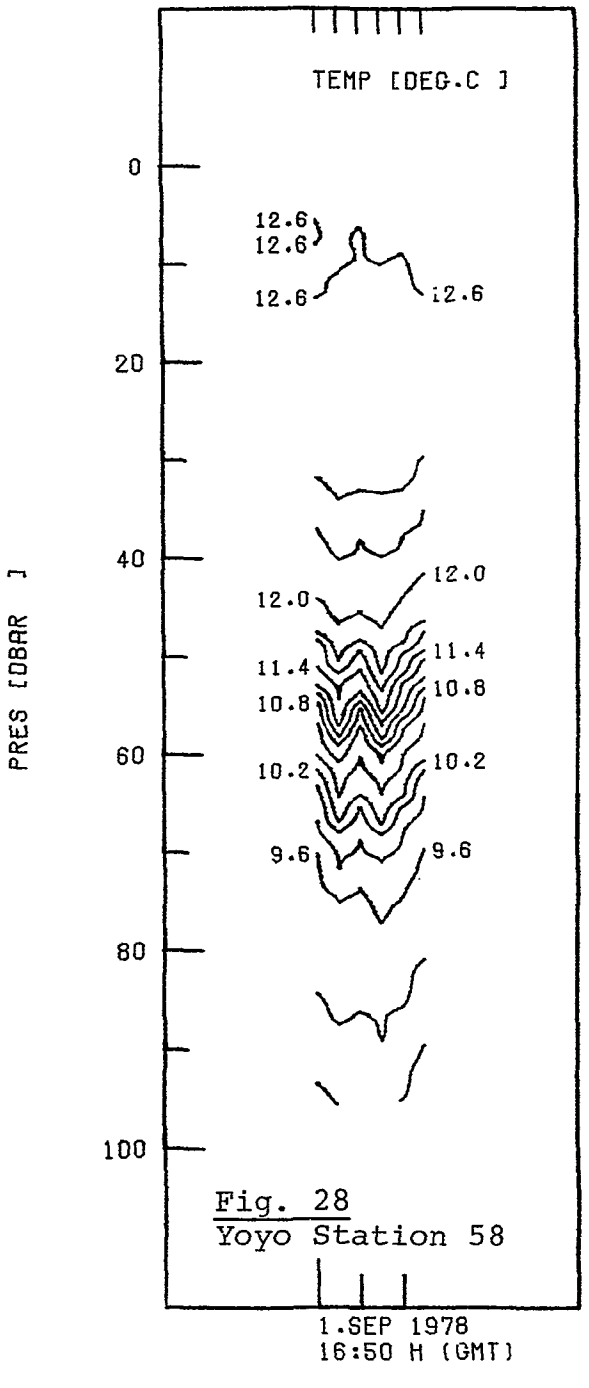

Fig. 28
Yoyo Station 58

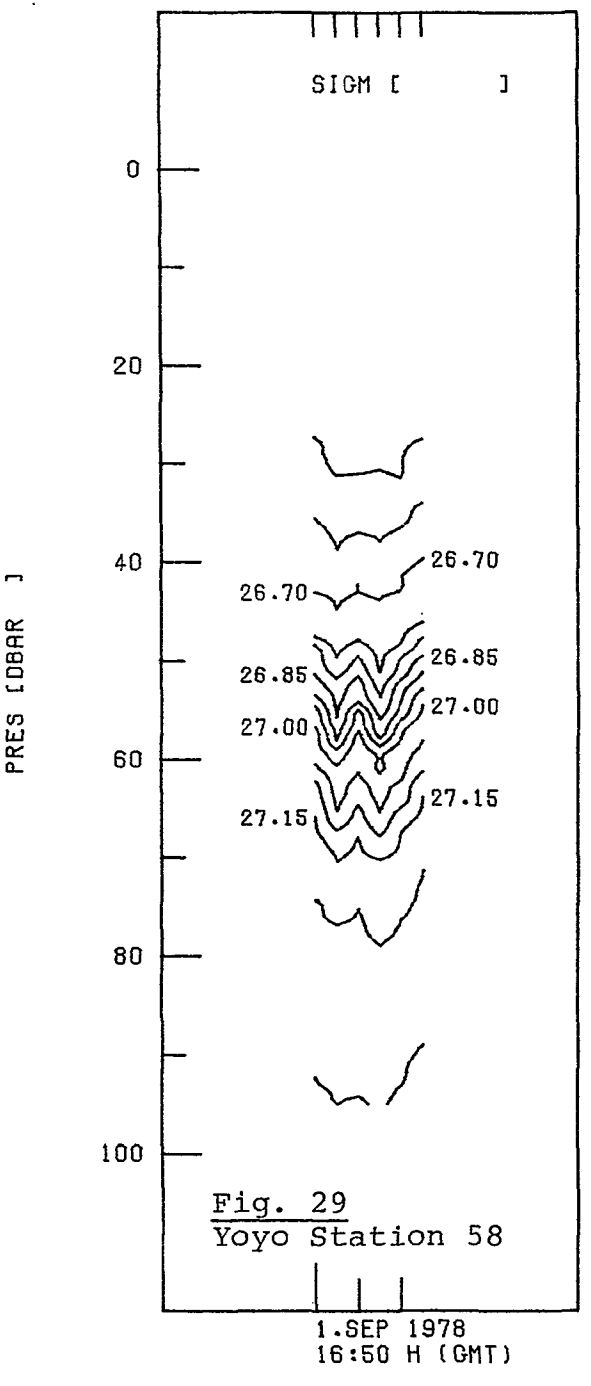

Fig. 29
Yoyo Station 58

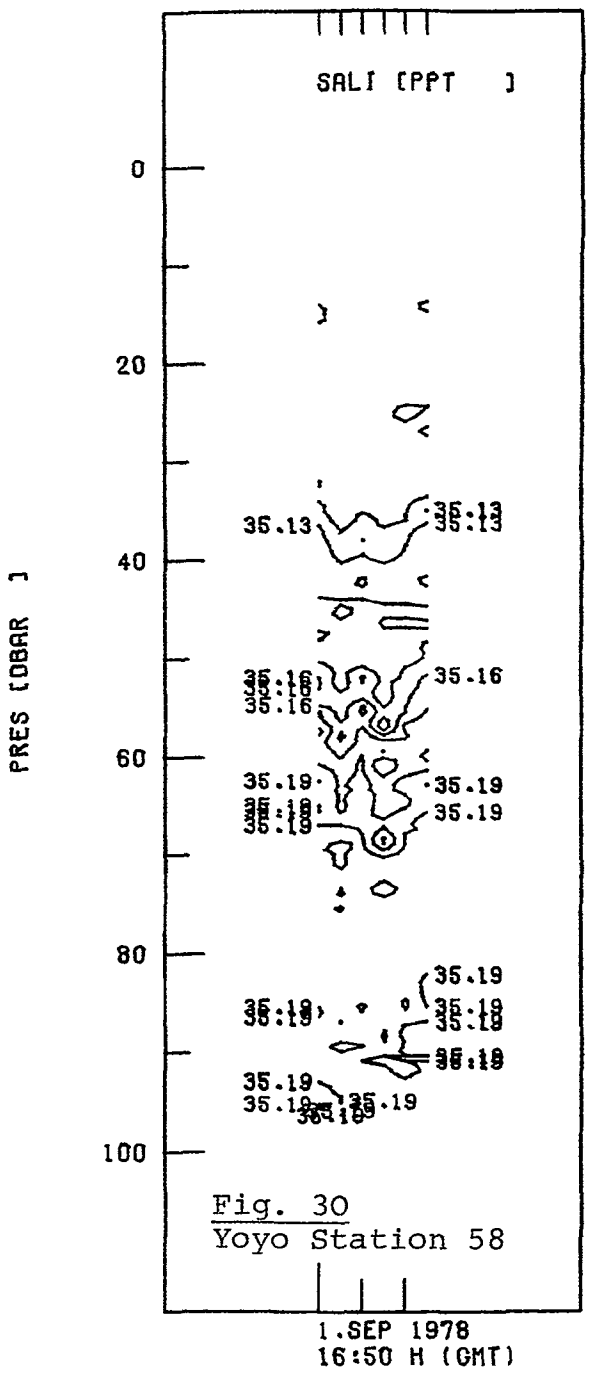

Fig. 30
Yoyo Station 58

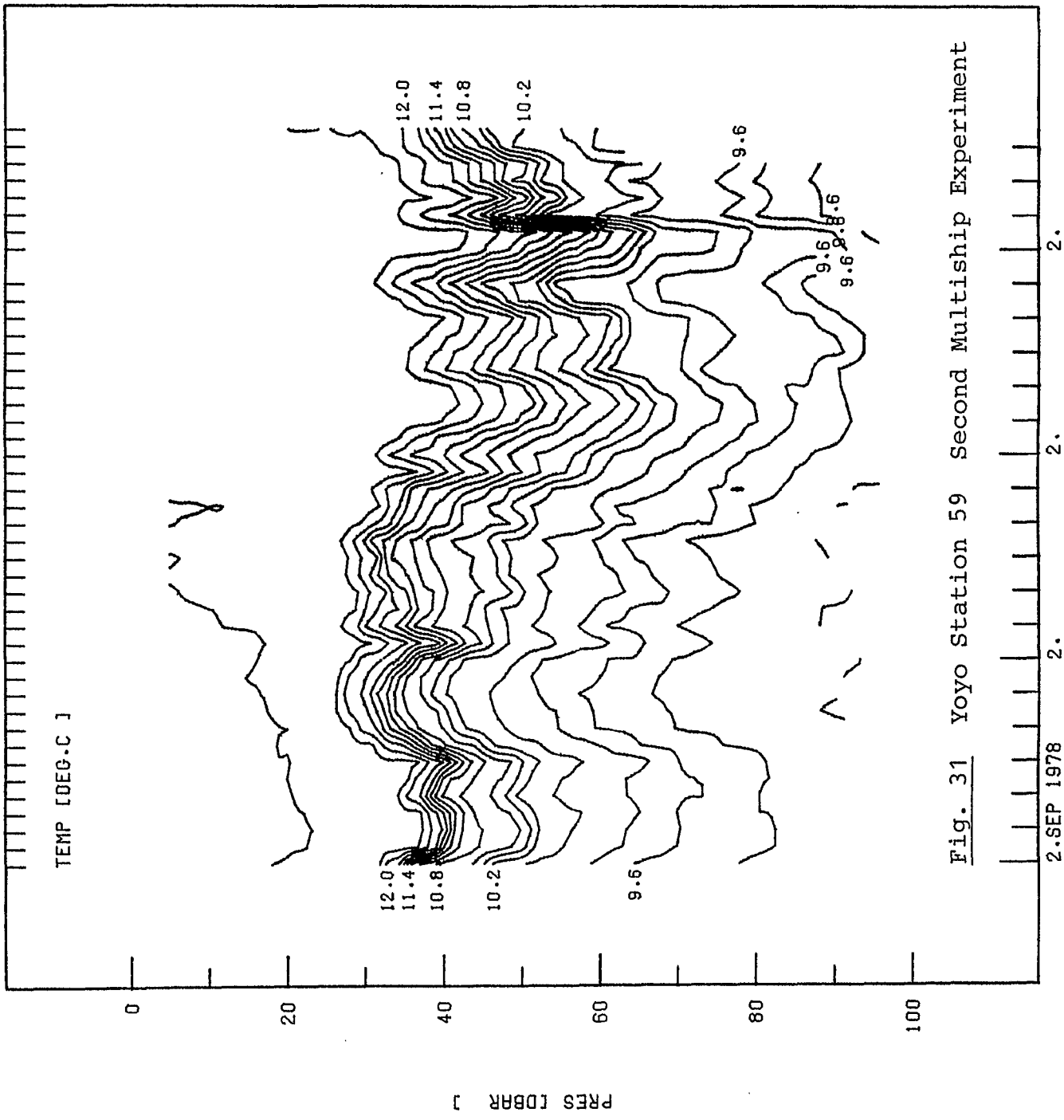

Fig. 31 Yoyo Station 59 Second Multiship Experiment

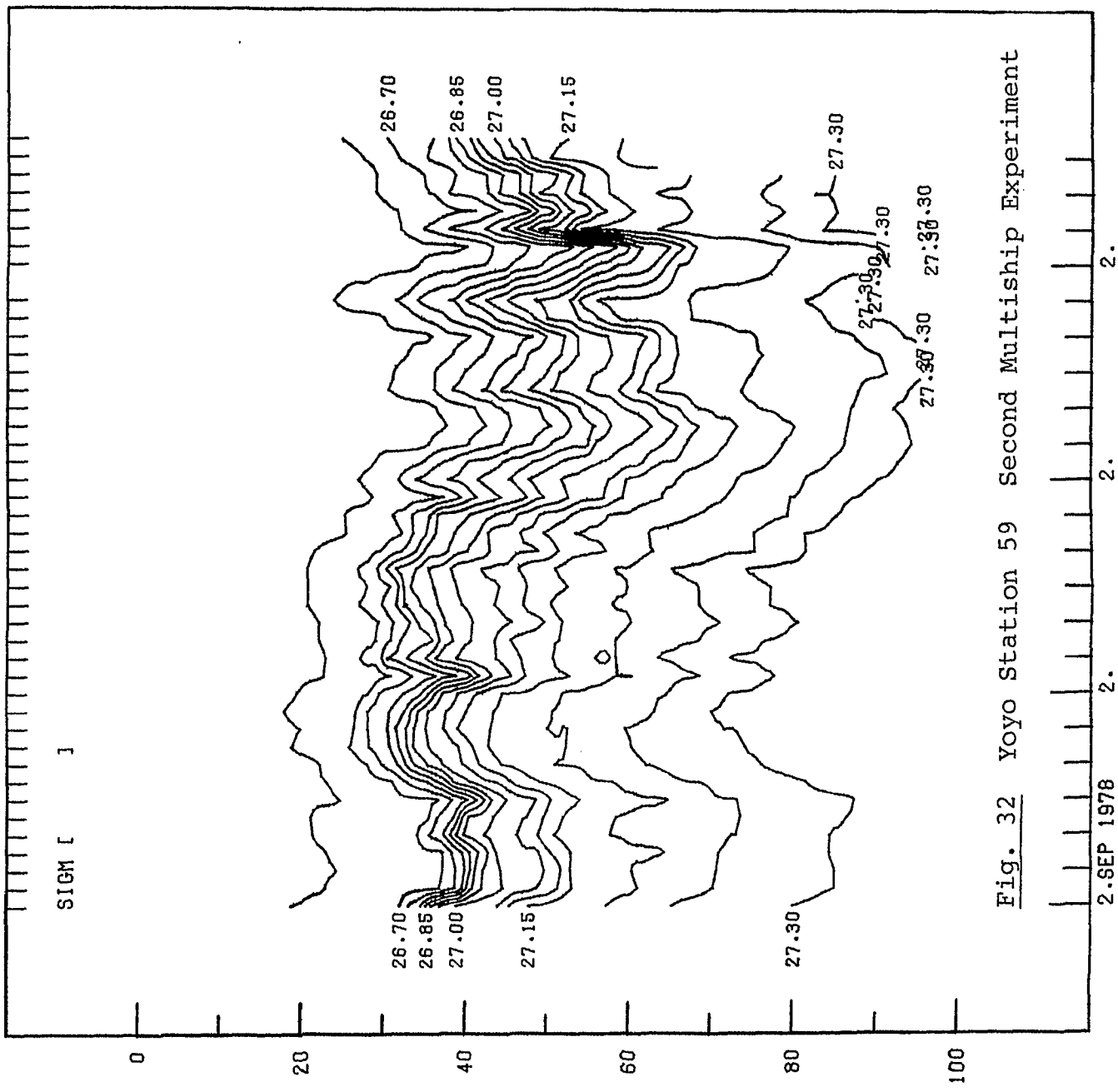

Fig. 32 Yoyo Station 59 Second Multiship Experiment

J301591125

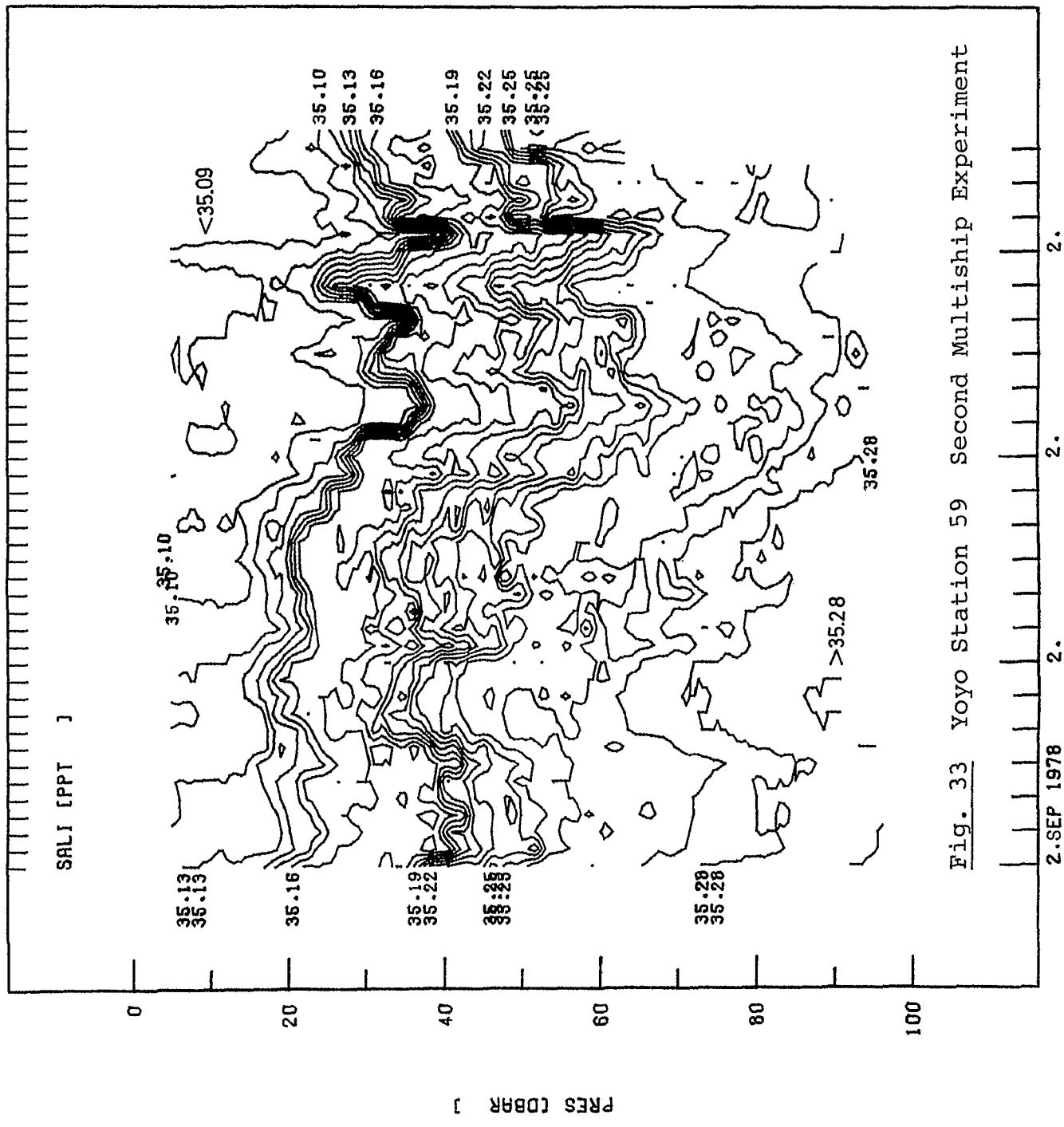

Fig. 33 Yoyo Station 59 Second Multiship Experiment

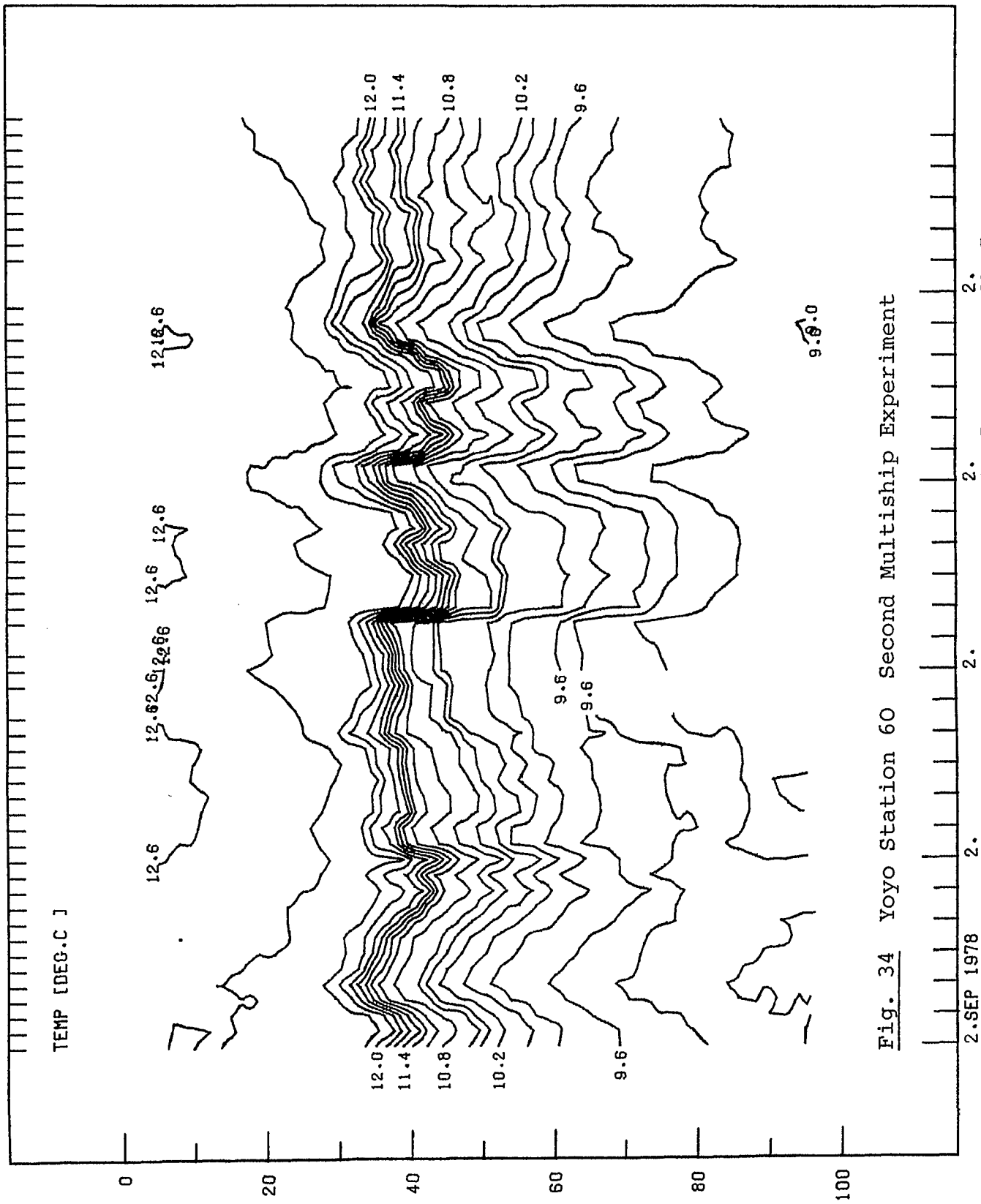

Fig. 34 Yoyo Station 60 Second Multiship Experiment

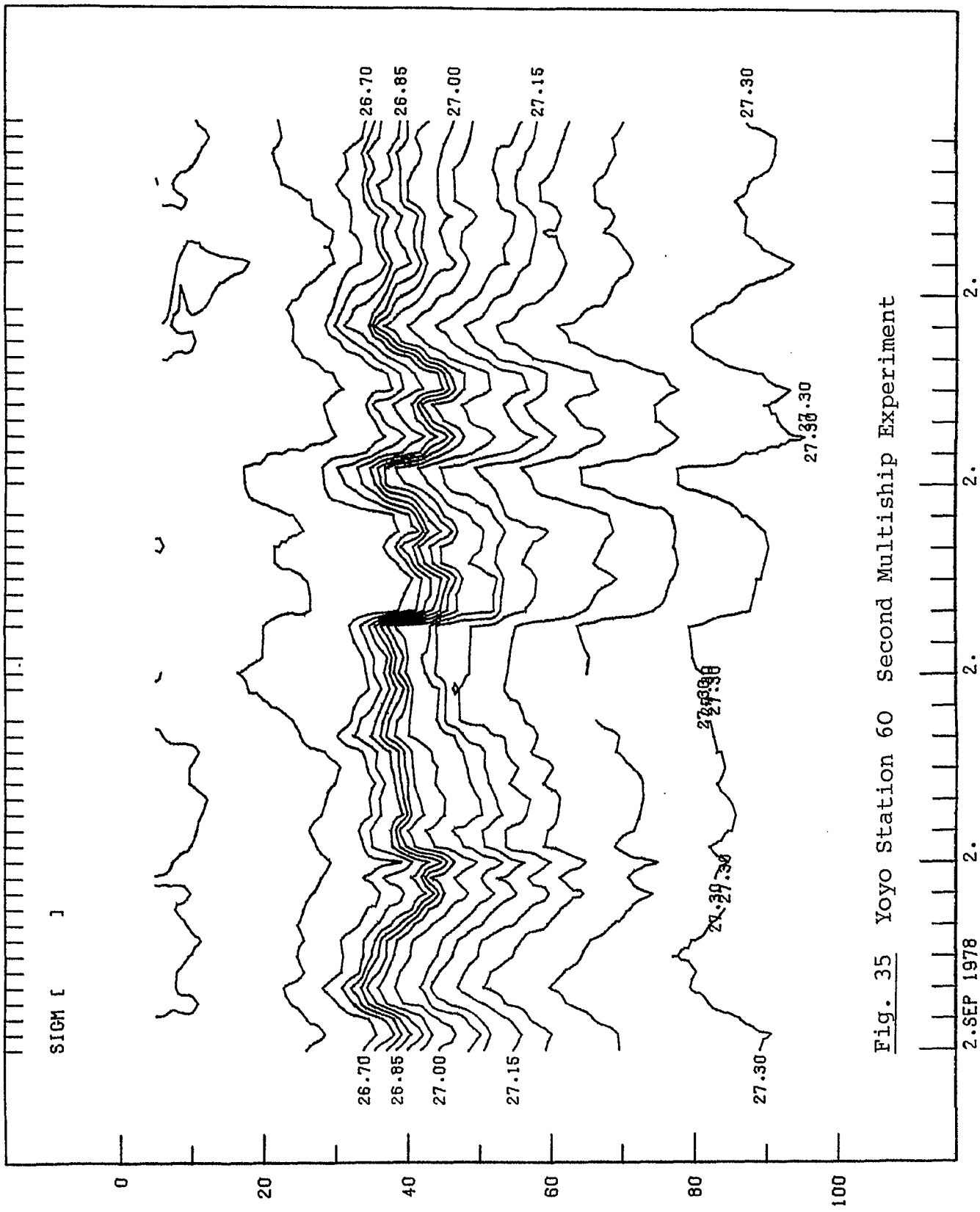

Fig. 35 Yoyo Station 60 Second Multiship Experiment

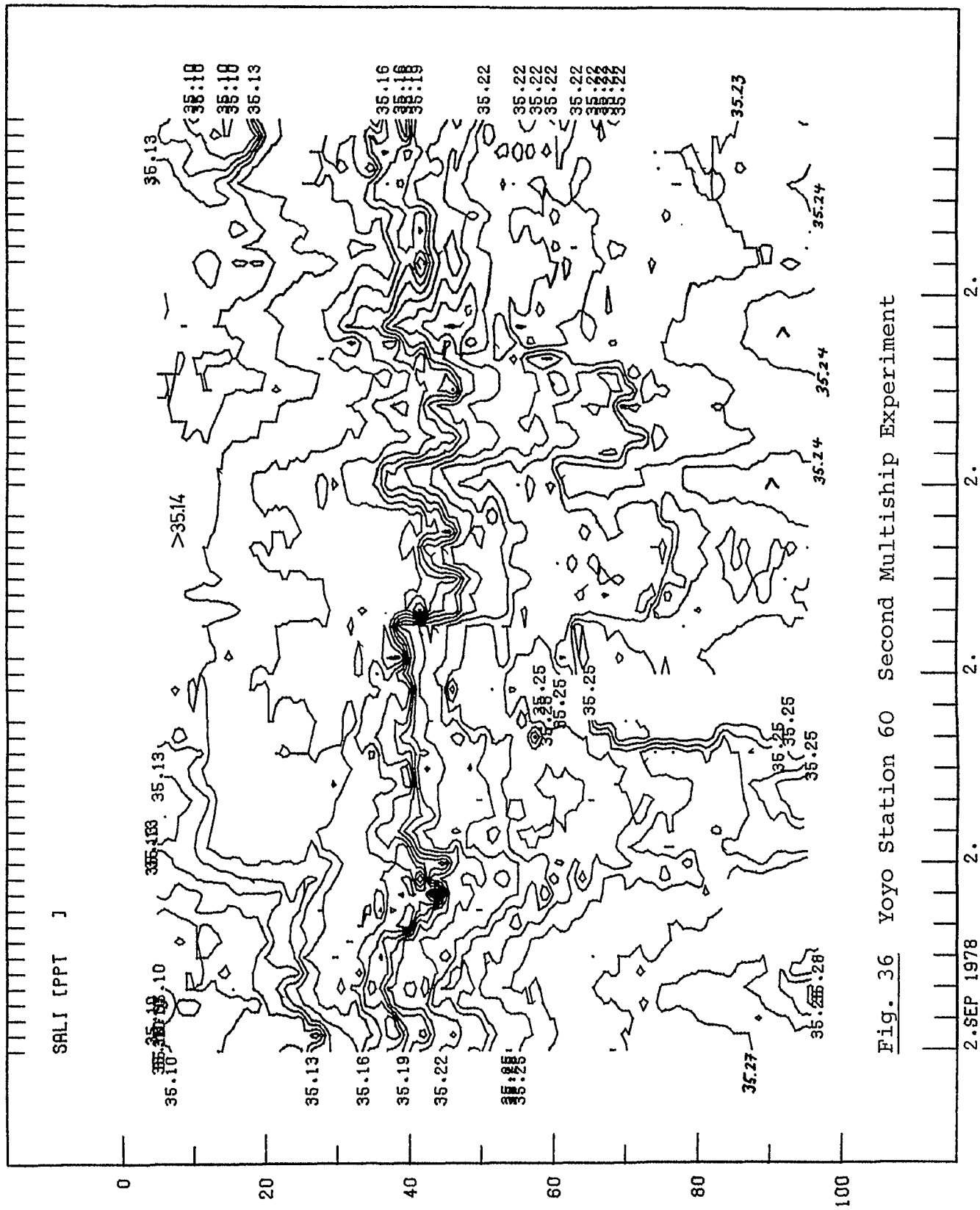

Fig. 36 Yoyo Station 60 Second Multiship Experiment

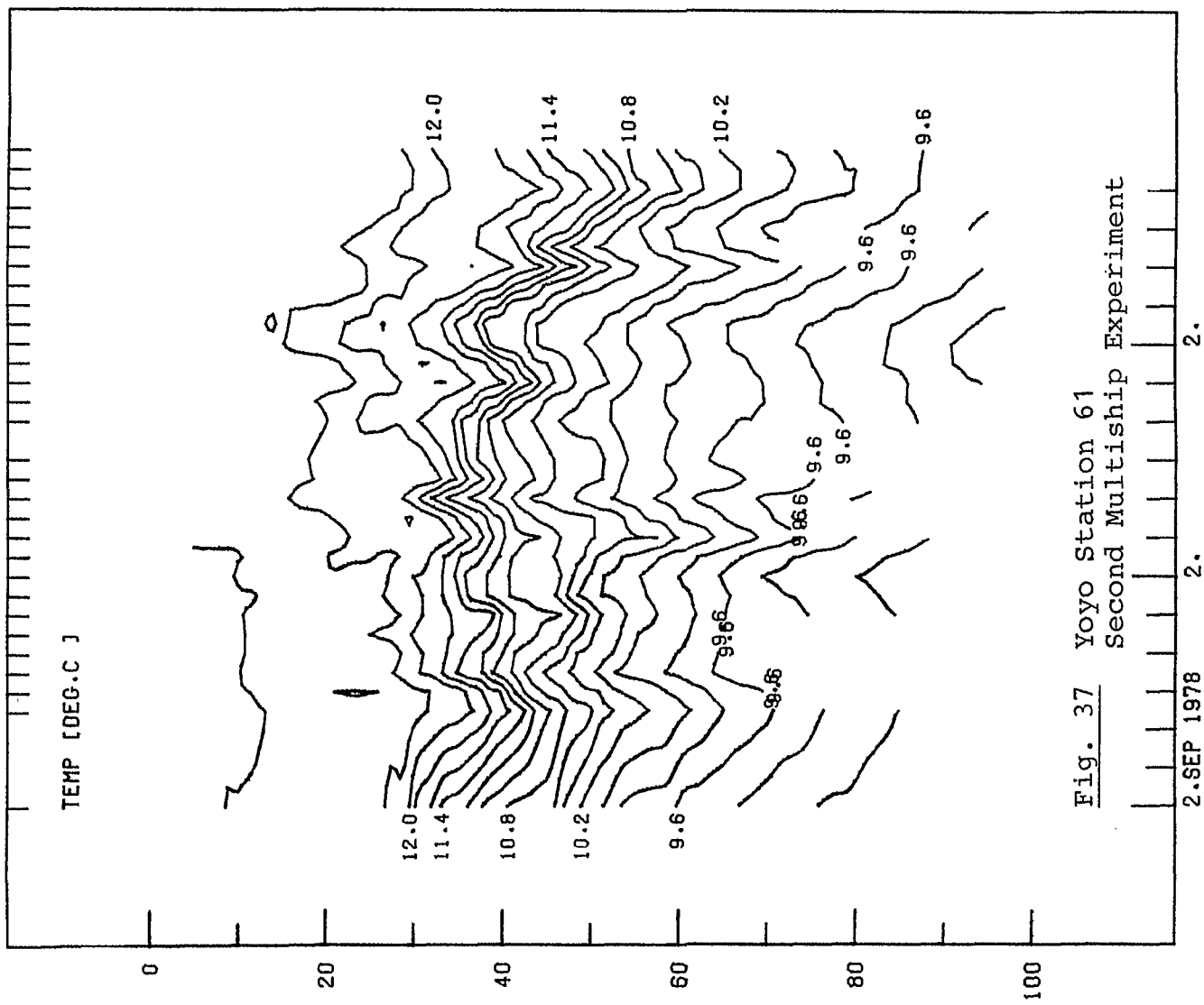

Fig. 37 Yoyo Station 61
Second Multiship Experiment

J301610000

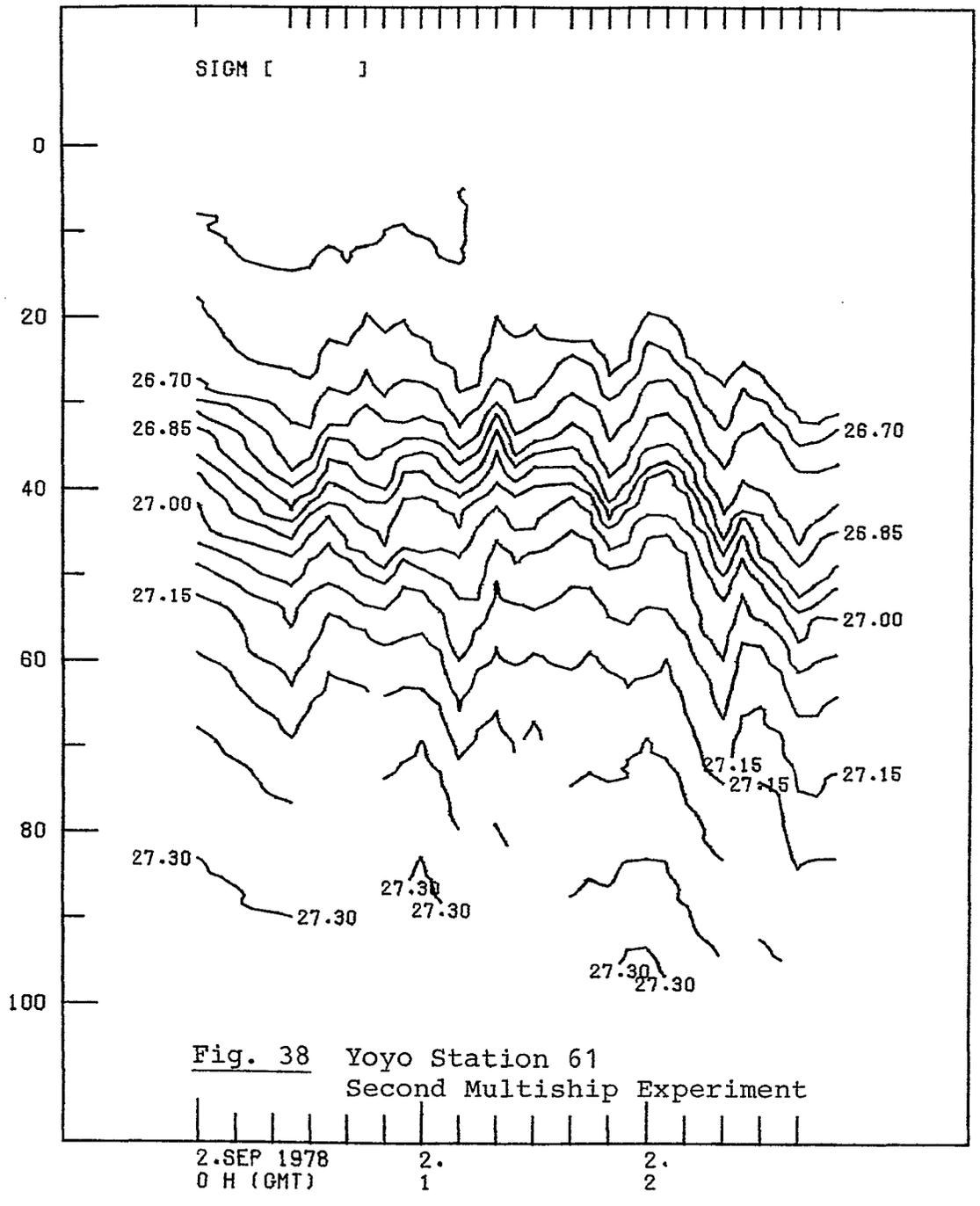

Fig. 38 Yoyo Station 61
Second Multiship Experiment

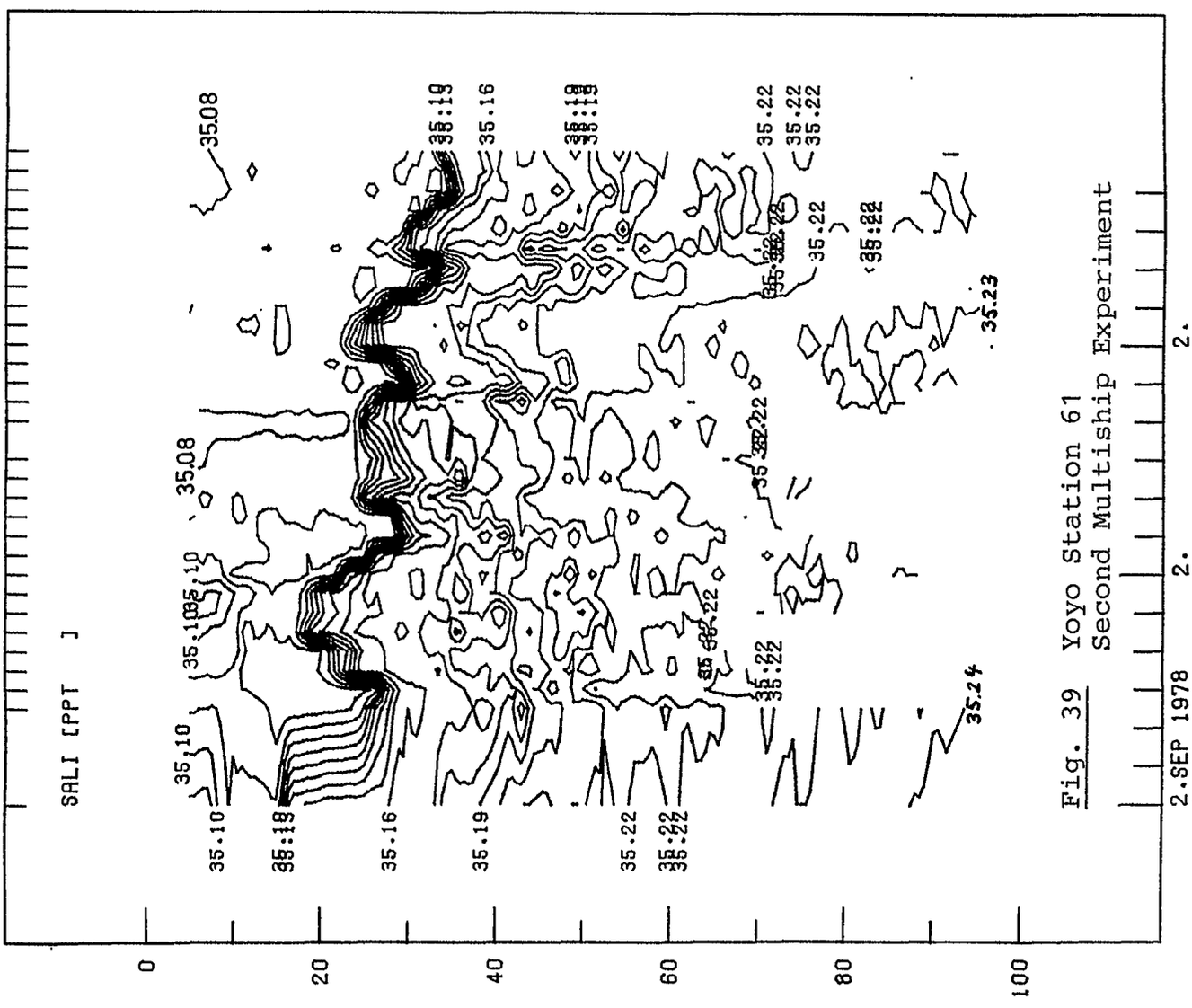

Fig. 39 Yoyo Station 61
Second Multiship Experiment

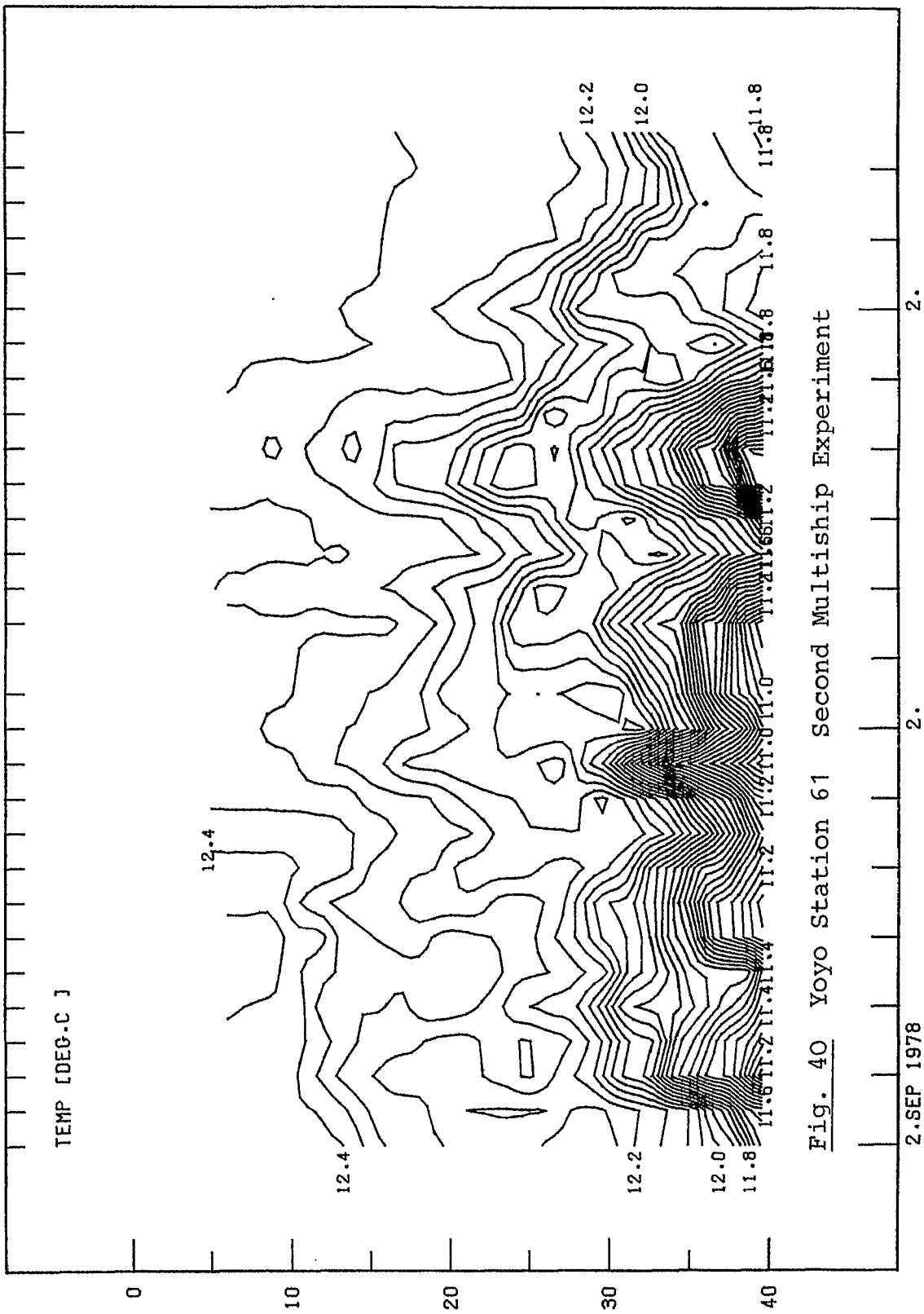

Fig. 40 Yoyo Station 61 Second Multiship Experiment

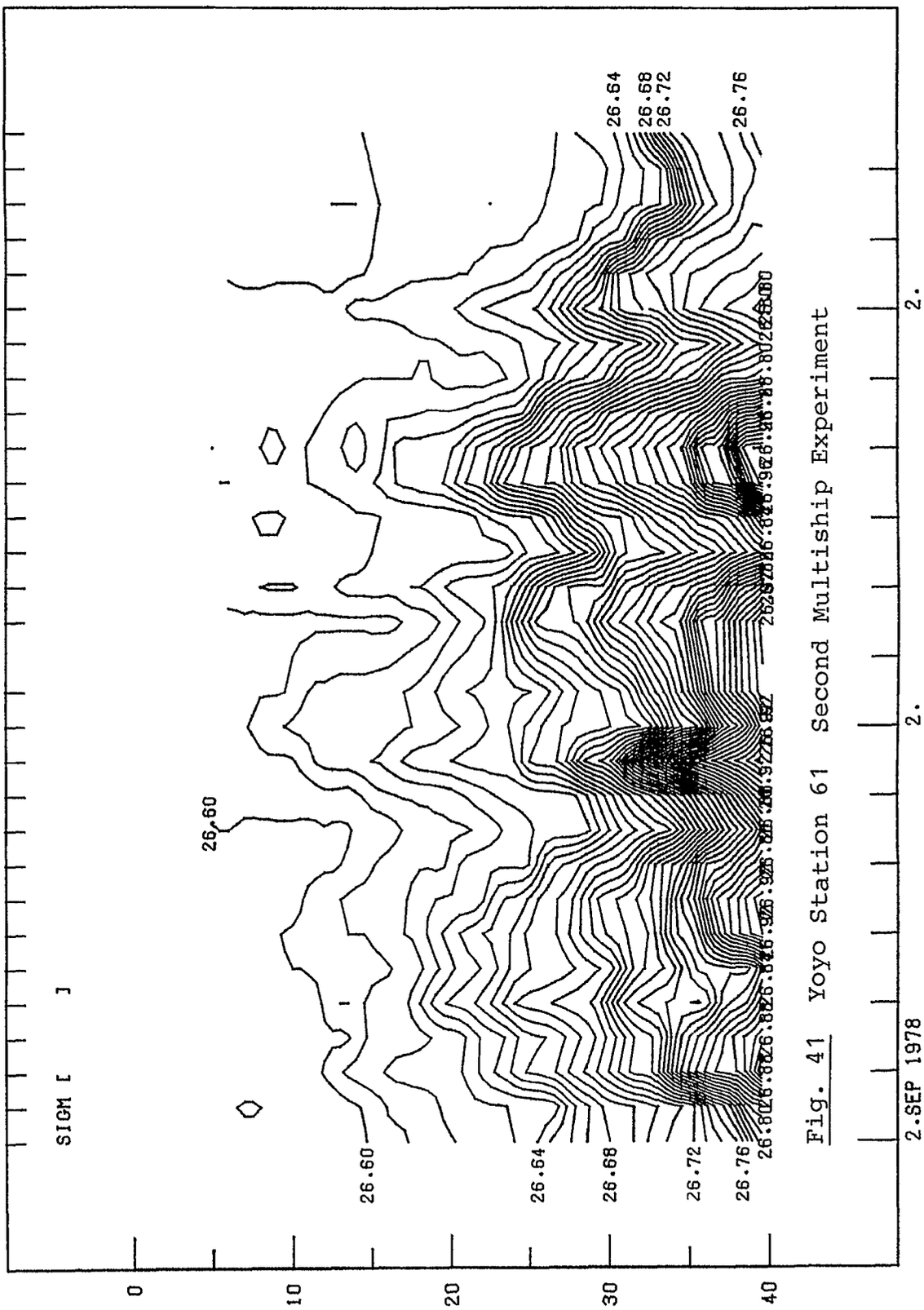

Fig. 41 Yoyo Station 61 Second Multiship Experiment

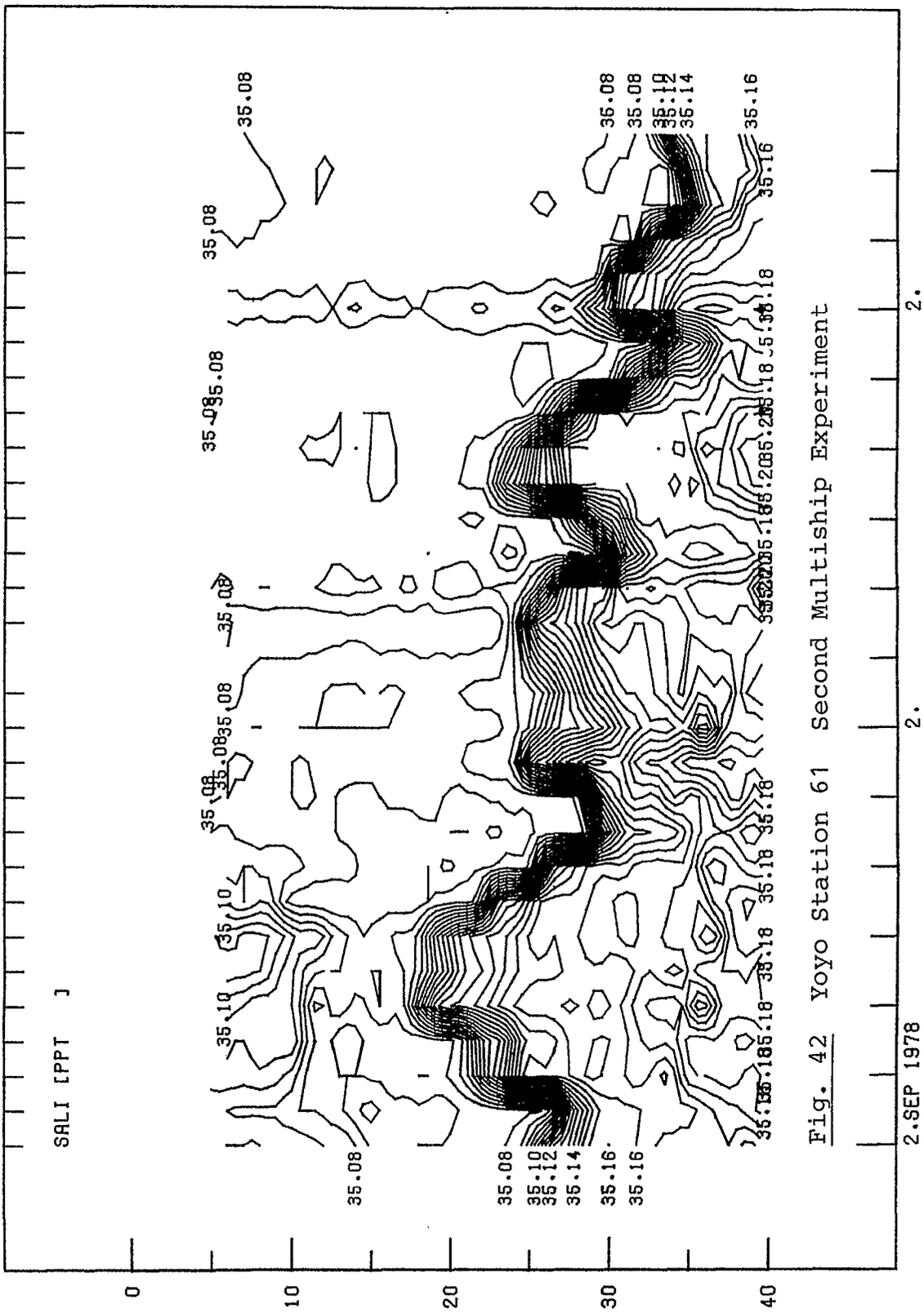

Fig. 42 Yoyo Station 61 Second Multiship Experiment

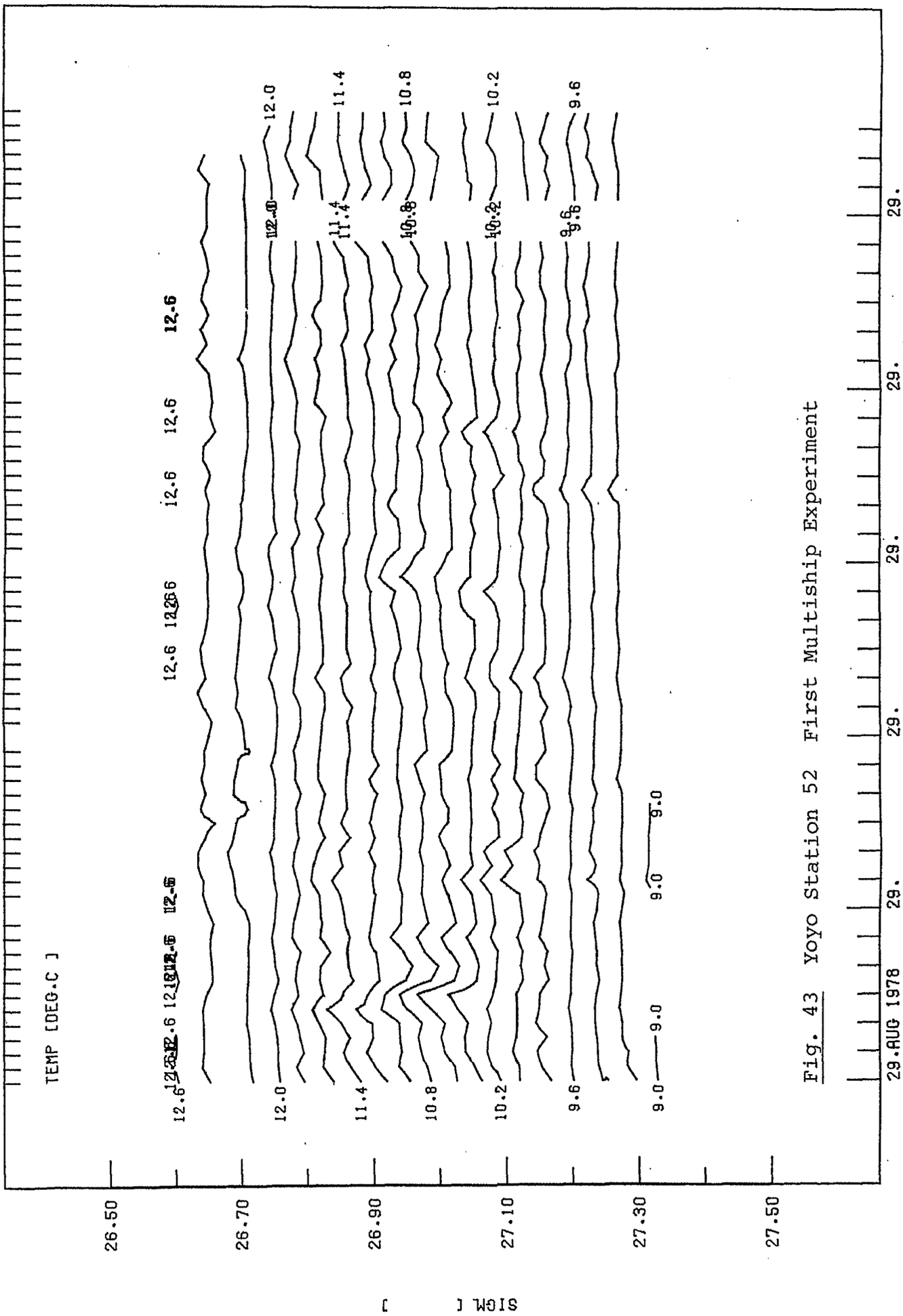

Fig. 43 Yoyo Station 52 First Multiship Experiment

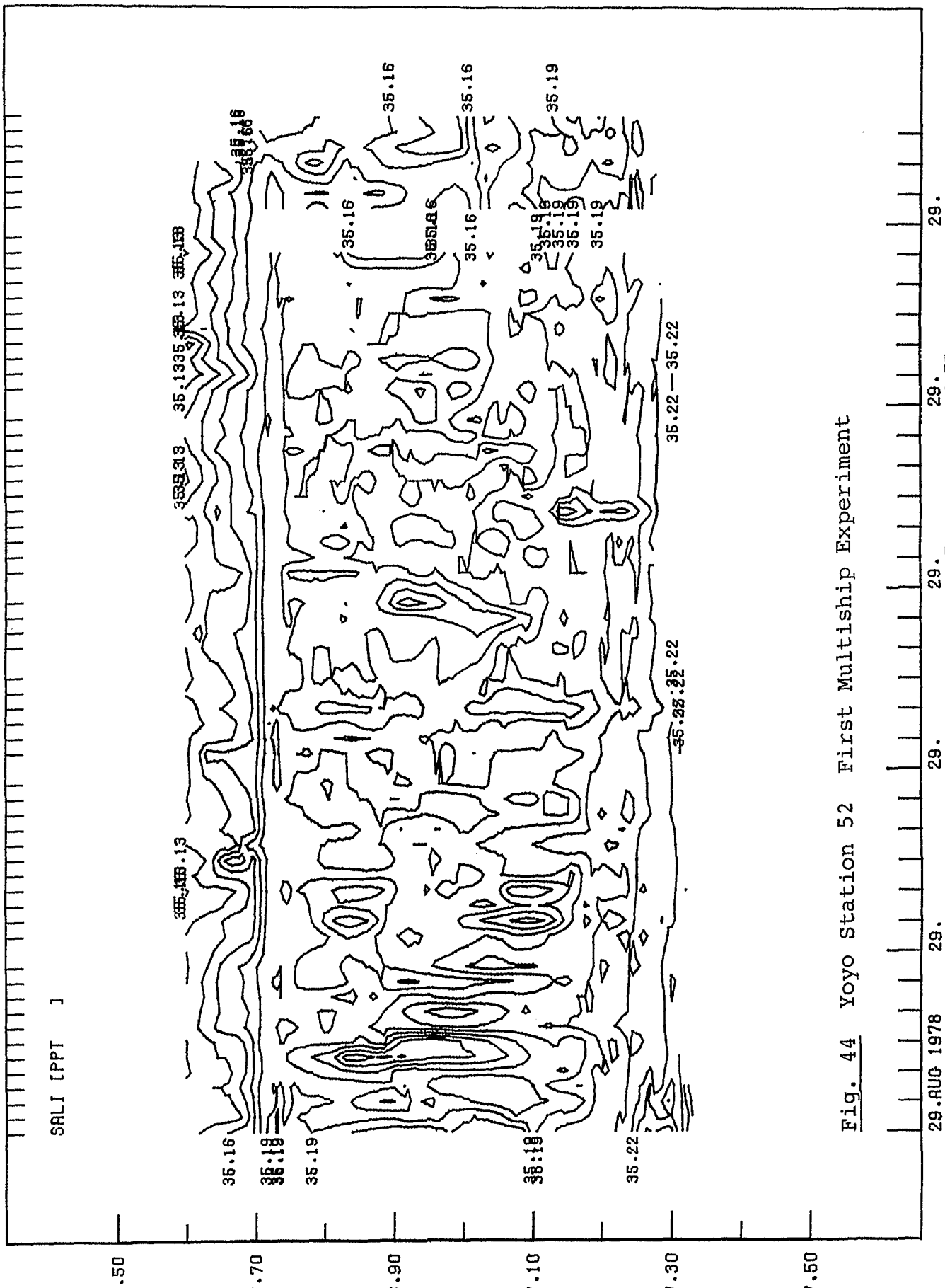

Fig. 44 Yoyo Station 52 First Multiship Experiment

J300521155

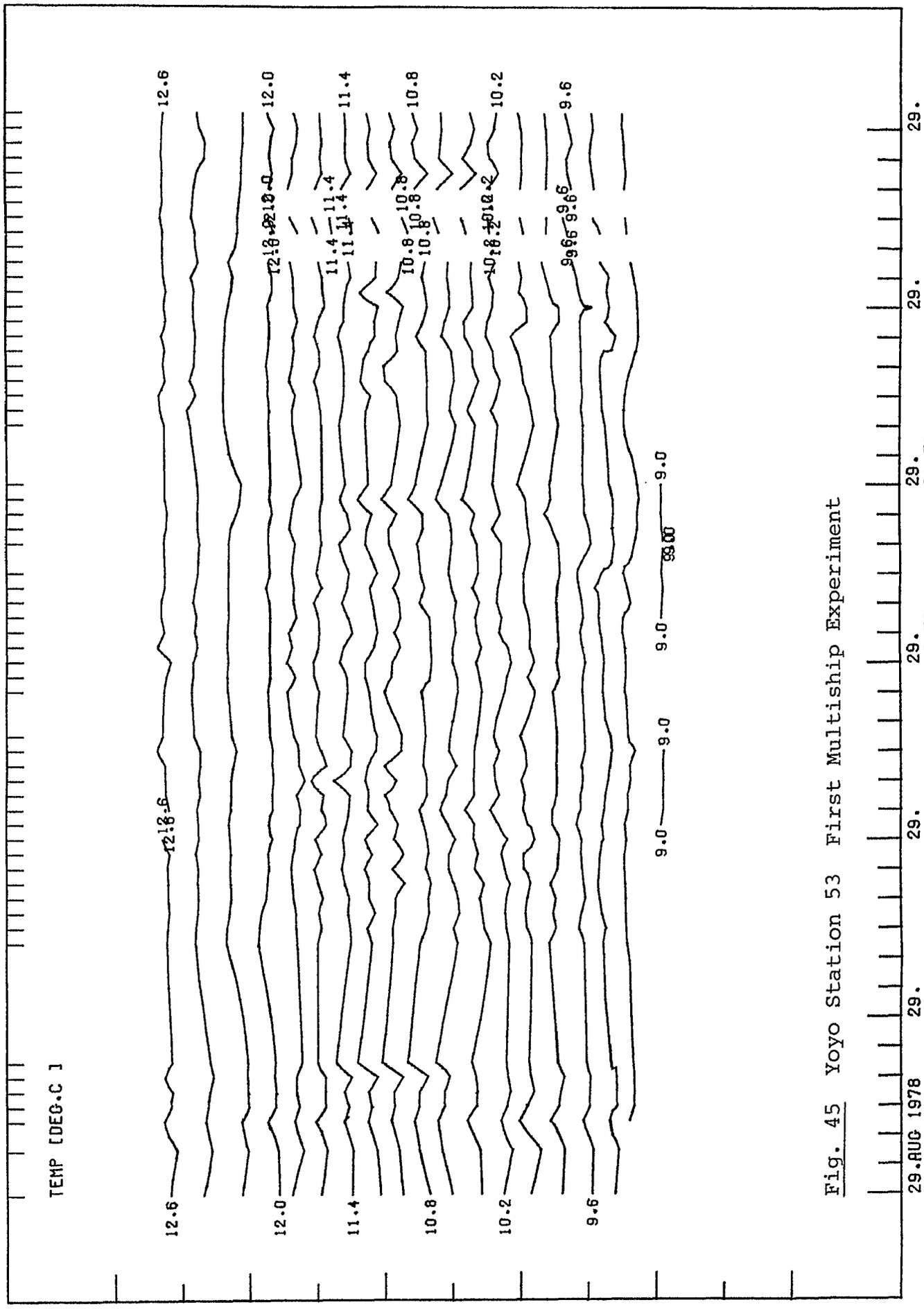

Fig. 45 Yoyo Station 53 First Multiship Experiment

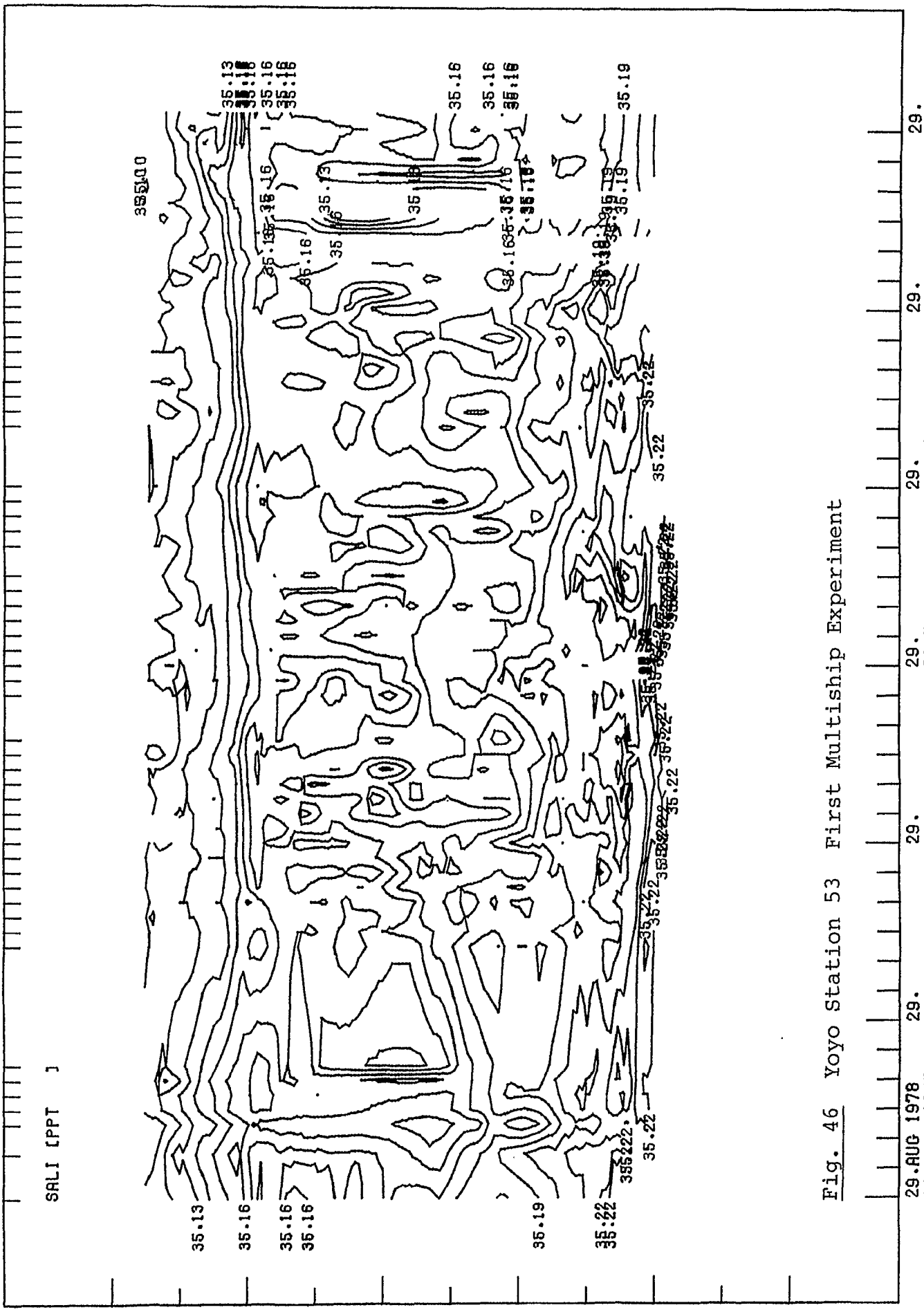

Fig. 46 Yoyo Station 53 First Multiship Experiment

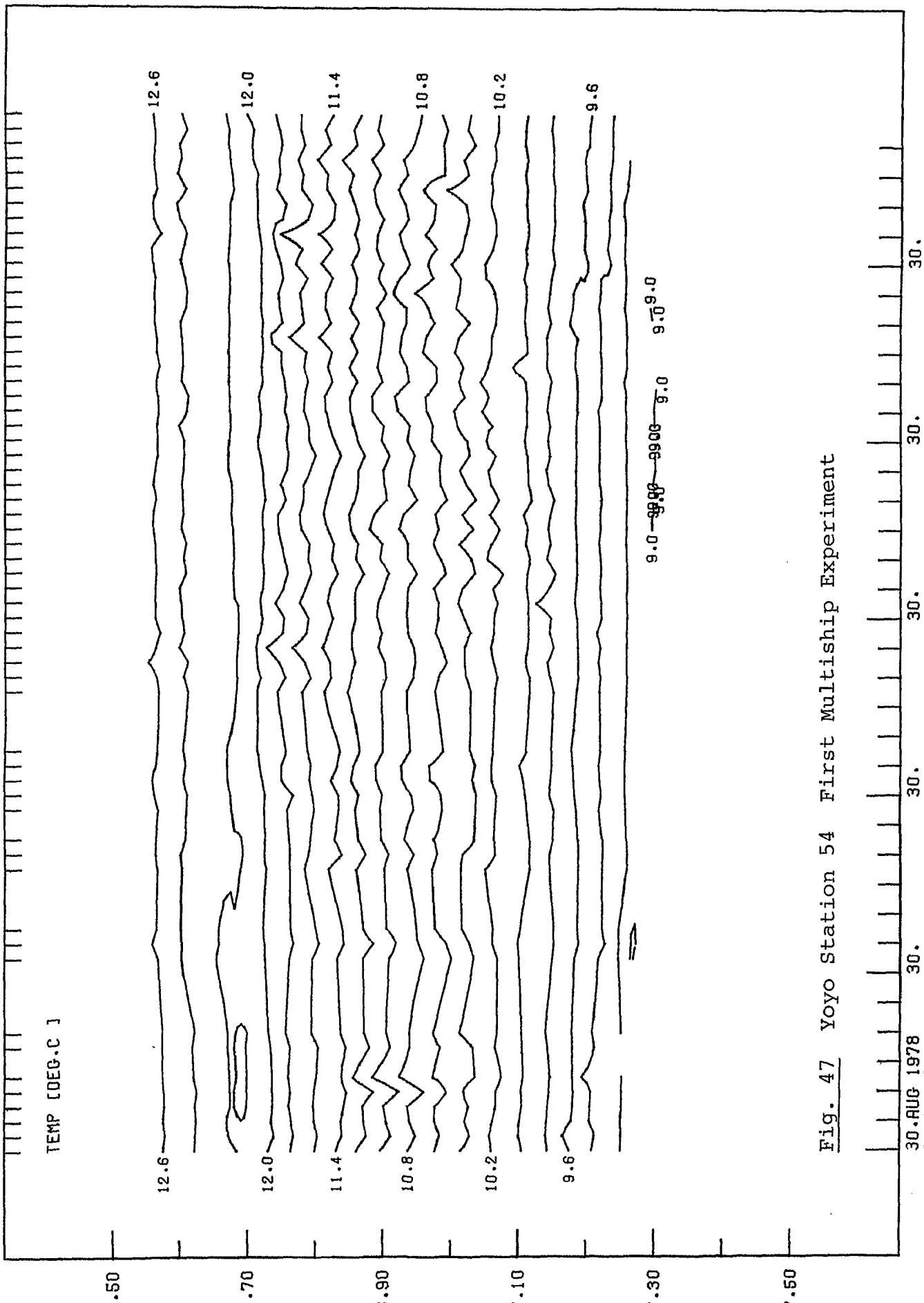

Fig. 47 Yoyo Station 54 First Multiship Experiment

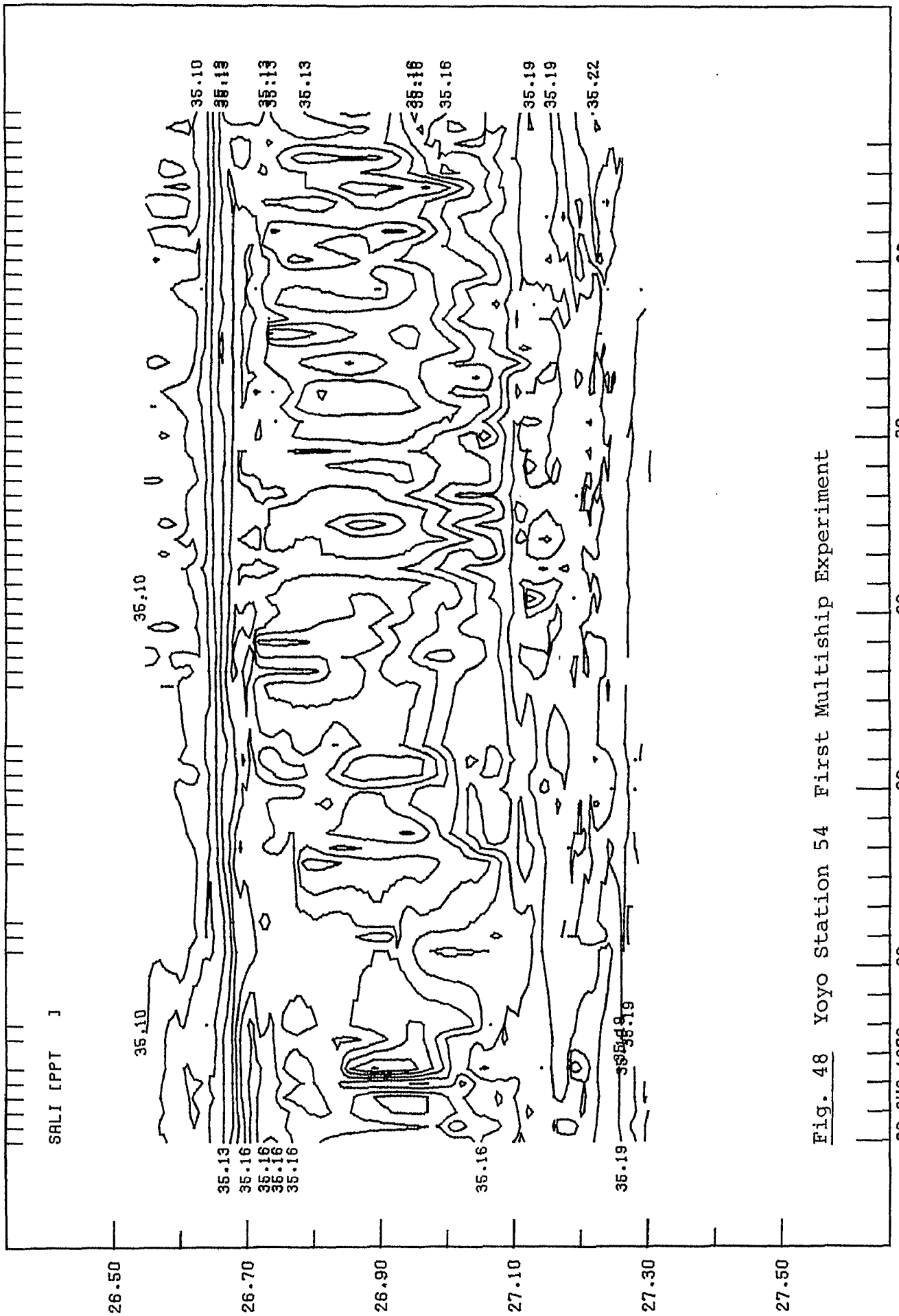

Fig. 48 Yoyo Station 54 First Multiship Experiment

J30D540010

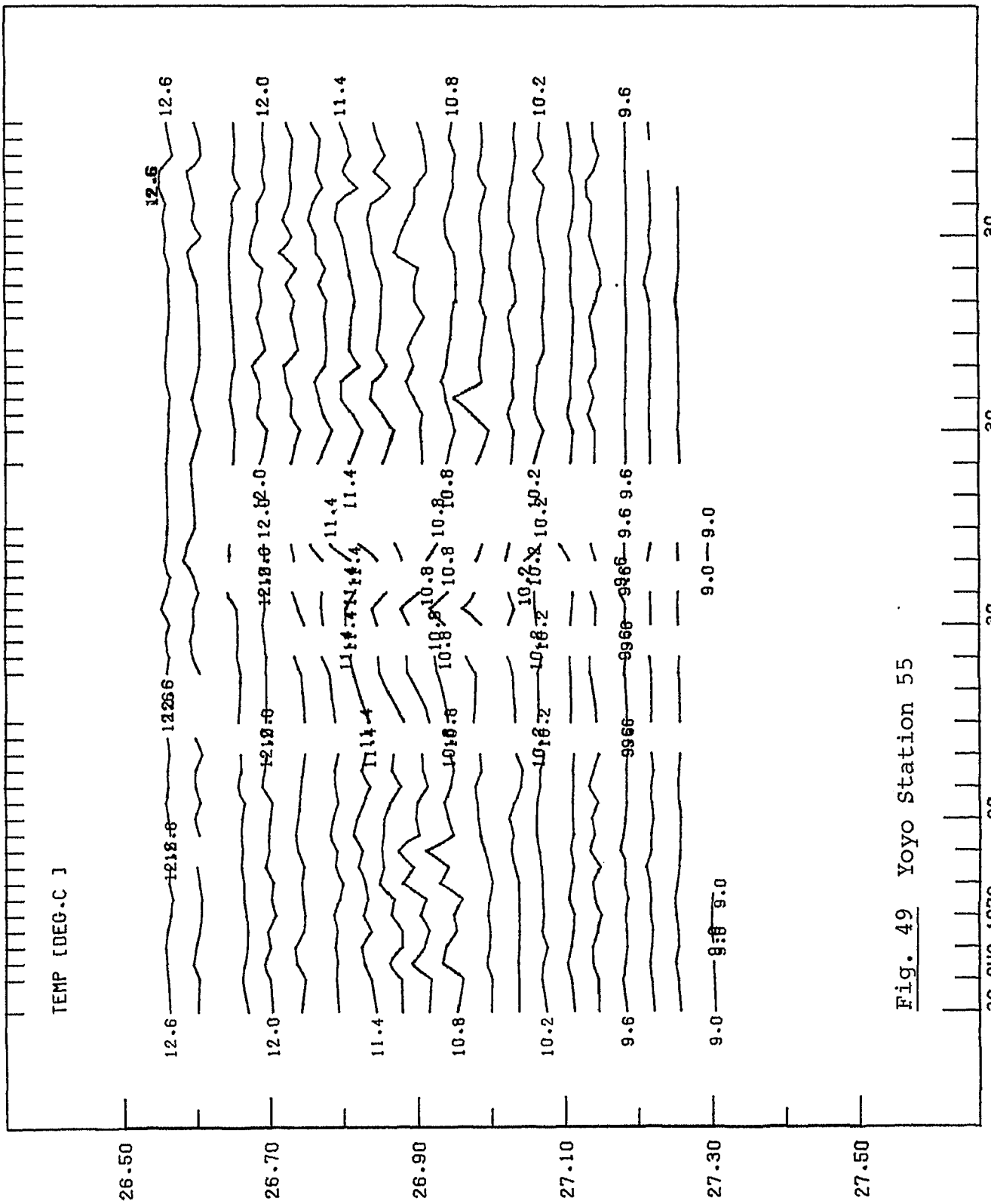

Fig. 49 Yoyo Station 55

J300550950

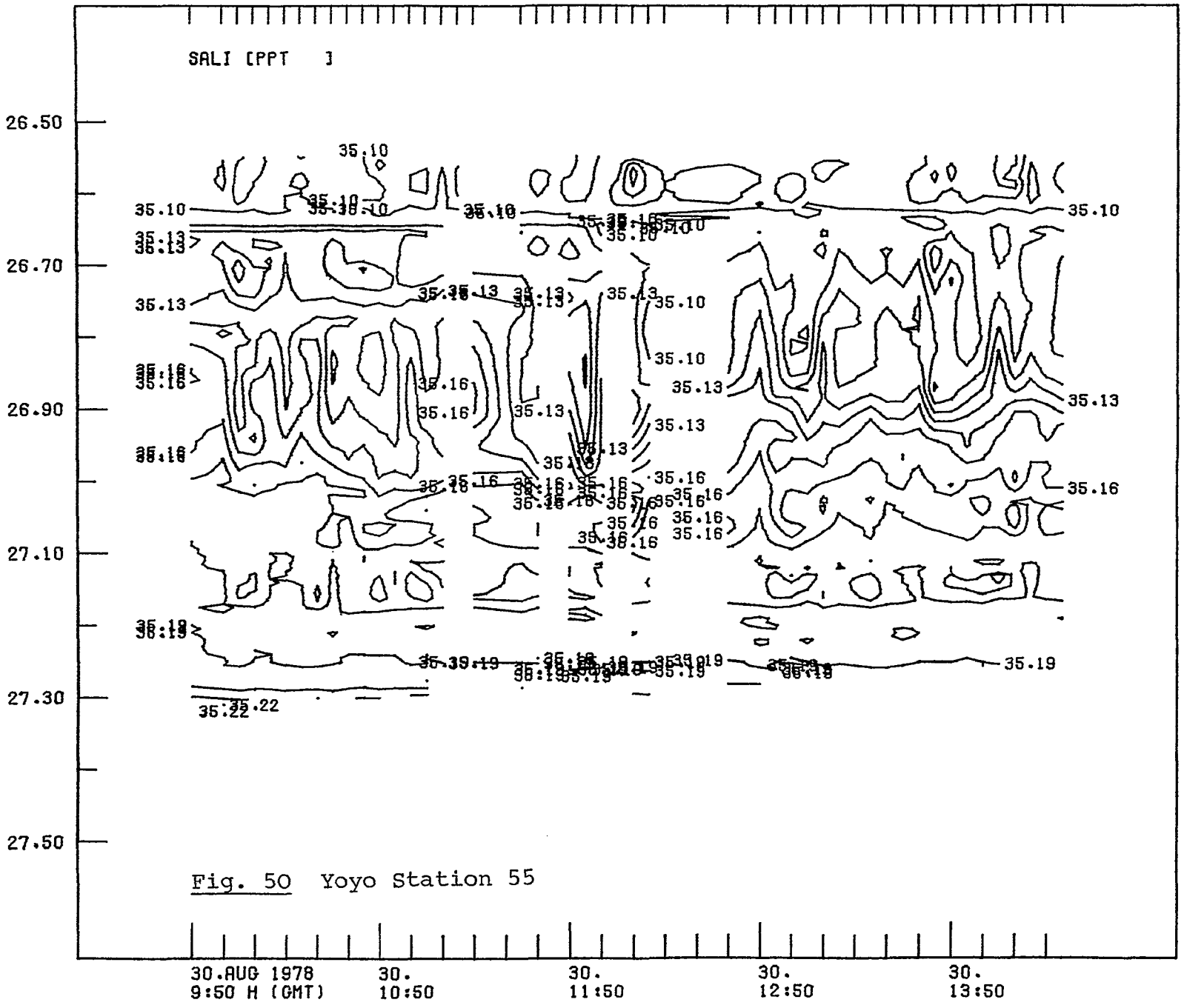

Fig. 50 Yoyo Station 55

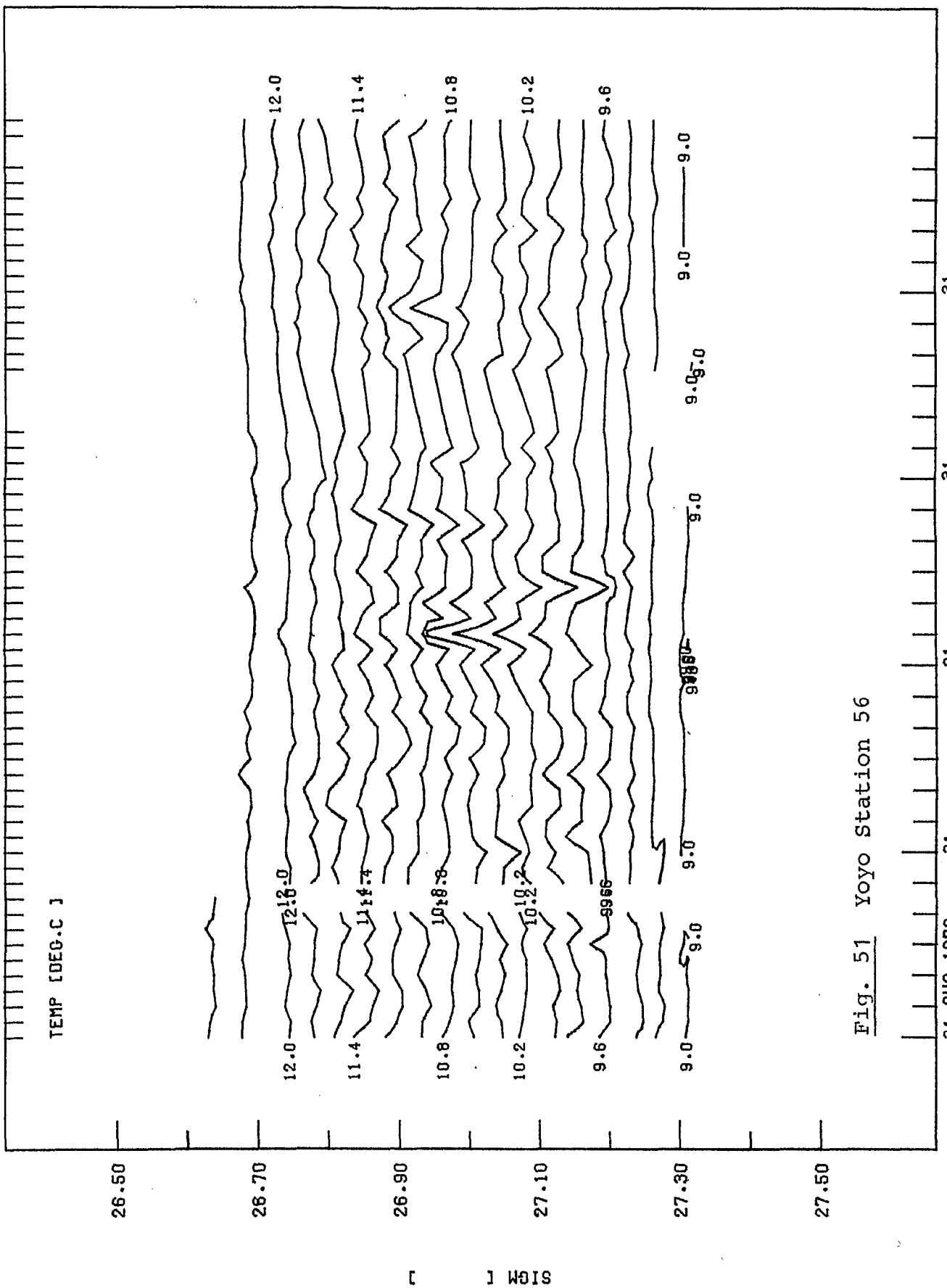

Fig. 51 Yoyo Station 56

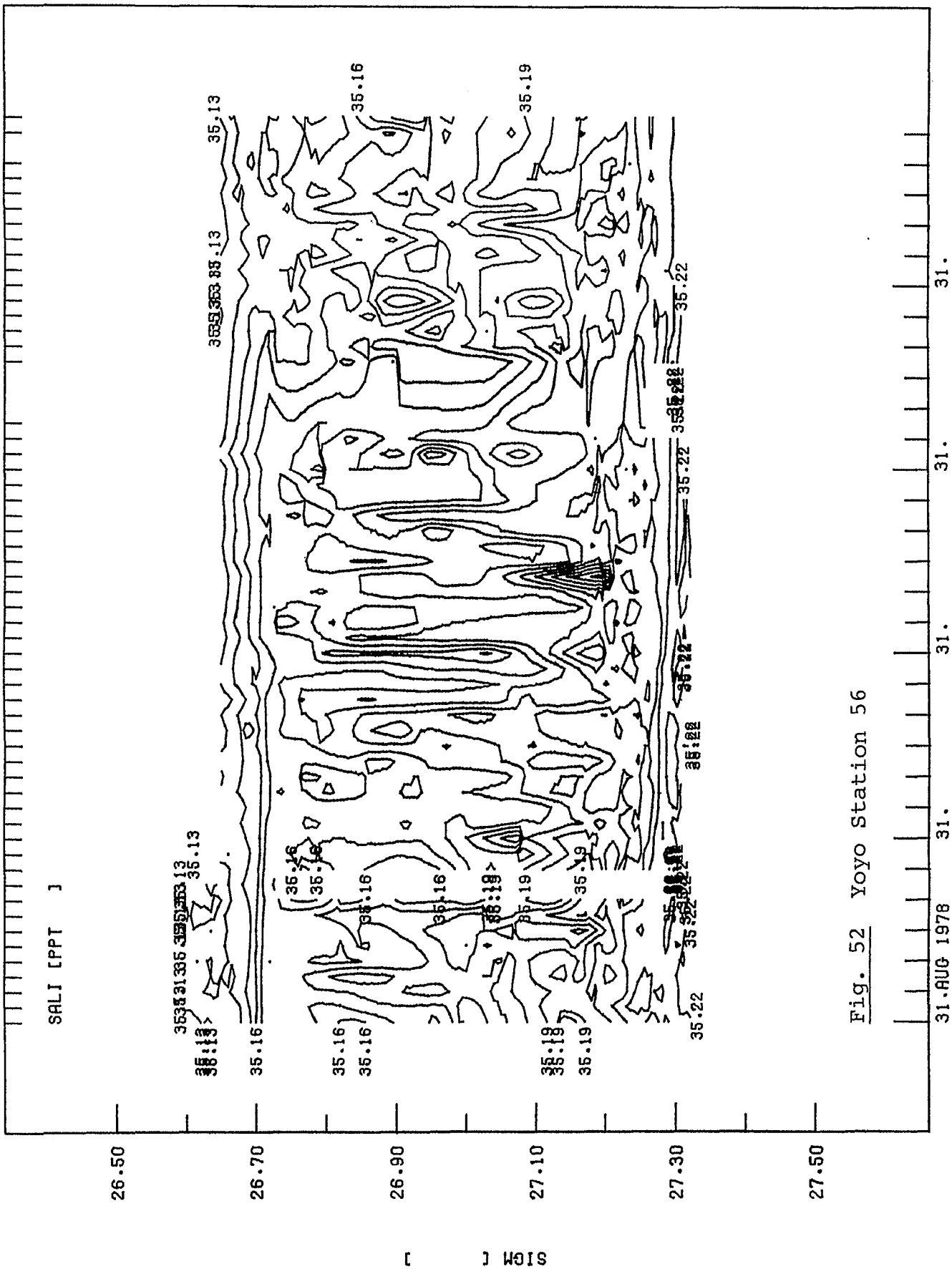

Fig. 52 Yoyo Station 56

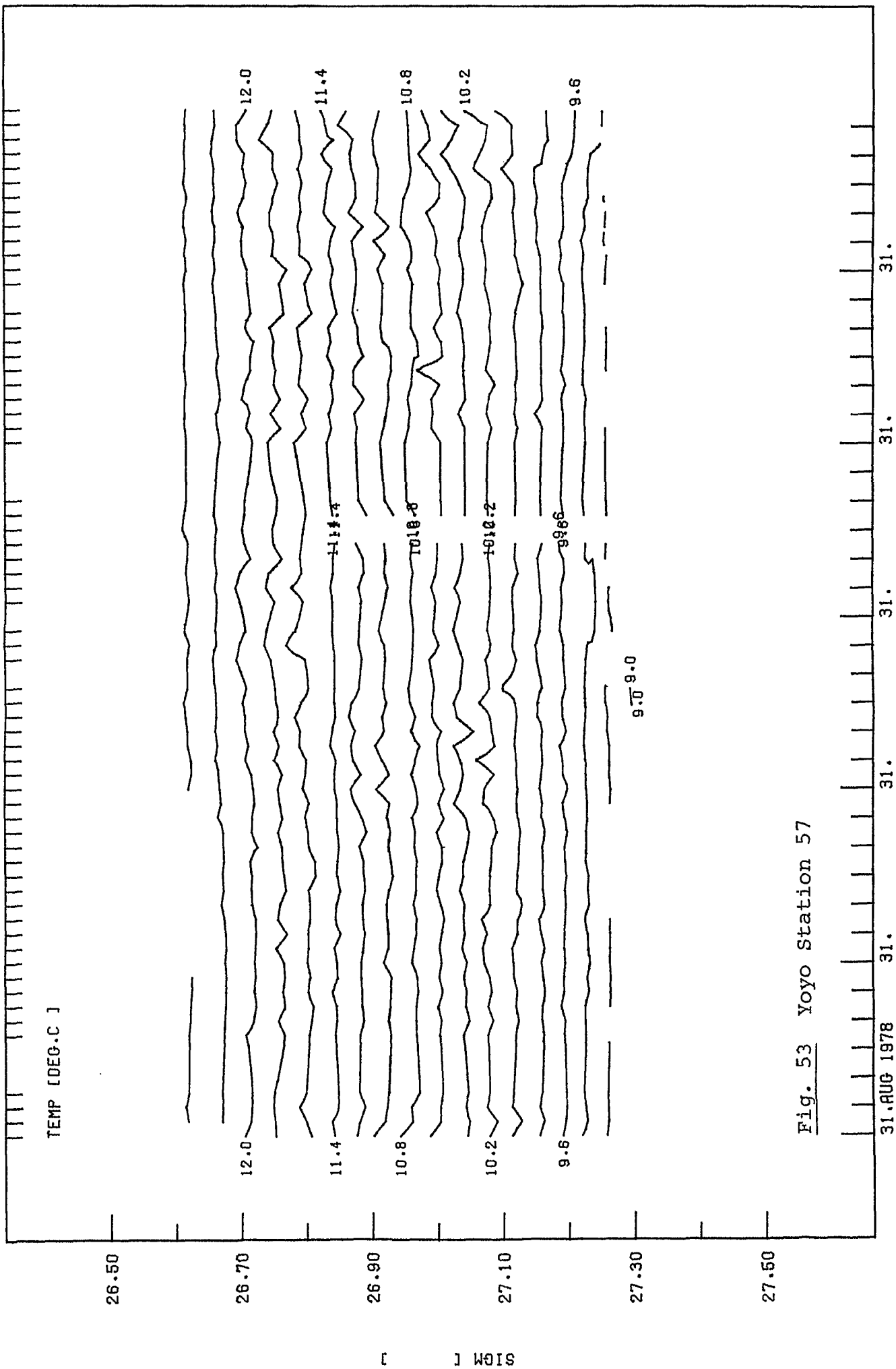

Fig. 53 Yoyo Station 57

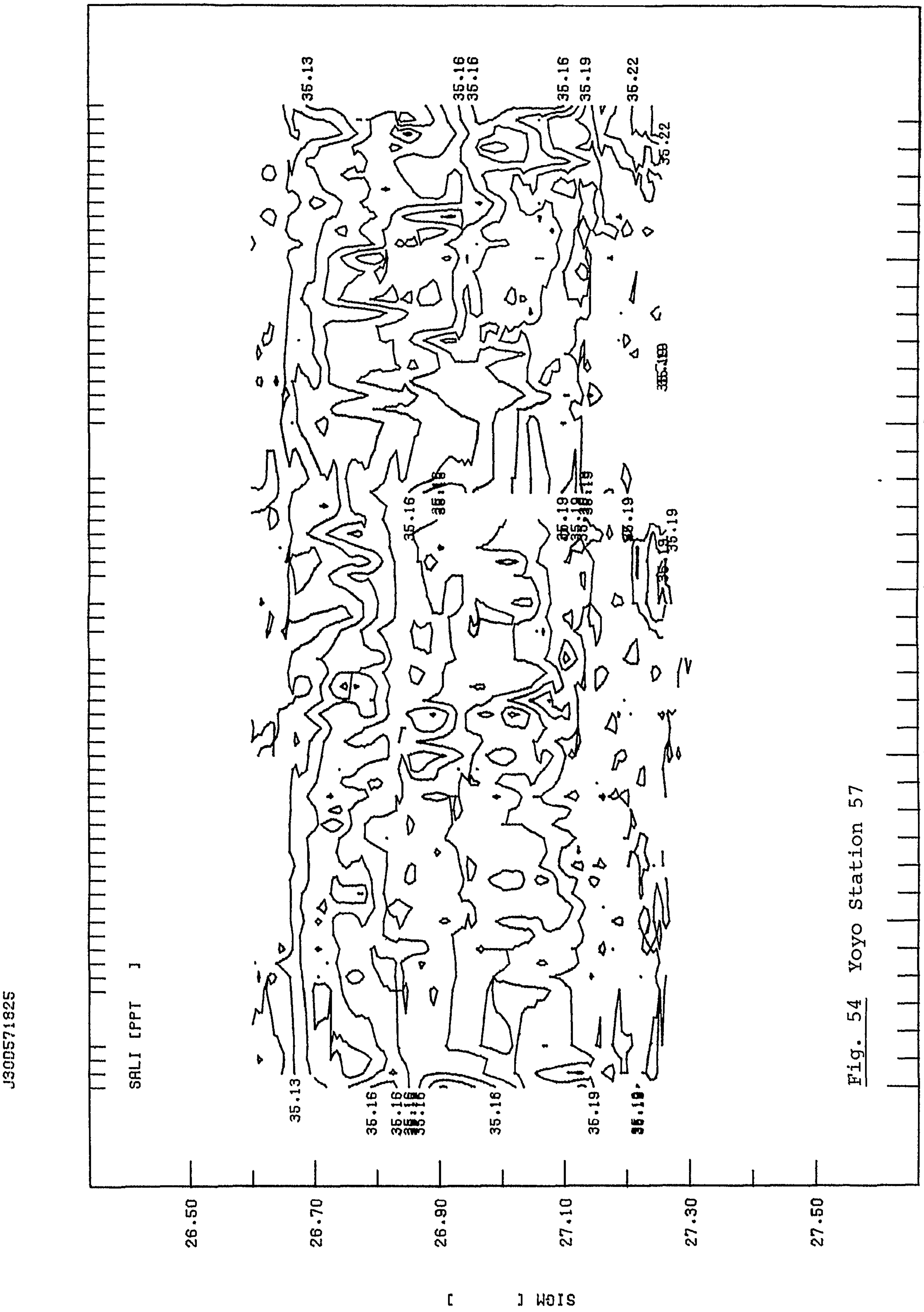

Fig. 54 Yoyo Station 57

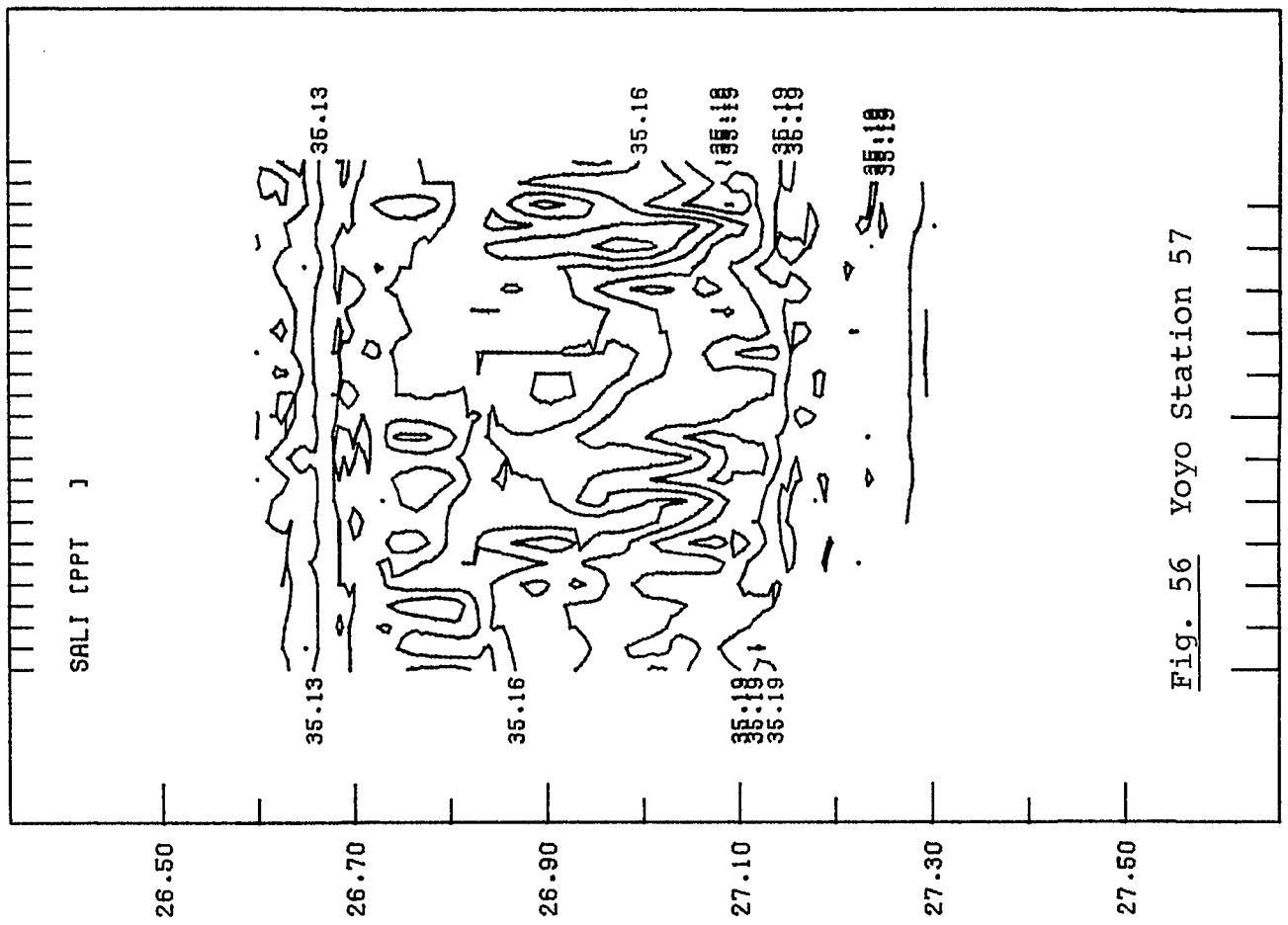

Fig. 56 Yoyo Station 57

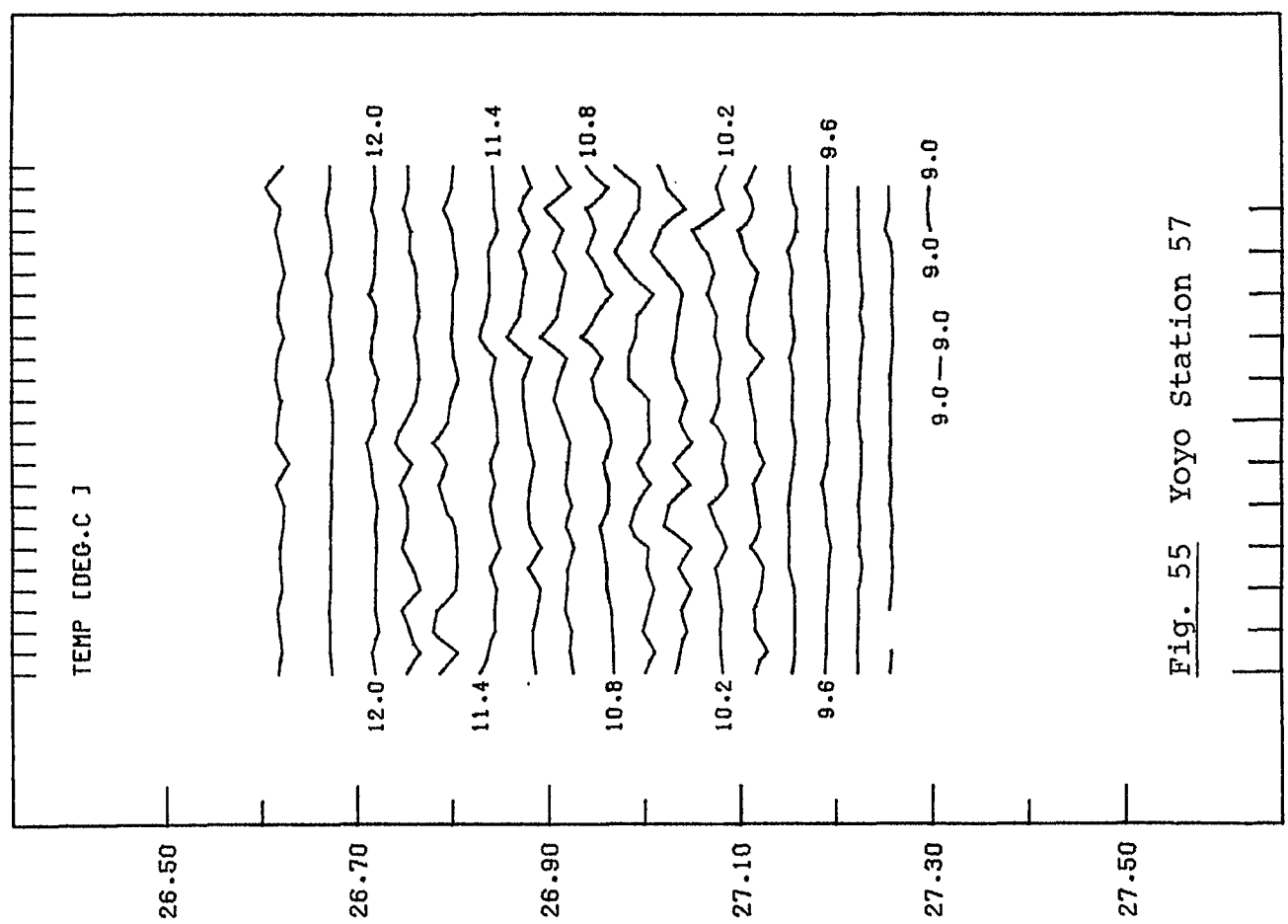

Fig. 55 Yoyo Station 57

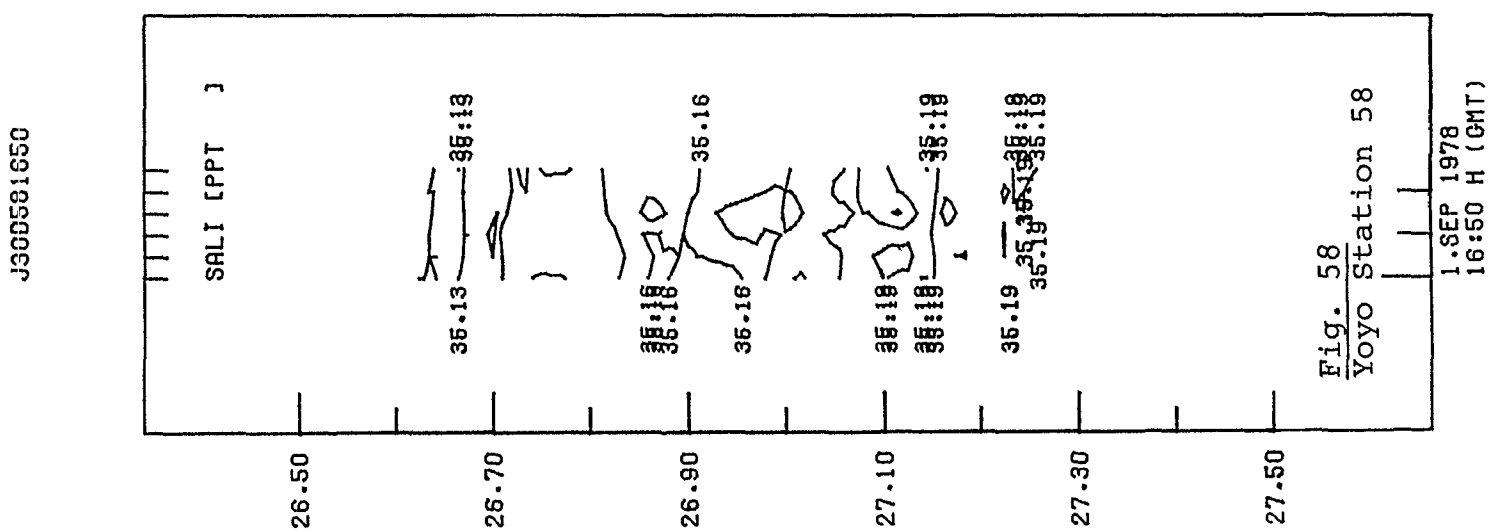

Fig. 58
Yoyo Station 58
1.SEP 1978
16:50 H (GMT)

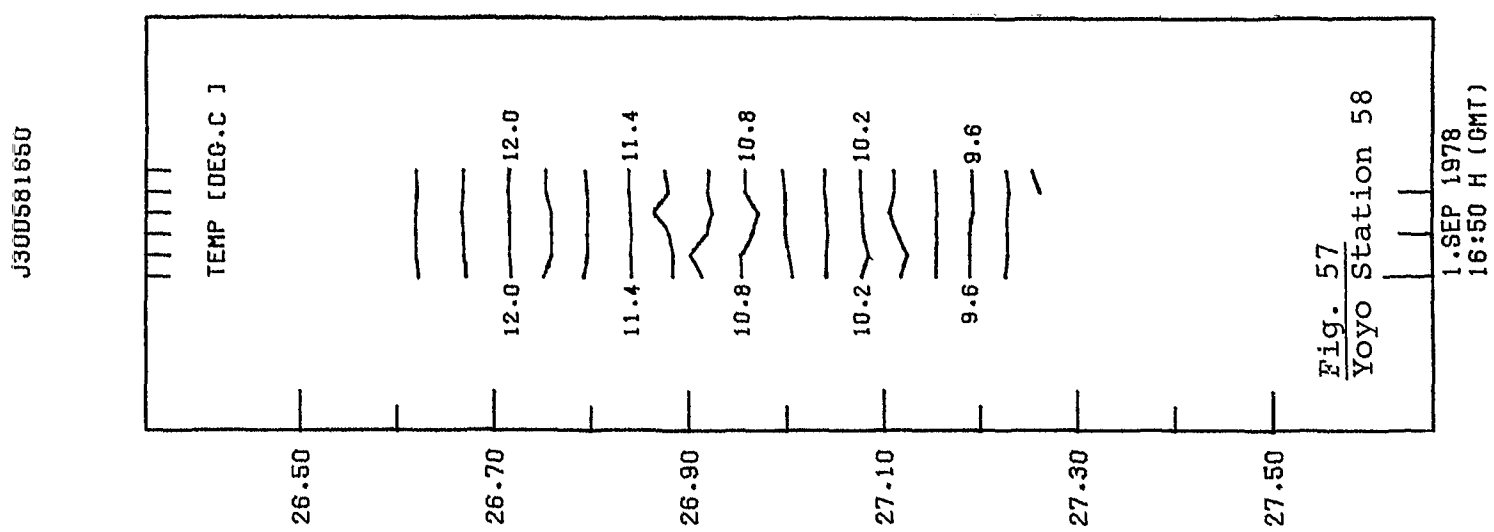

Fig. 57
Yoyo Station 58
1.SEP 1978
16:50 H (GMT)

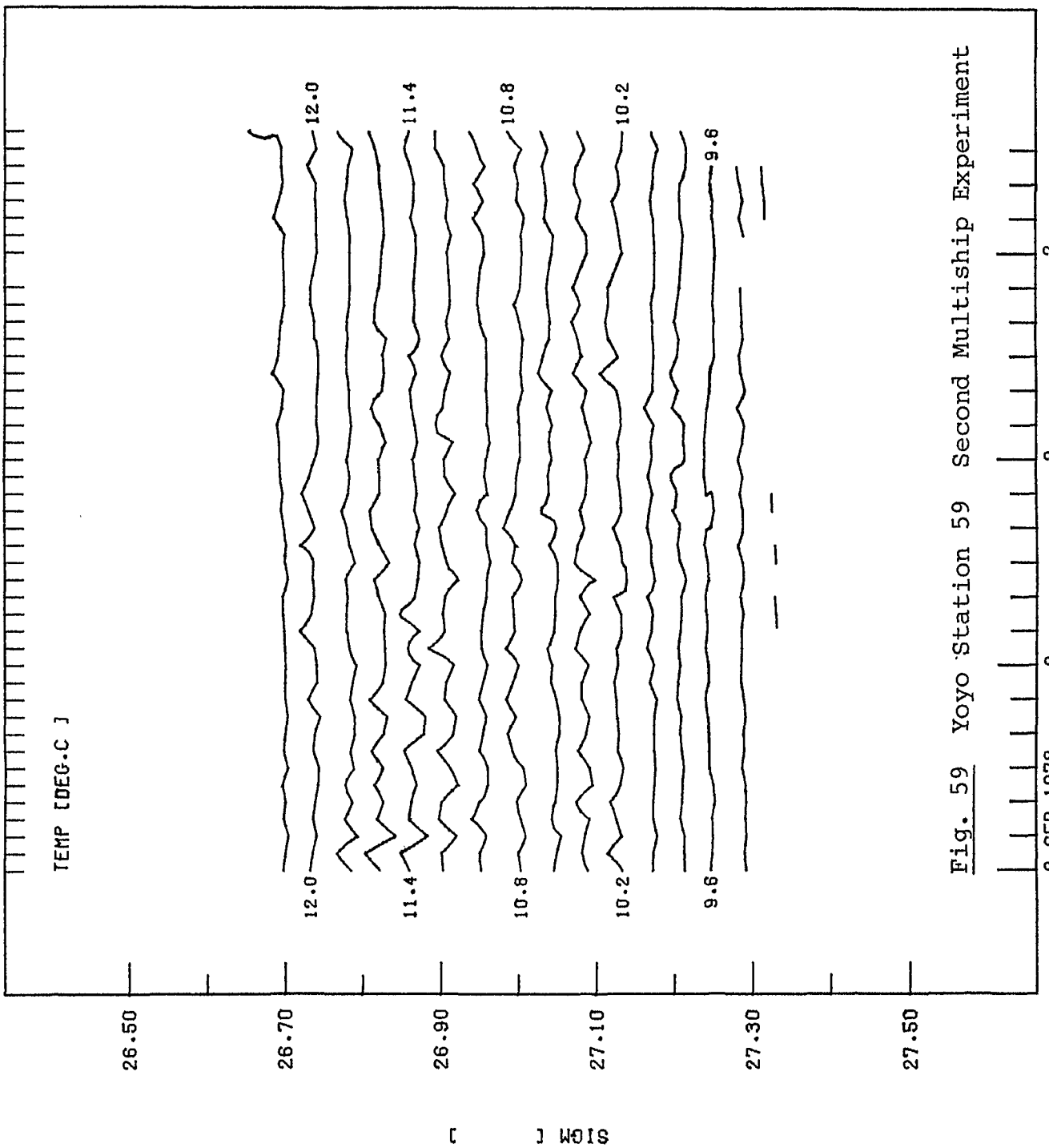

Fig. 59 Yoyo Station 59 Second Multiship Experiment

J300591125

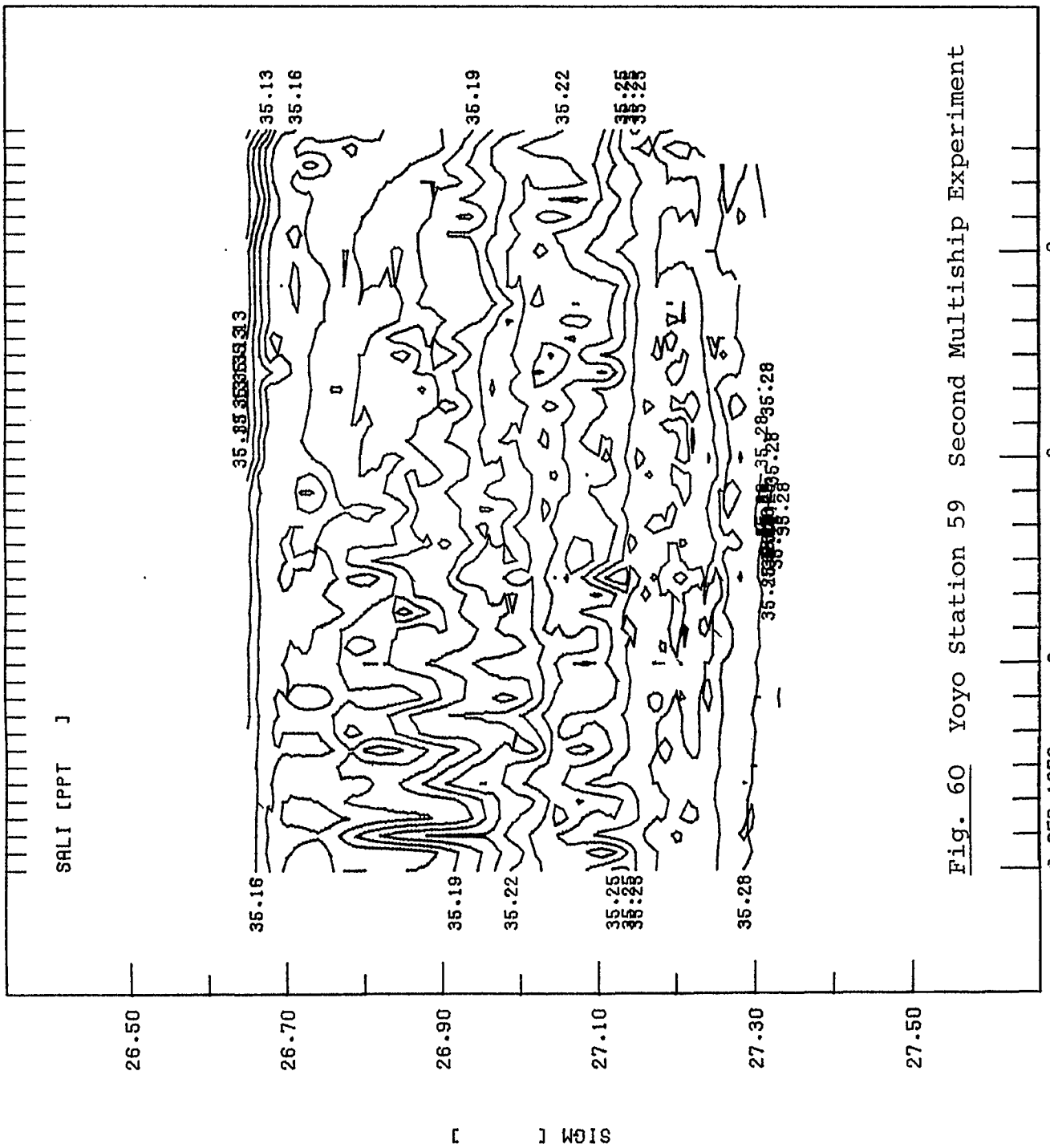

Fig. 60 Yoyo Station 59 Second Multiship Experiment

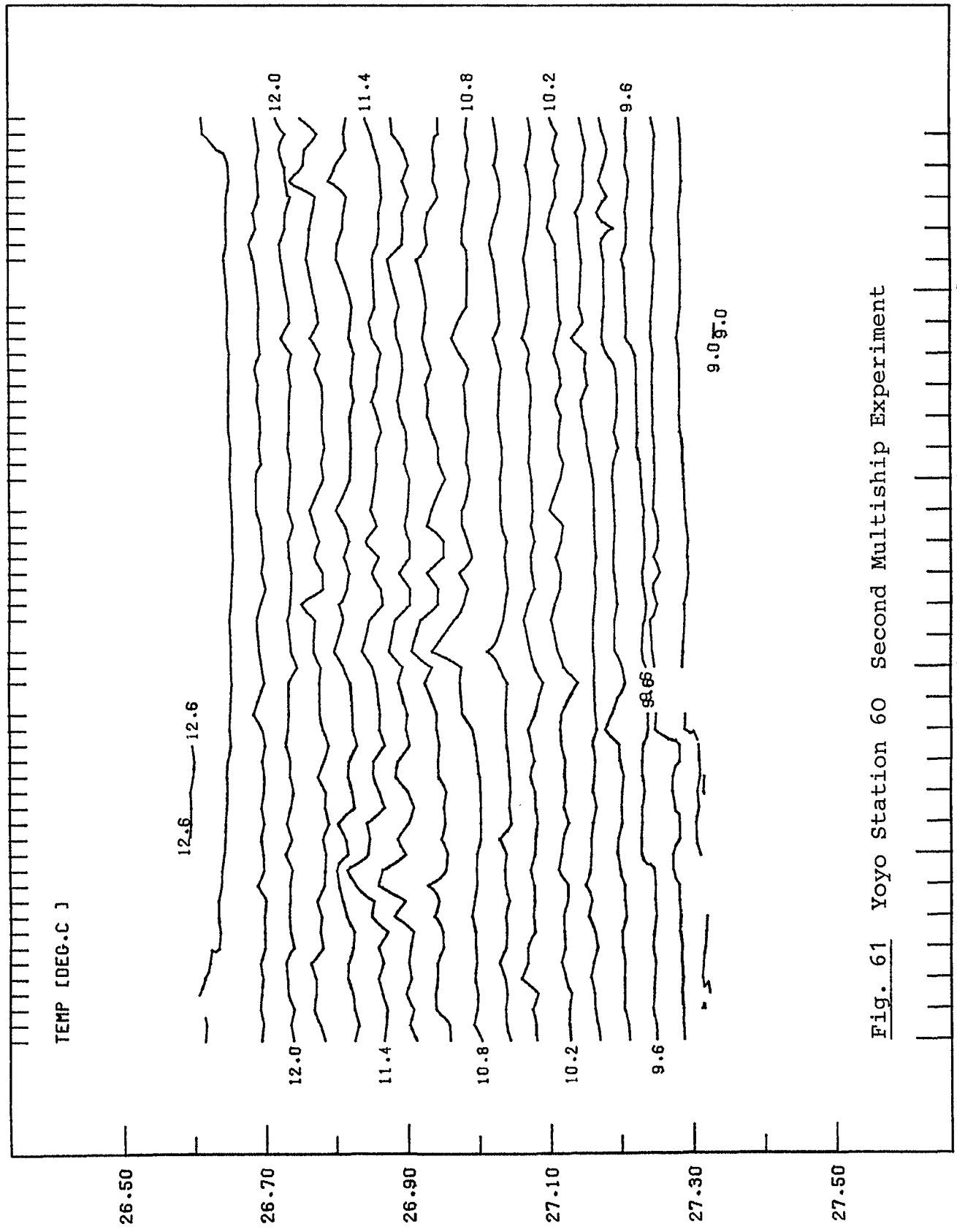

Fig. 61 Yoyo Station 60 Second Multiship Experiment

J3006G1645

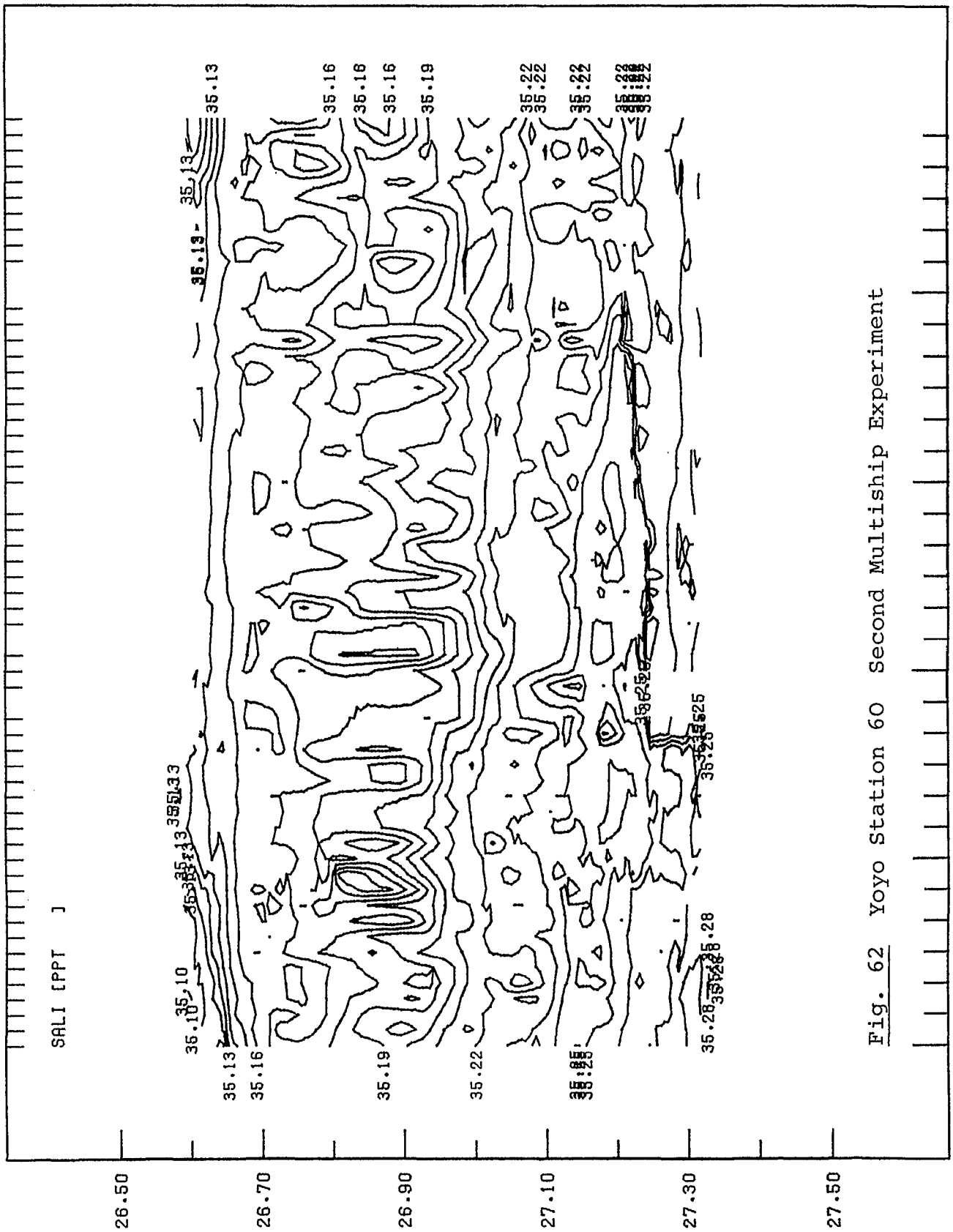

Fig. 62 Yoyo Station 60 Second Multiship Experiment

J30D601845

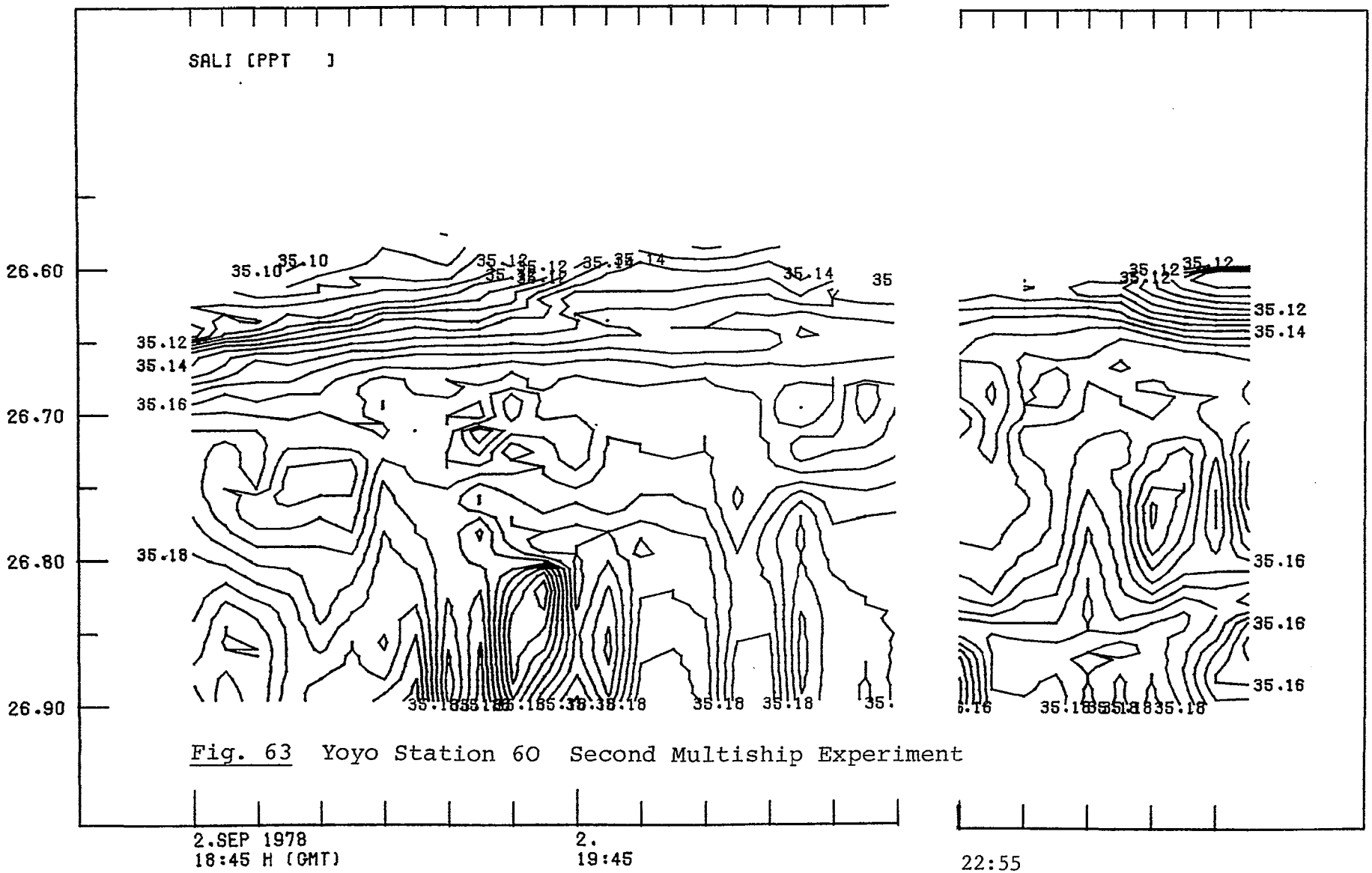

Fig. 63 Yoyo Station 60 Second Multiship Experiment

J30D601845

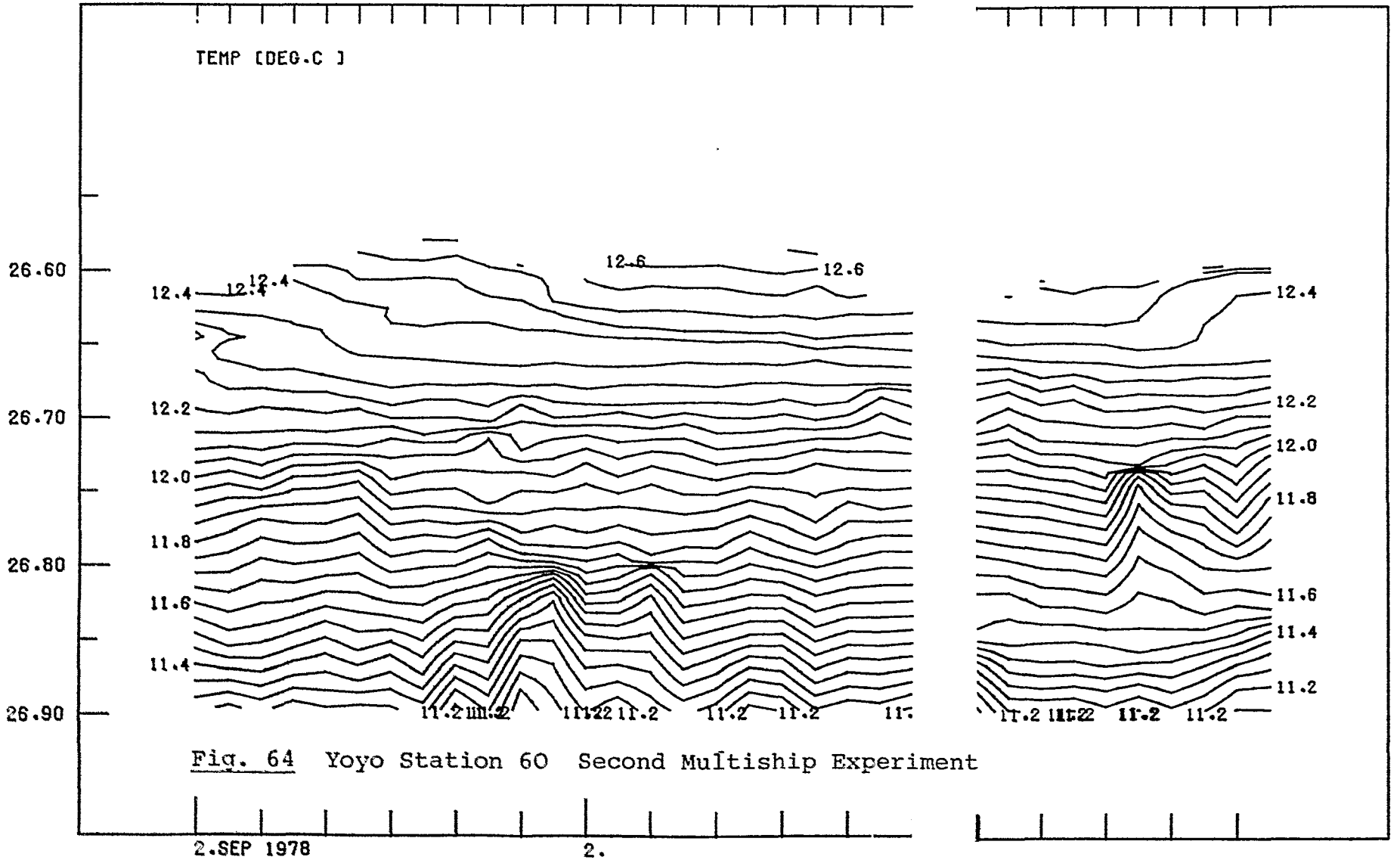

Fig. 64 Yoyo Station 60 Second Multiship Experiment

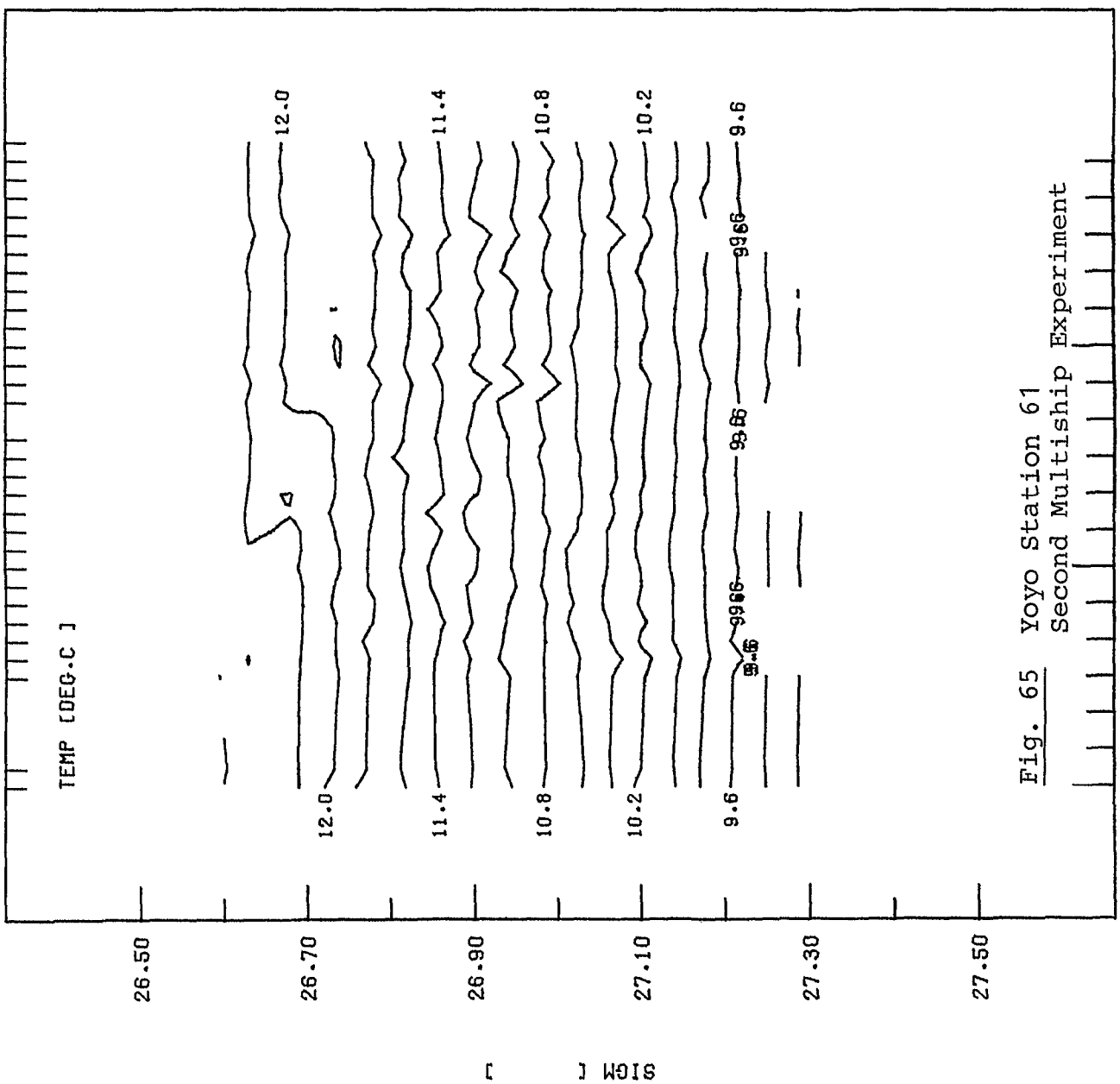

Fig. 65

J300612355

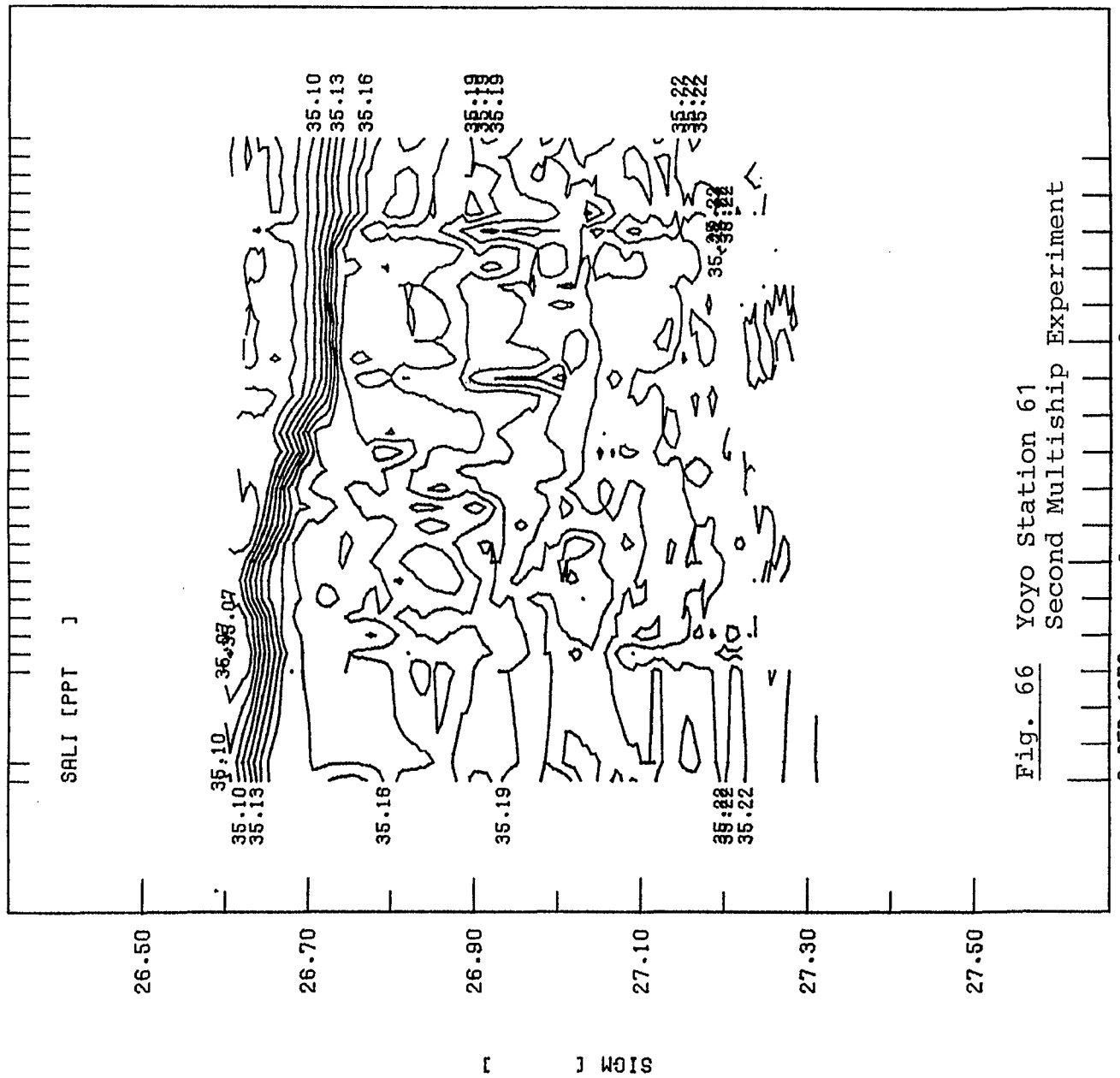

Fig. 66 Yoyo Station 61
Second Multiship Experiment

J30D612355

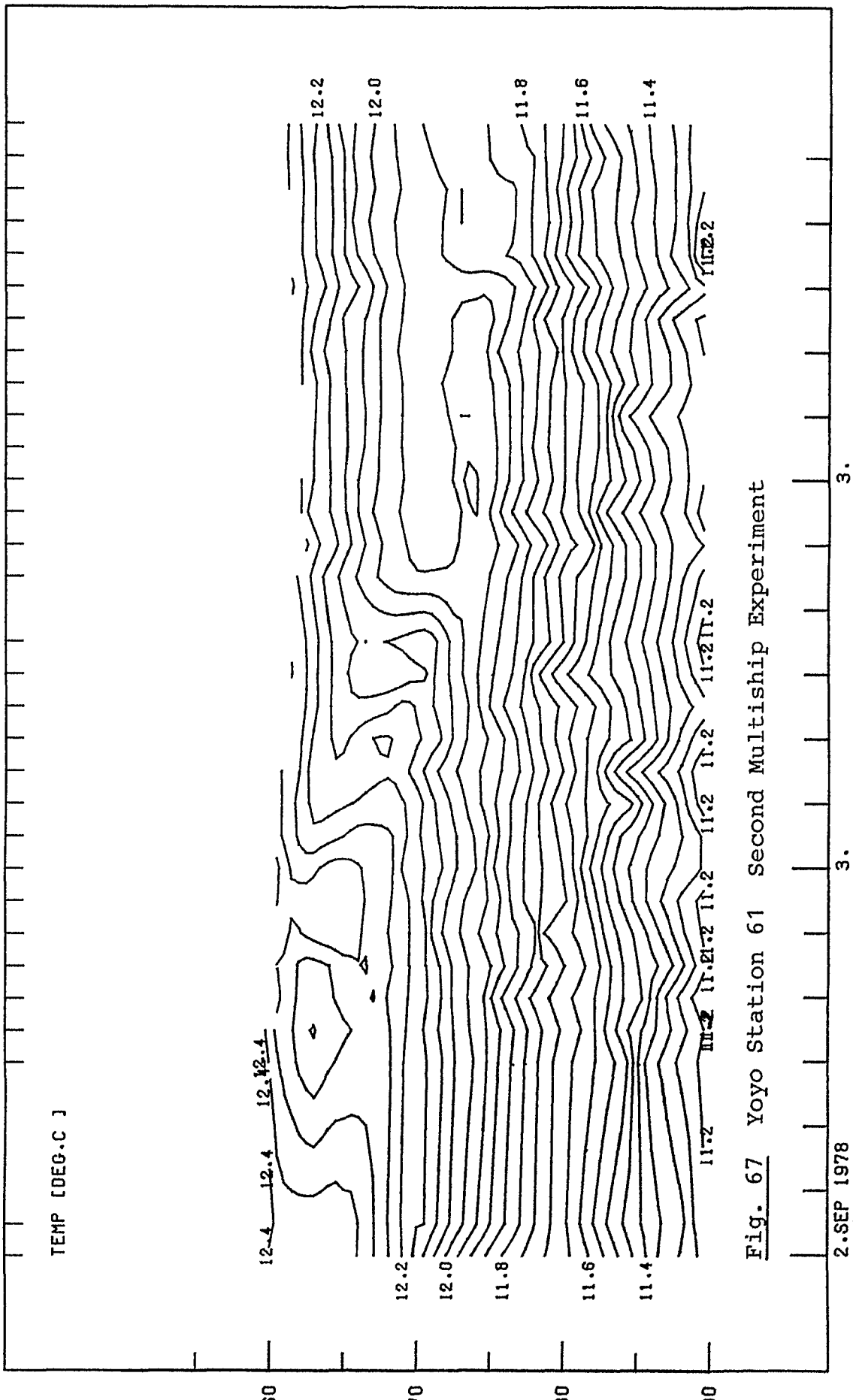

Fig. 67 Yoyo Station 61 Second Multiship Experiment

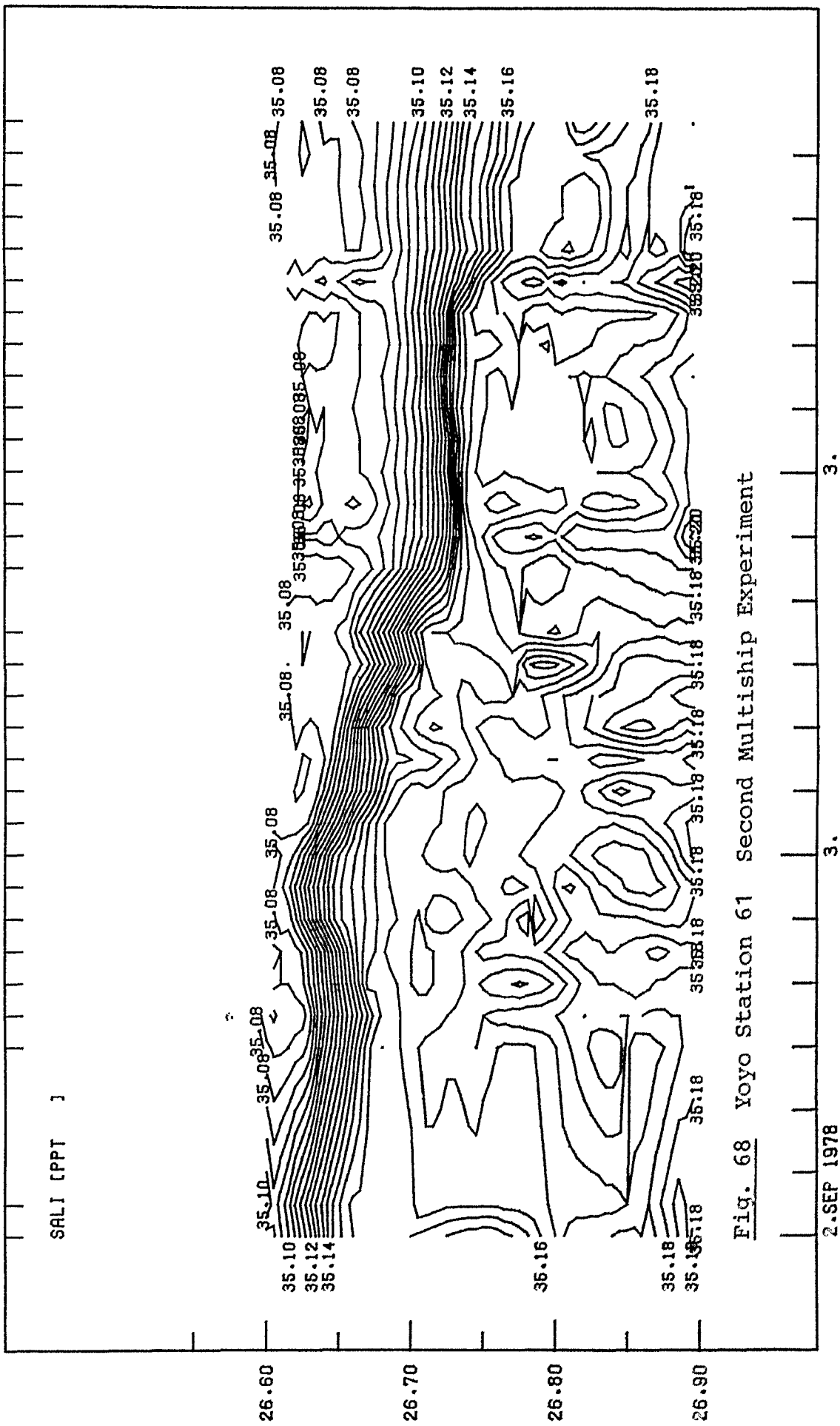

Fig. 68 Yoyo Station 61 Second Multiship Experiment

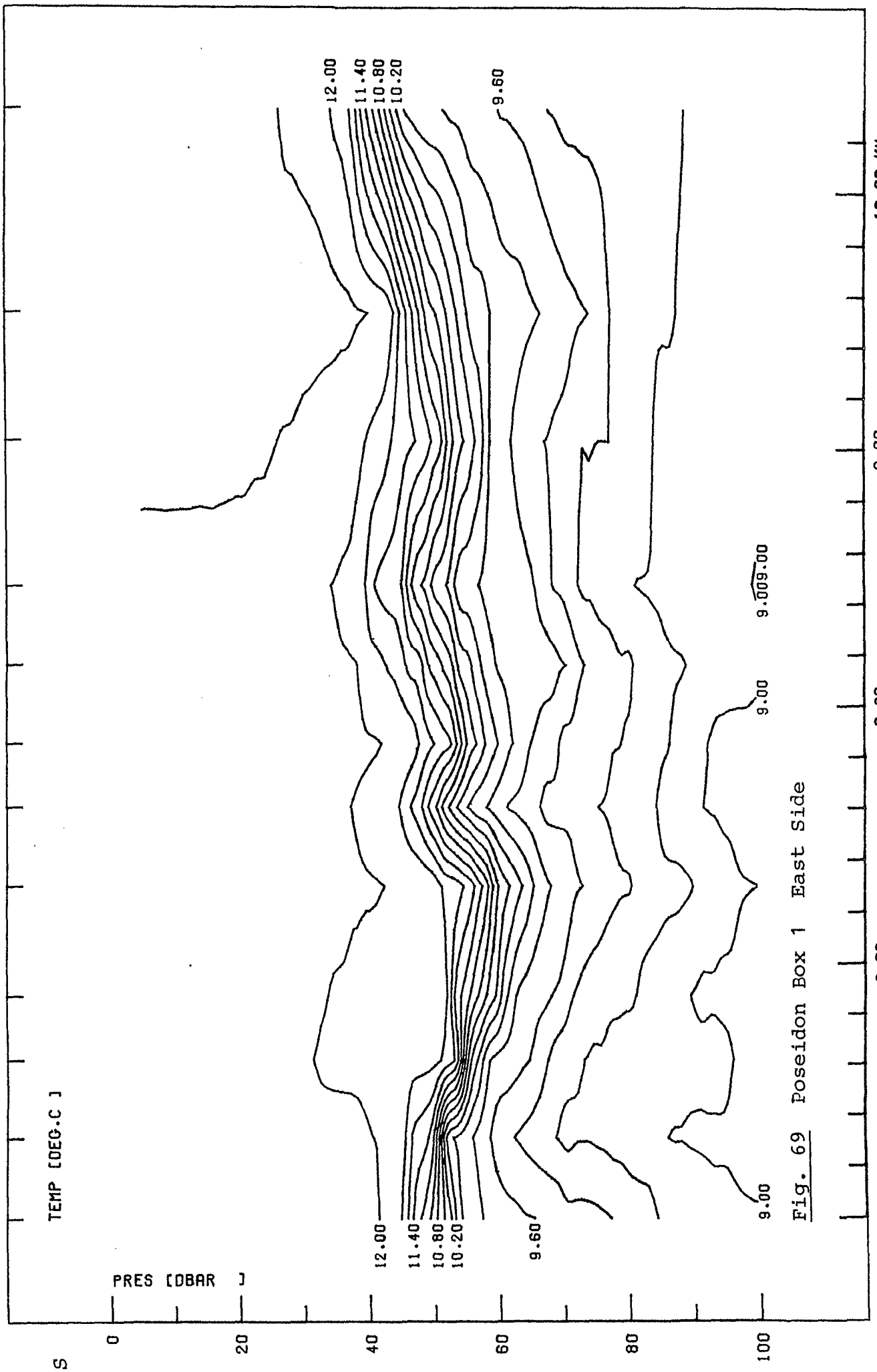

Fig. 69 Poseidon Box 1 East Side

PJC003T

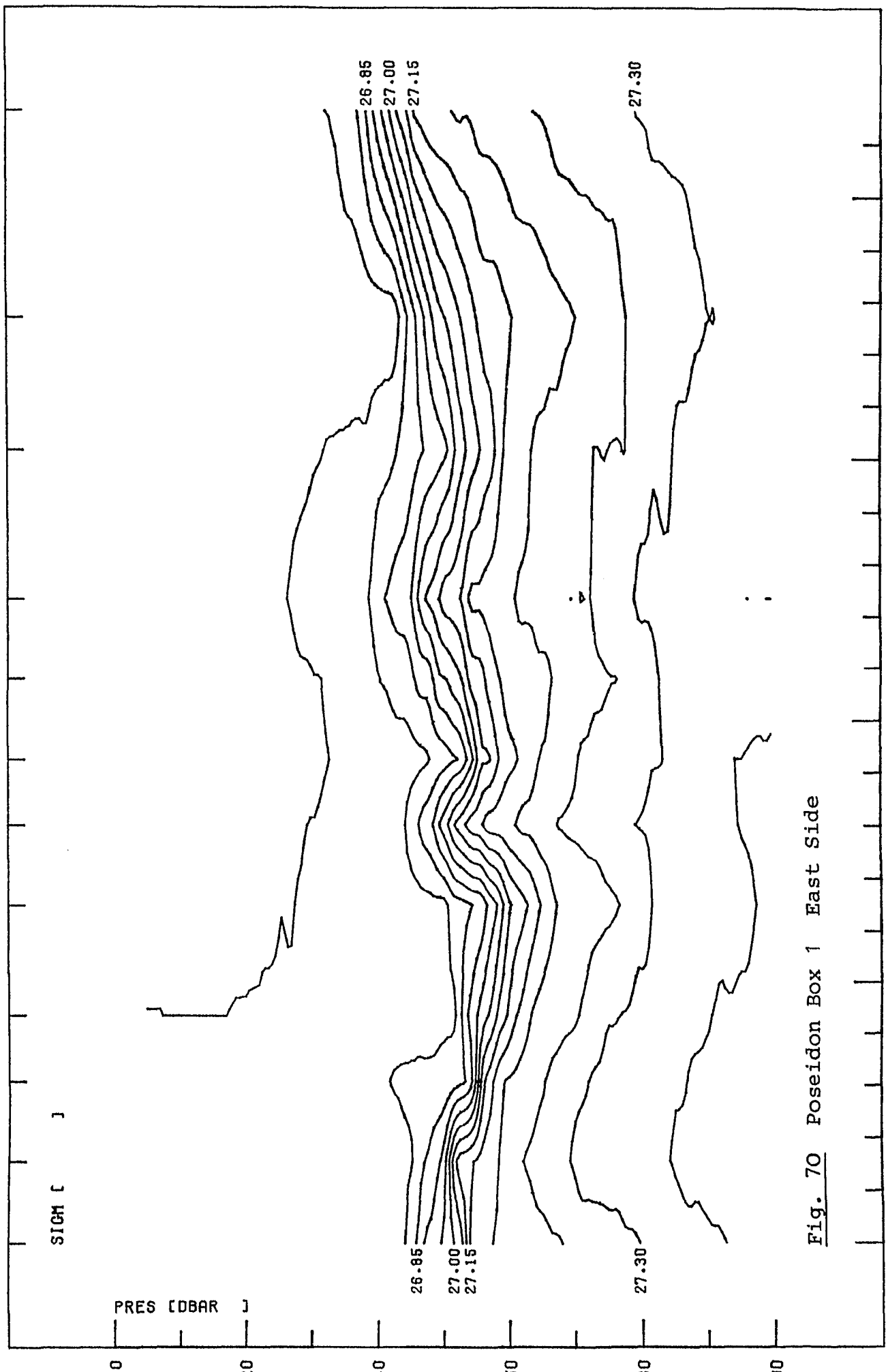

Fig. 70 Poseidon Box 1 East Side

PJC003F

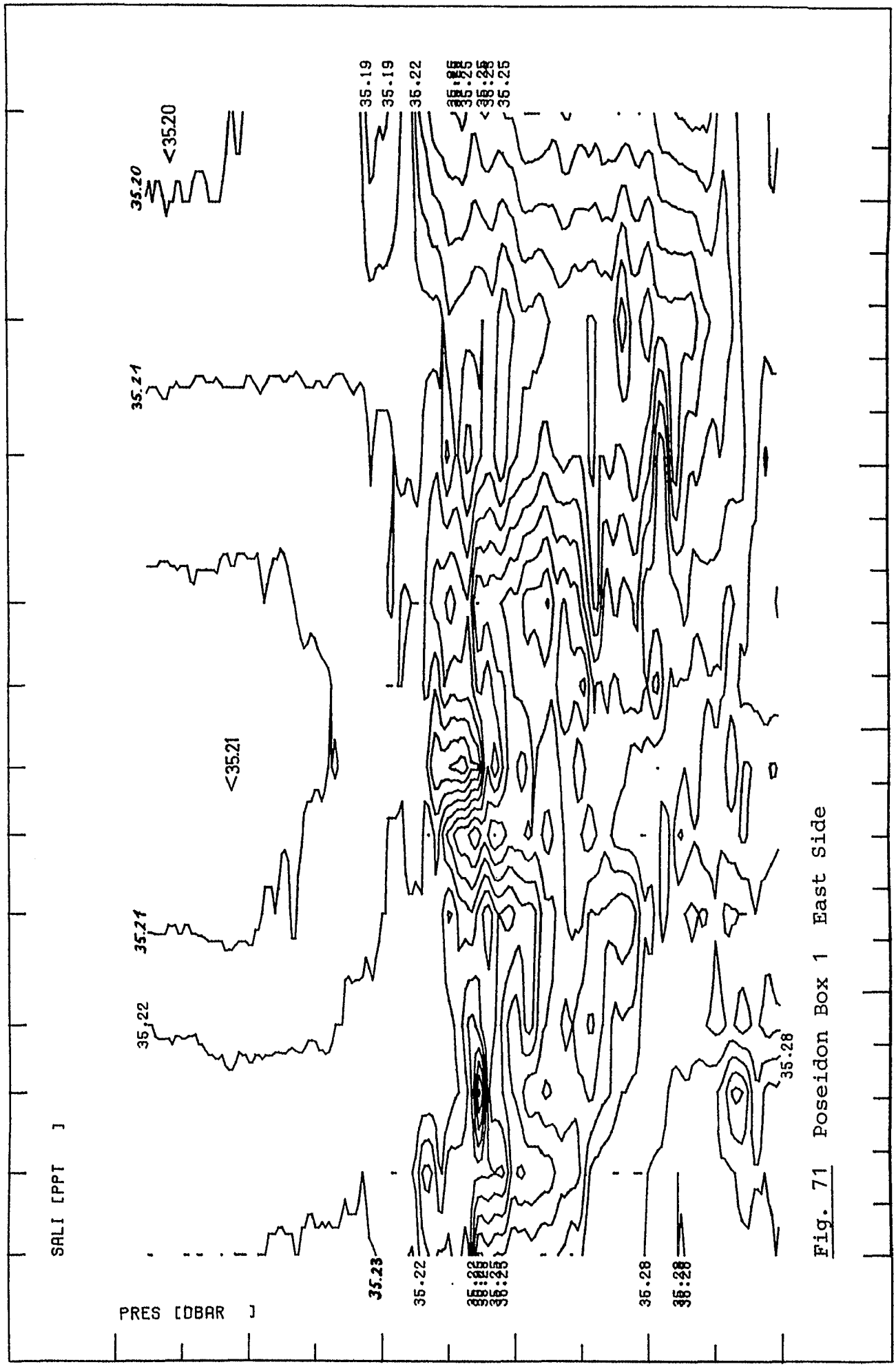

Fig. 71 Poseidon Box 1 East Side

PJC003T

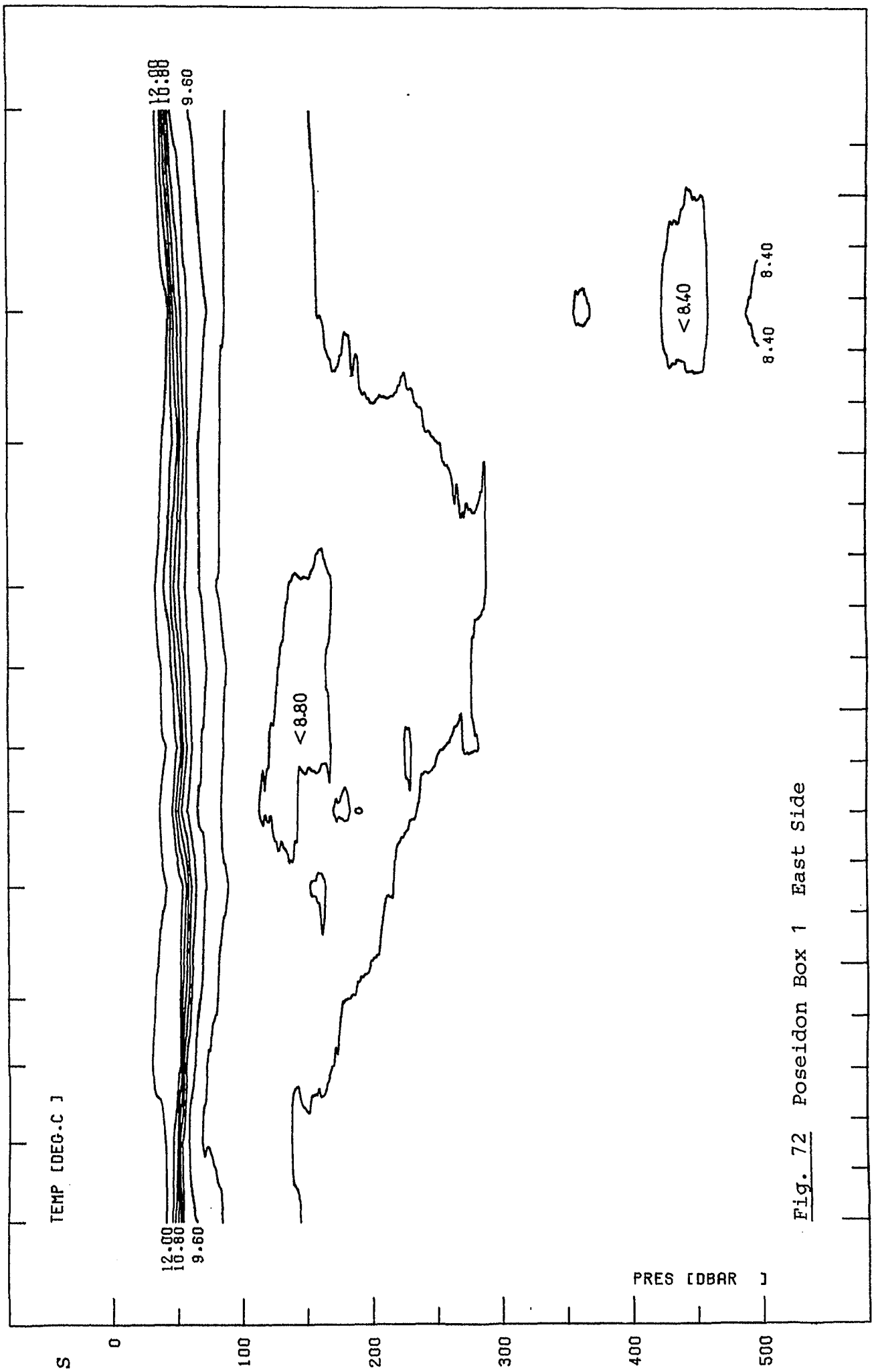

Fig. 72 Poseidon Box 1 East Side

PJC003T

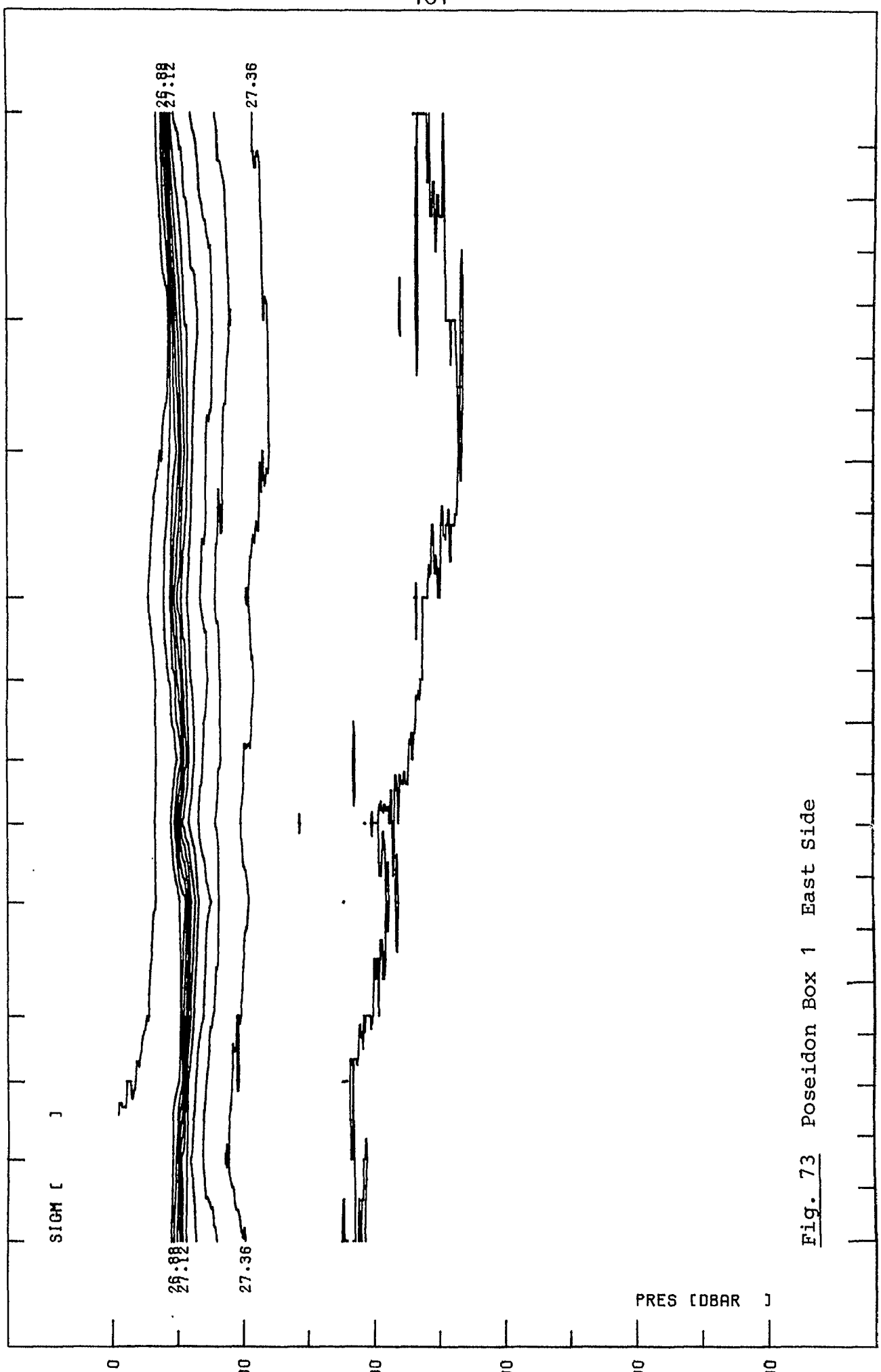

Fig. 73 Poseidon Box 1 East Side

PJC003T

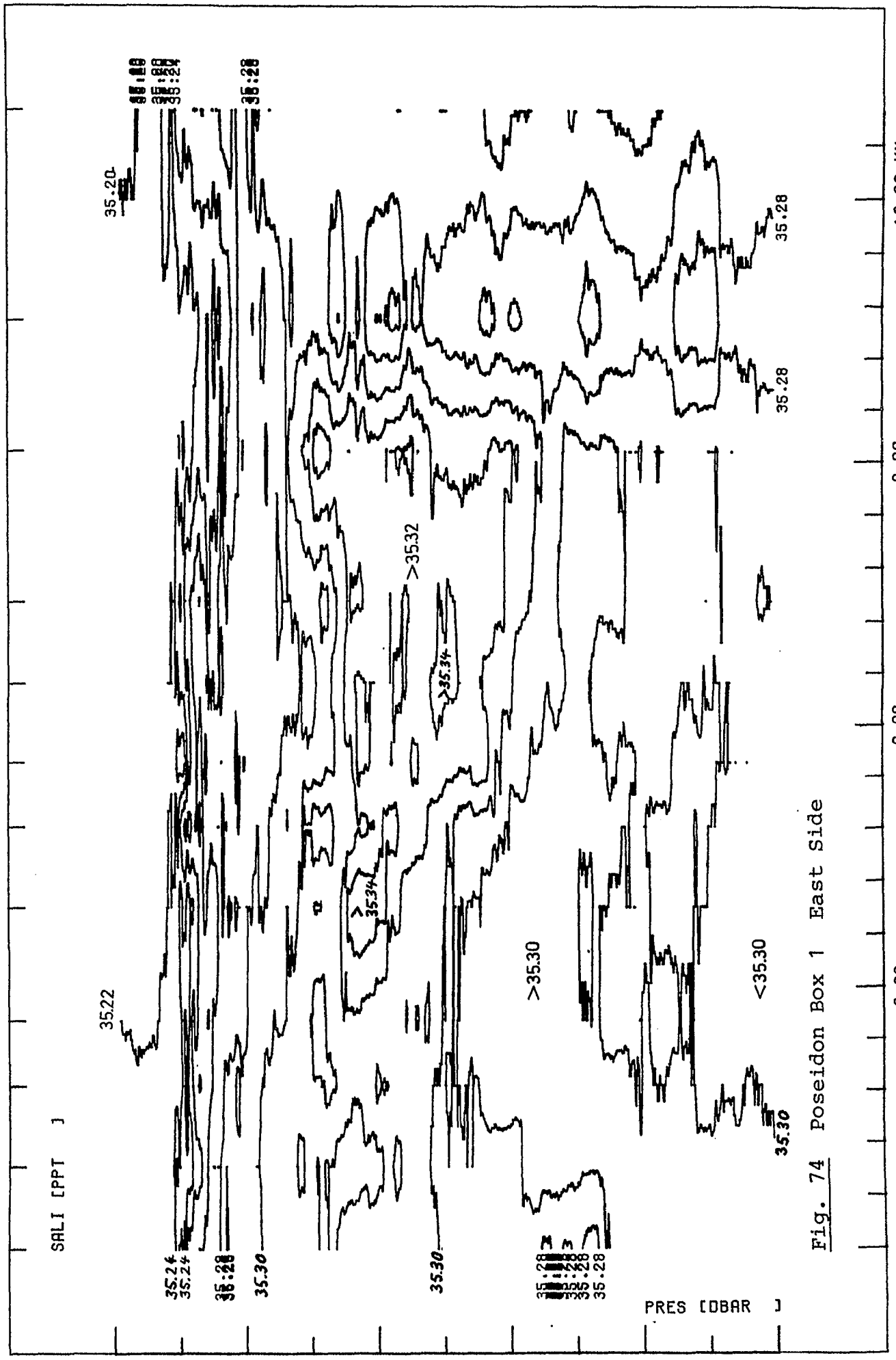

Fig. 74 Poseidon Box 1 East Side

PJC003T

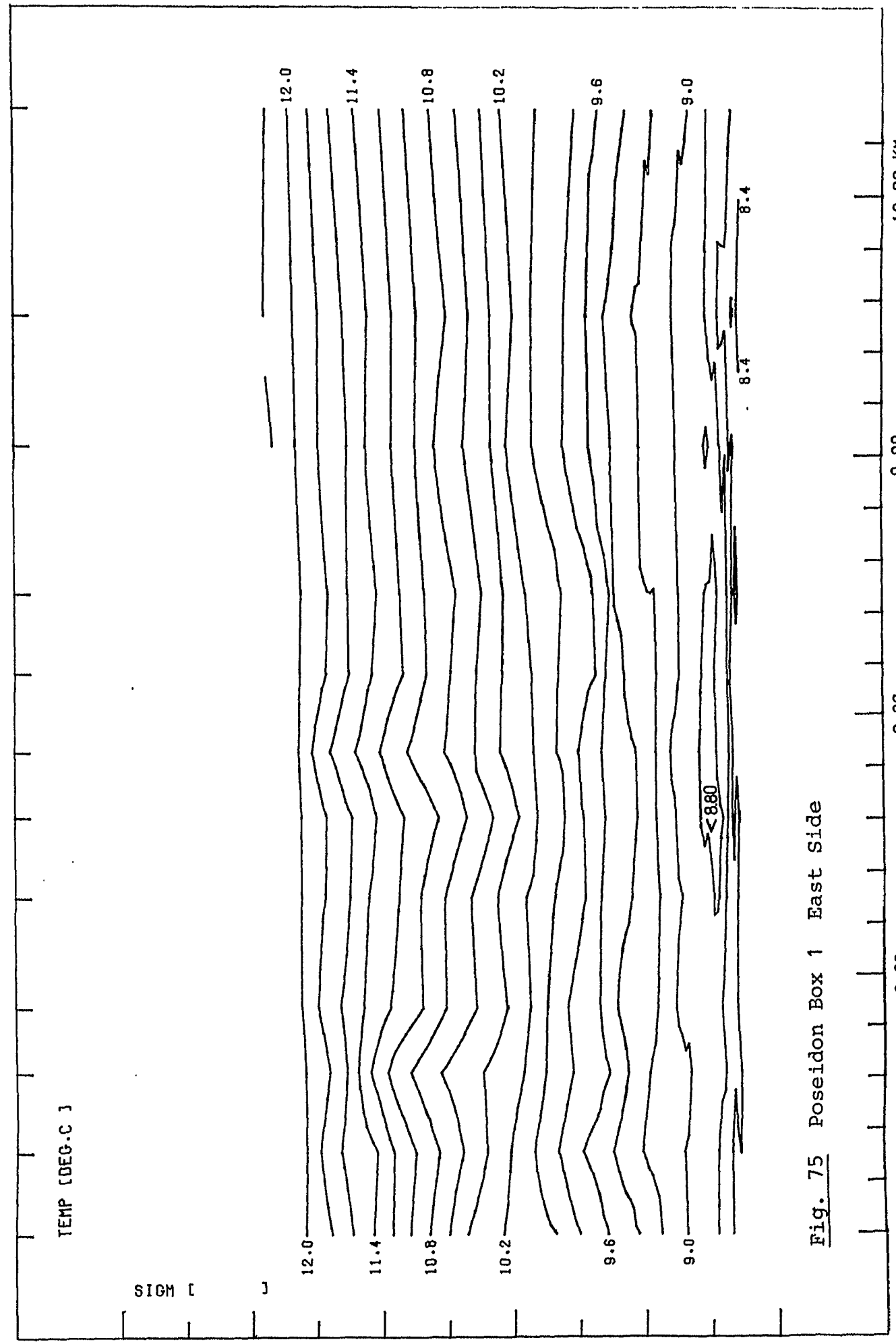

Fig. 75 Poseidon Box 1 East Side

PJC003

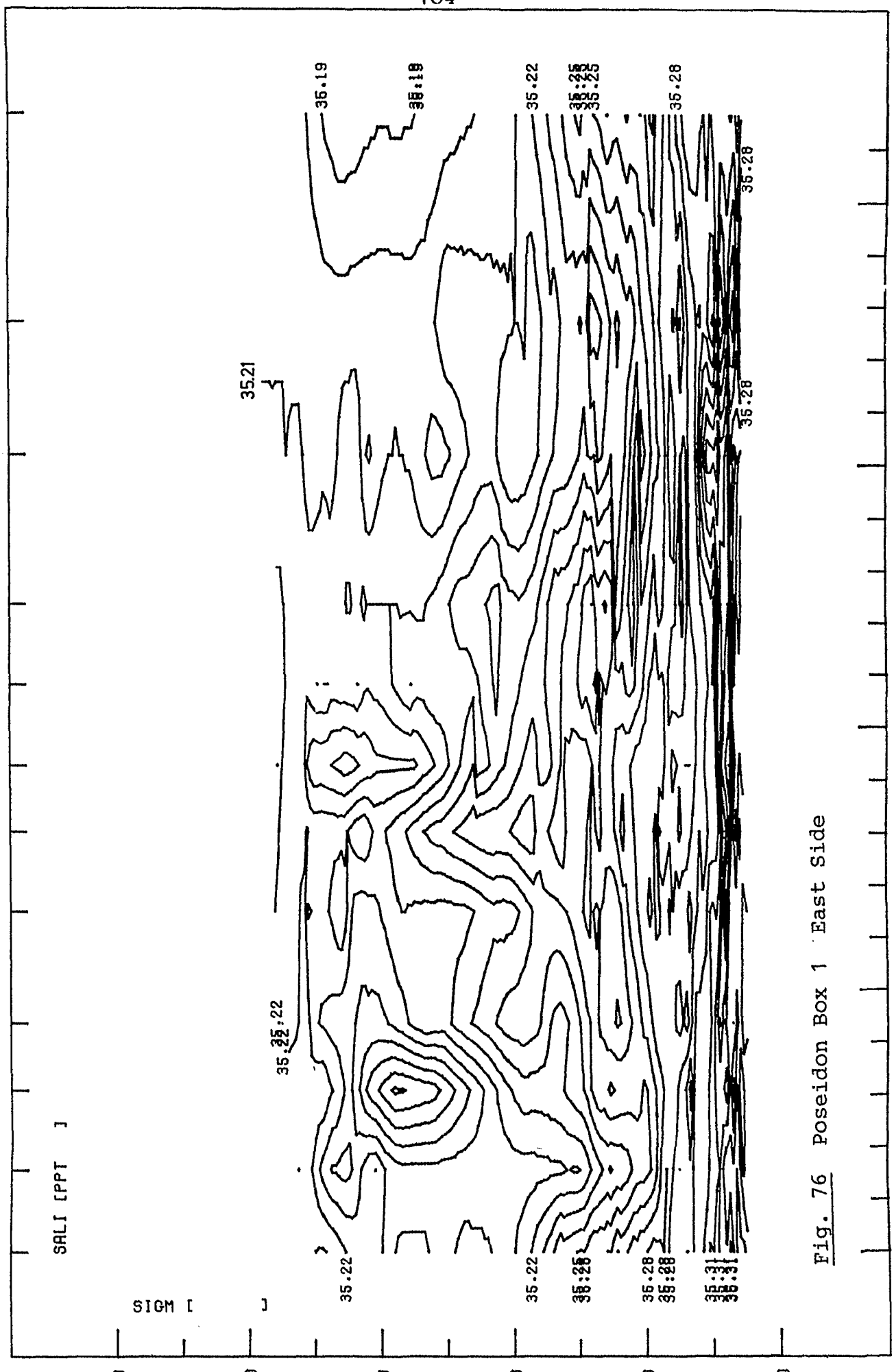

Fig. 76 Poseidon Box 1 East Side

PJC003

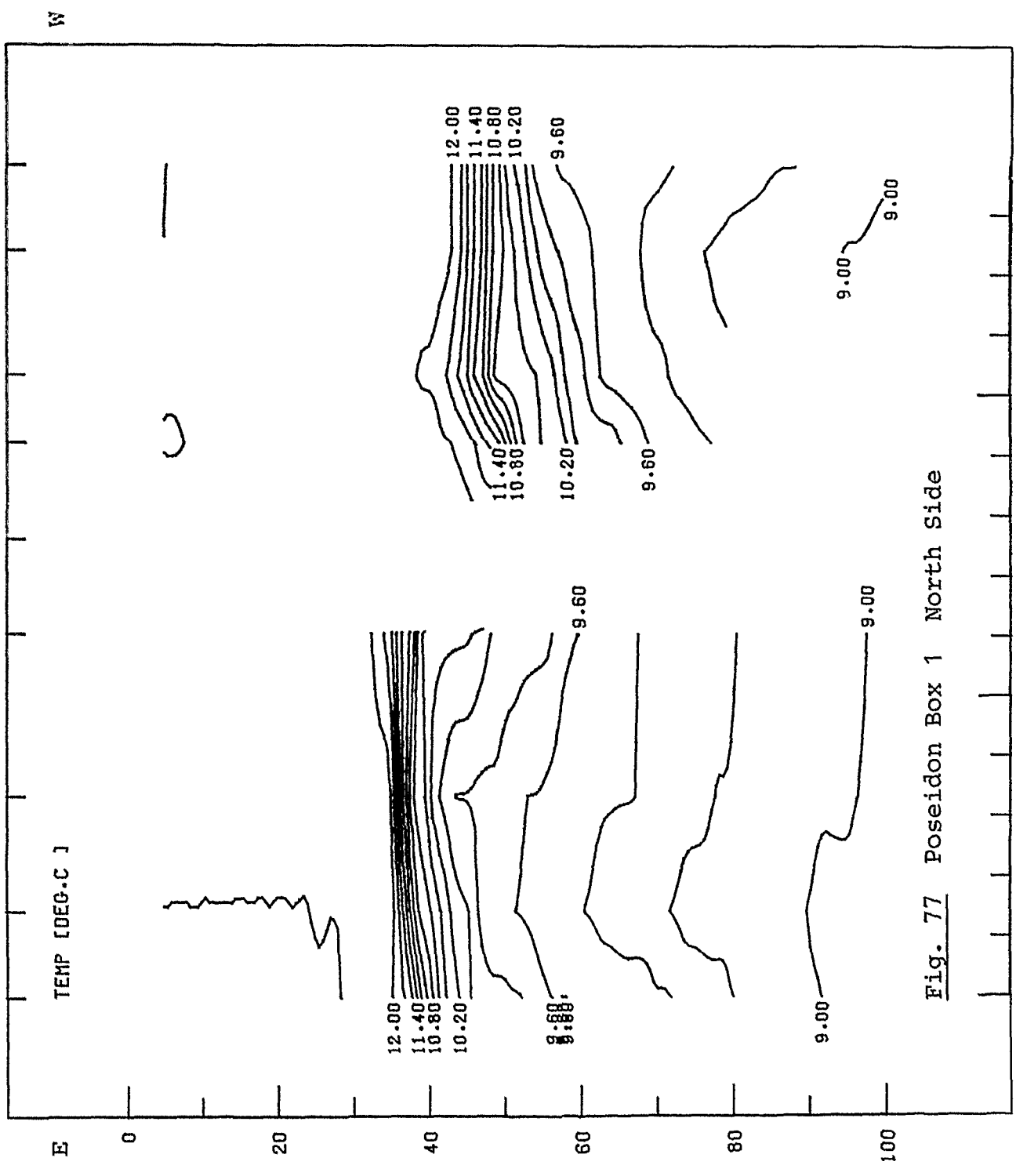

Fig. 77 Poseidon Box 1 North Side

PJC016T

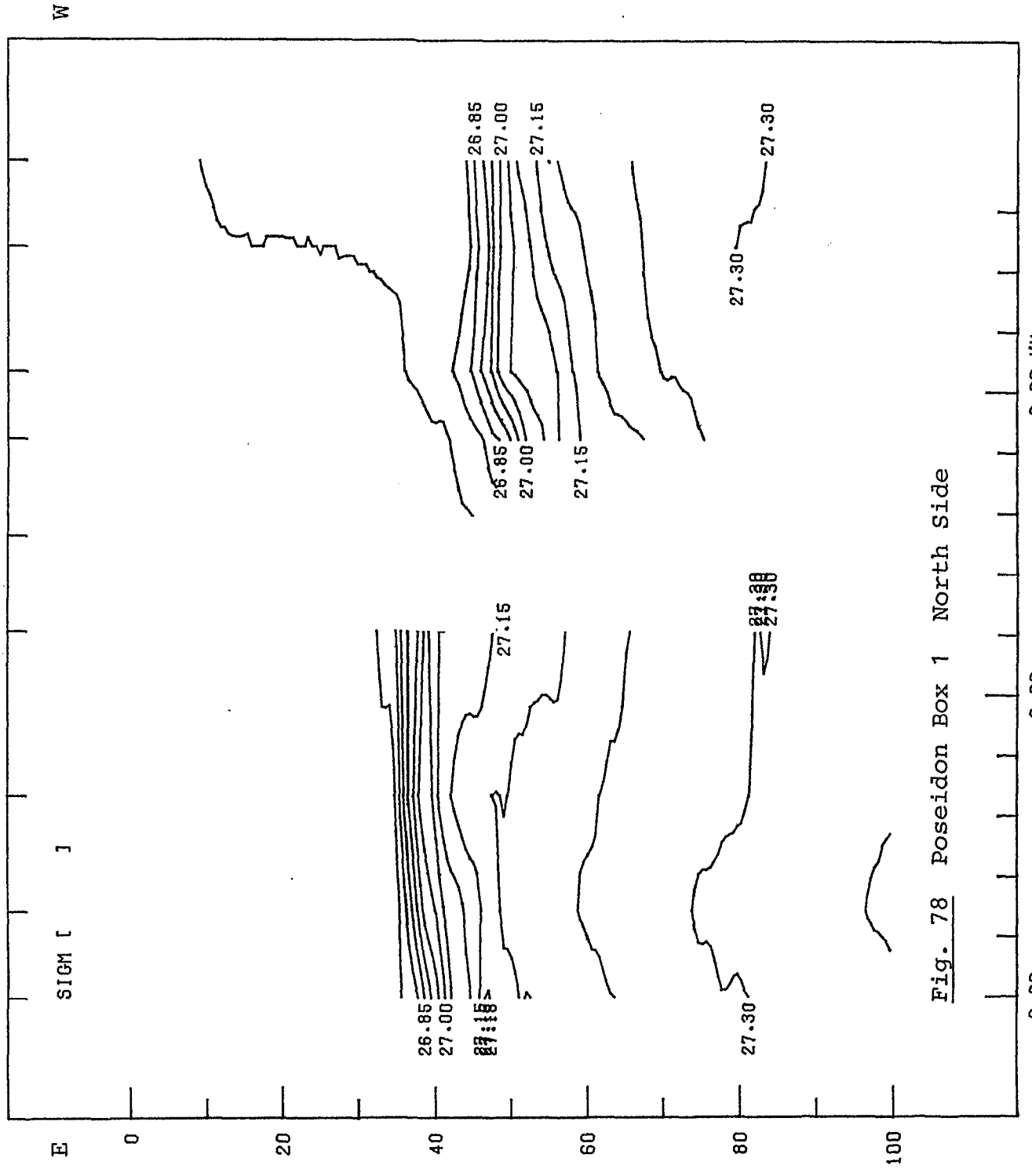

Fig. 78 Poseidon Box 1 North Side

PJC016T

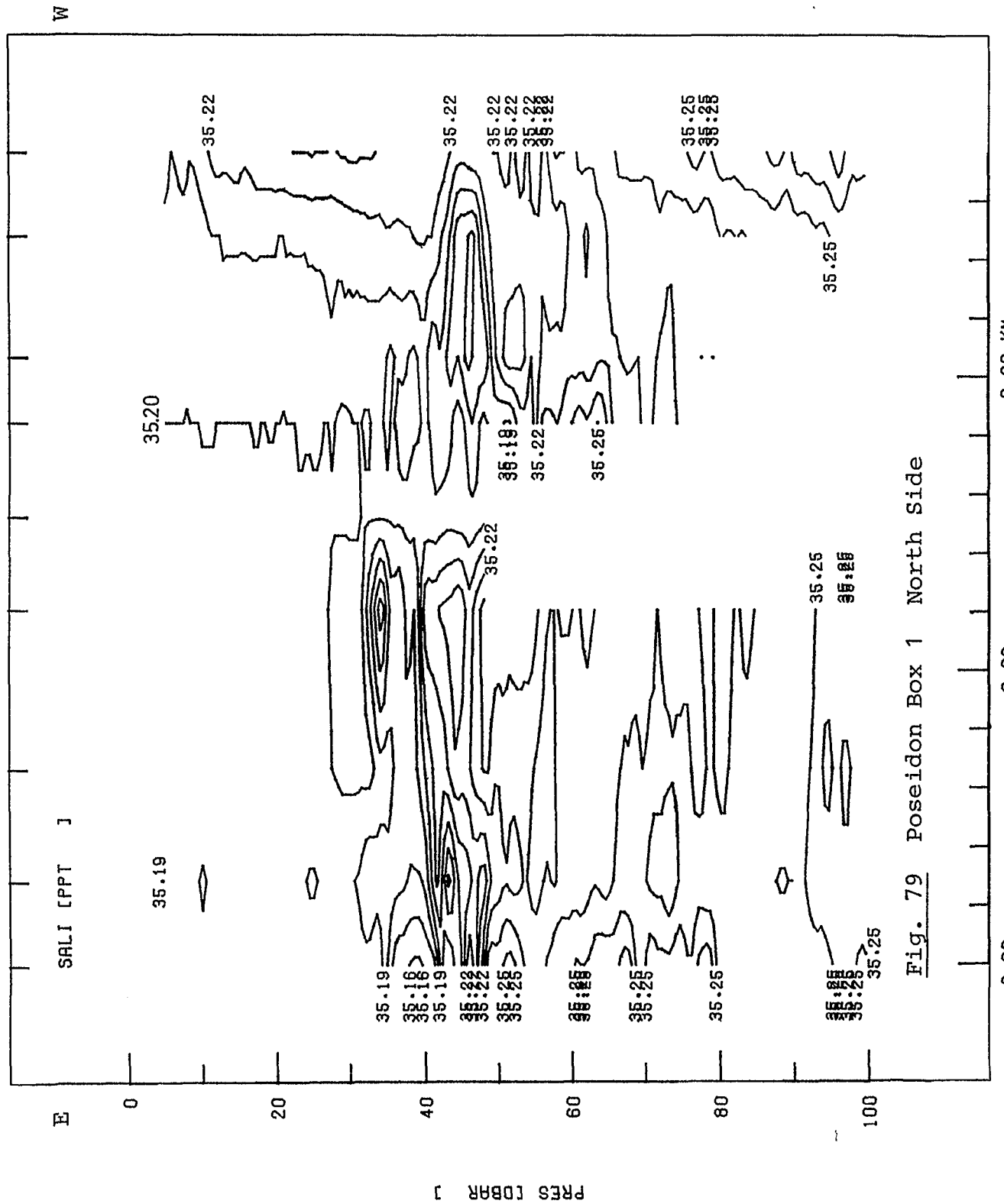

Fig. 79 Poseidon Box 1 North Side

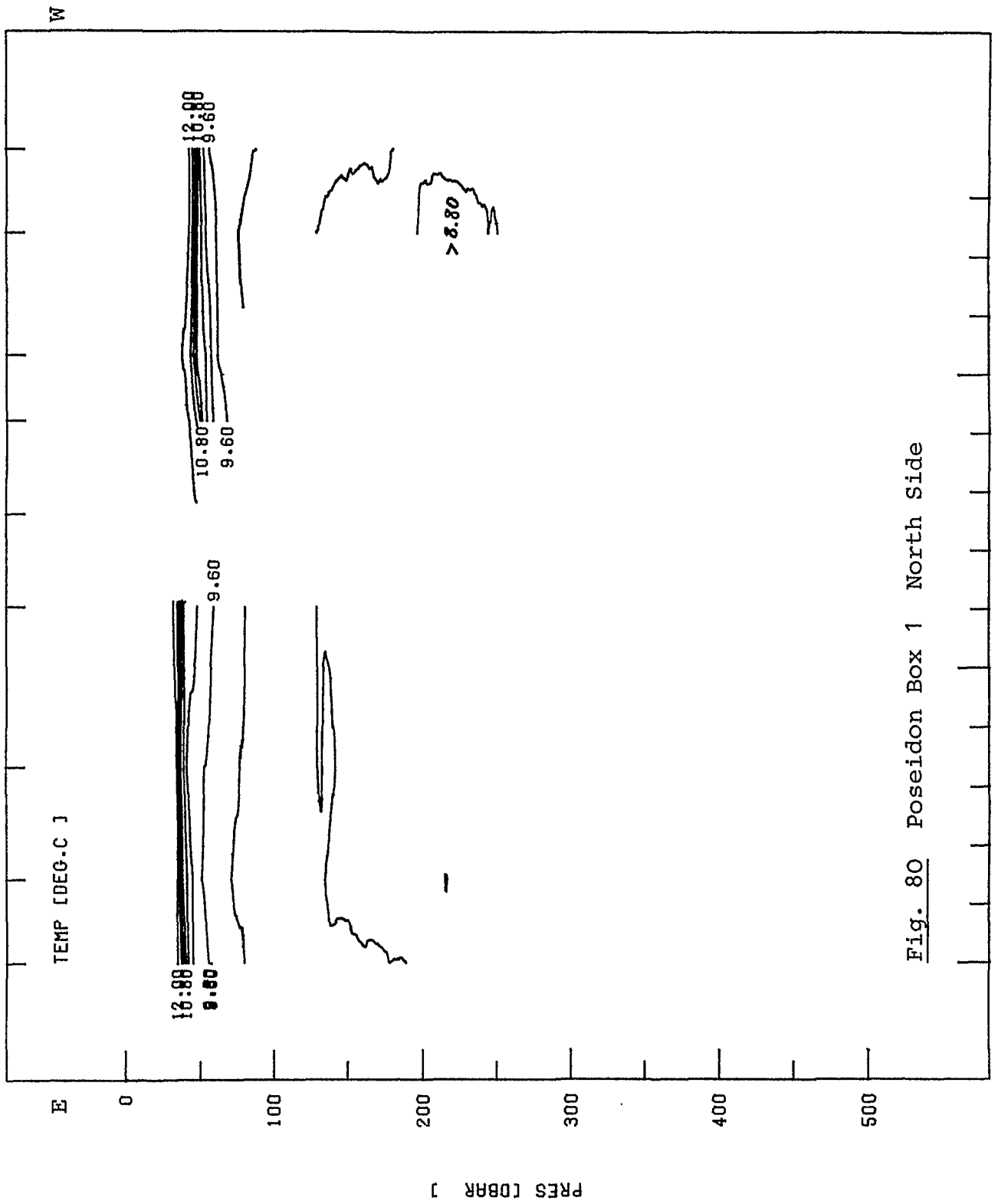

Fig. 80 Poseidon Box 1 North Side

PJC016T

PJC016T

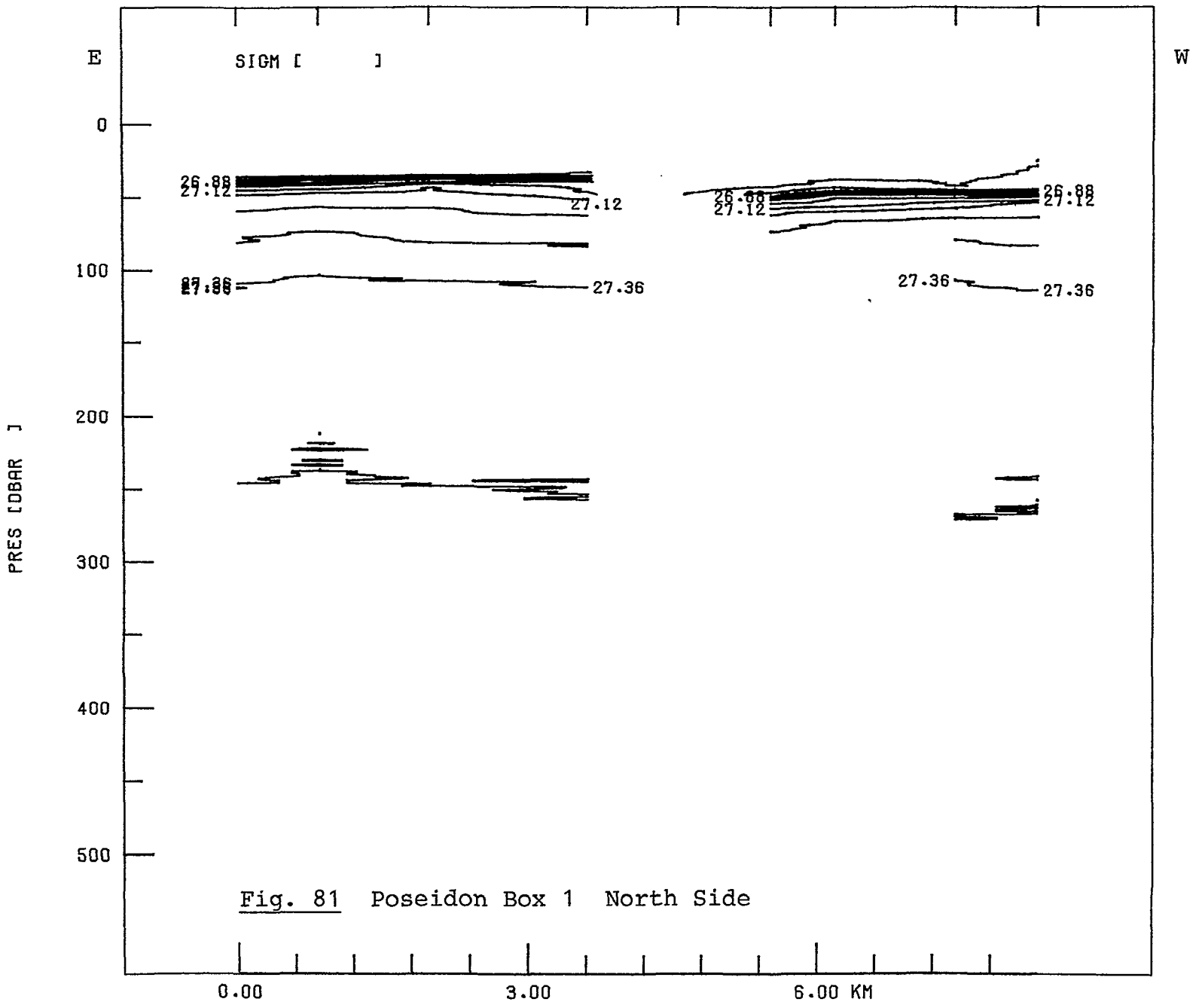

Fig. 81 Poseidon Box 1 North Side

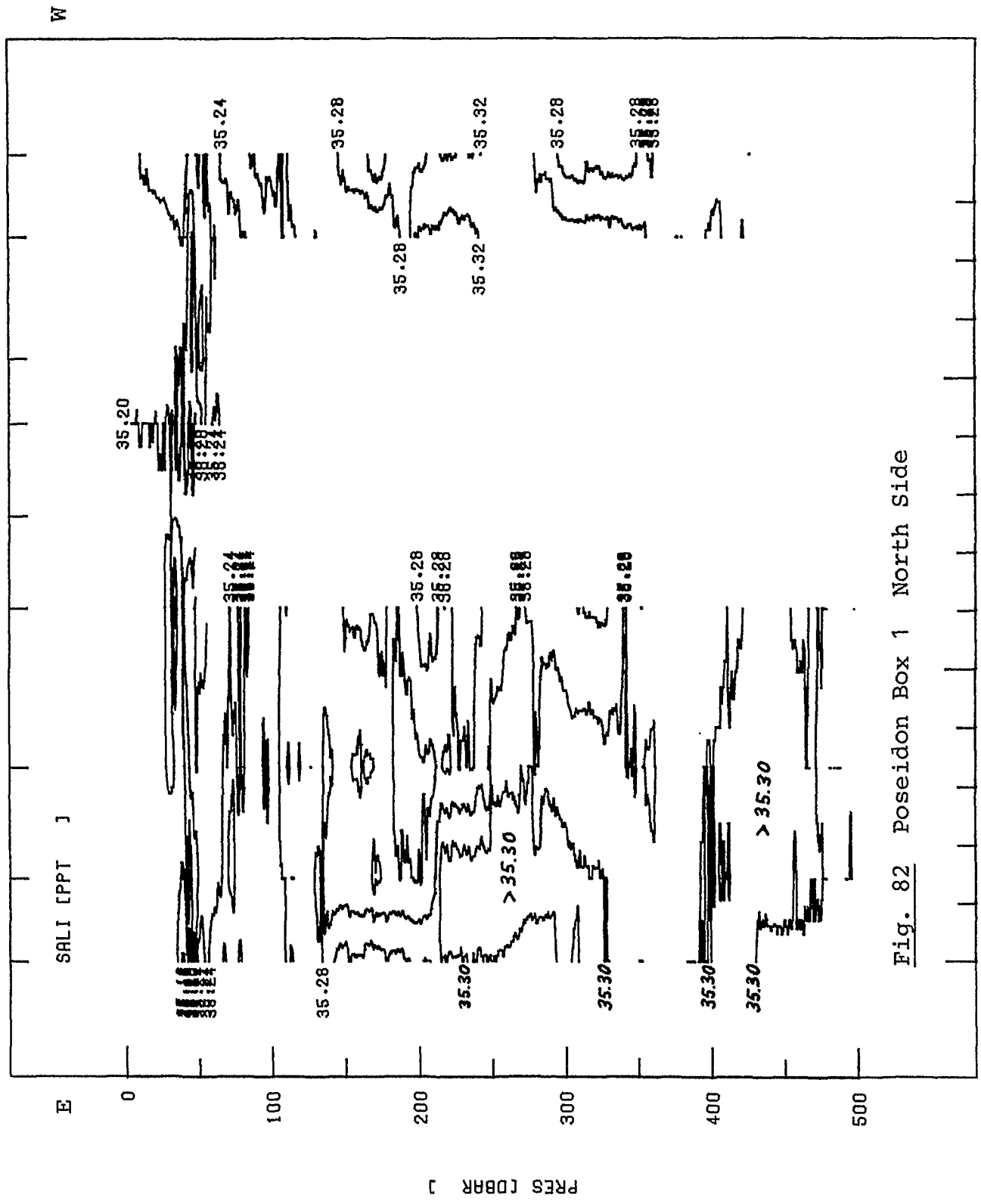

Fig. 82 Poseidon Box 1 North Side

PJC016T

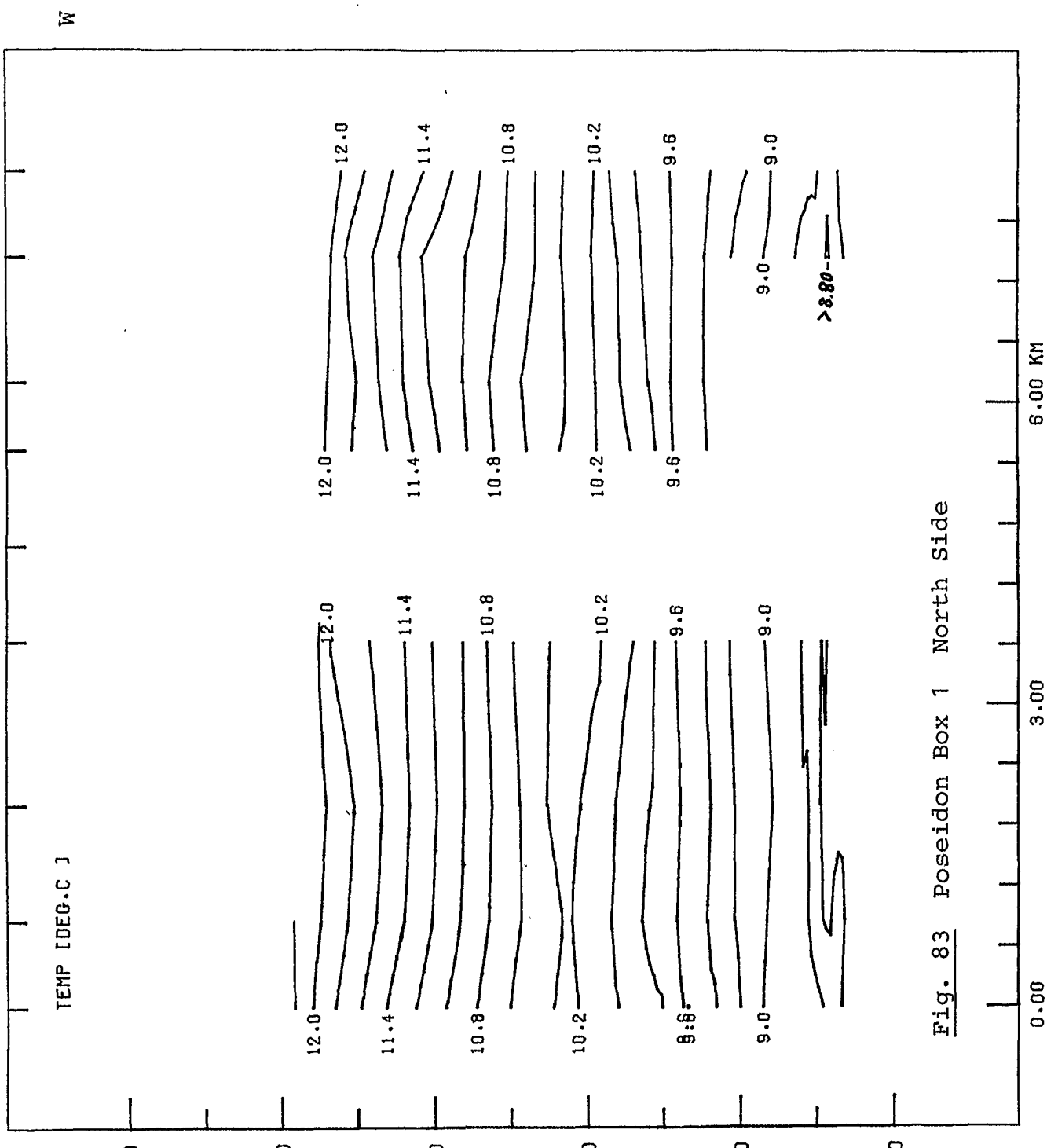

Fig. 83 Poseidon Box 1 North Side

PJC016

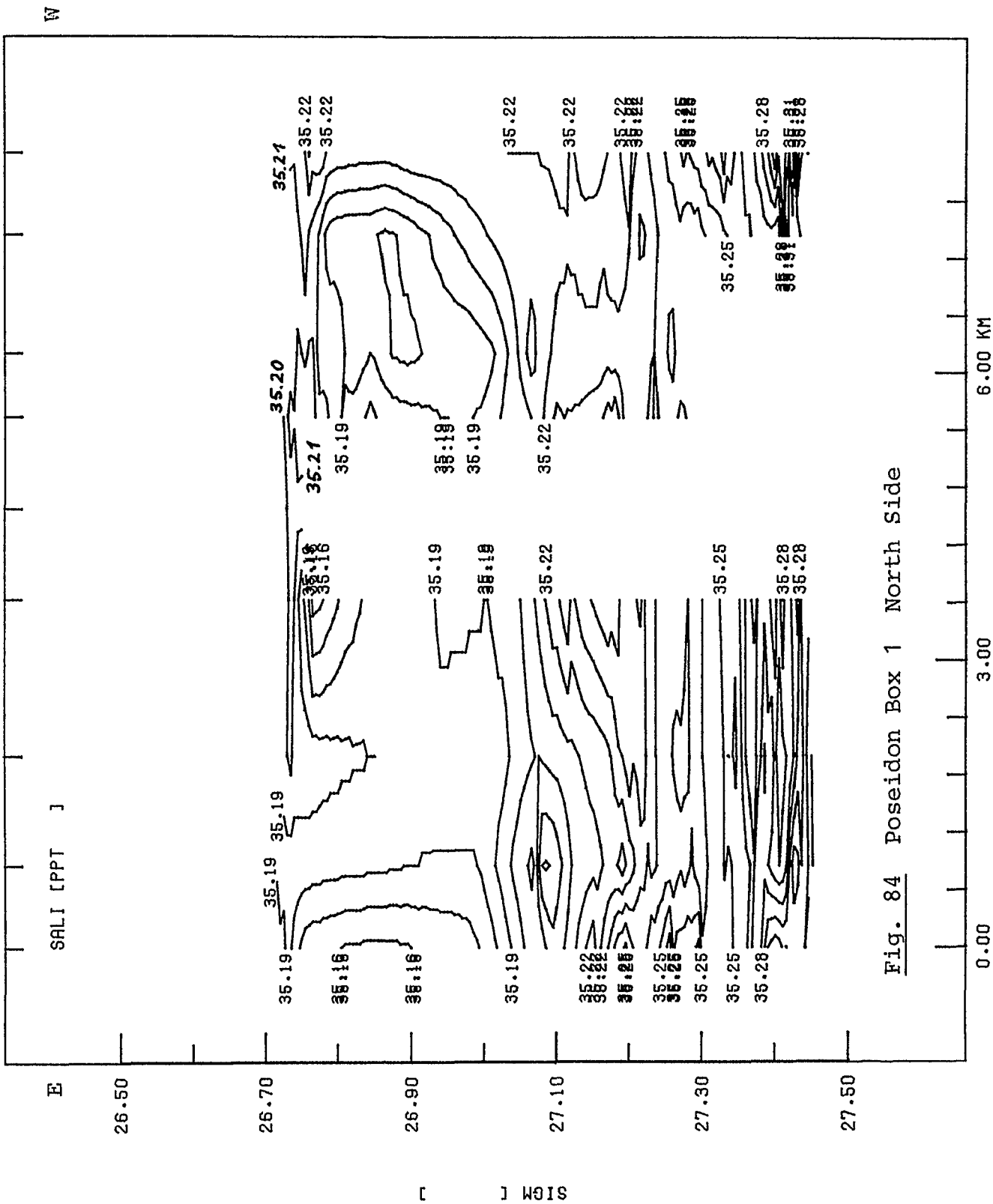

Fig. 84 Poseidon Box 1 North Side

PJC016

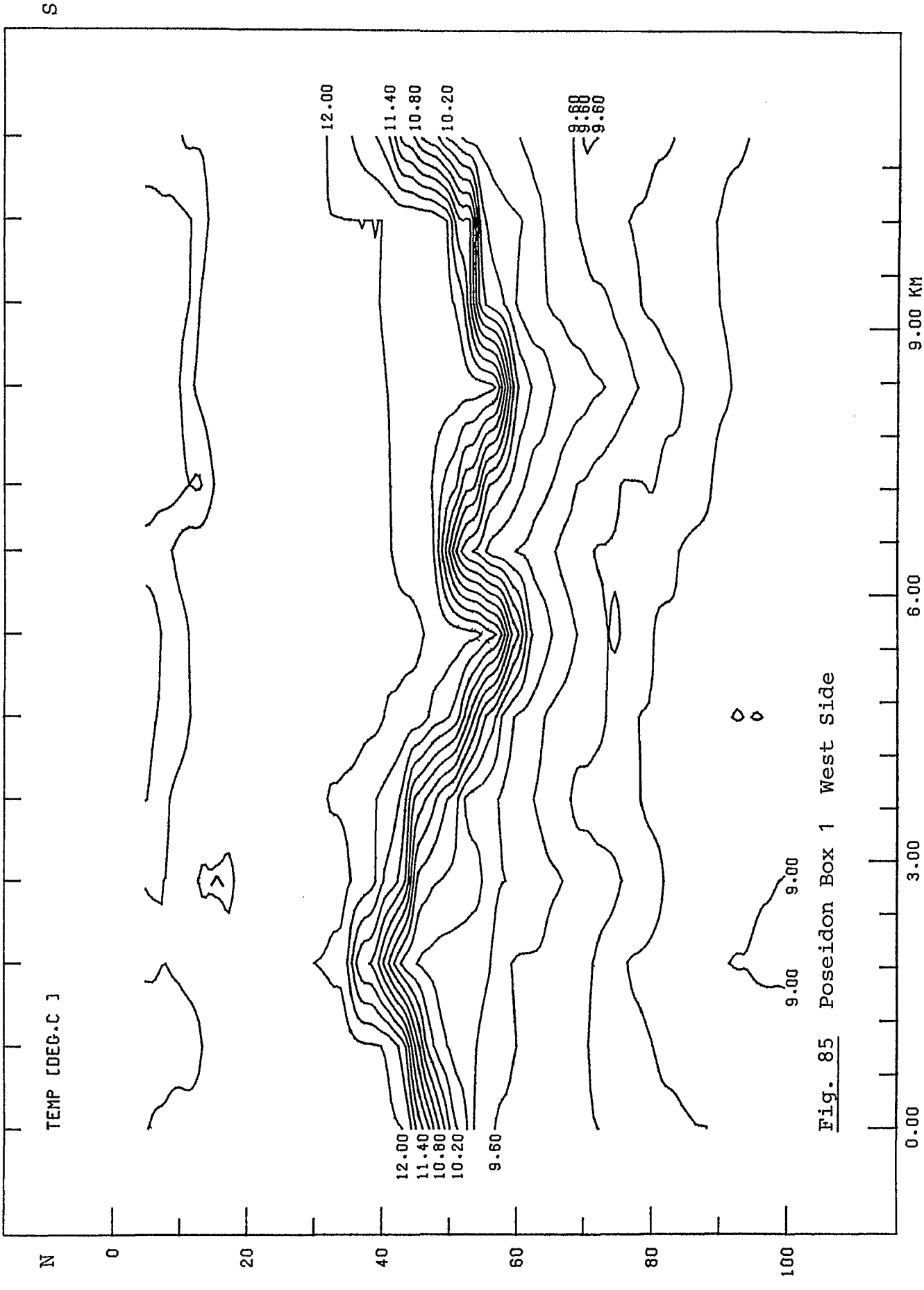

Fig. 85 Poseidon Box 1 West Side

PJC025T

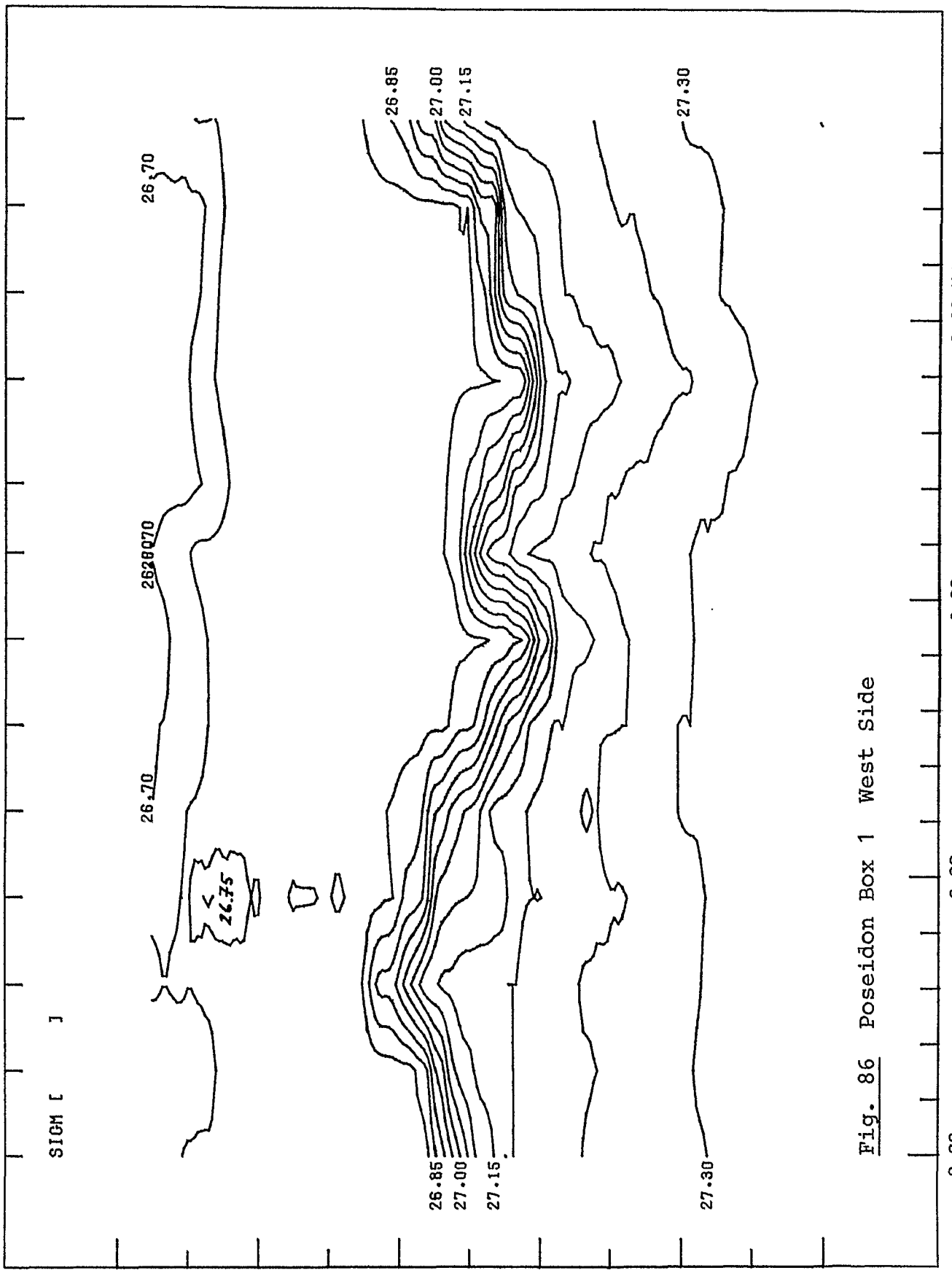

Fig. 86 Poseidon Box 1 West Side

PJC025T

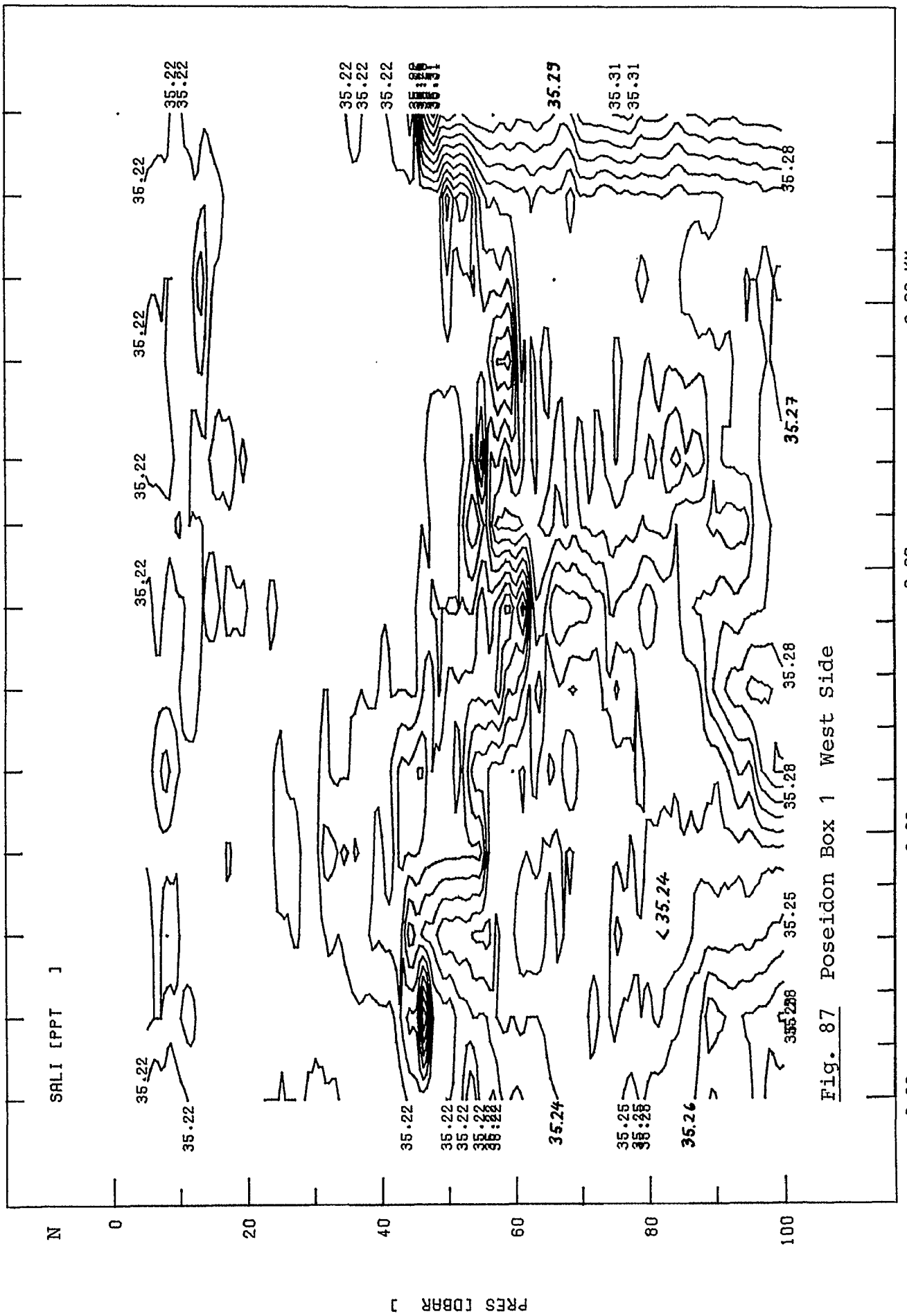

Fig. 87 Poseidon Box 1 West Side

PJC025T

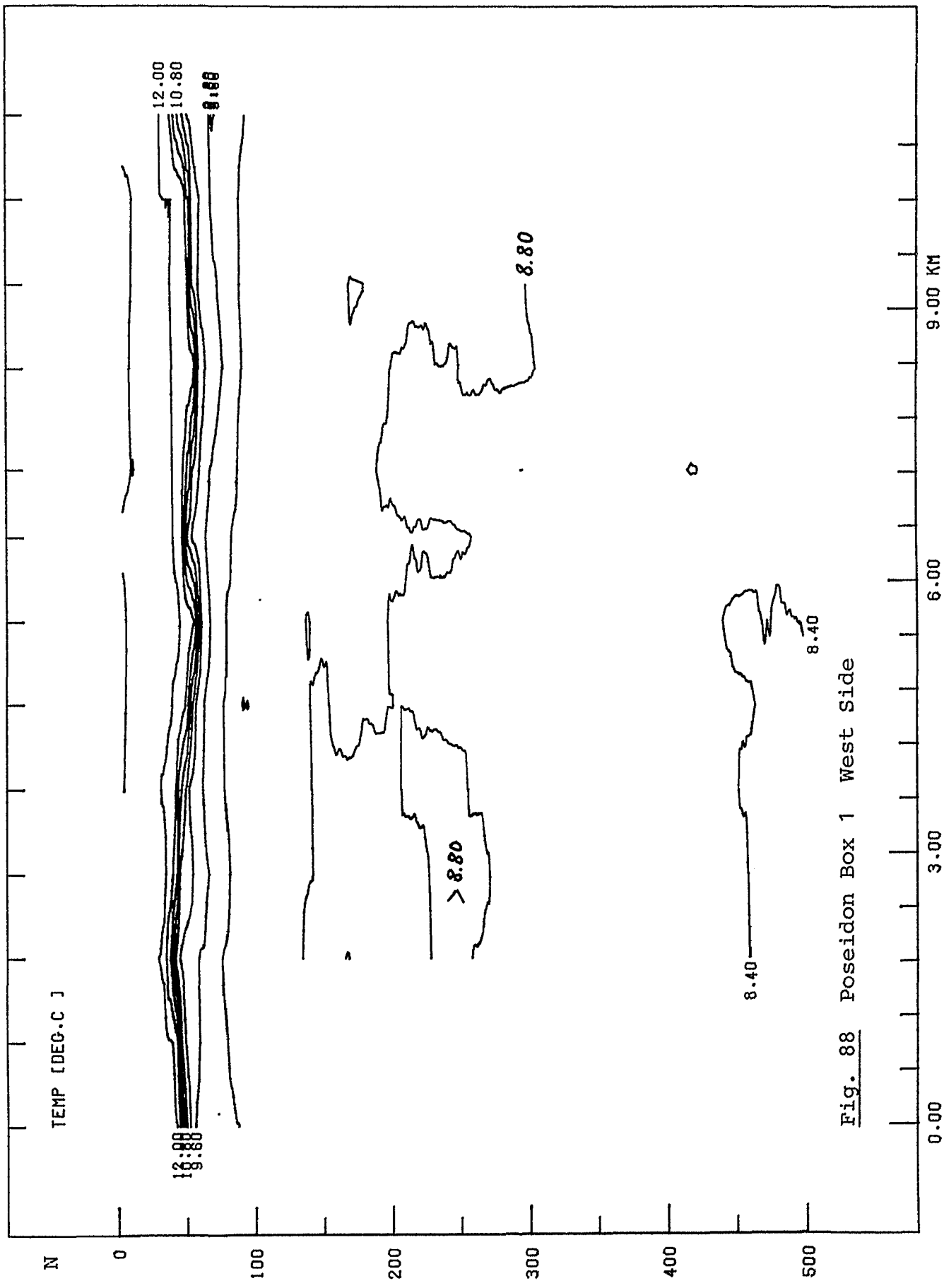

Fig. 88 Poseidon Box 1 West Side

PJC025T

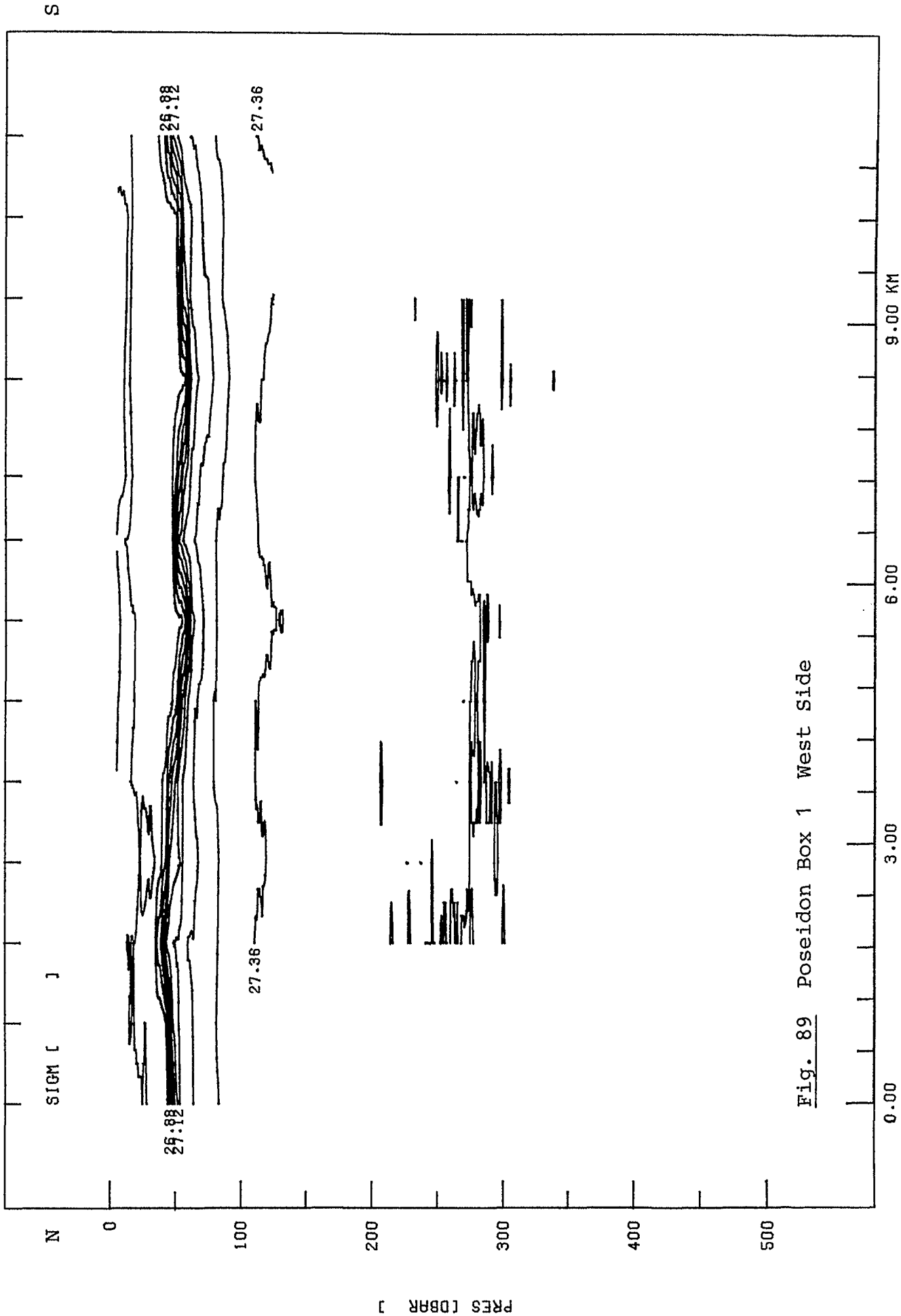

Fig. 89 Poseidon Box 1 West Side

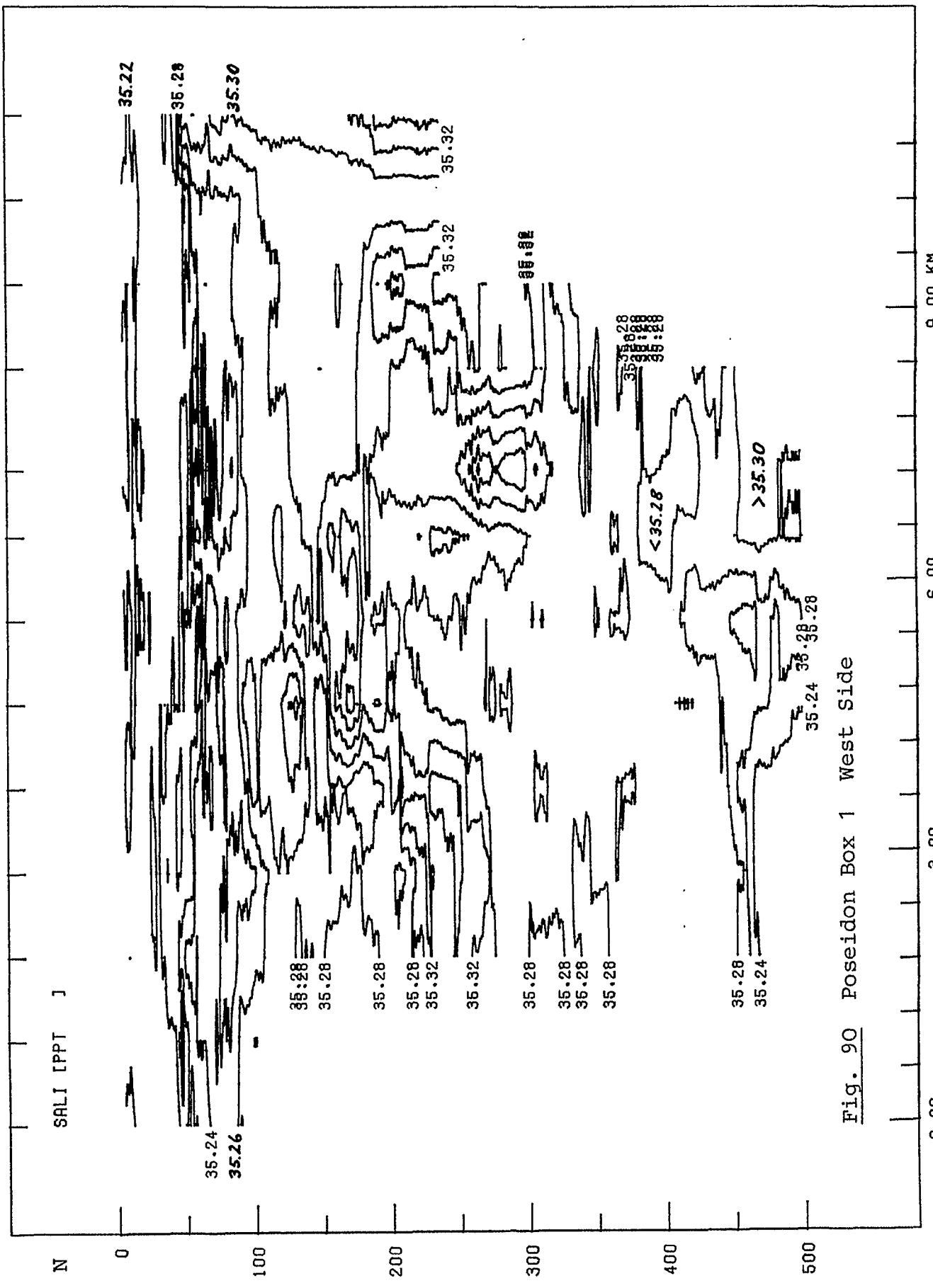

Fig. 90 Poseidon Box 1 West Side

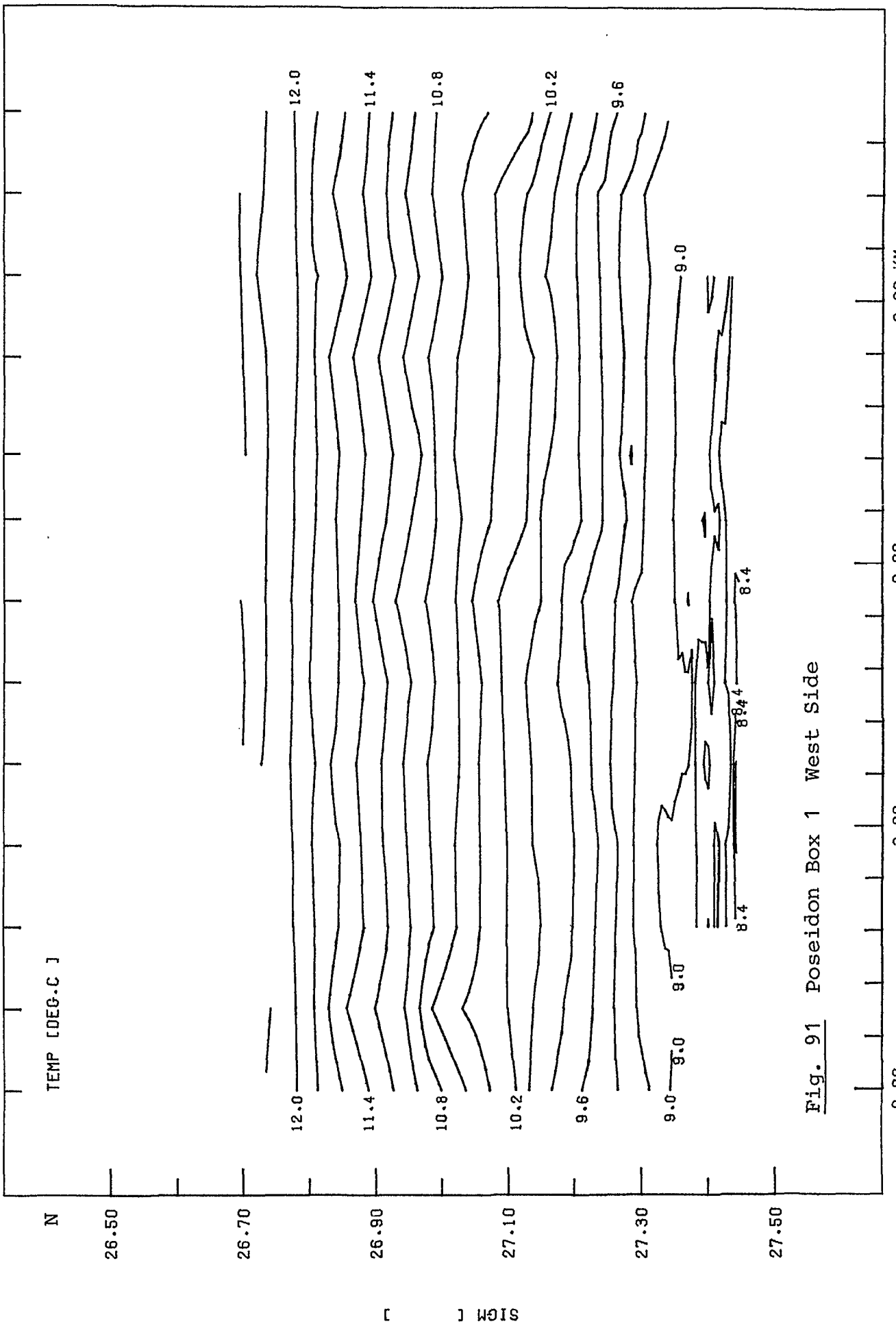

Fig. 91 Poseidon Box 1 West Side

PJC025

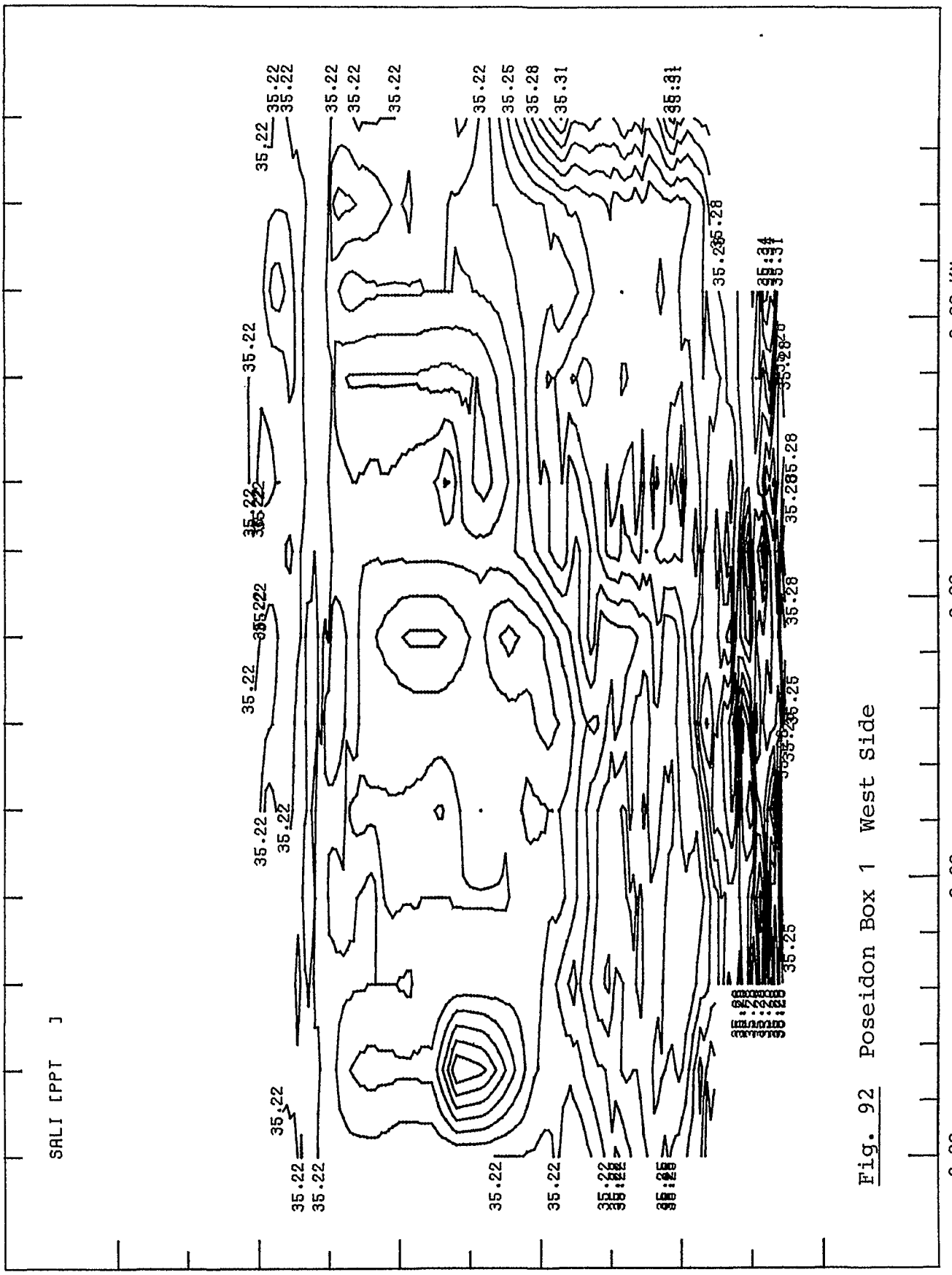

Fig. 92 Poseidon Box 1 West Side

PJC025

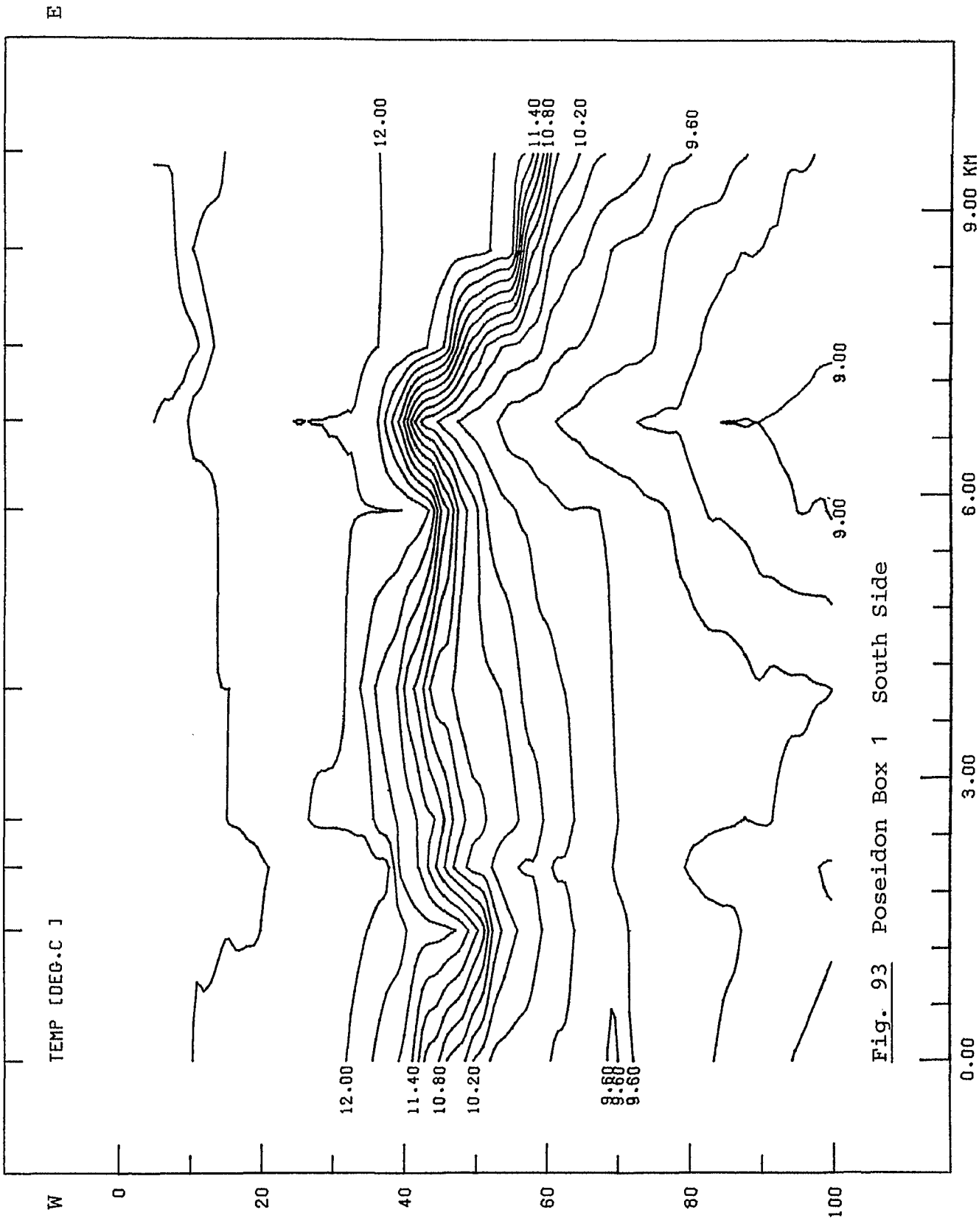

Fig. 93 Poseidon Box 1 South Side

PJC037T

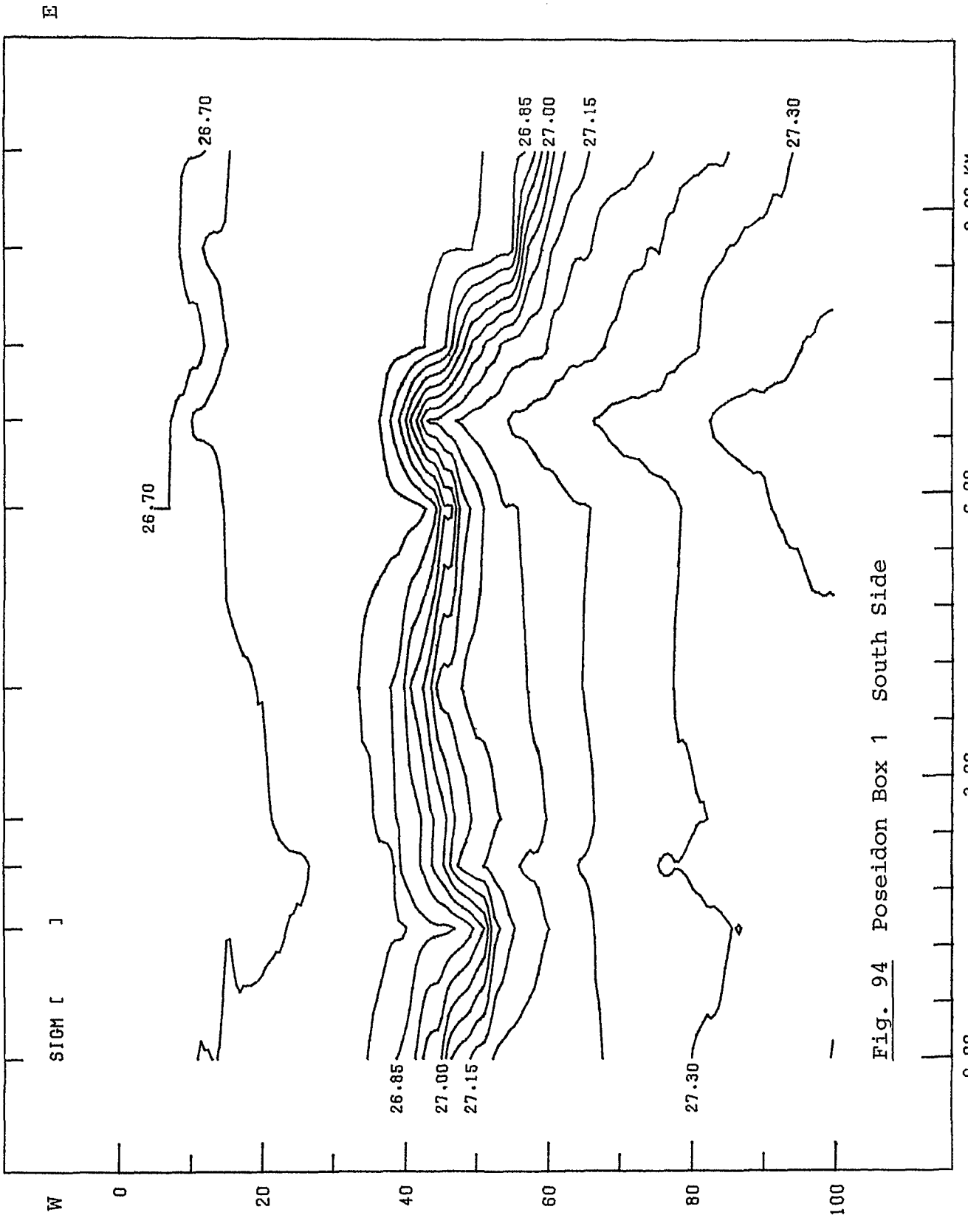

Fig. 94 Poseidon Box 1 South Side

PJC037T

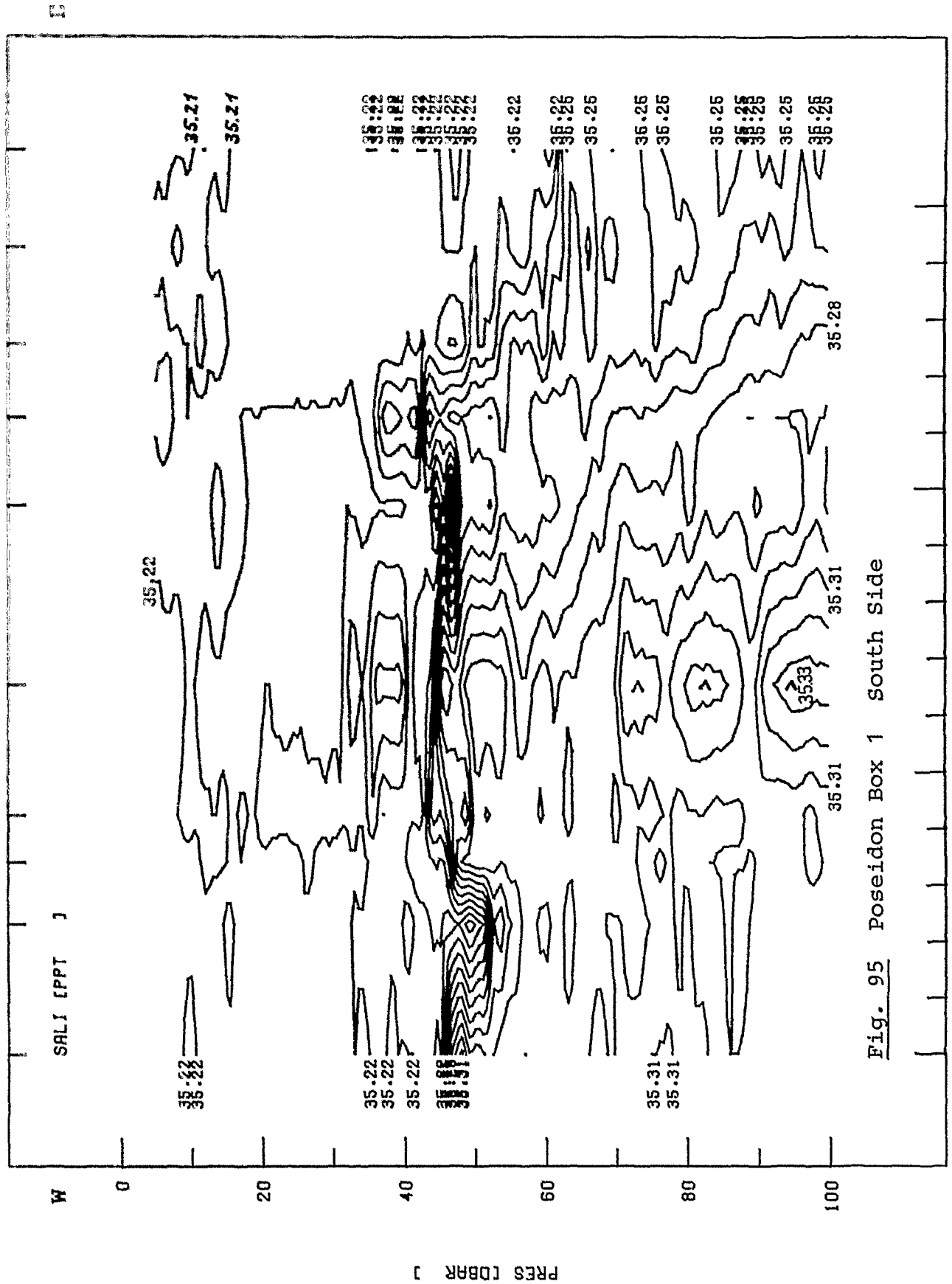

Fig. 95 Poseidon Box 1 South Side

PJC037T

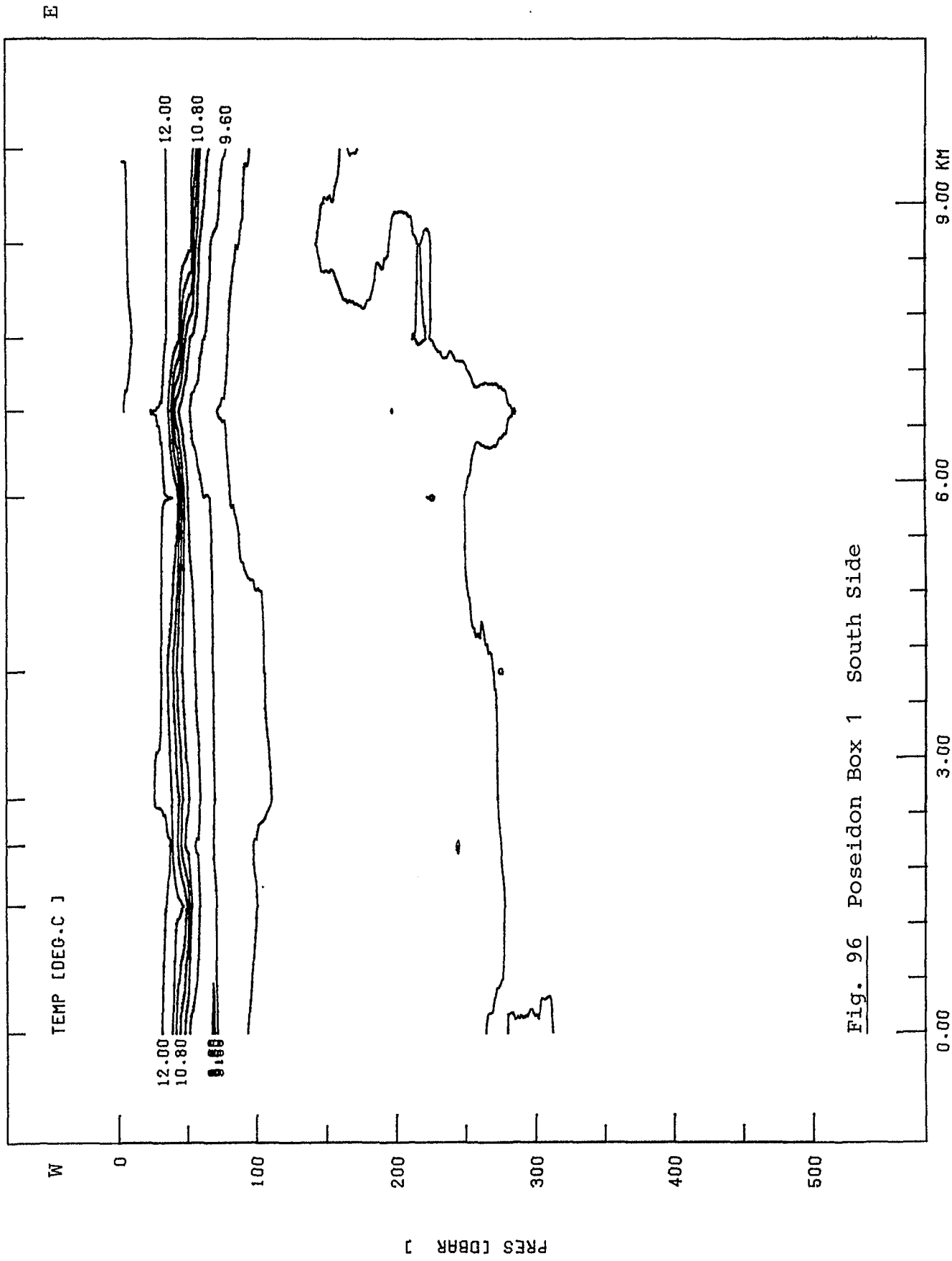

Fig. 96 Poseidon Box 1 South Side

PJC037T

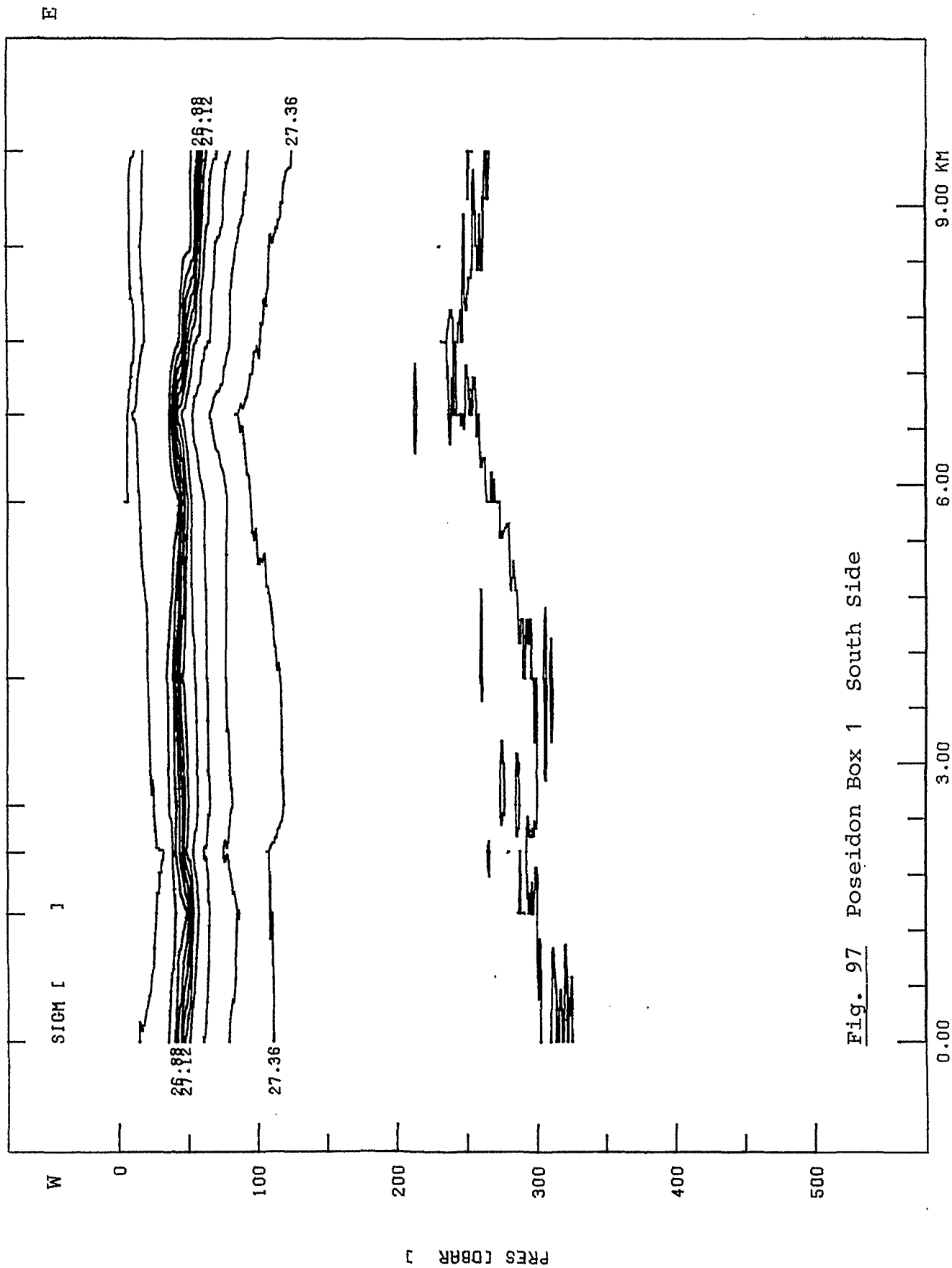

Fig. 97 Poseidon Box 1 South Side

PJC037T

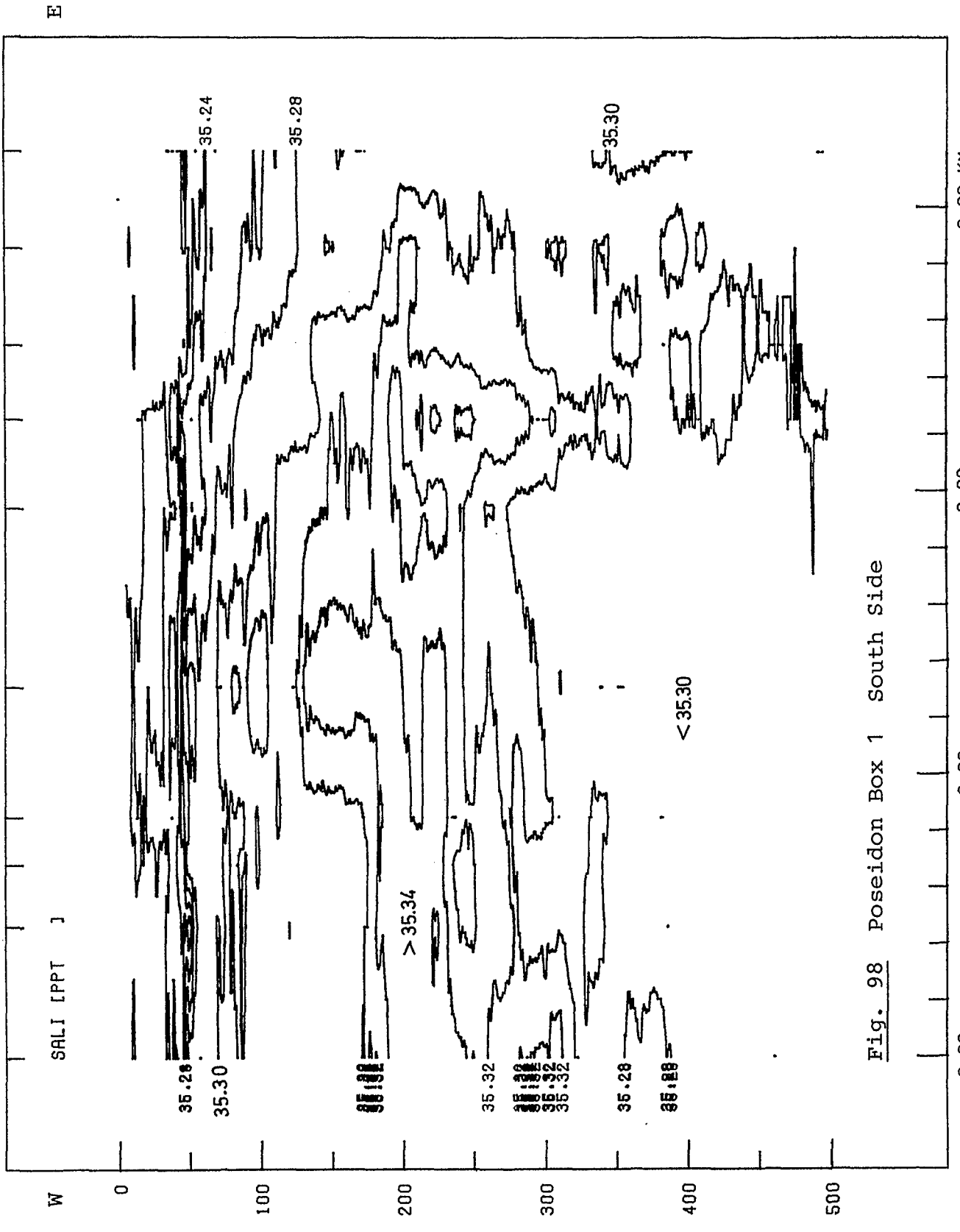

Fig. 98 Poseidon Box 1 South Side

PJC037T

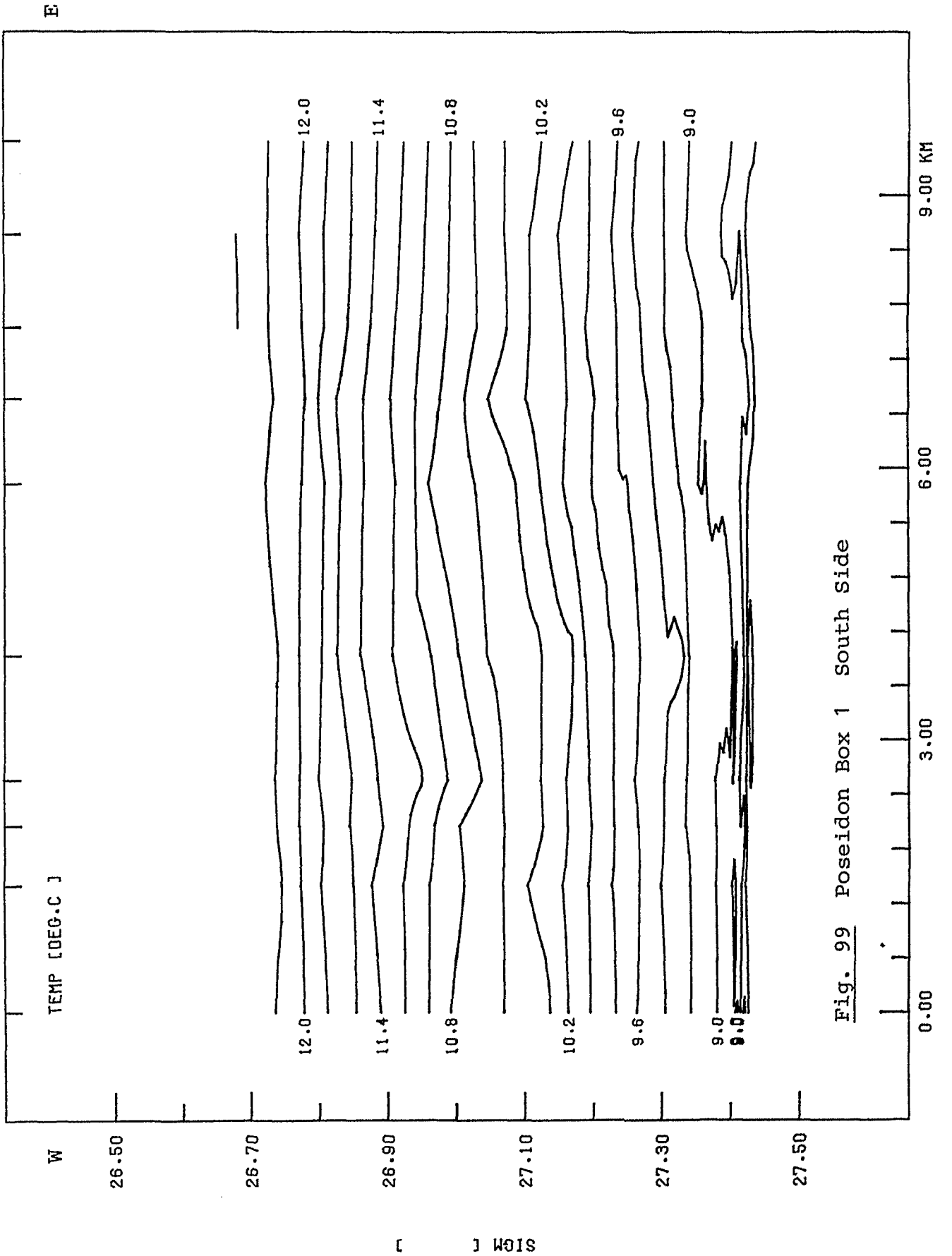

Fig. 99 Poseidon Box 1 South Side

PJC037

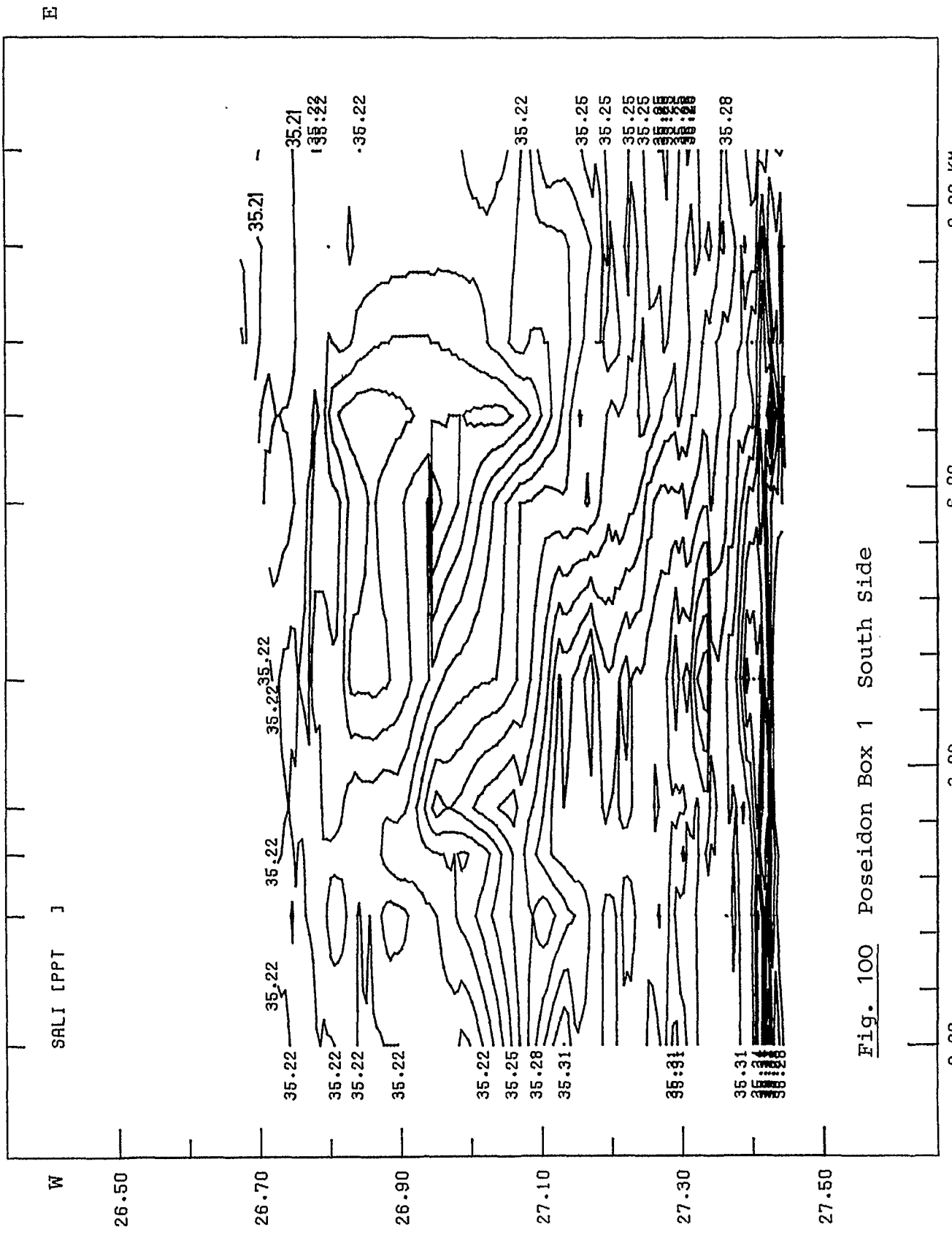

Fig. 100 Poseidon Box 1 South Side

PJC037

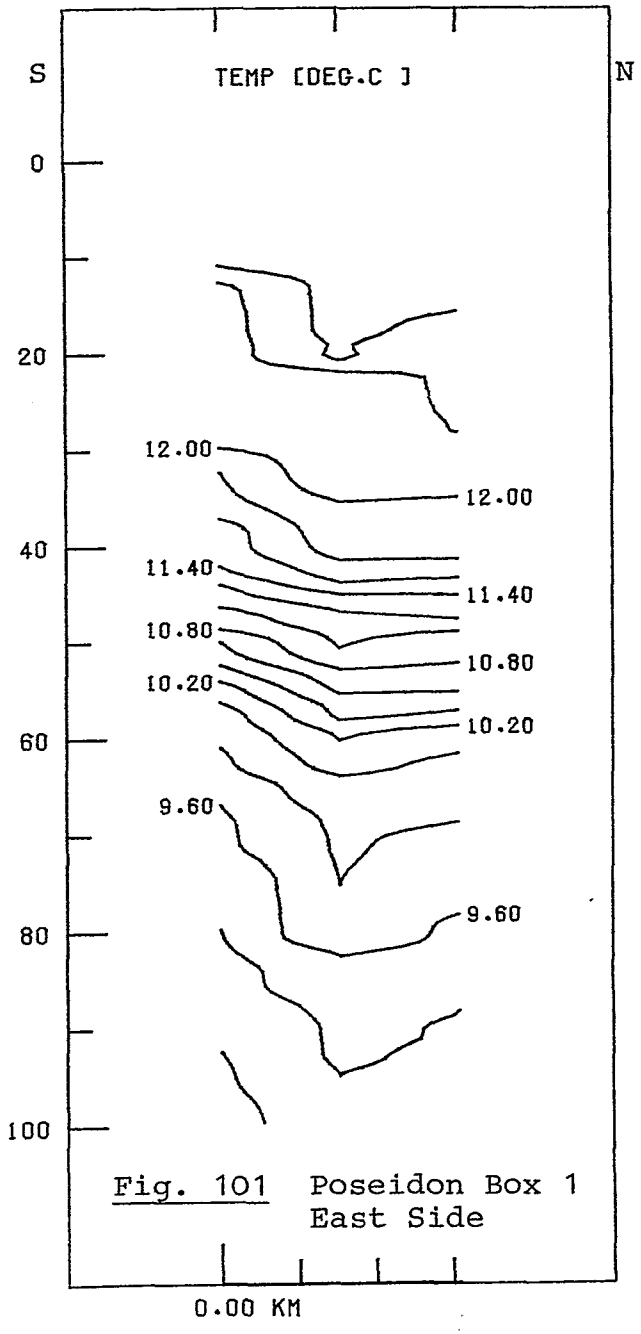

Fig. 101 Poseidon Box 1
East Side

PJC048T

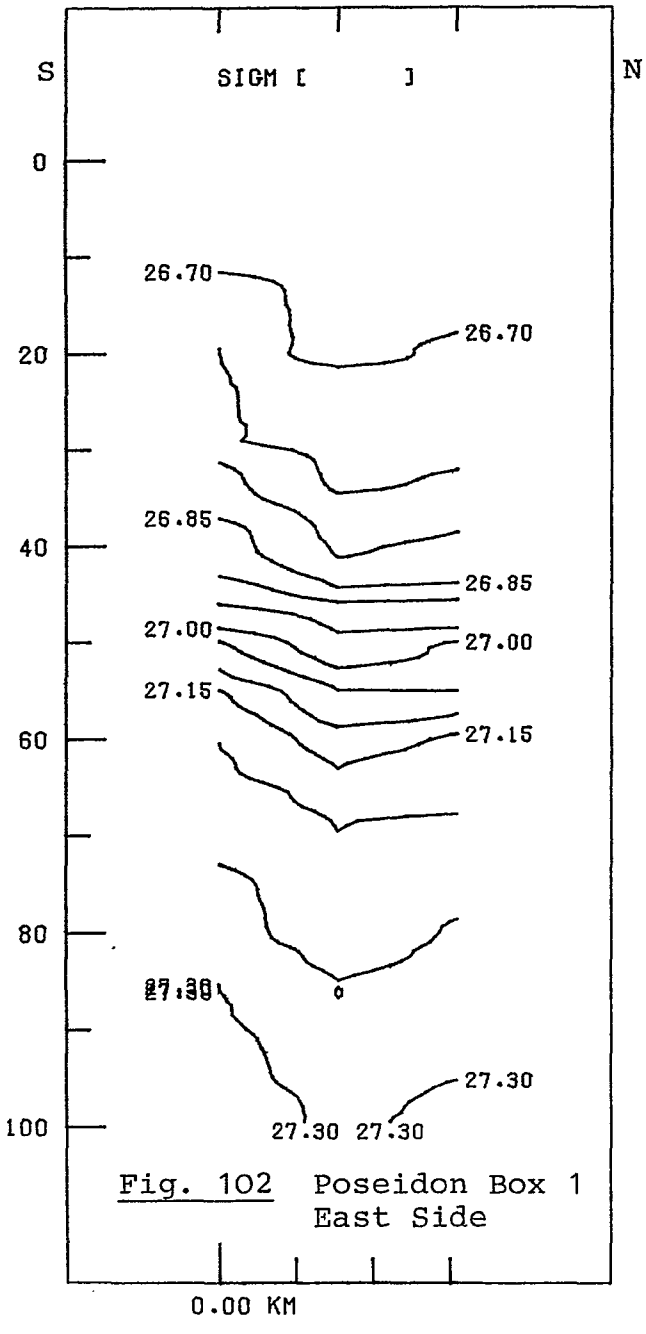

Fig. 102 Poseidon Box 1
East Side

PJC048T

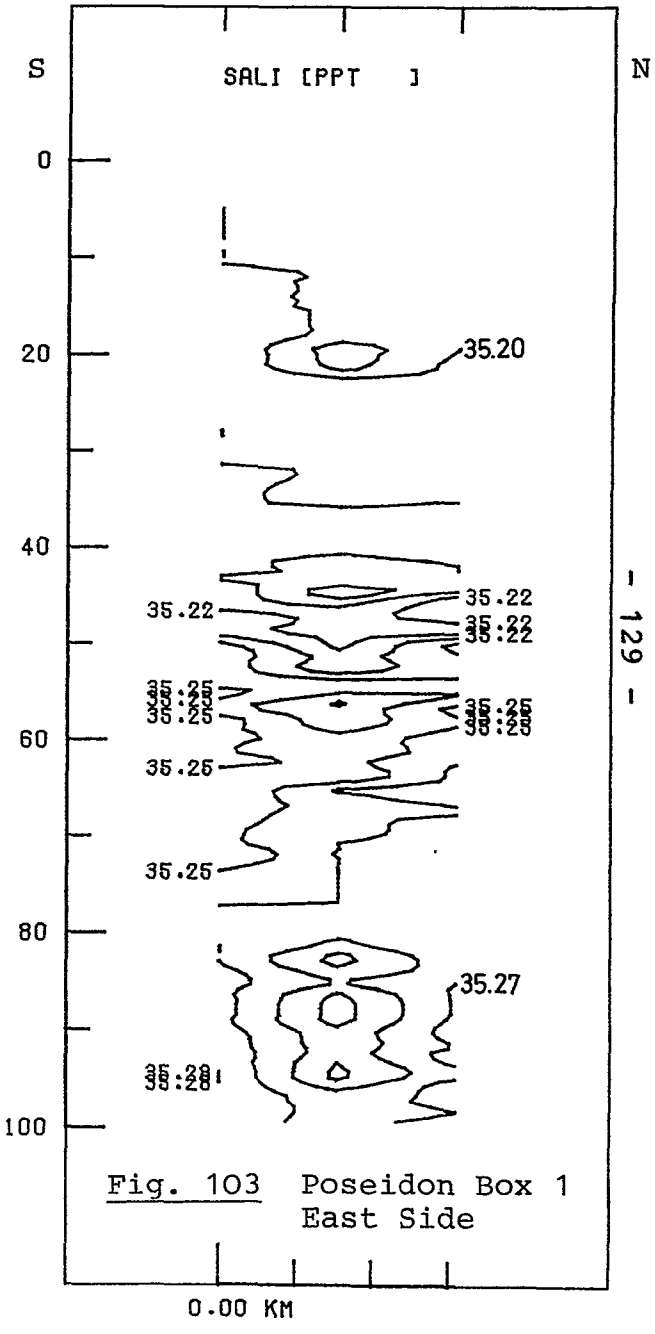

Fig. 103 Poseidon Box 1
East Side

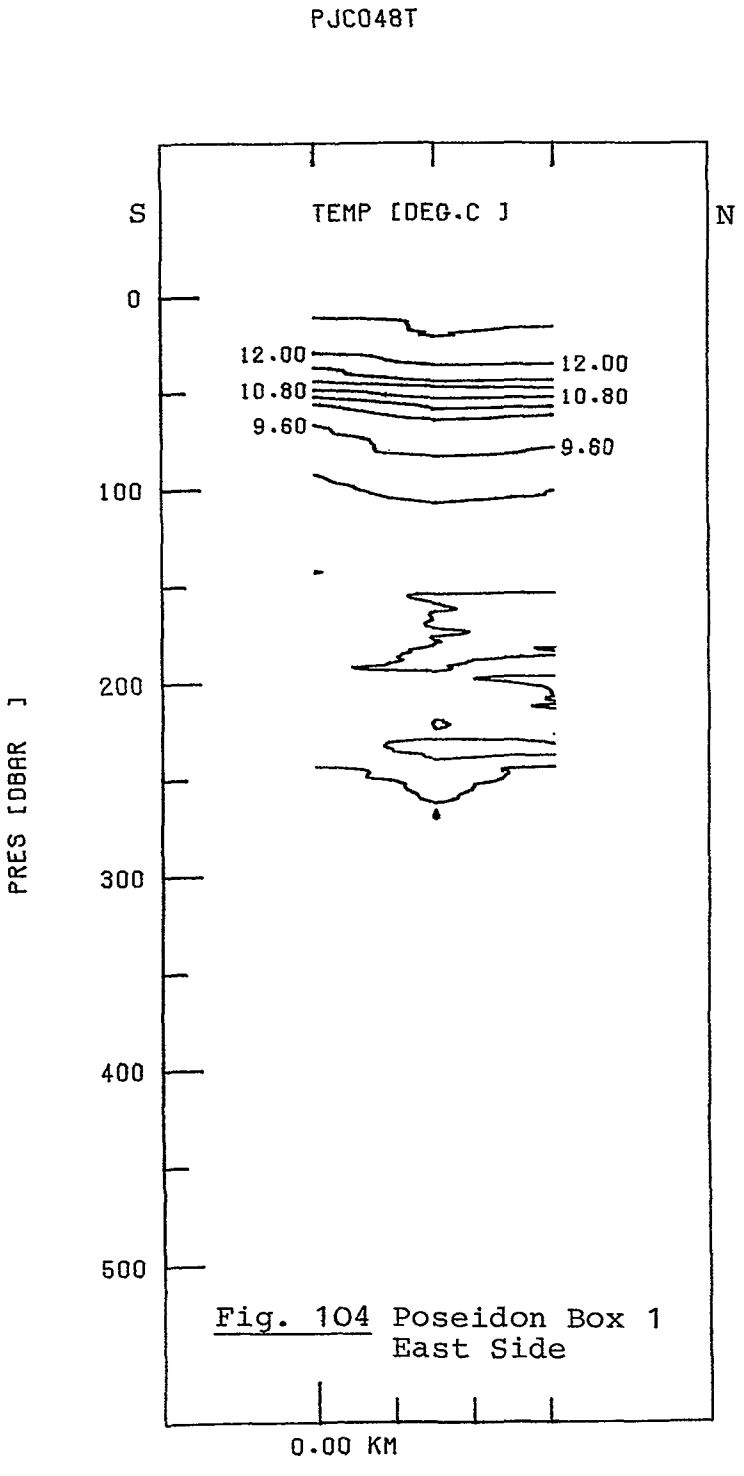

Fig. 104 Poseidon Box 1
East Side

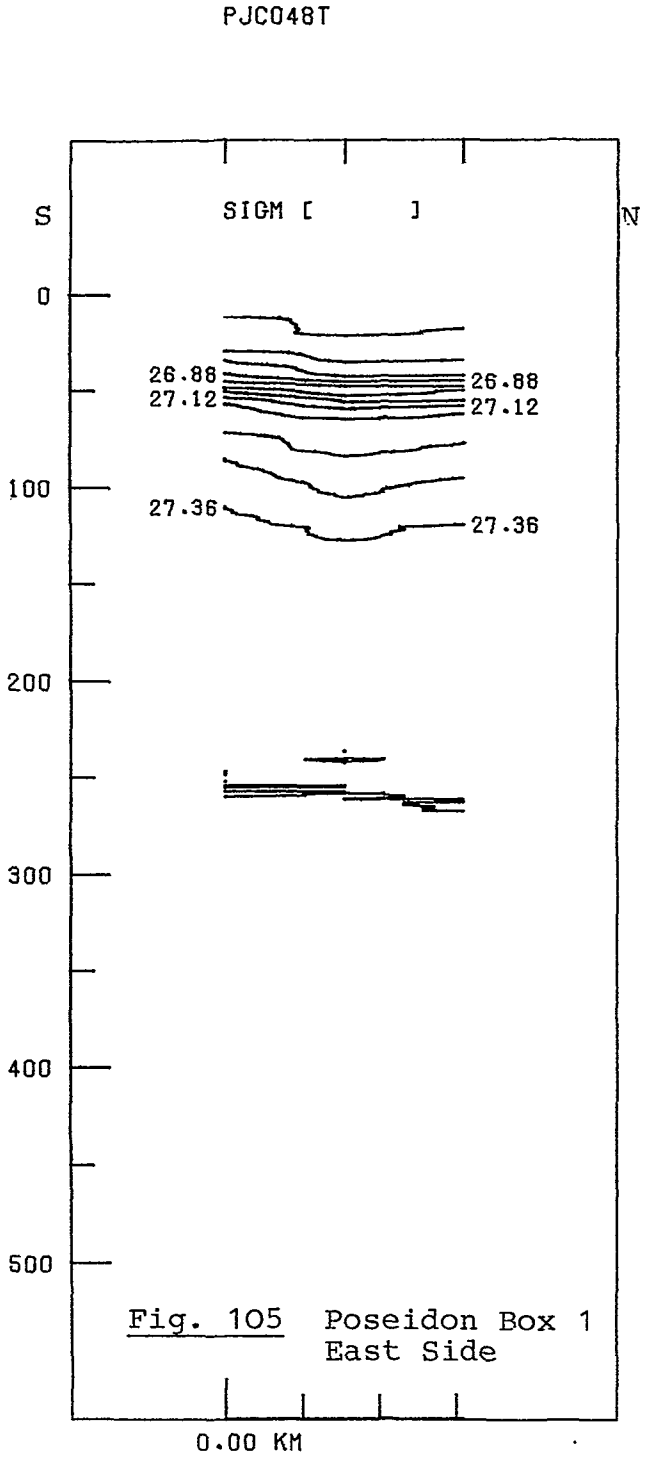

Fig. 105 Poseidon Box 1
East Side

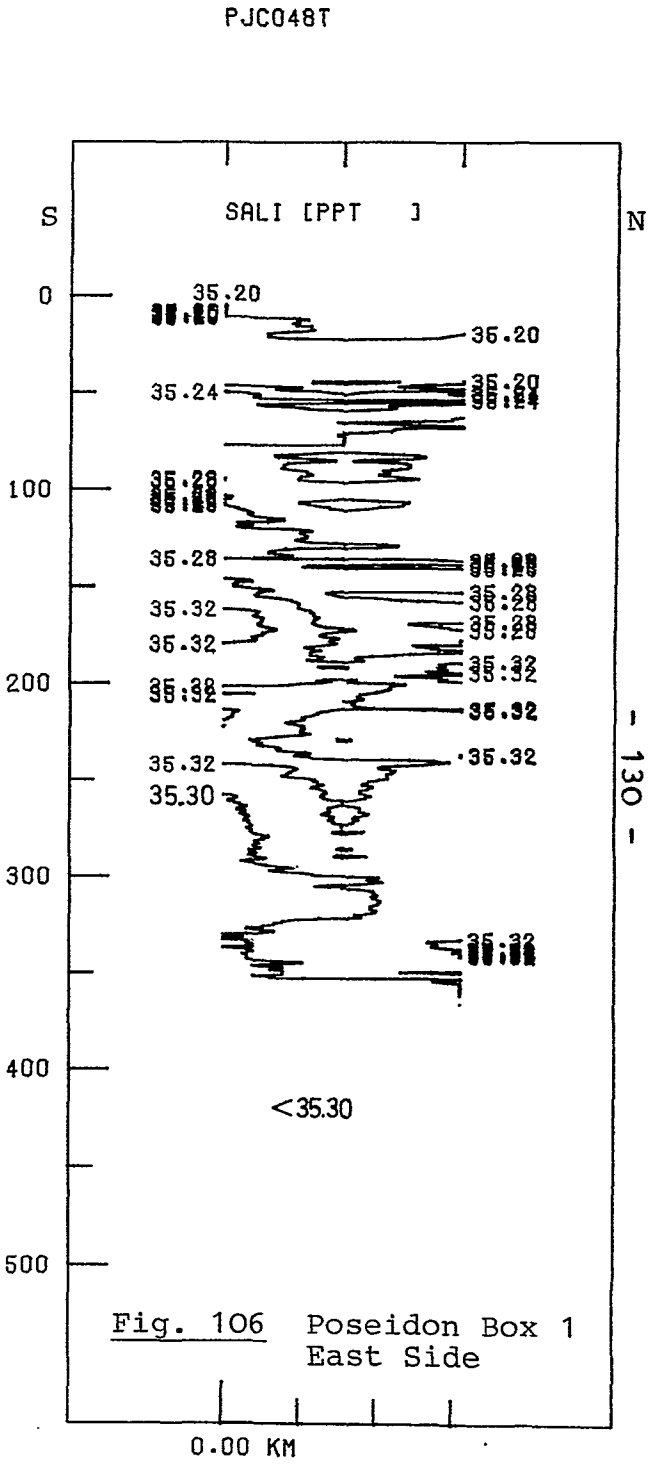

Fig. 106 Poseidon Box 1
East Side

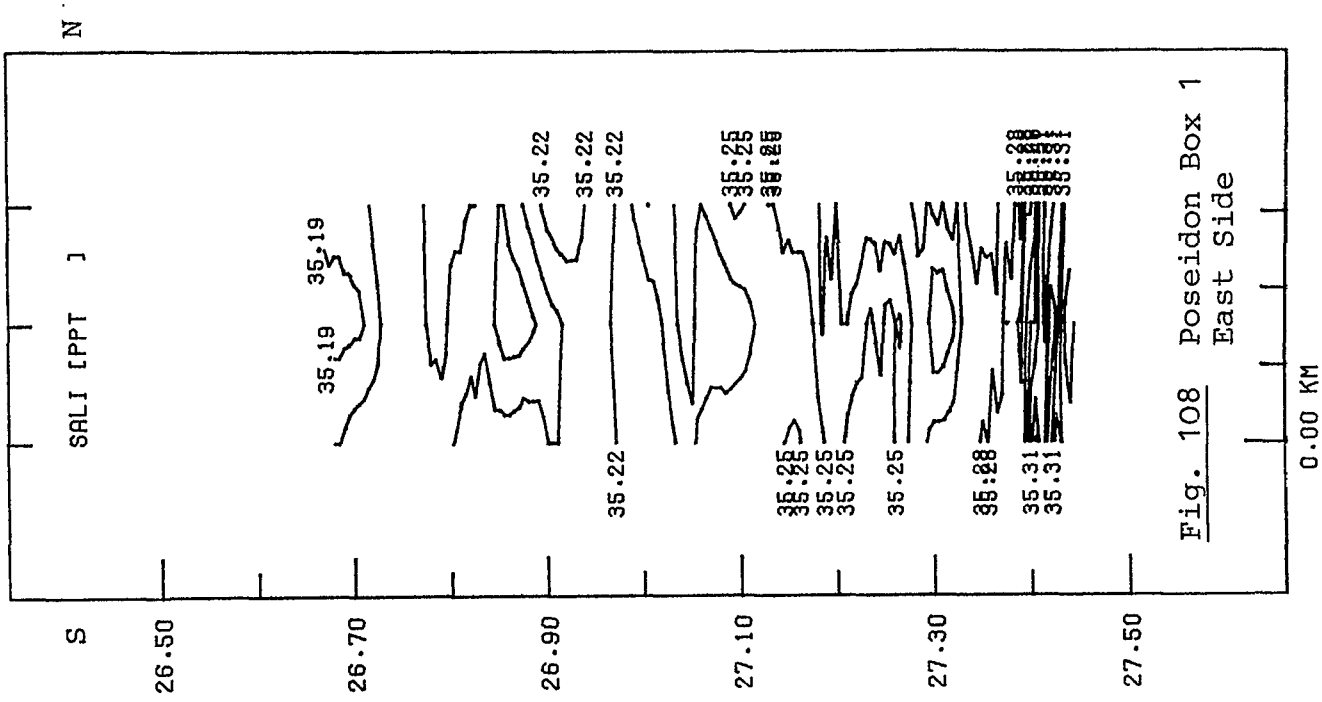

Fig. 108 Poseidon Box 1
East Side

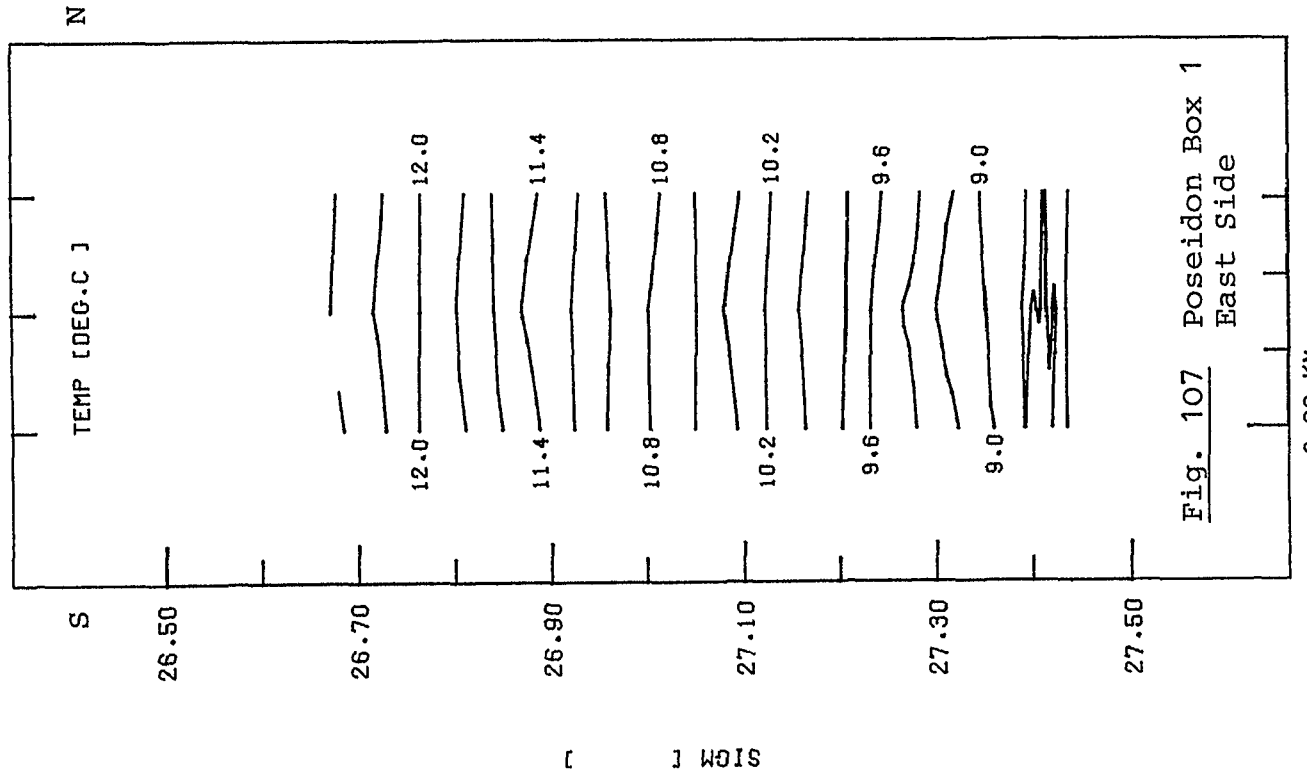

Fig. 107 Poseidon Box 1
East Side

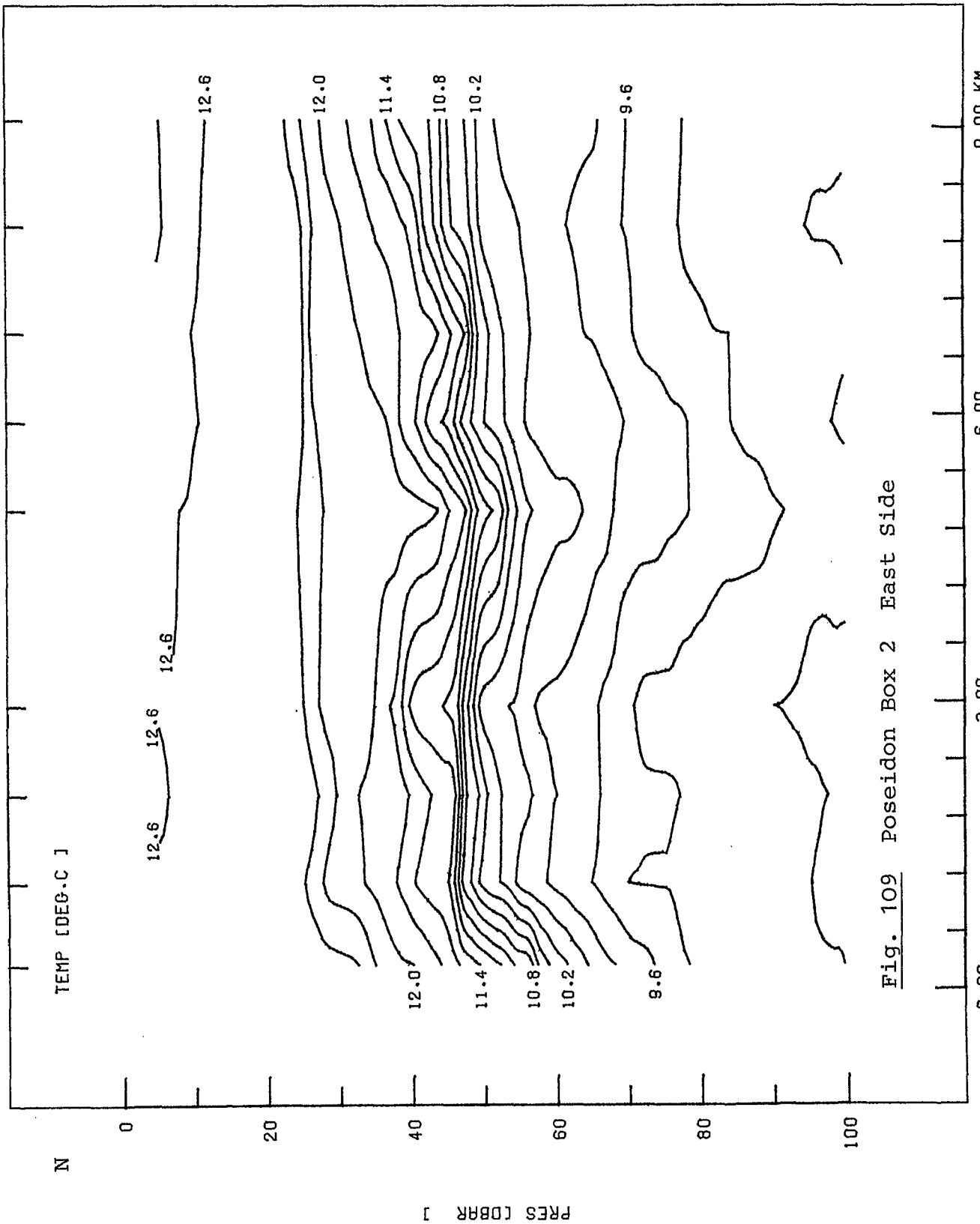

Fig. 109 Poseidon Box 2 East Side

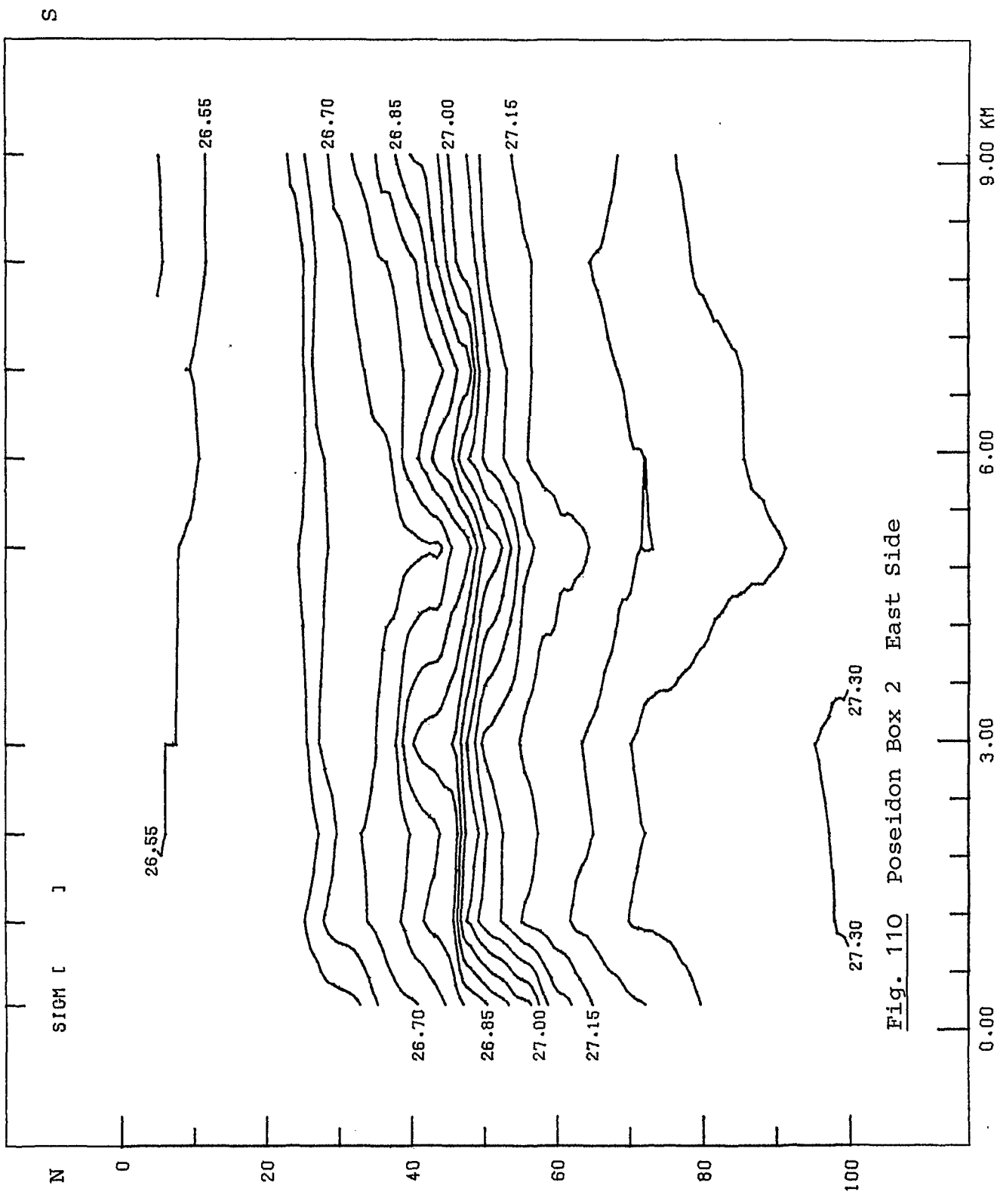

Fig. 110 Poseidon Box 2 East Side

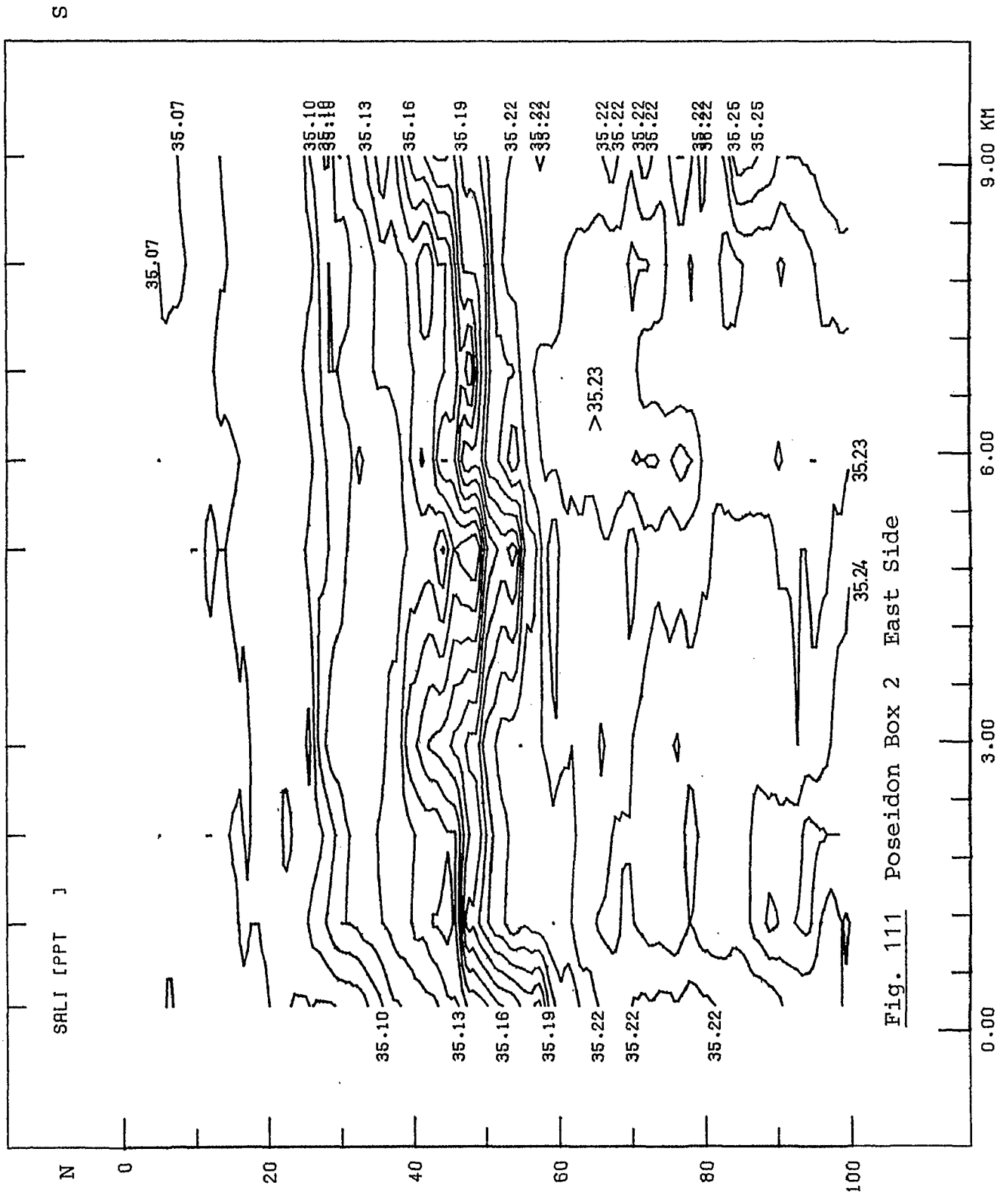

Fig. 111 Poseidon Box 2 East Side

PJC062T

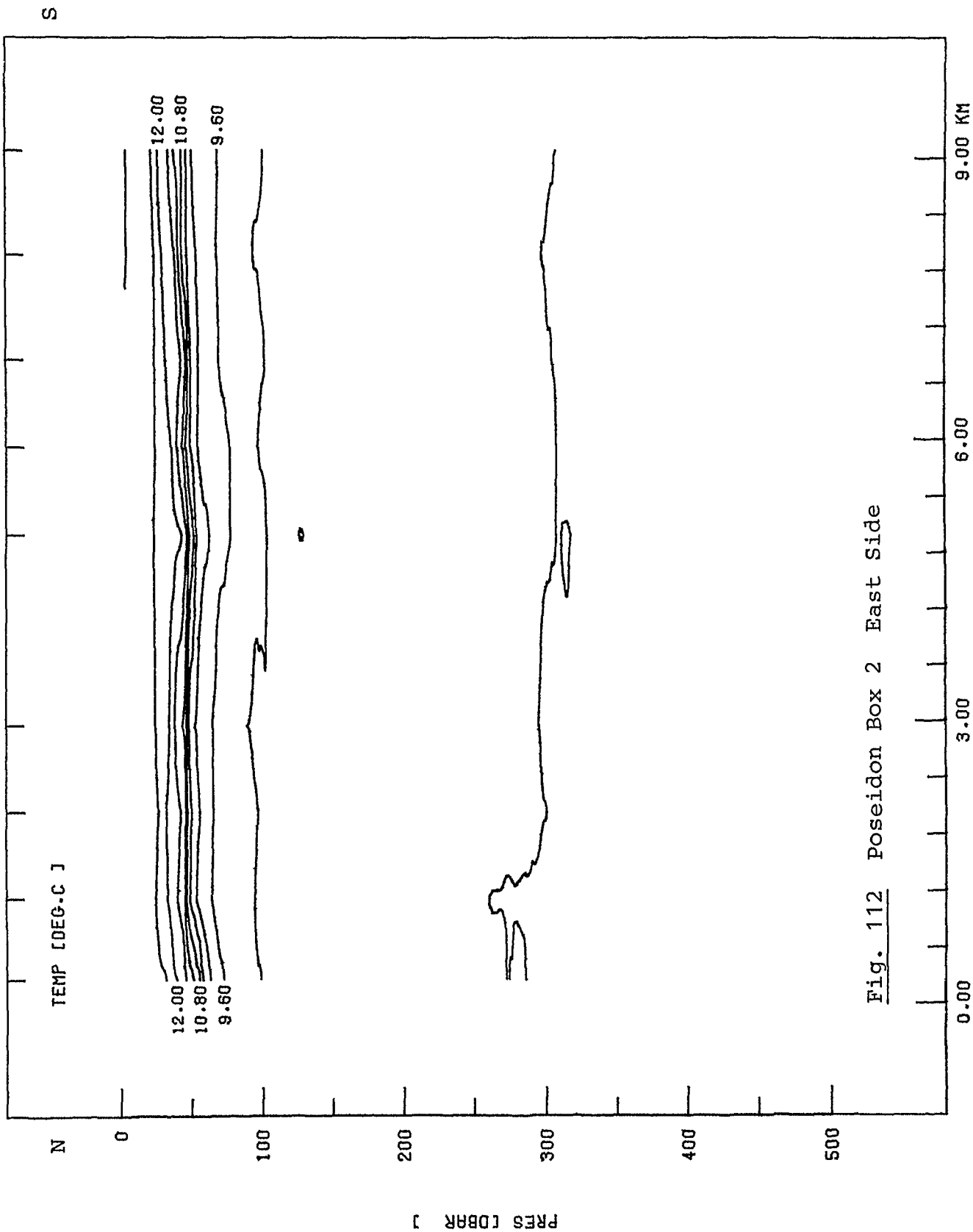

Fig. 112 Poseidon Box 2 East Side

PJC062T

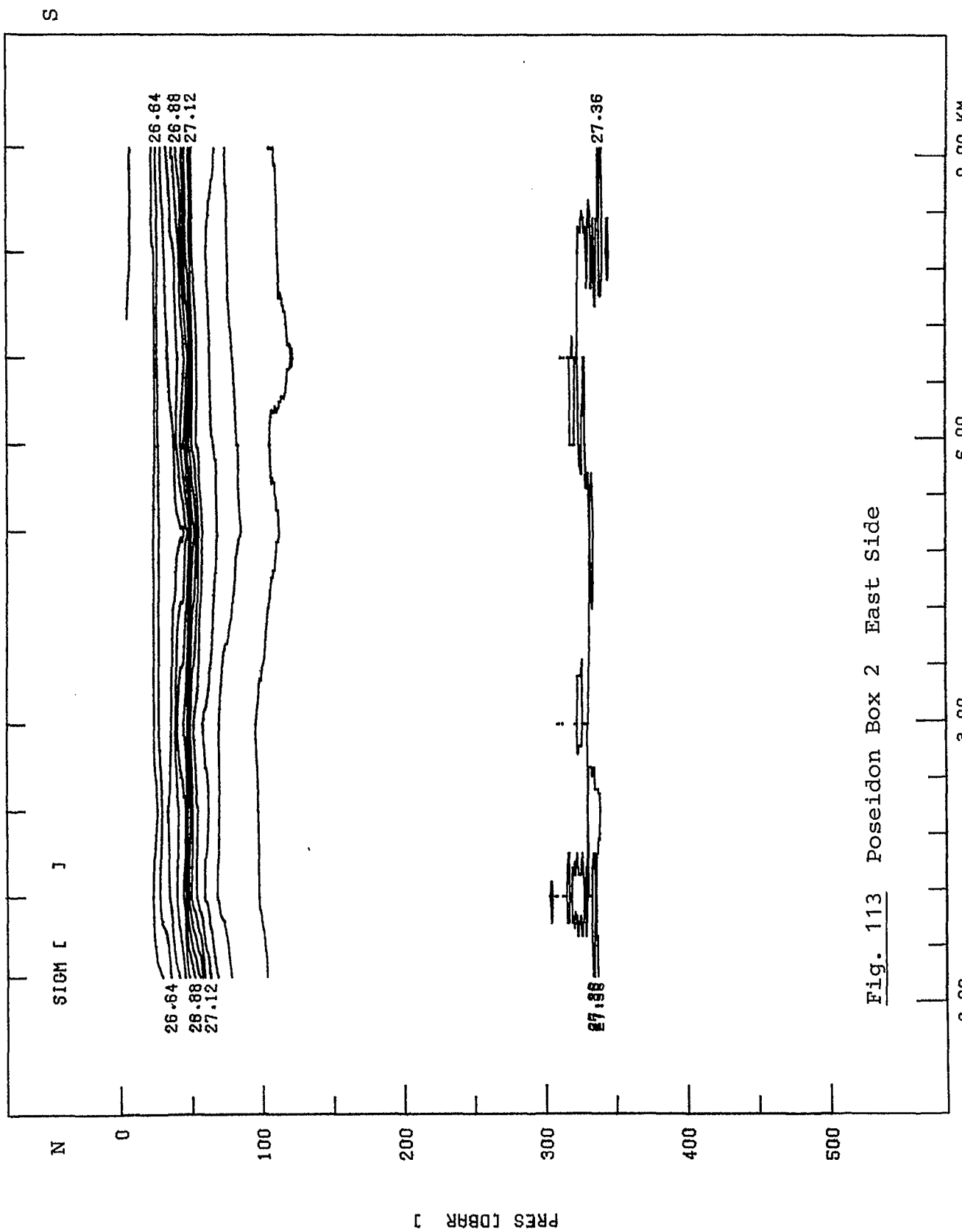

Fig. 113 Poseidon Box 2 East Side

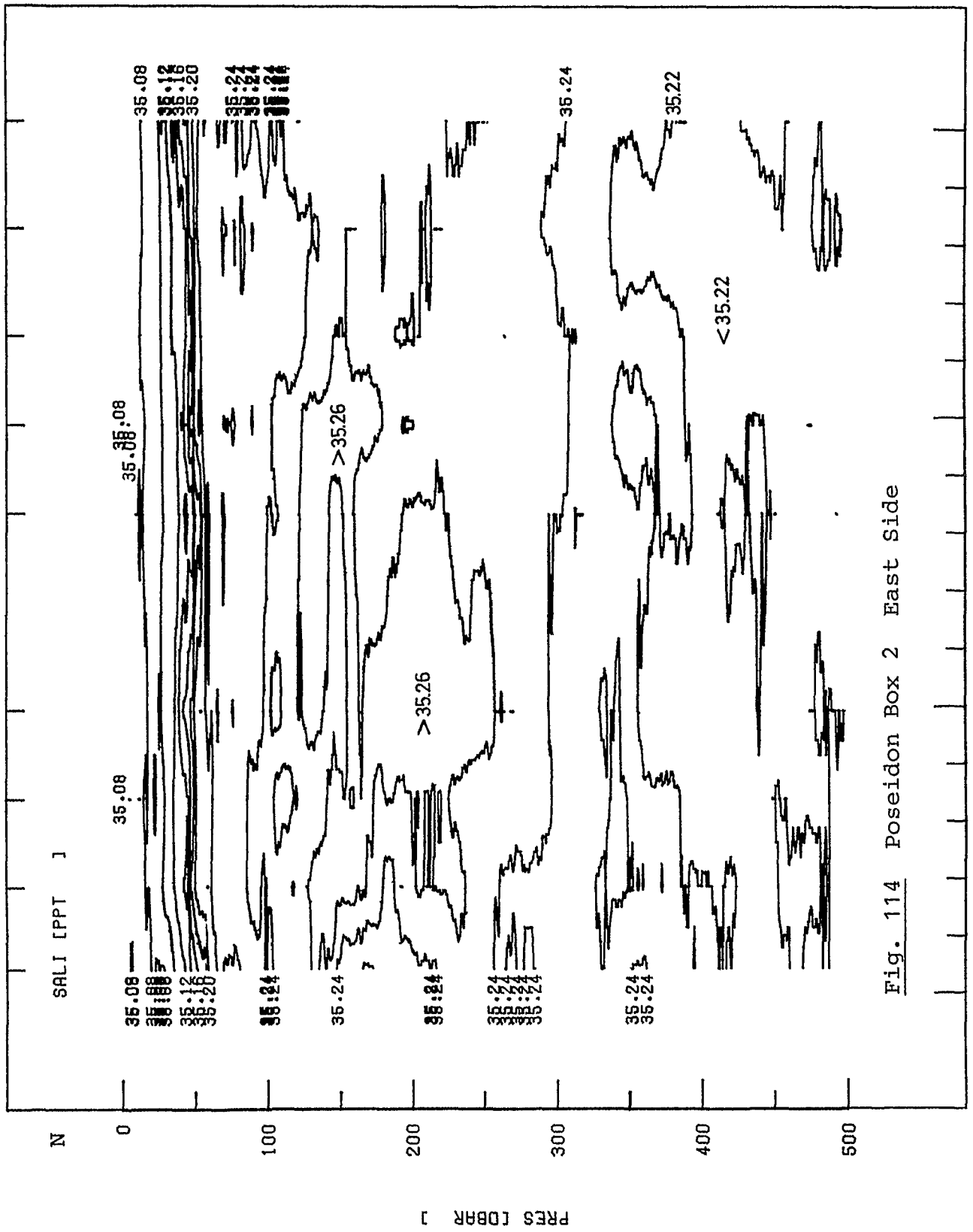
S
N
SALI [PPT]
PRES [DBAR]
0
100
200
300
400
500
0.00
3.00
6.00
9.00 KM
35.08
35.12
35.16
35.20
35.24
>35.26
<35.22
Fig. 114 Poseidon Box 2 East Side

PJC062T

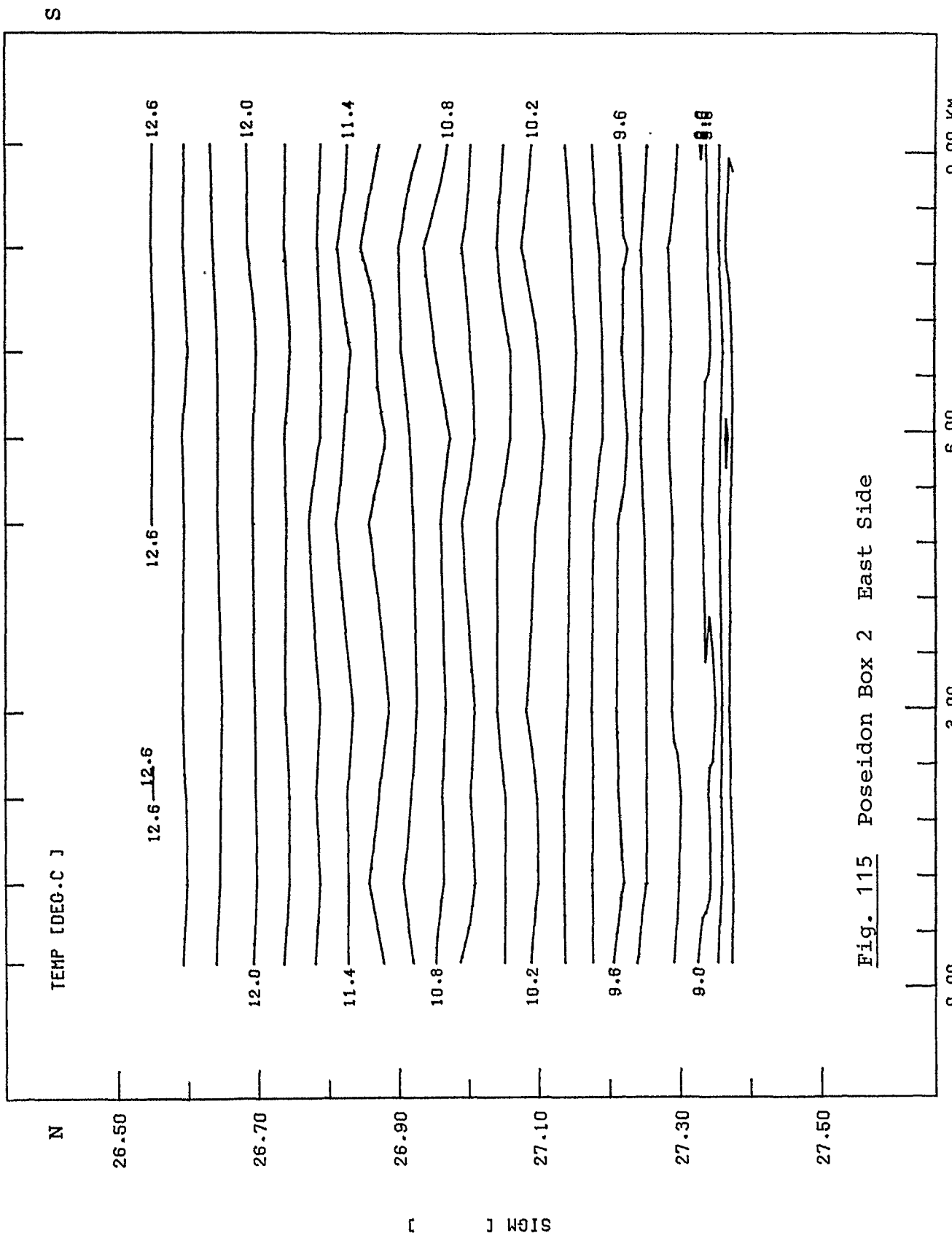

Fig. 115 Poseidon Box 2 East Side

P1501D

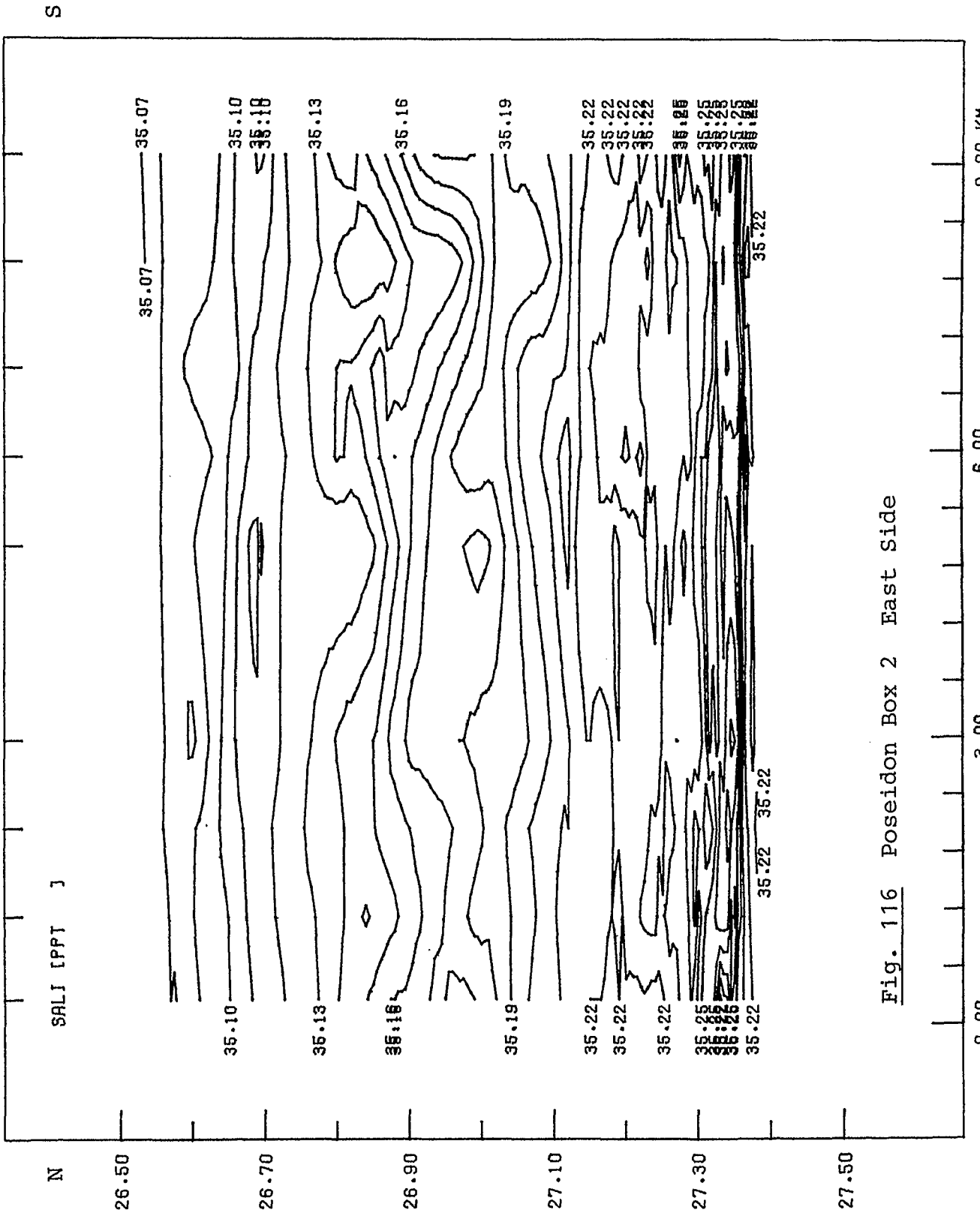

Fig. 116 Poseidon Box 2 East Side

P1501D

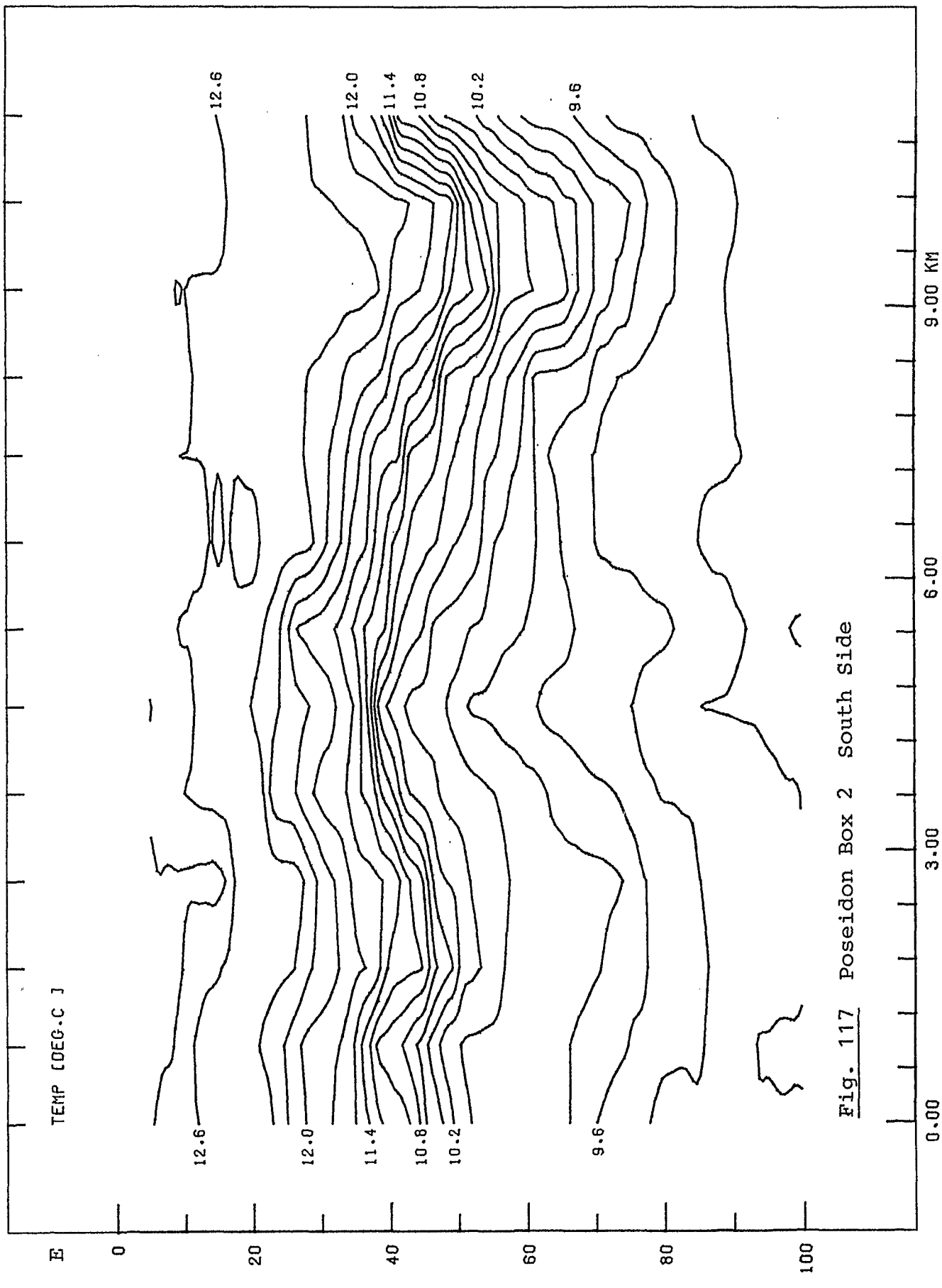

Fig. 117 Poseidon Box 2 South Side

PJC071T

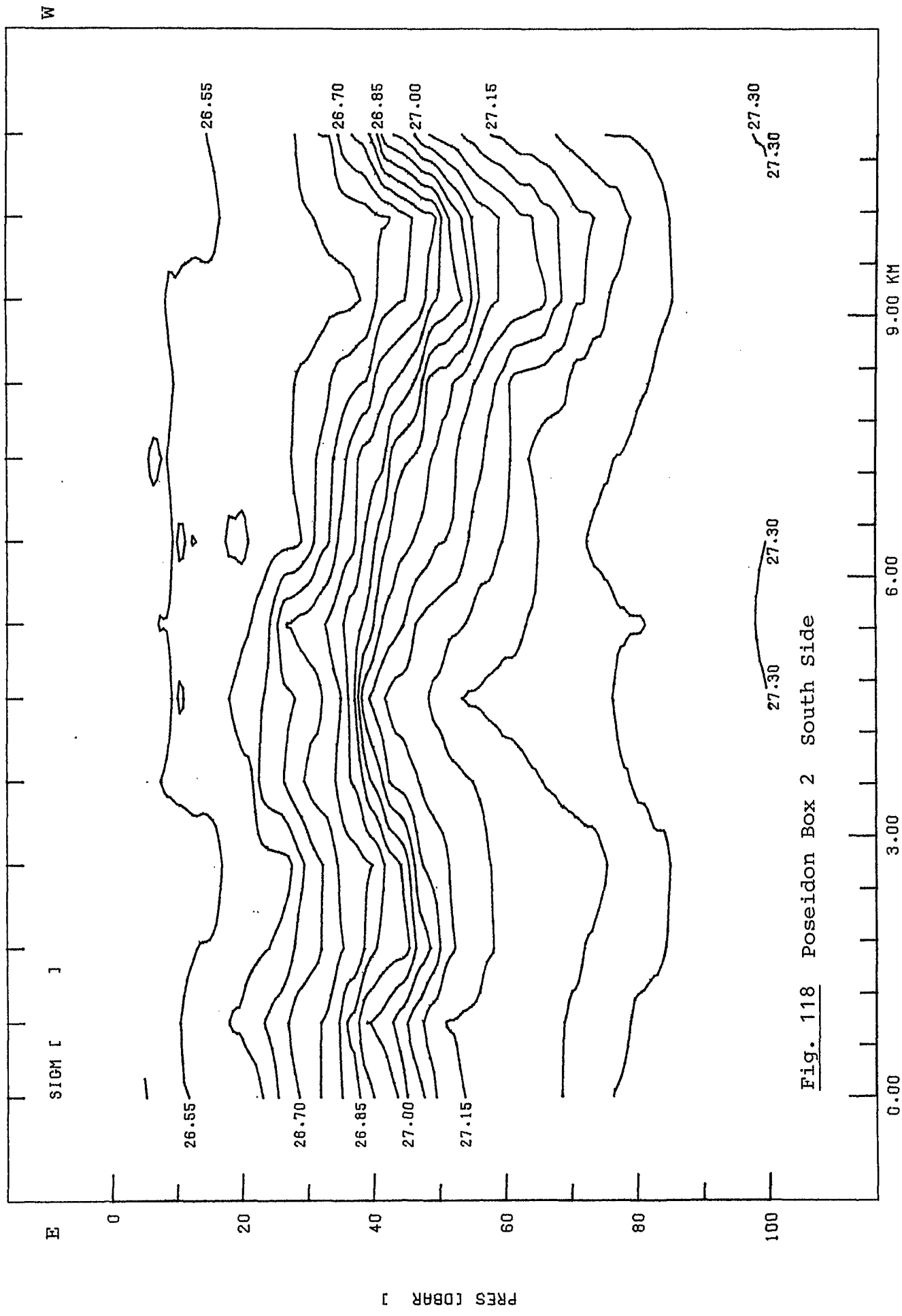

Fig. 118 Poseidon Box 2 South Side

PJC071T

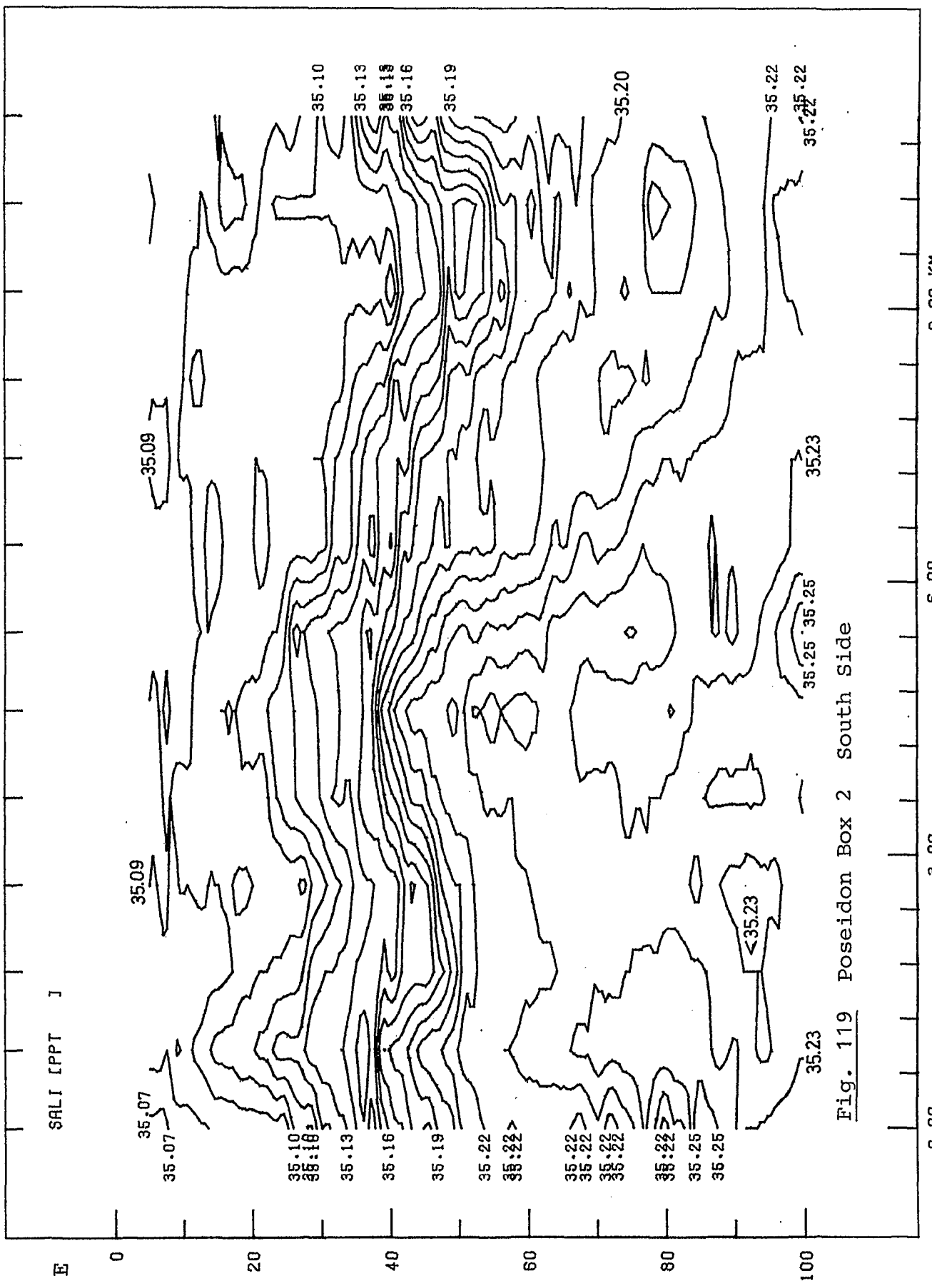

Fig. 119 Poseidon Box 2 South Side

PJC071T

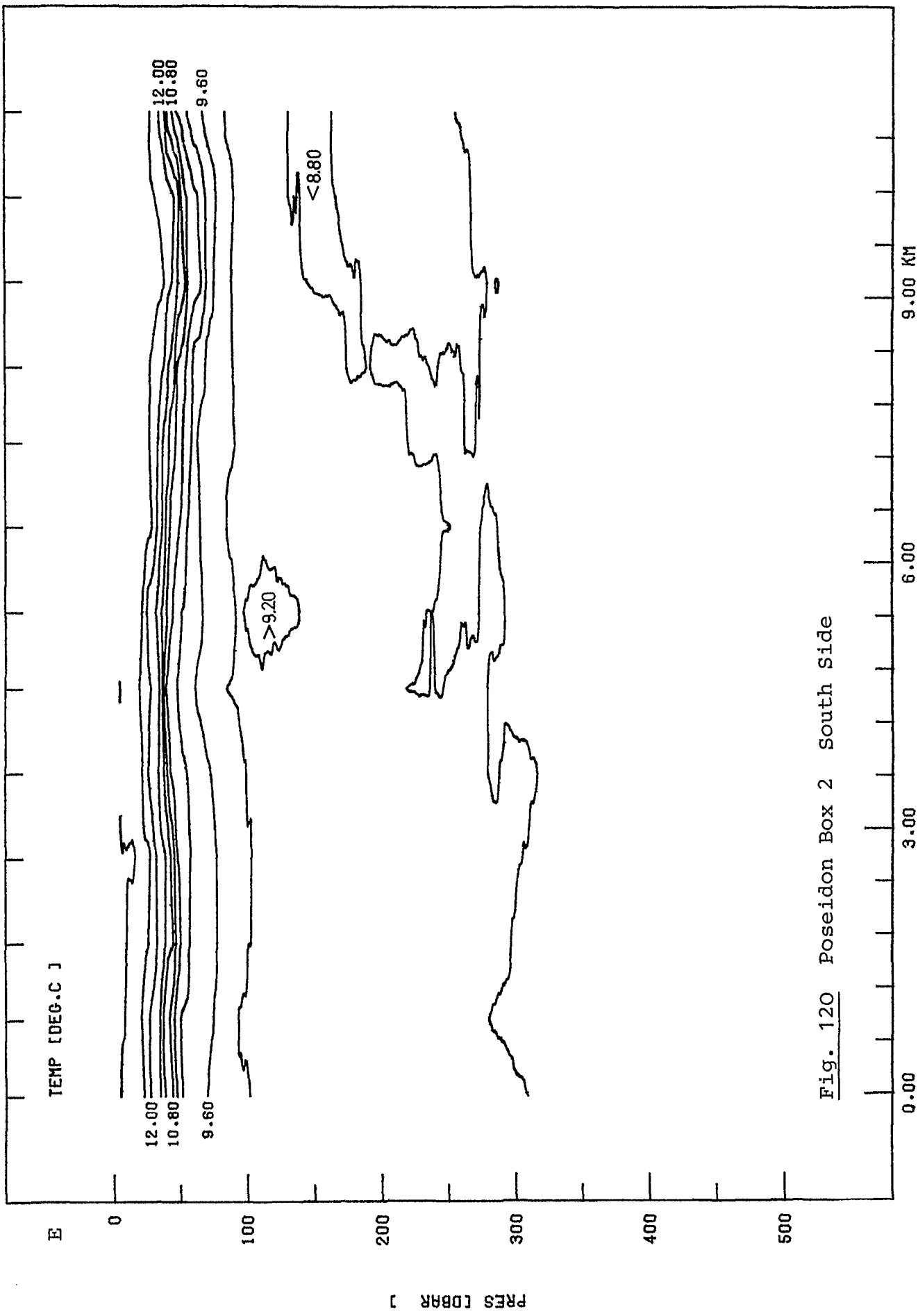

Fig. 120 Poseidon Box 2 South Side

PJC071T

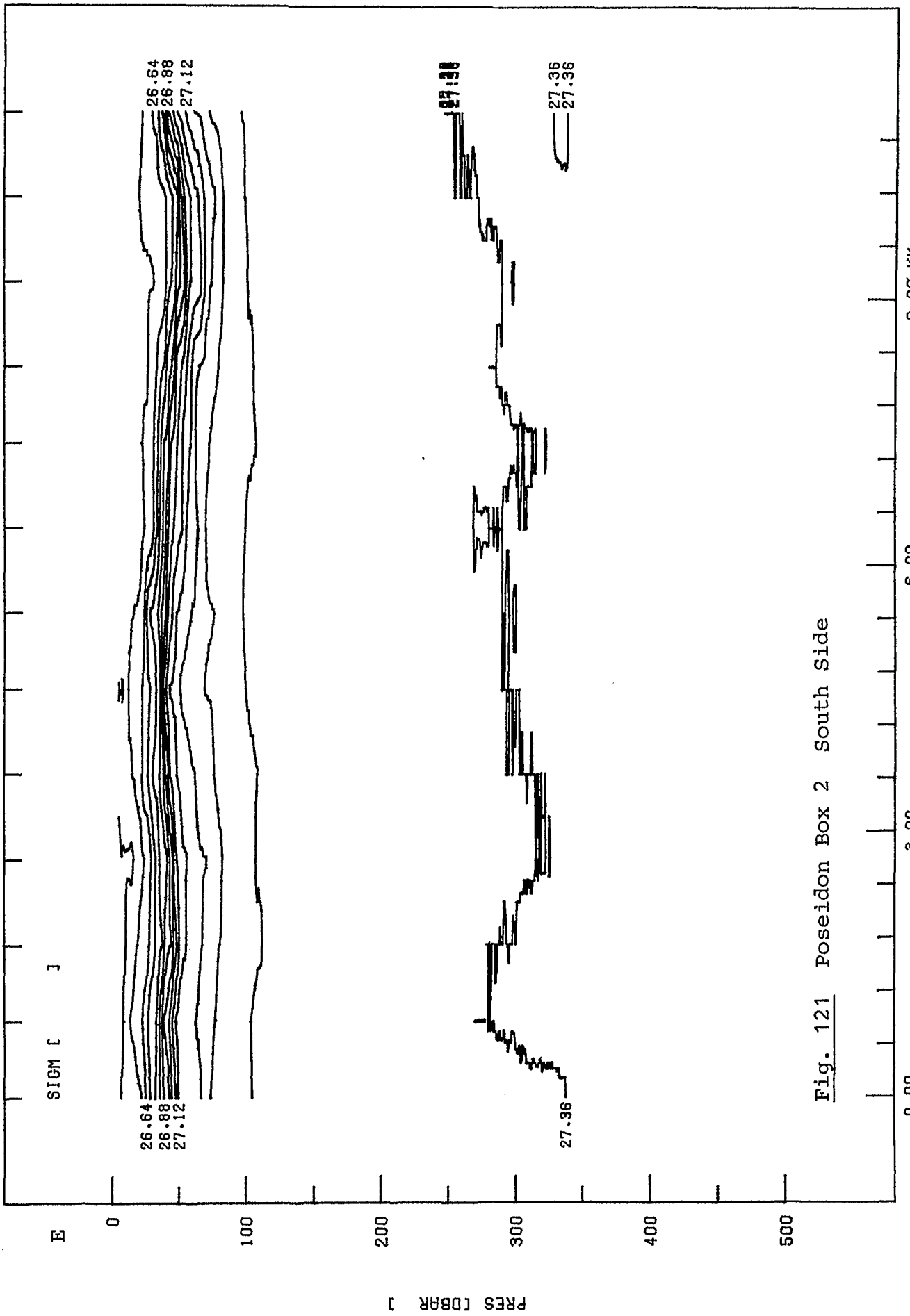

Fig. 121 Poseidon Box 2 South Side

PJC071T

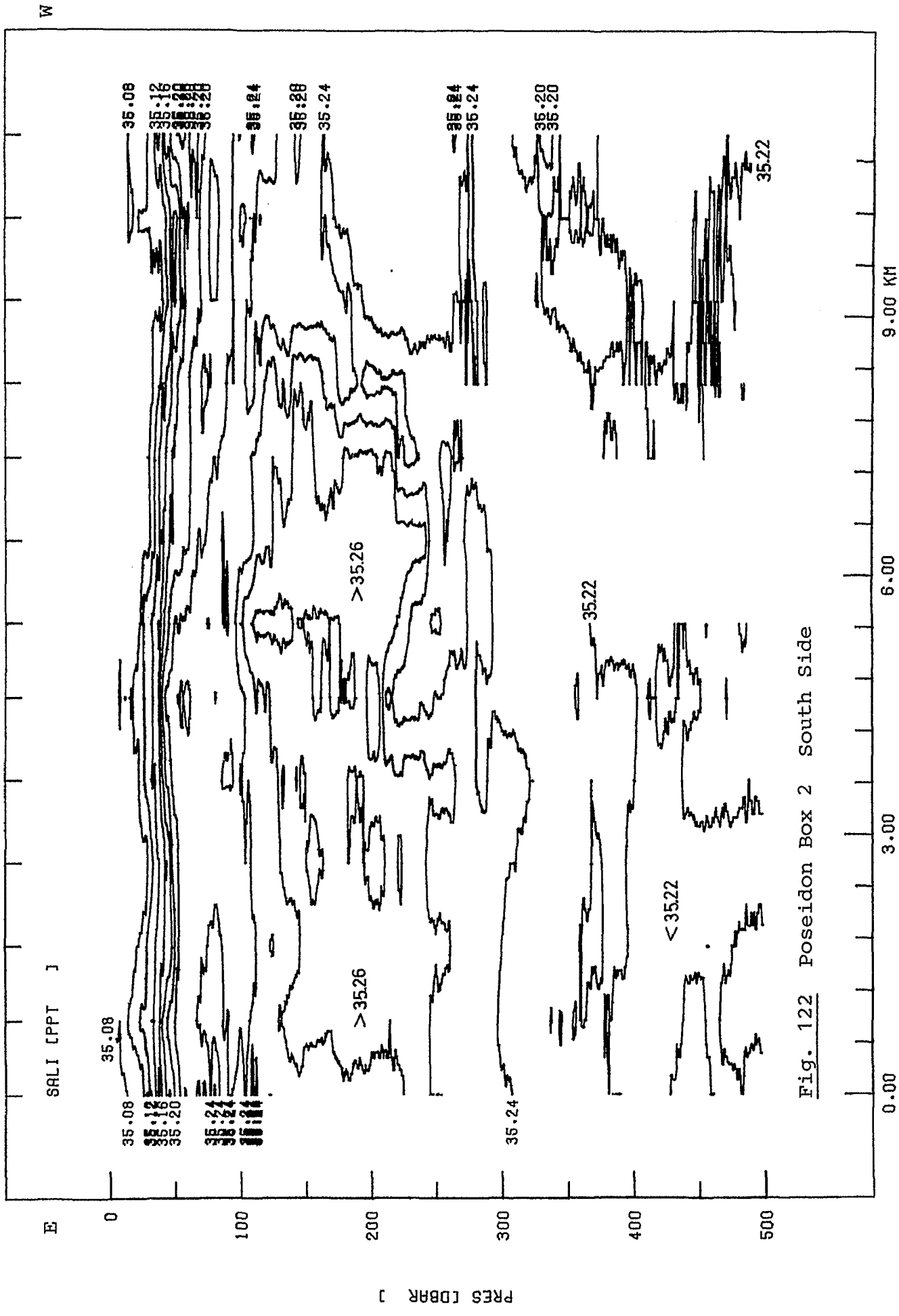

Fig. 122 Poseidon Box 2 South Side

PJC071T

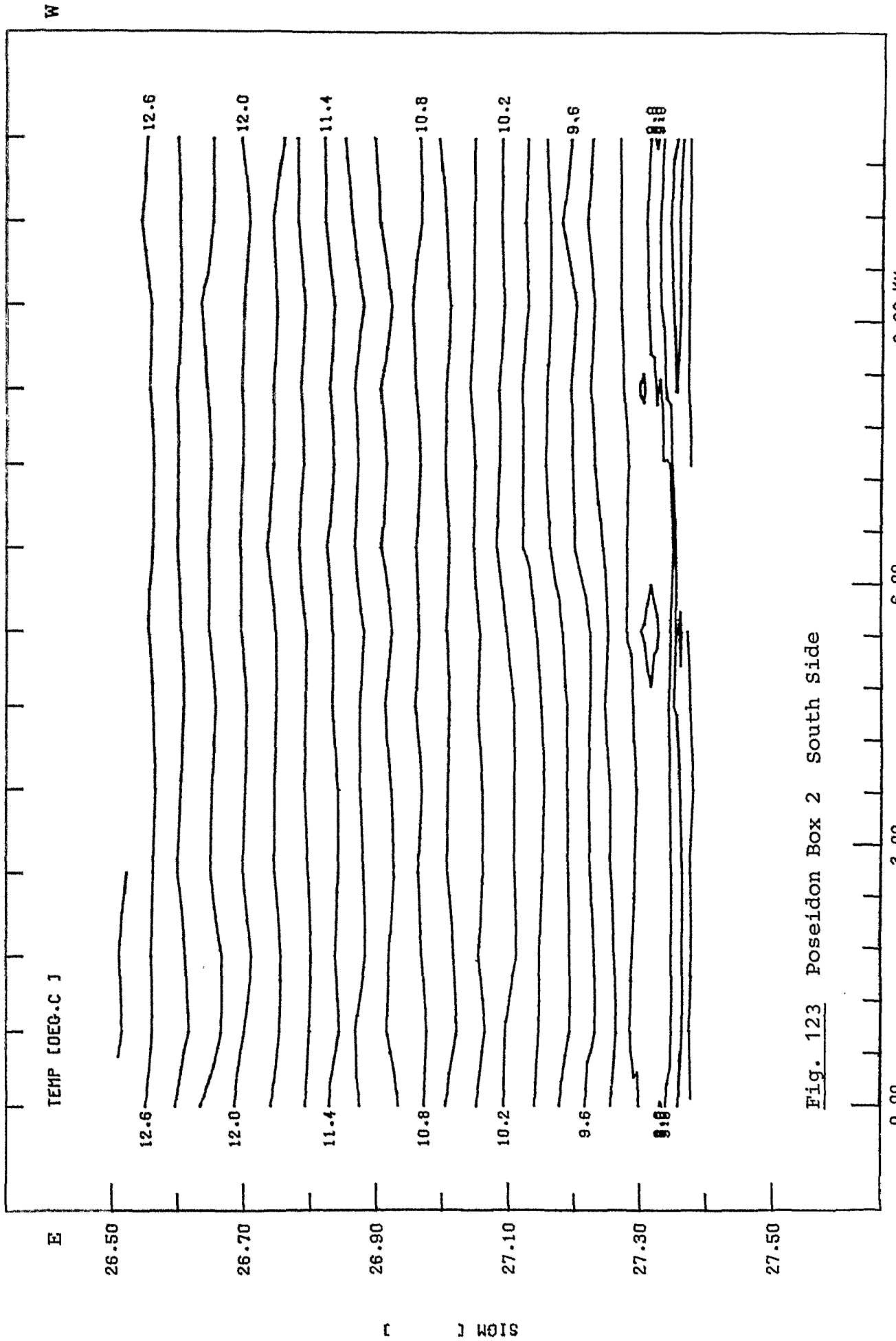

Fig. 123 Poseidon Box 2 South Side

P15100

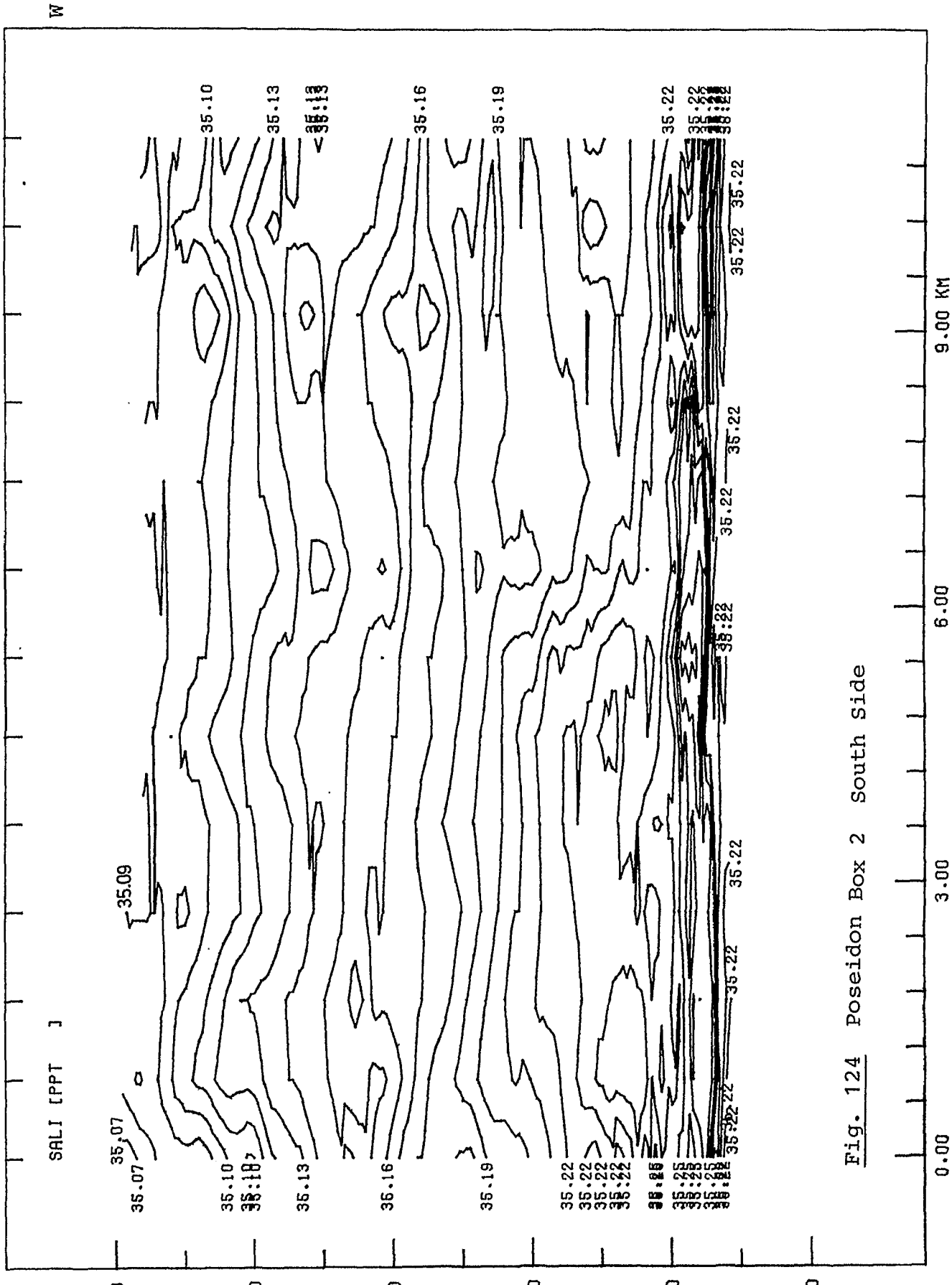

Fig. 124 Poseidon Box 2 South Side

P1510D

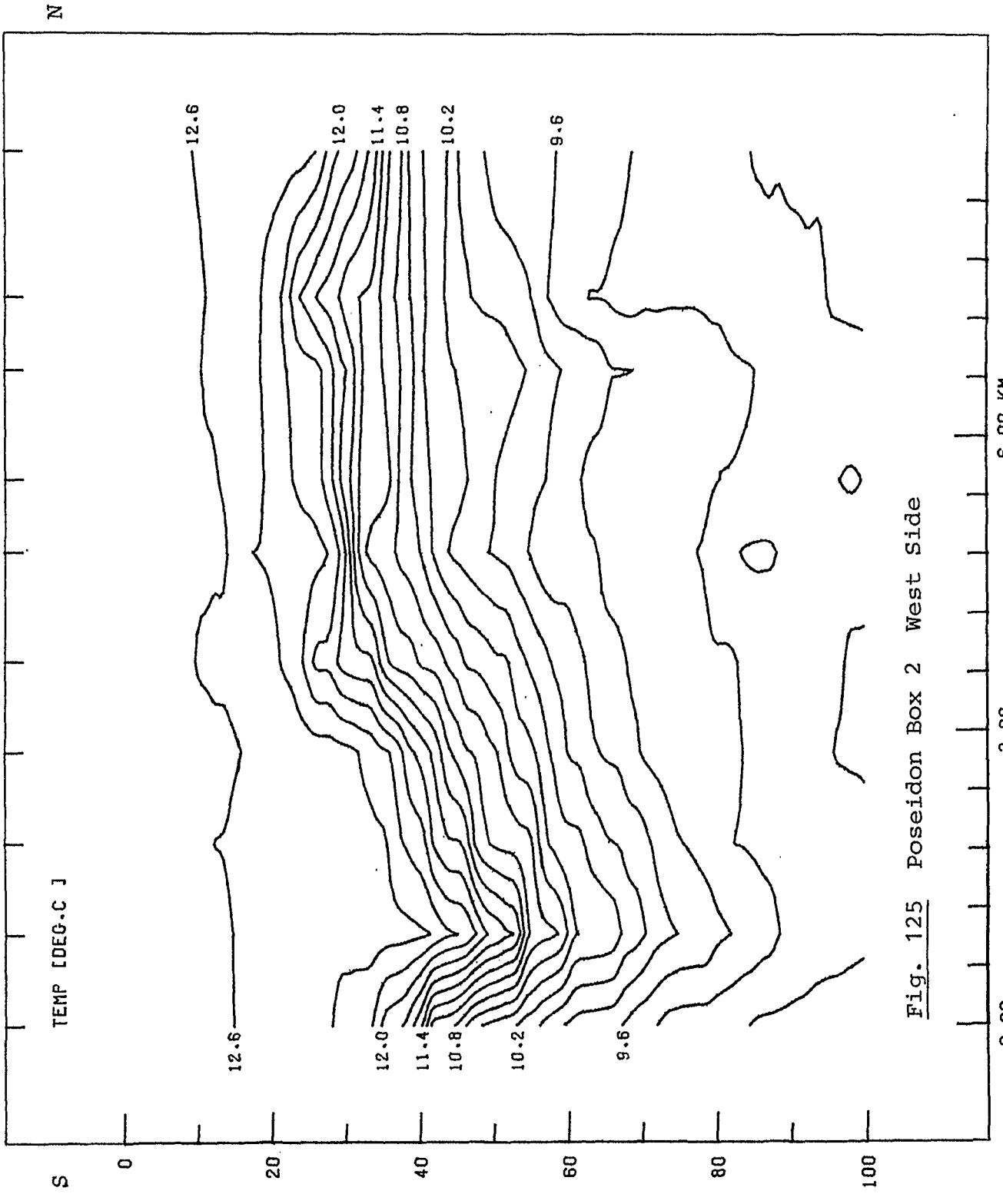

Fig. 125 Poseidon Box 2 West Side

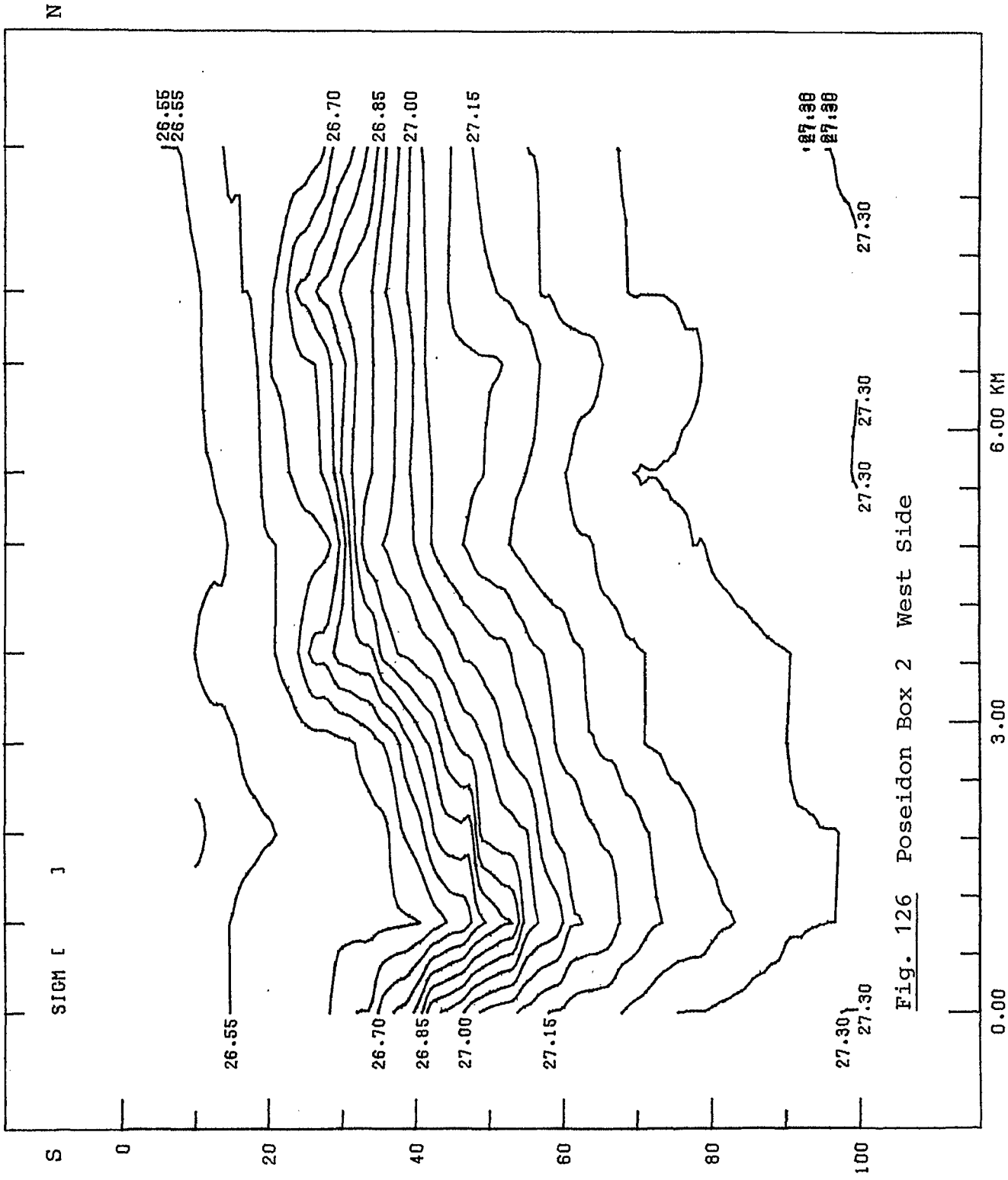

Fig. 126 Poseidon Box 2 West Side

PJC084T

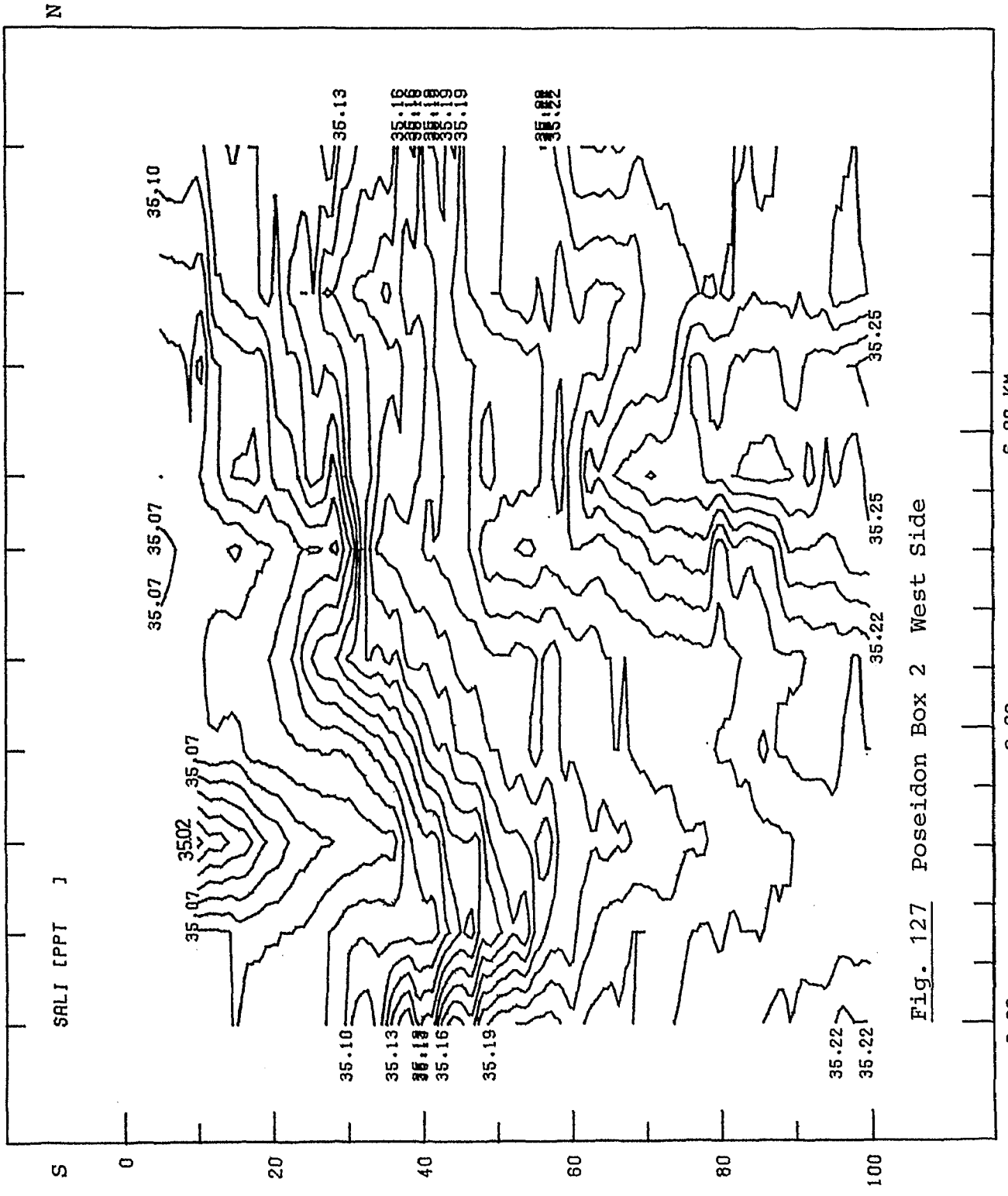

Fig. 127 Poseidon Box 2 West Side

PJC084T

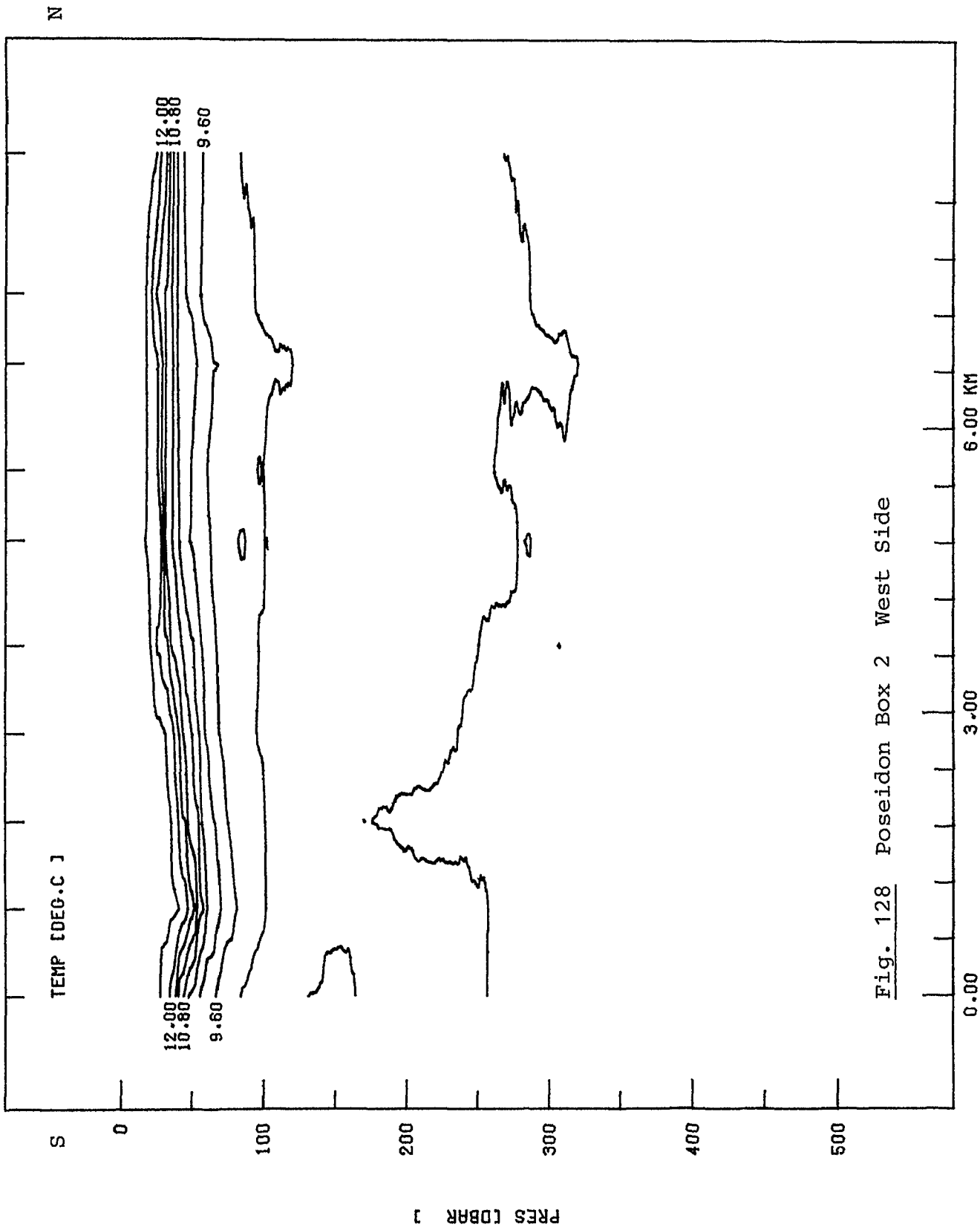

Fig. 128 Poseidon Box 2 West Side

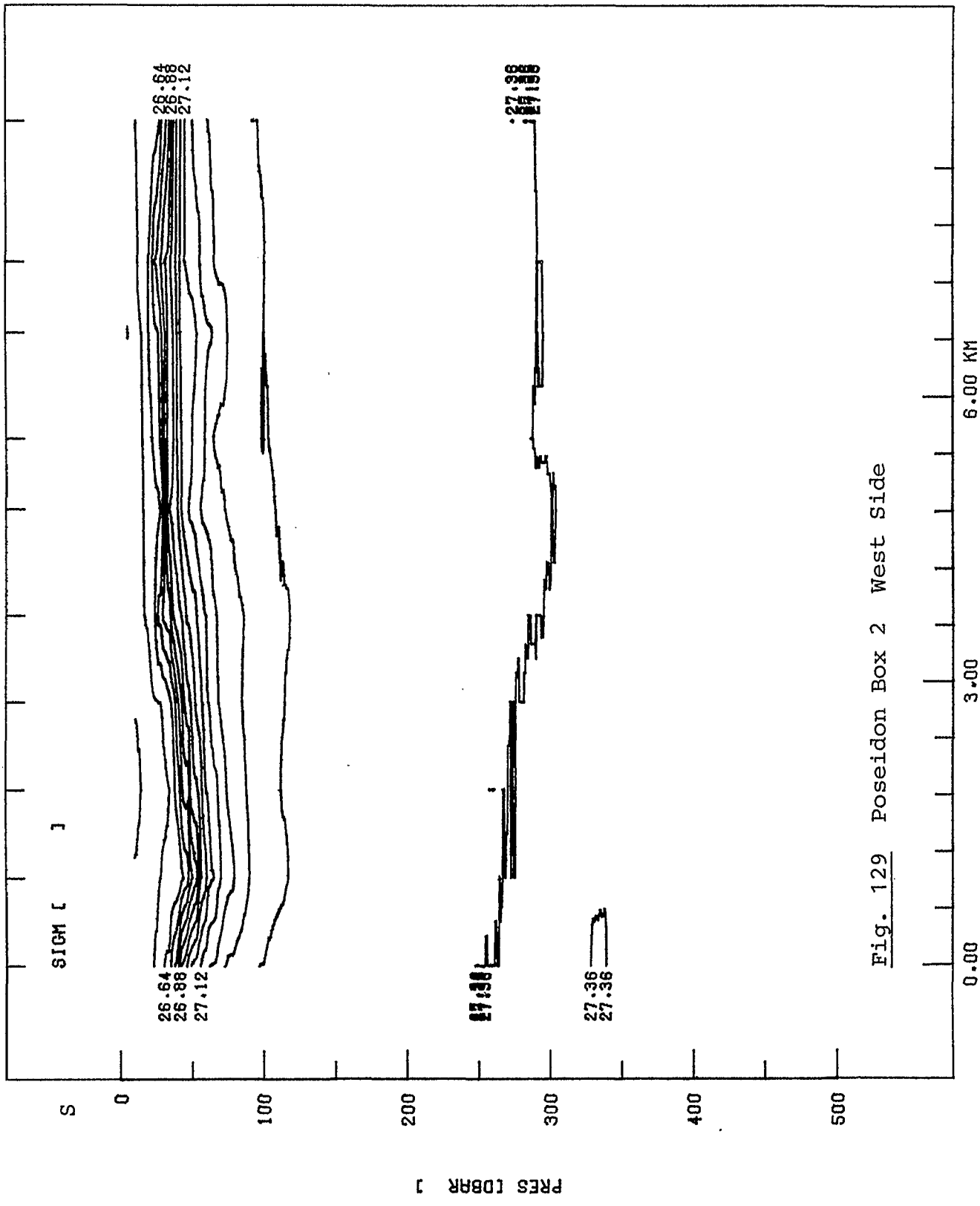

Fig. 129 Poseidon Box 2 West Side

PJC084T

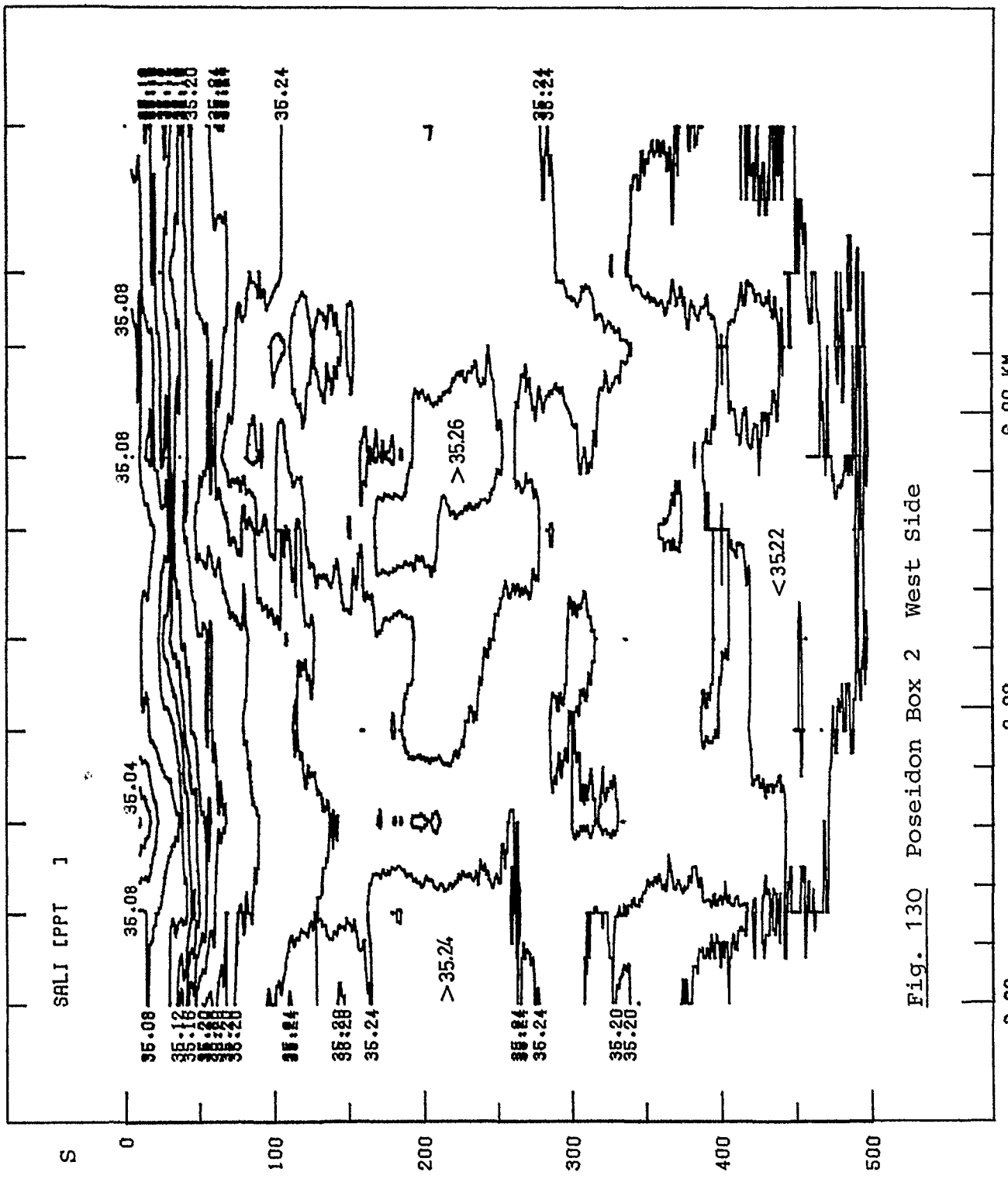

Fig. 130 Poseidon Box 2 West Side

PJC084T

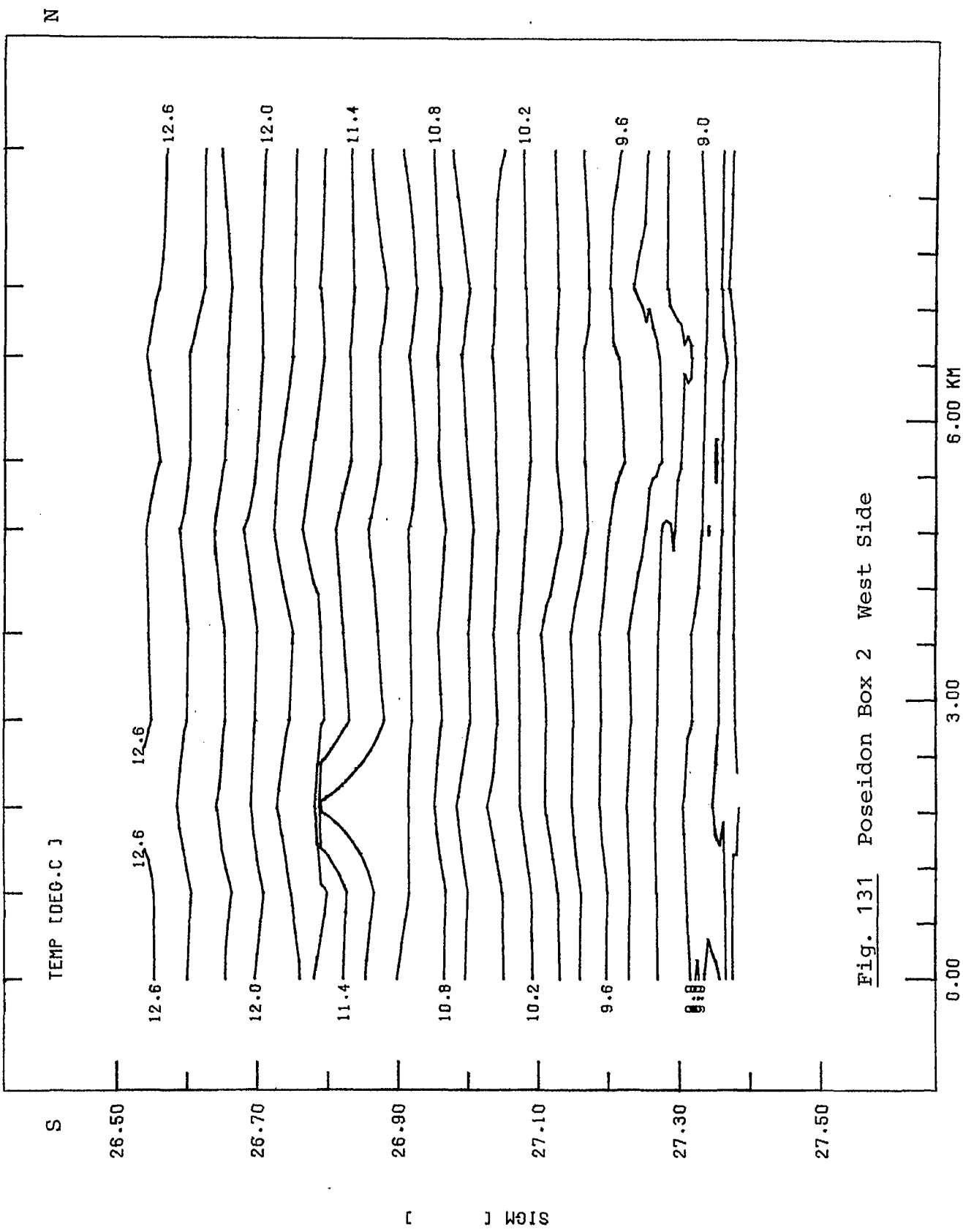

Fig. 131 Poseidon Box 2 West Side

P1524D

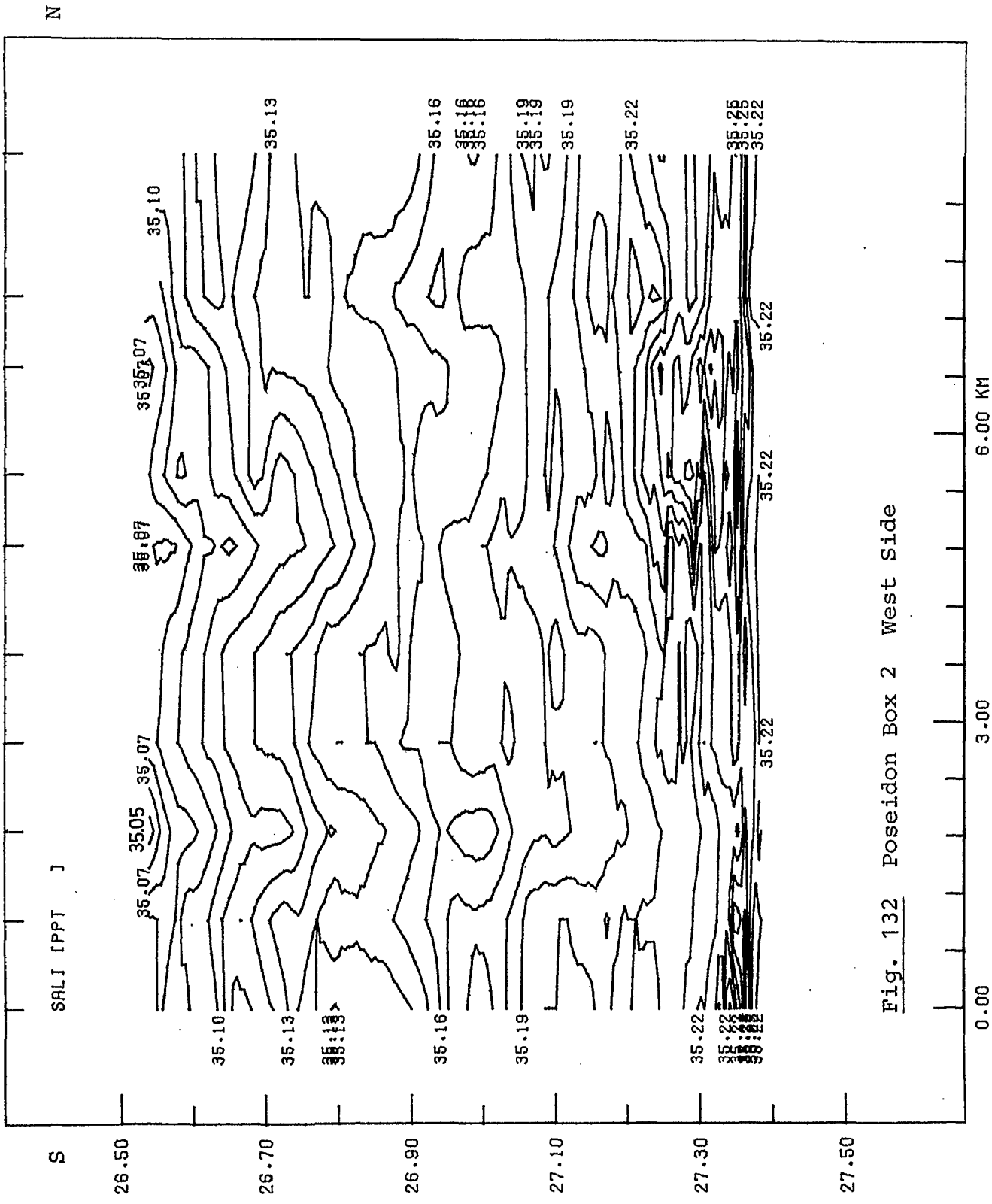

Fig. 132 Poseidon Box 2 West Side

P1524D

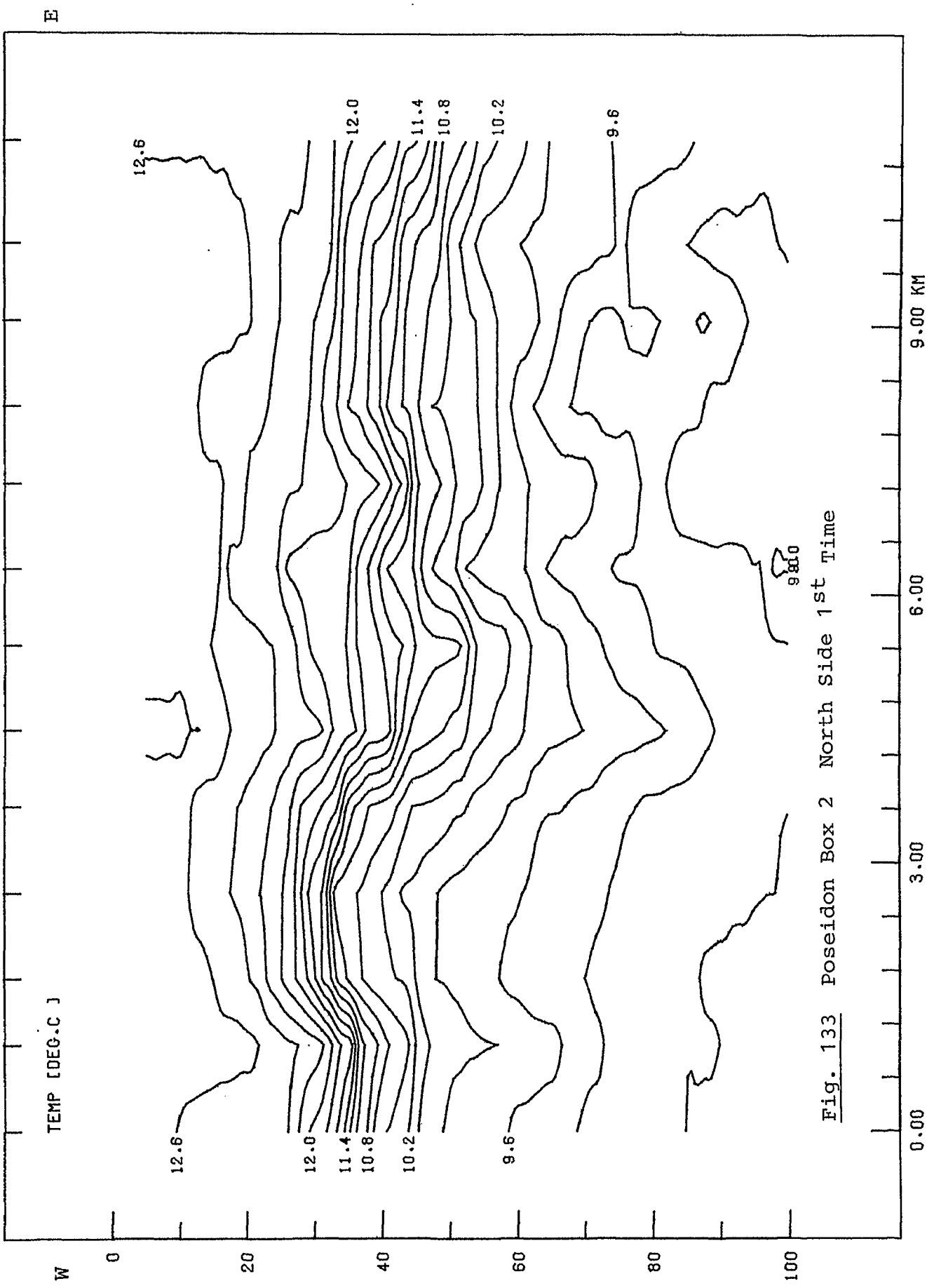

Fig. 133 Poseidon Box 2 North Side 1st Time

PJC093T

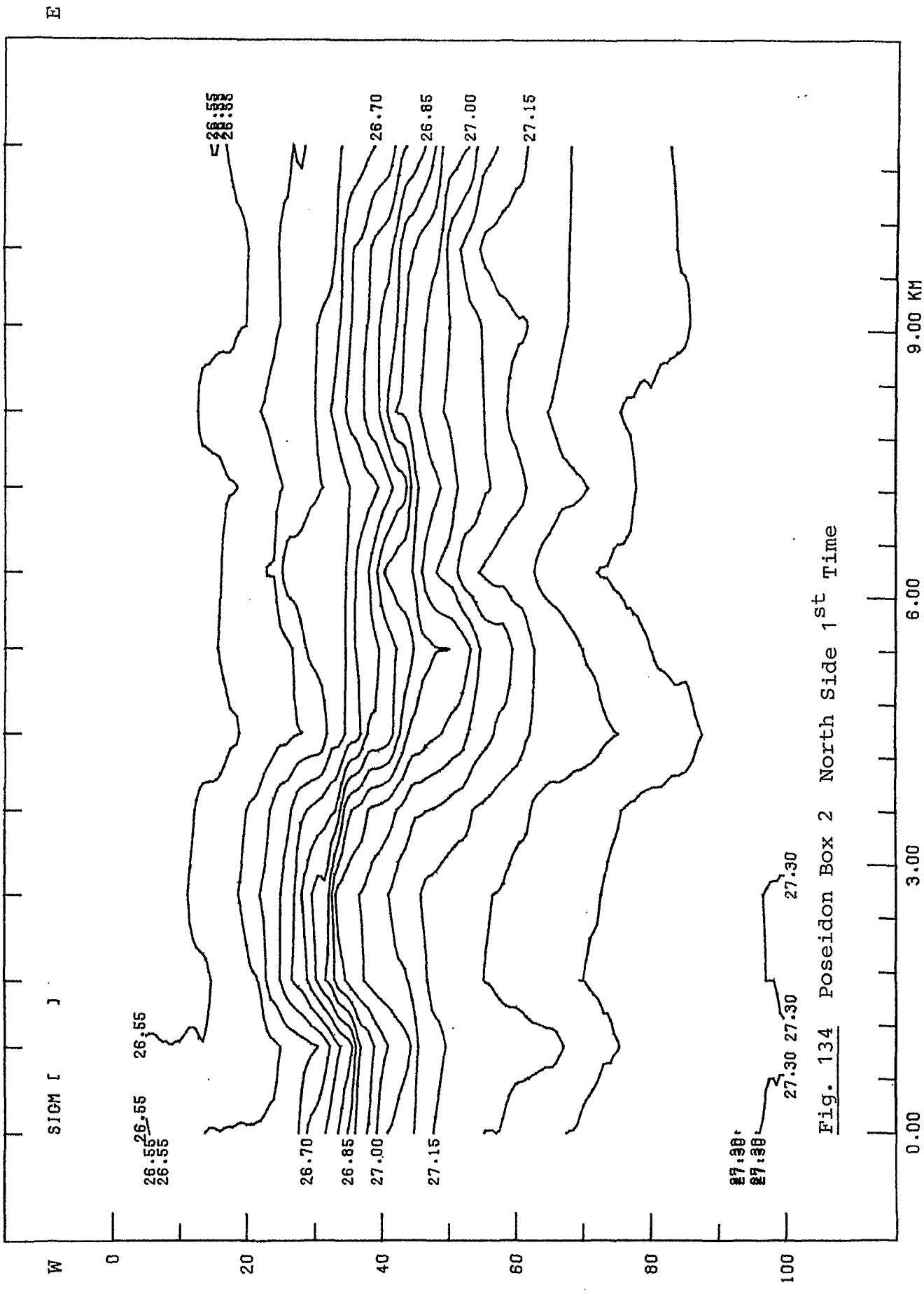

Fig. 134 Poseidon Box 2 North Side 1st Time

PJC093T

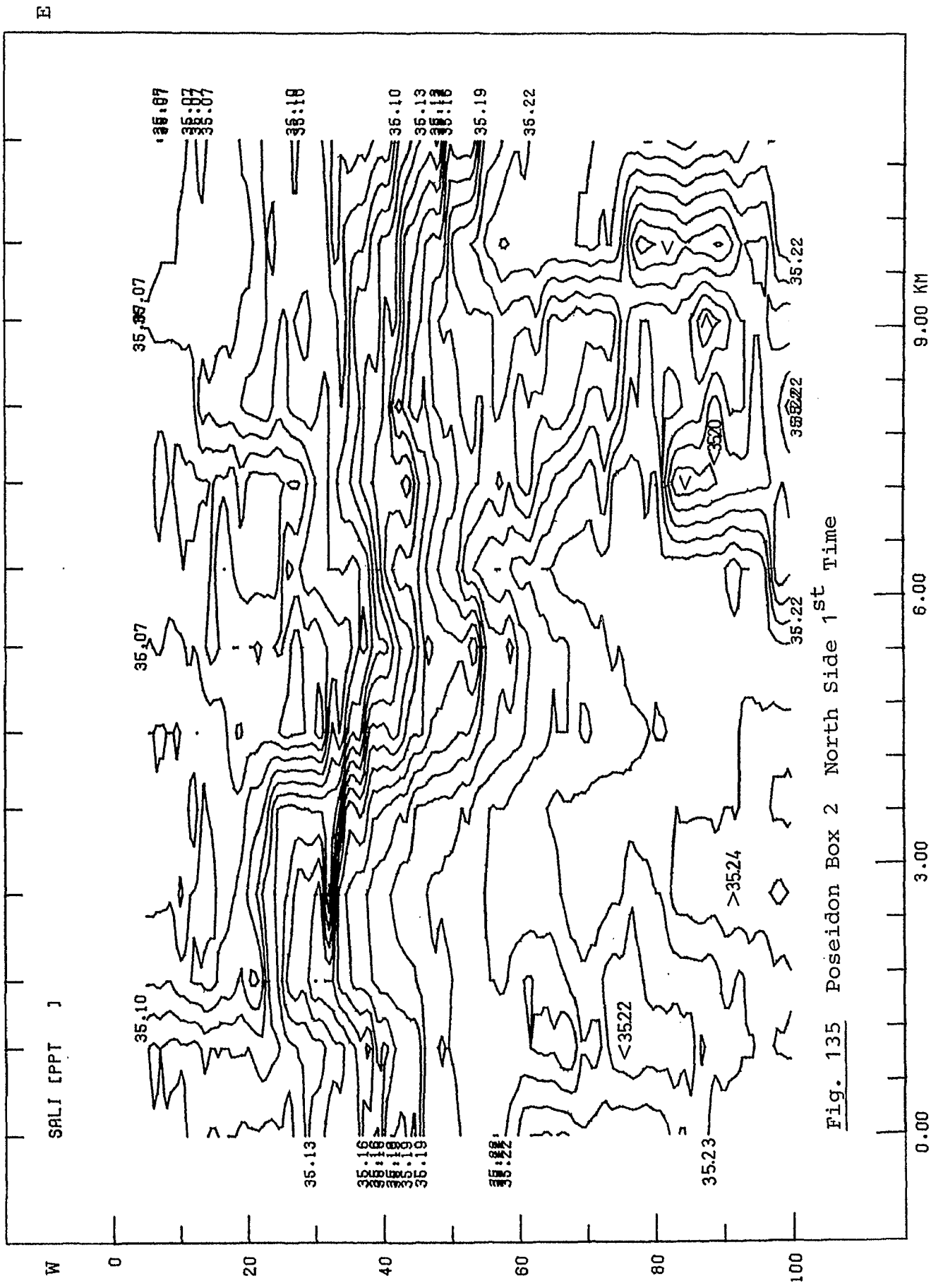

Fig. 135 Poseidon Box 2 North Side 1st Time

PJC093T

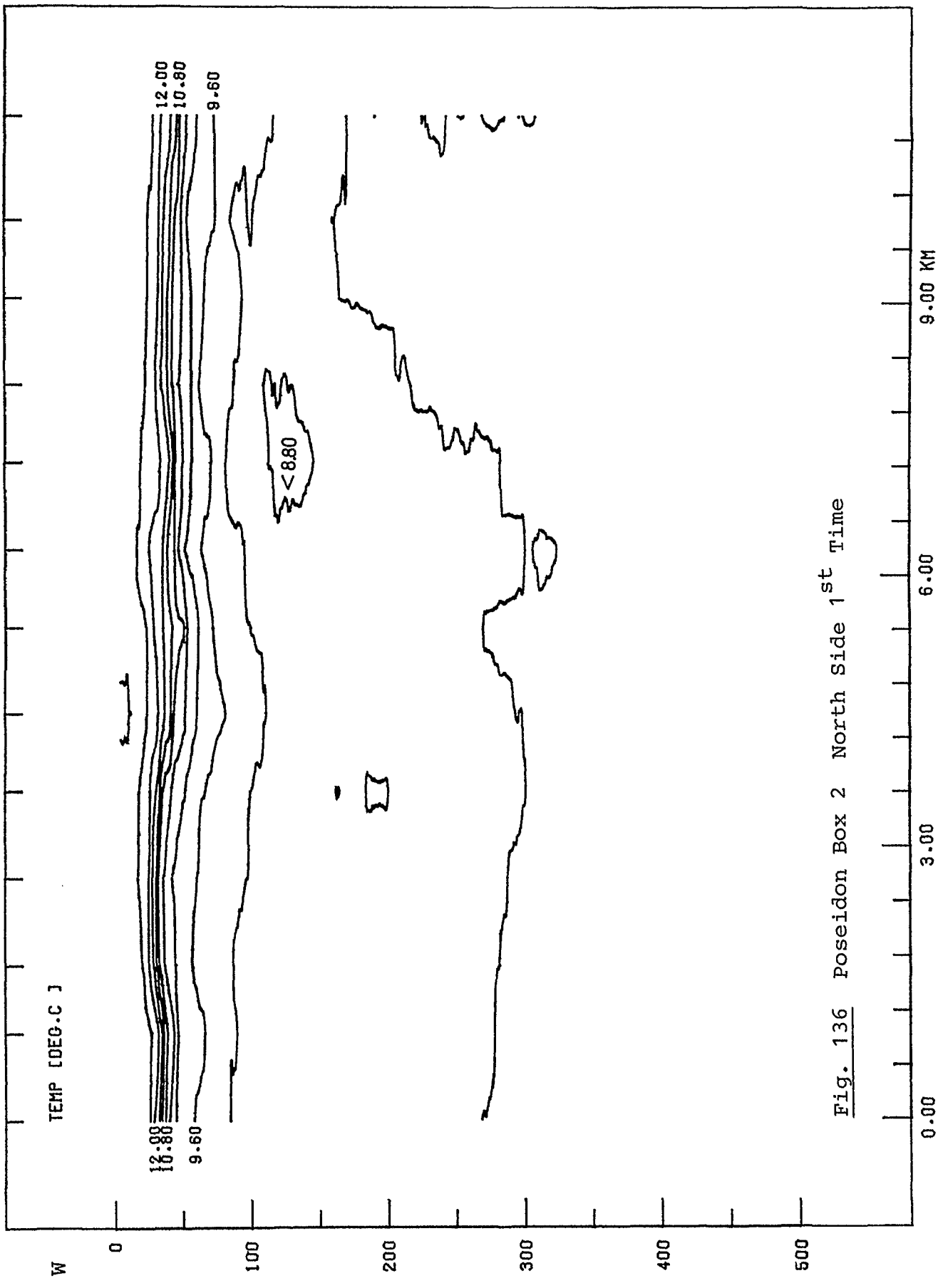

Fig. 136 Poseidon Box 2 North Side 1st Time

PJC093T

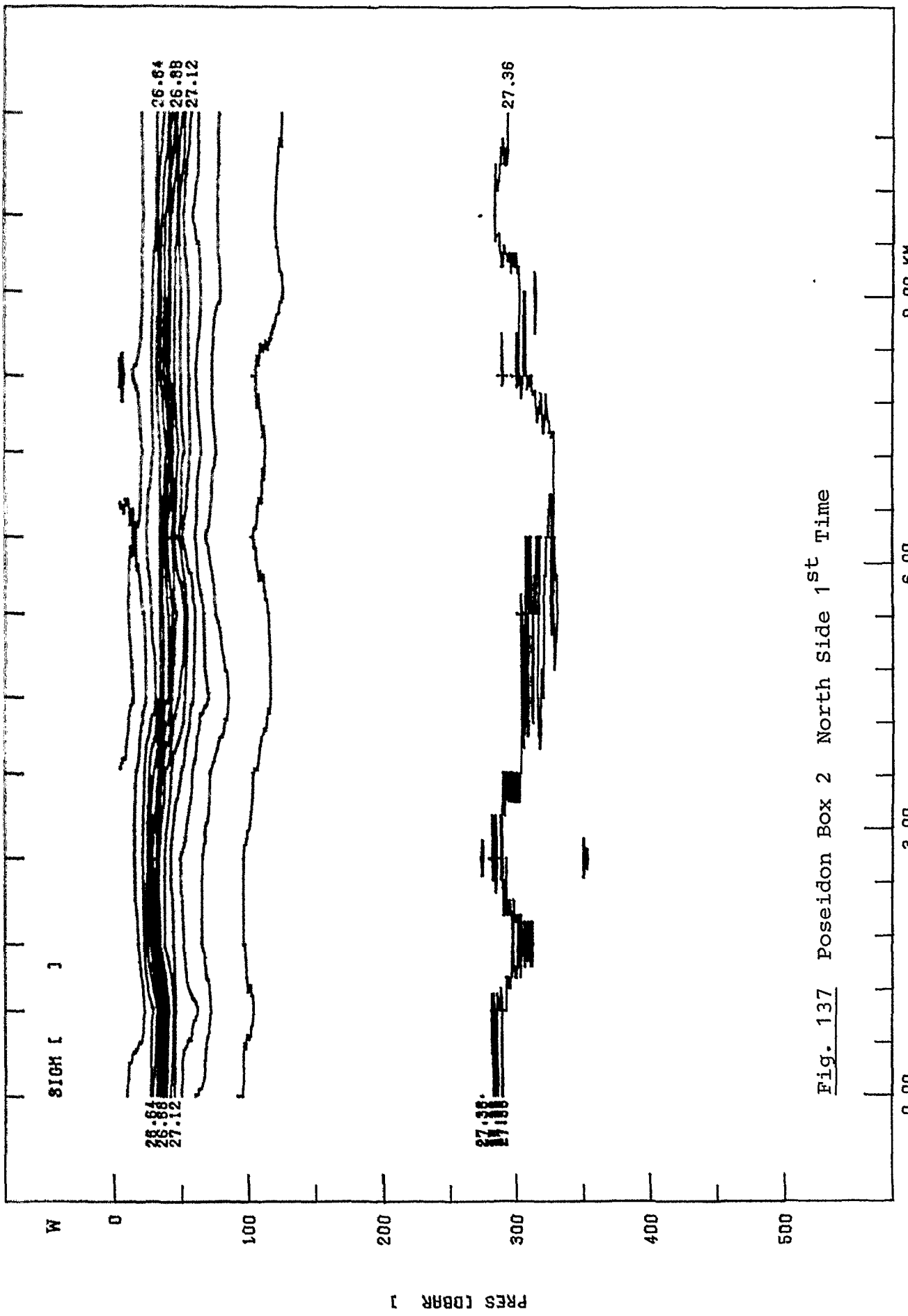

Fig. 137 Poseidon Box 2 North Side 1st Time

PJC093T

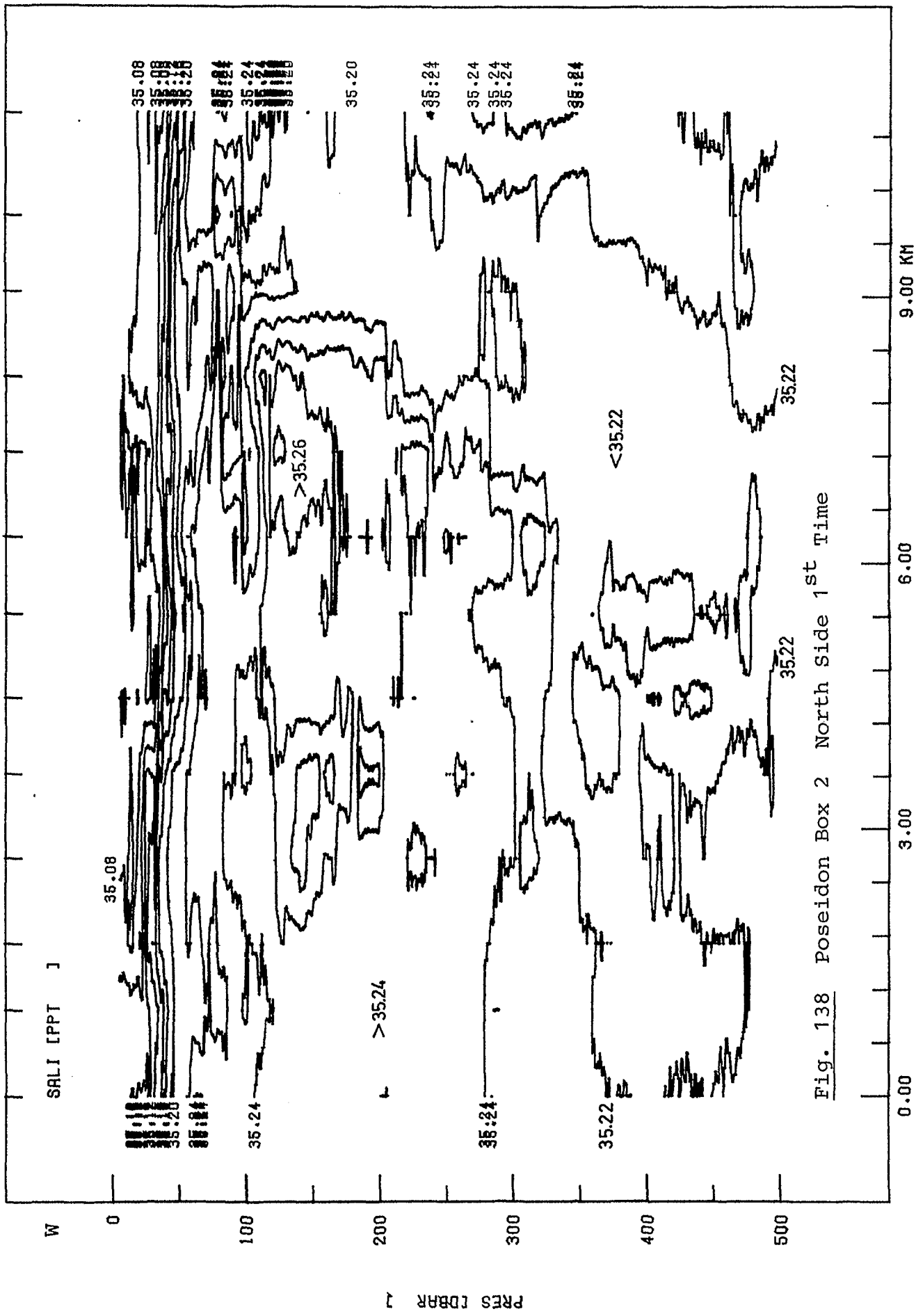

Fig. 138 Poseidon Box 2 North Side 1st Time

PJC093T

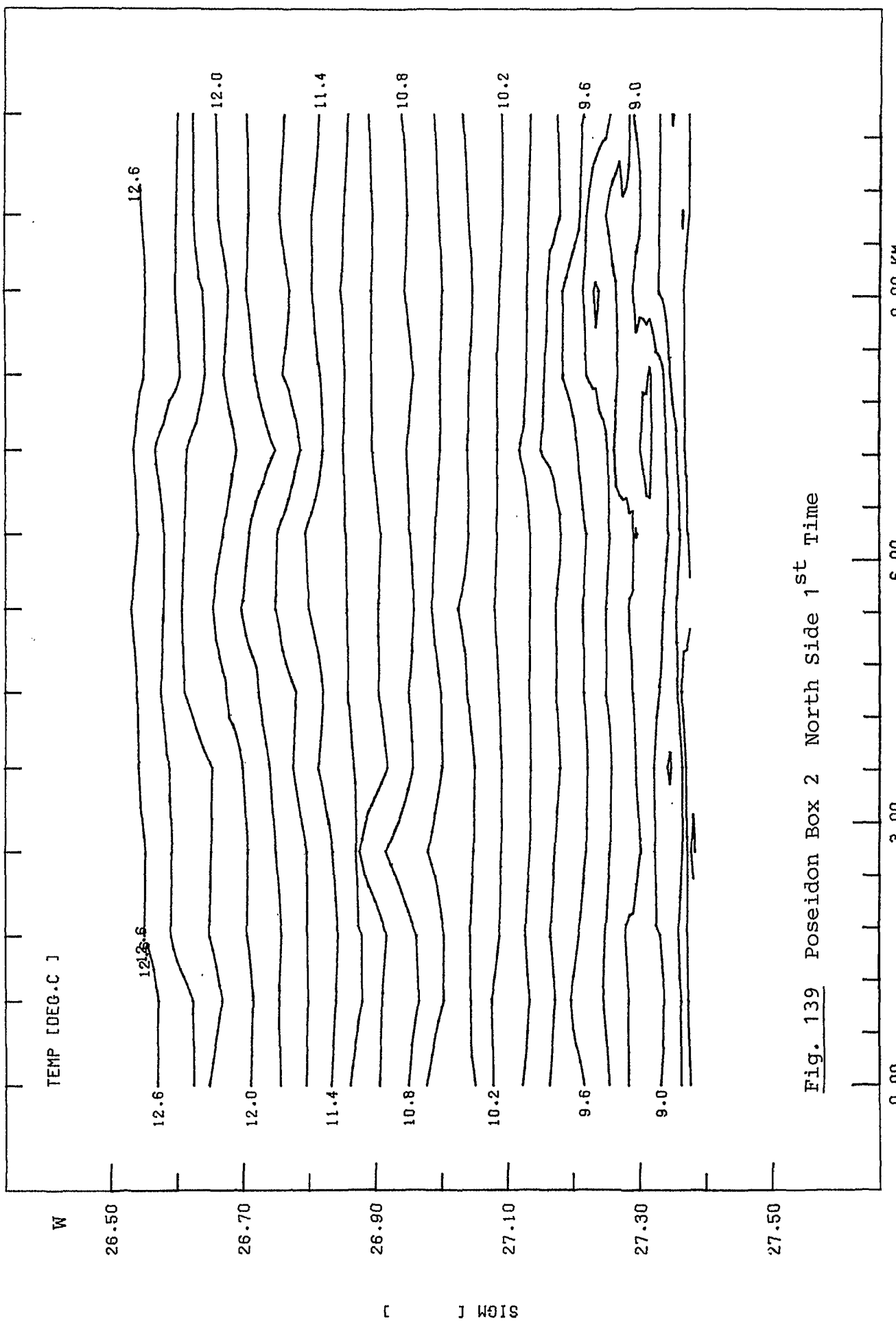

Fig. 139 Poseidon Box 2 North Side 1st Time

P1533D

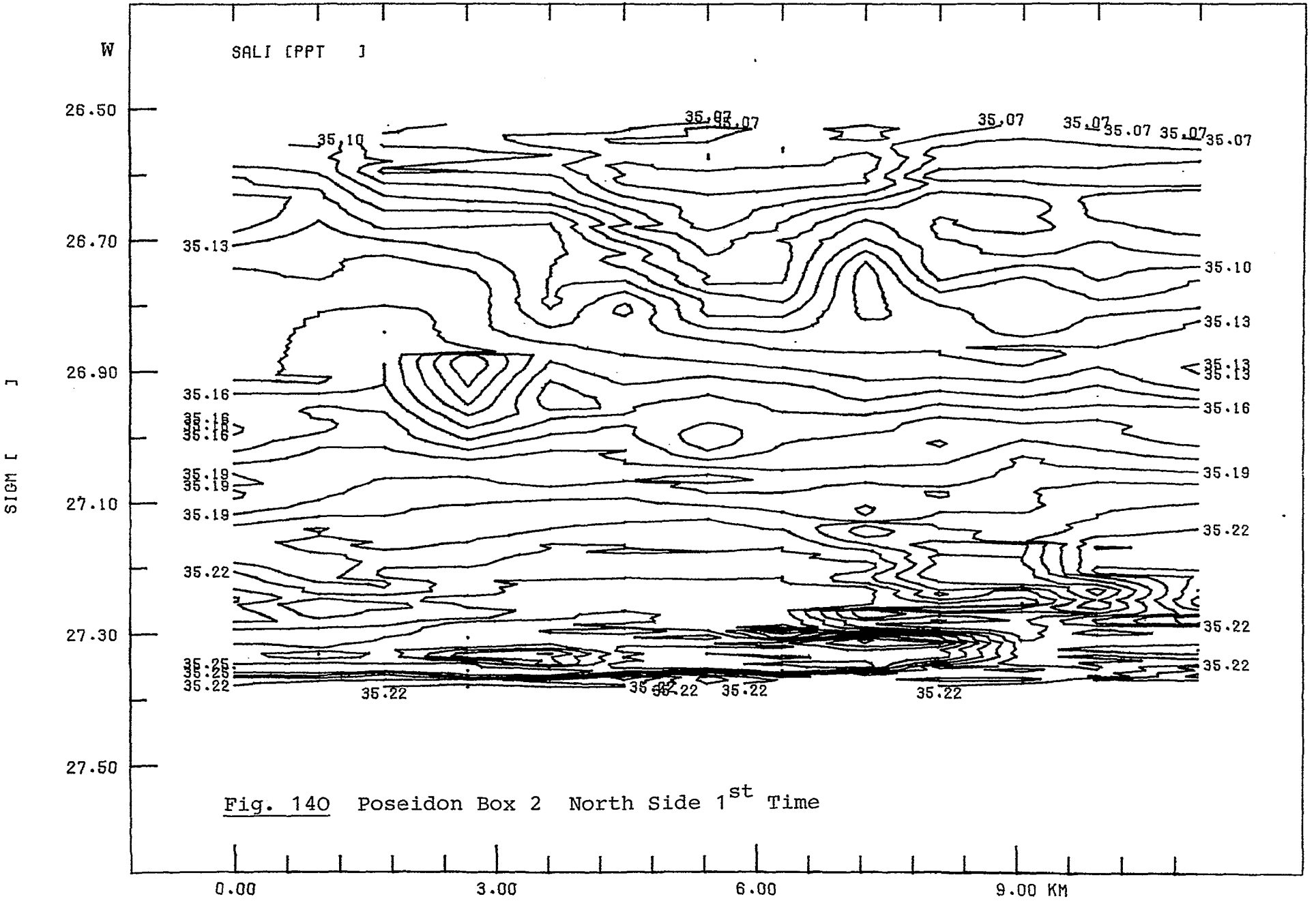

Fig. 140 Poseidon Box 2 North Side 1st Time

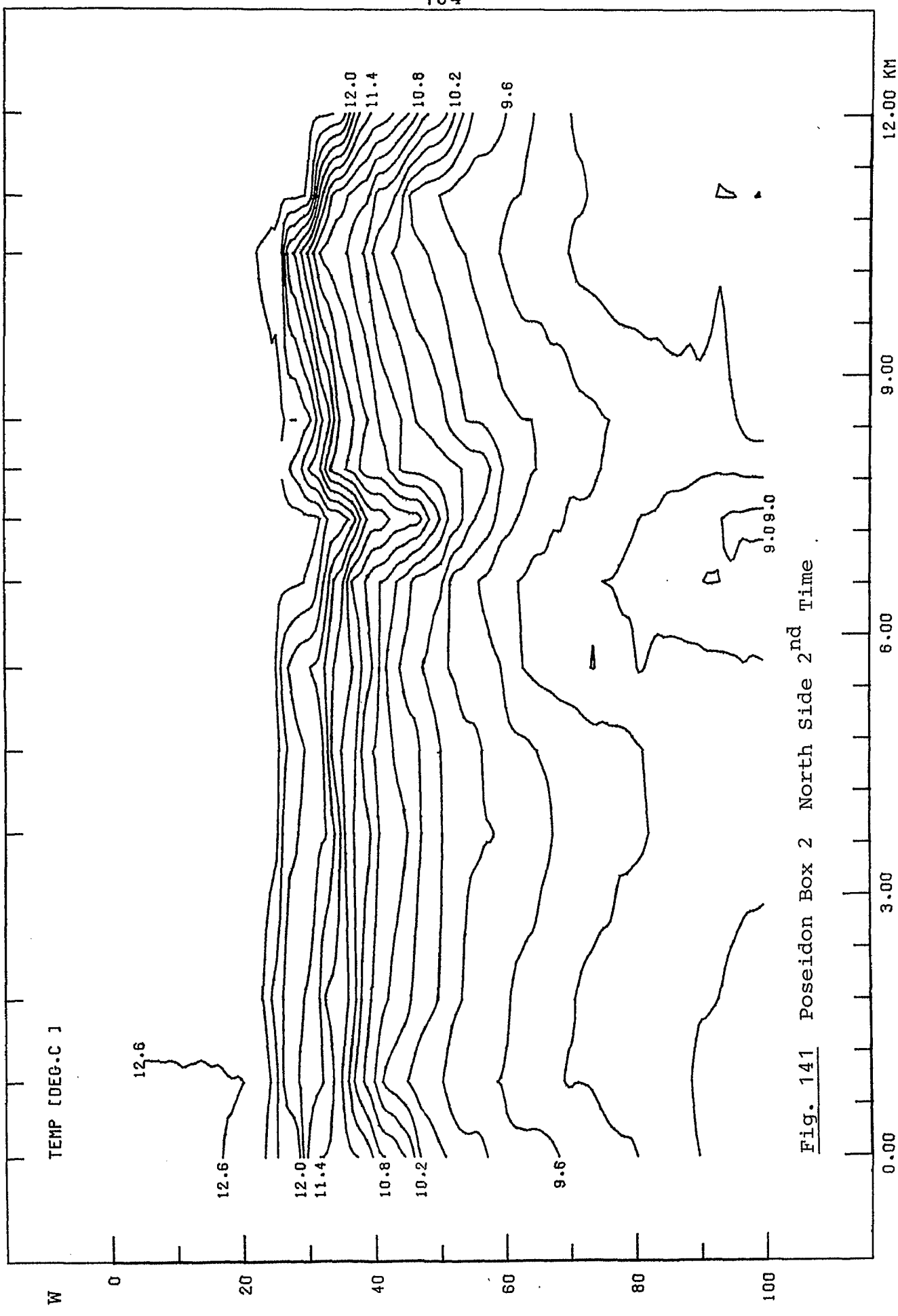

Fig. 141 Poseidon Box 2 North Side 2nd Time

PJC106T

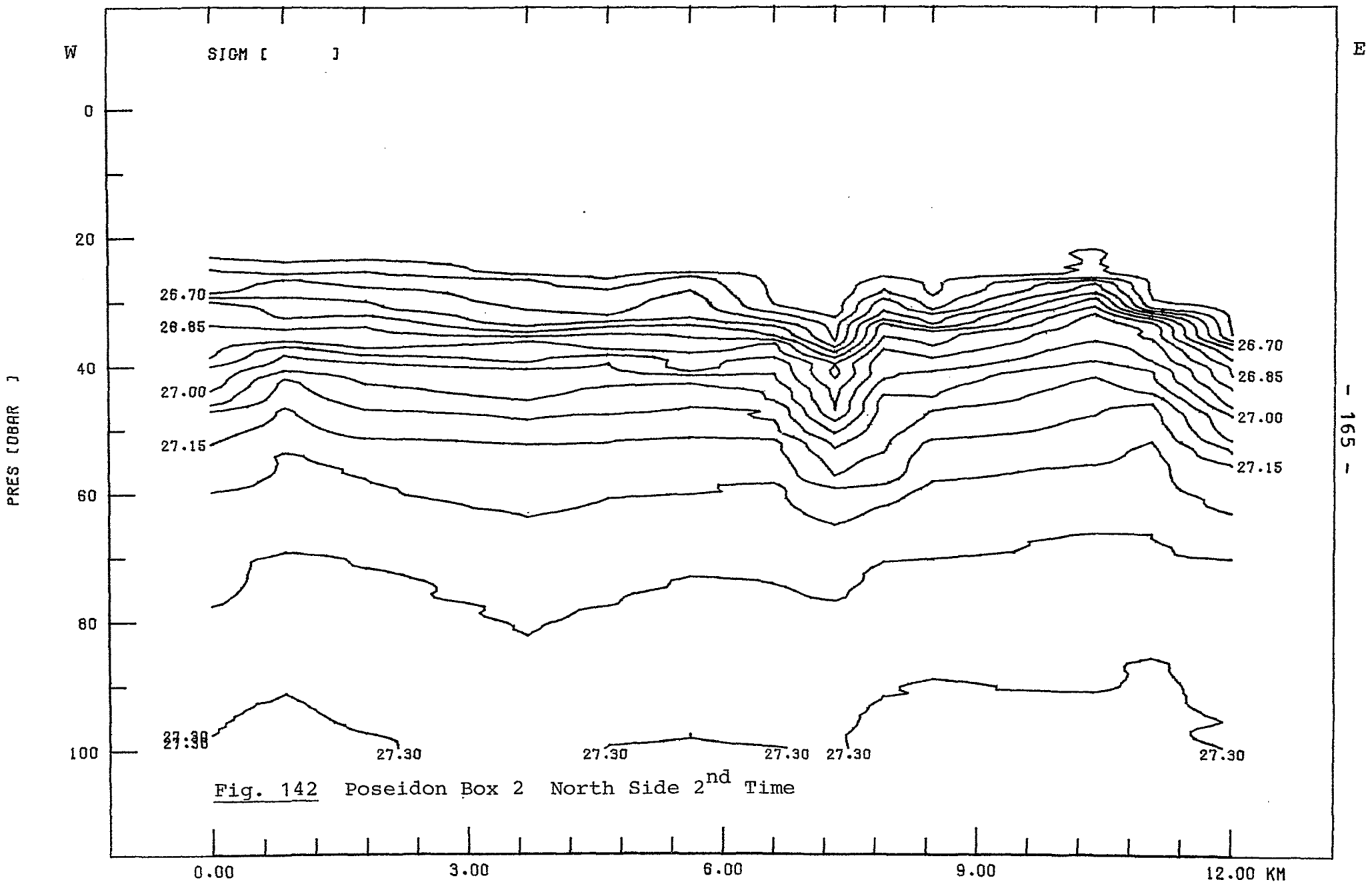

Fig. 142 Poseidon Box 2 North Side 2nd Time

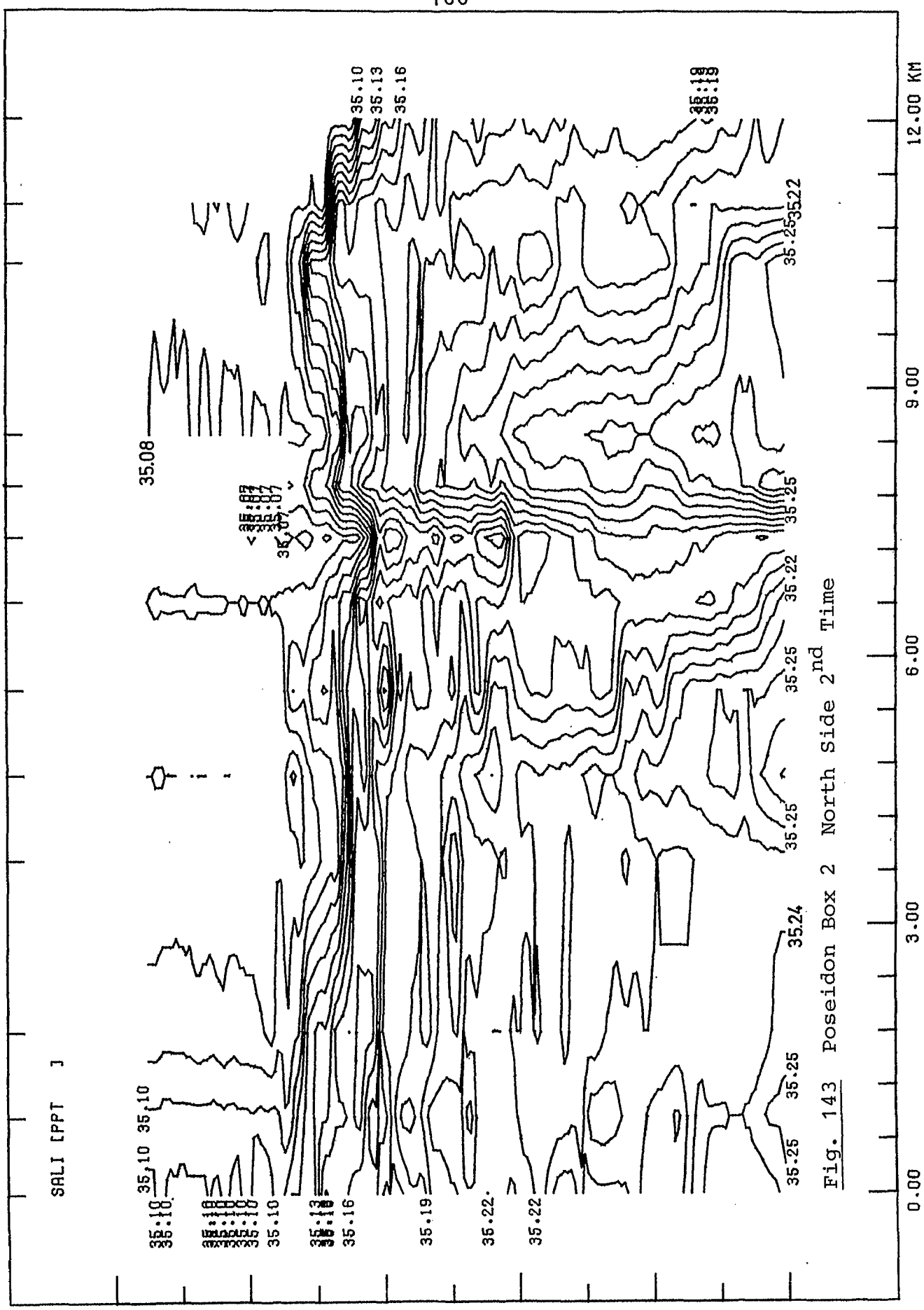

Fig. 143 Poseidon Box 2 North Side 2nd Time

PJC106T

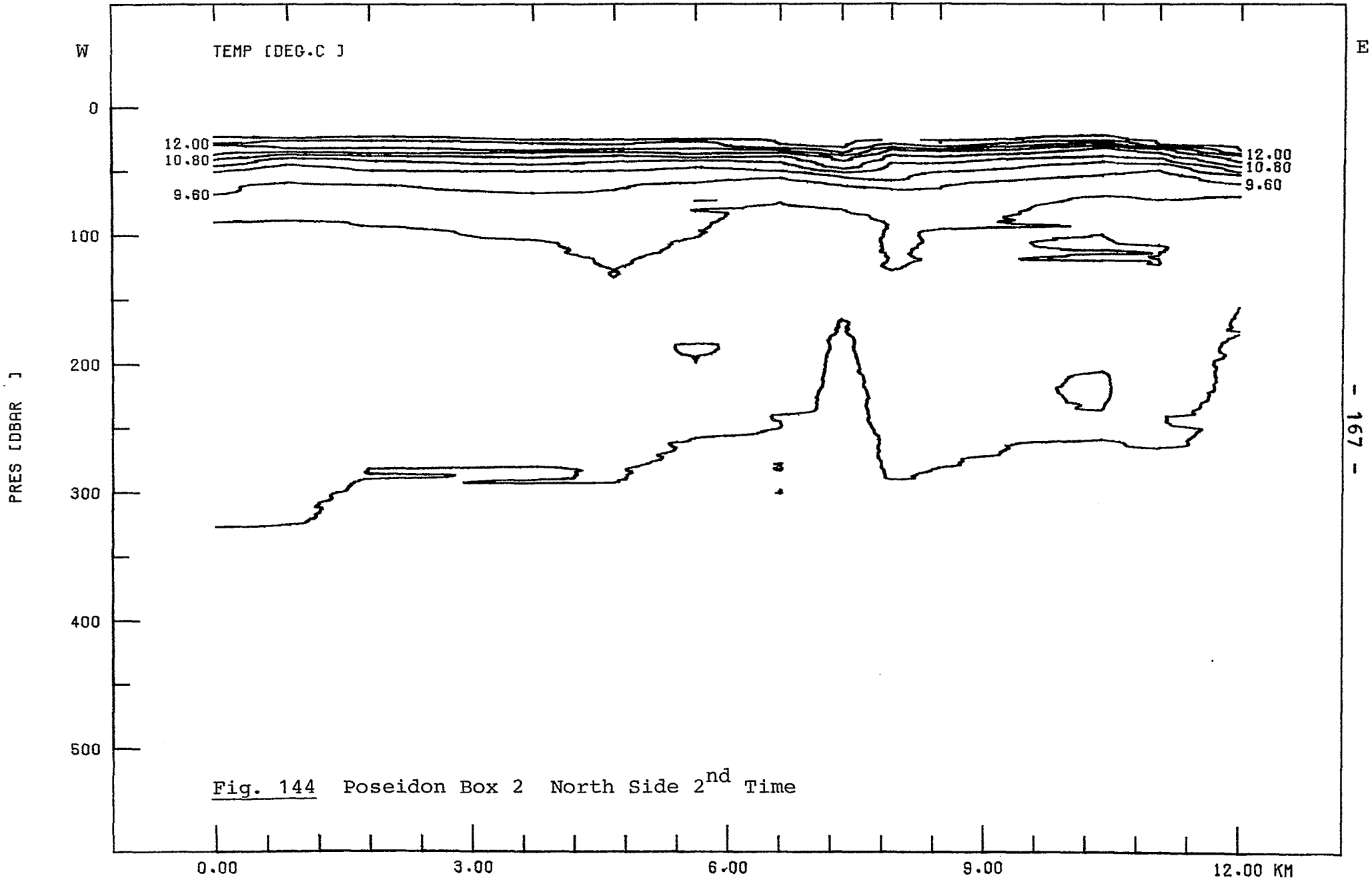

Fig. 144 Poseidon Box 2 North Side 2nd Time

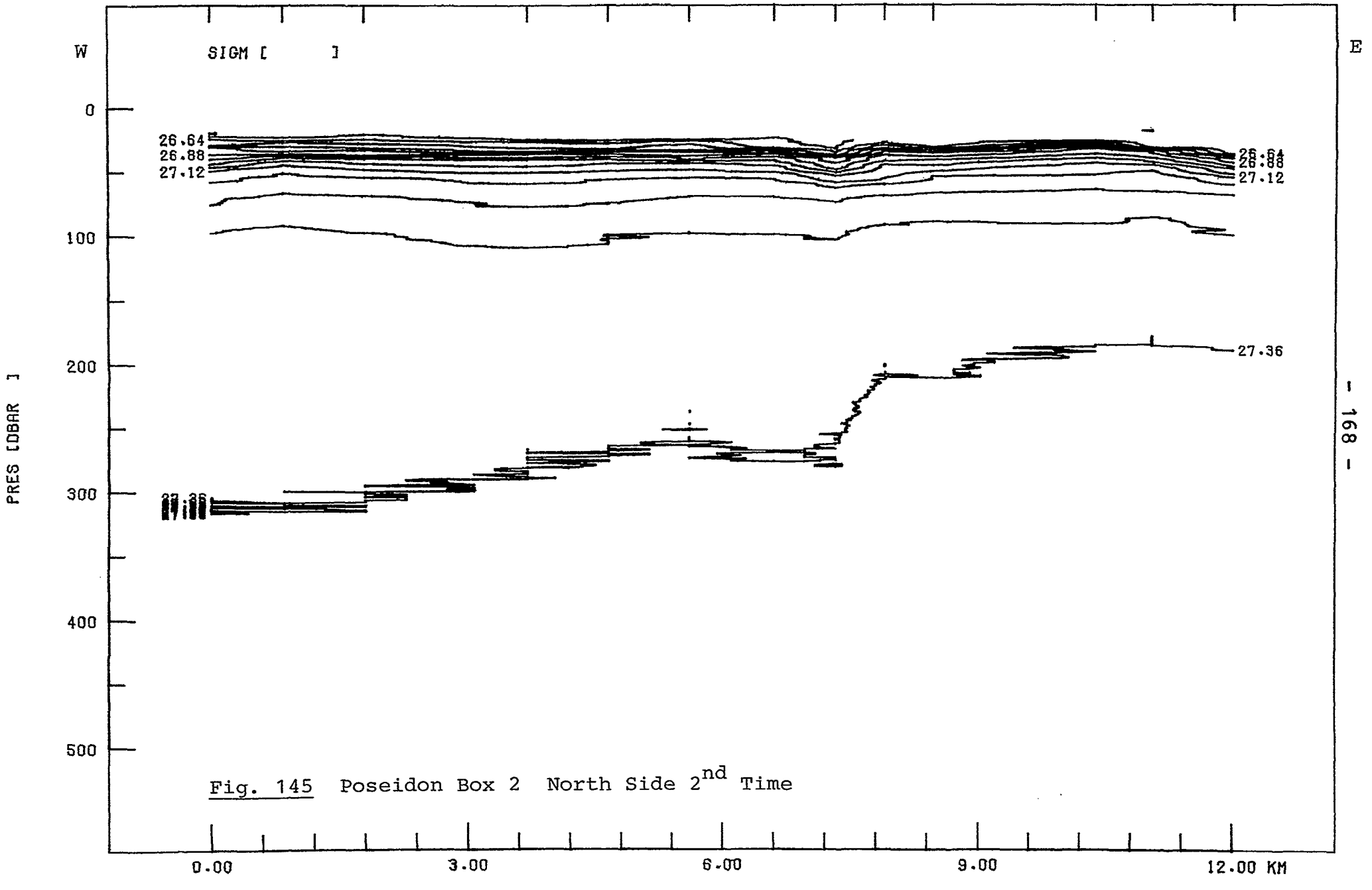

Fig. 145 Poseidon Box 2 North Side 2nd Time

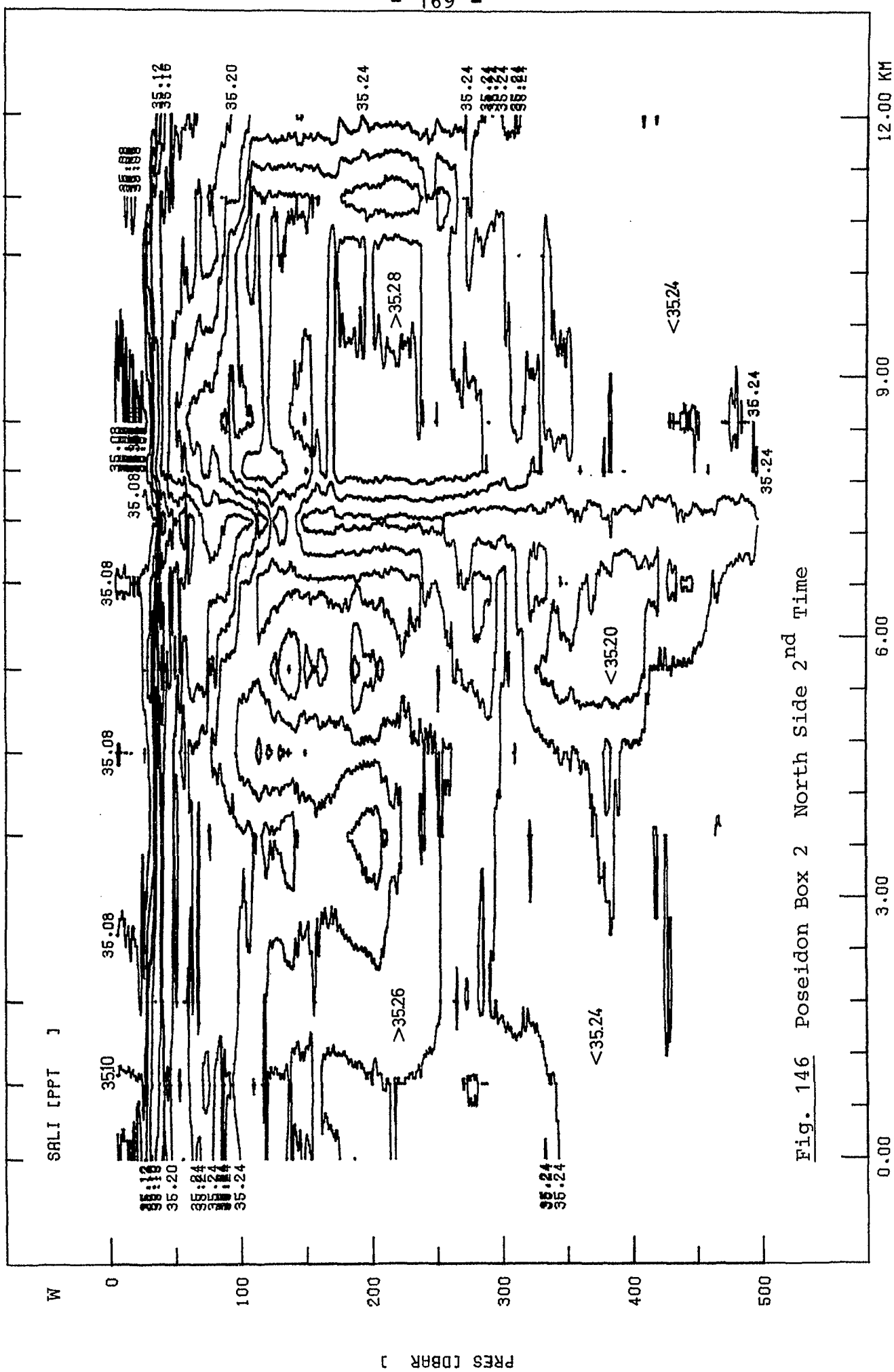

Fig. 146 Poseidon Box 2 North Side 2nd Time

PJC106T

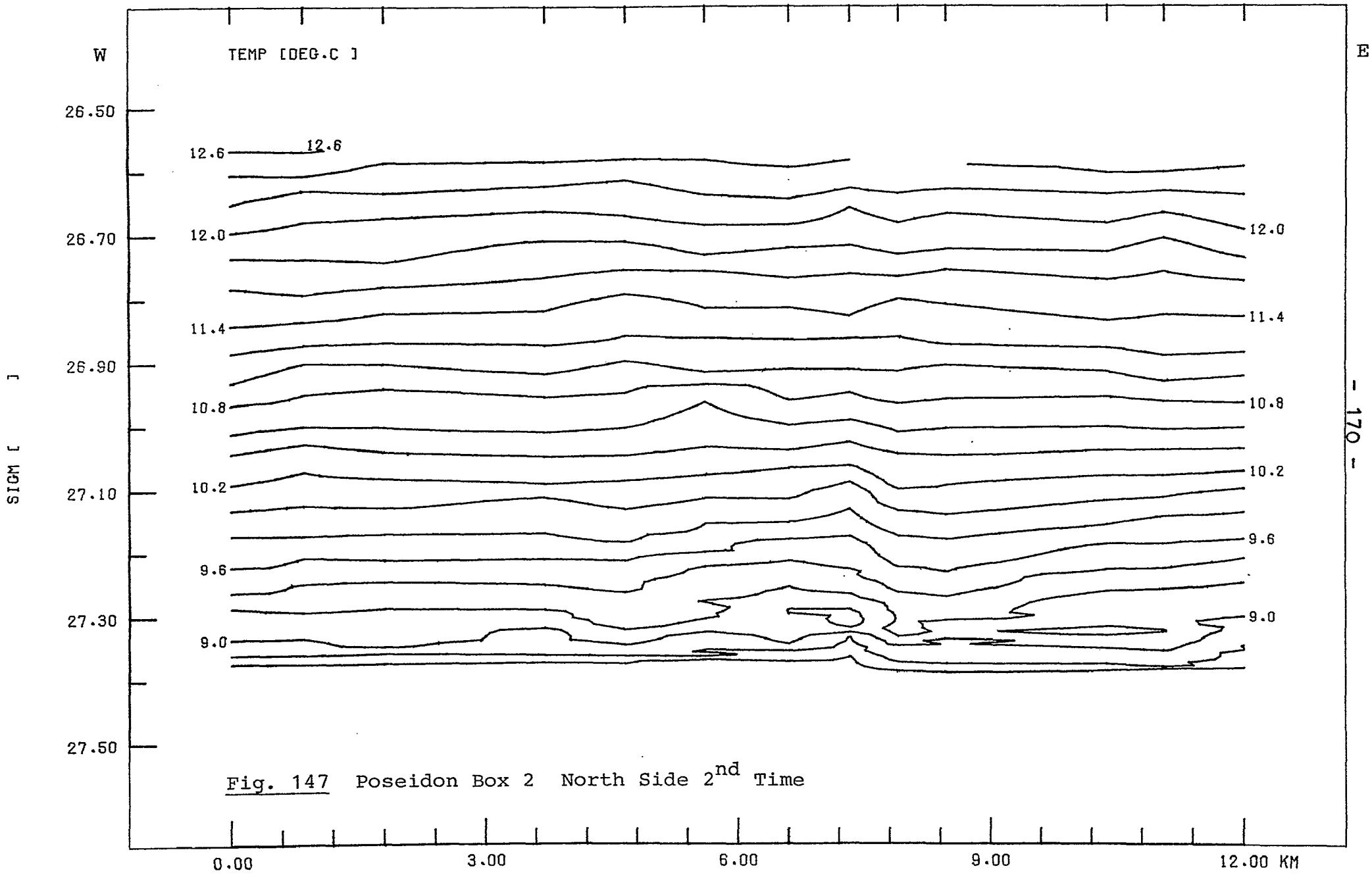

Fig. 147 Poseidon Box 2 North Side 2nd Time

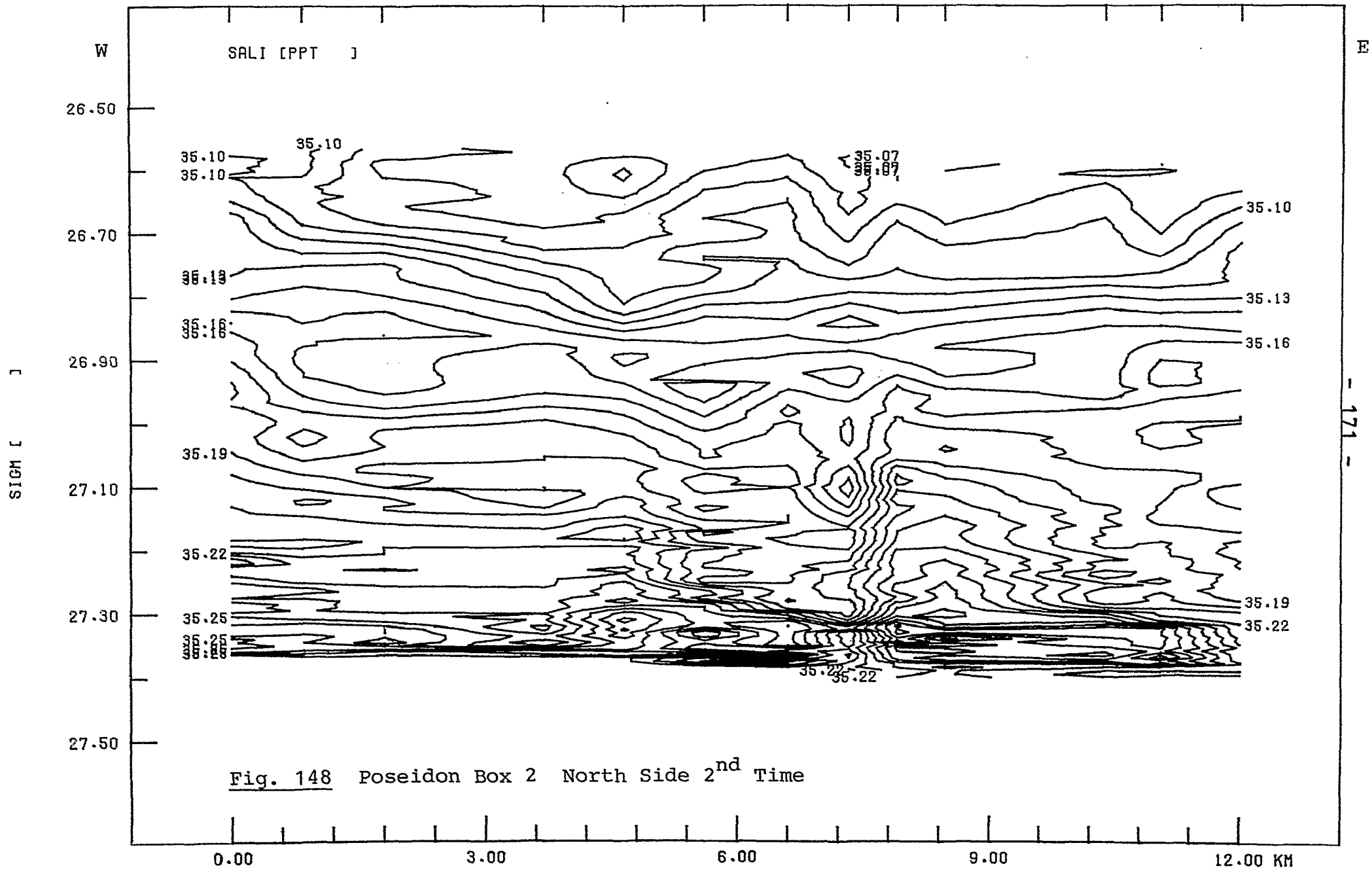

Fig. 148 Poseidon Box 2 North Side 2nd Time

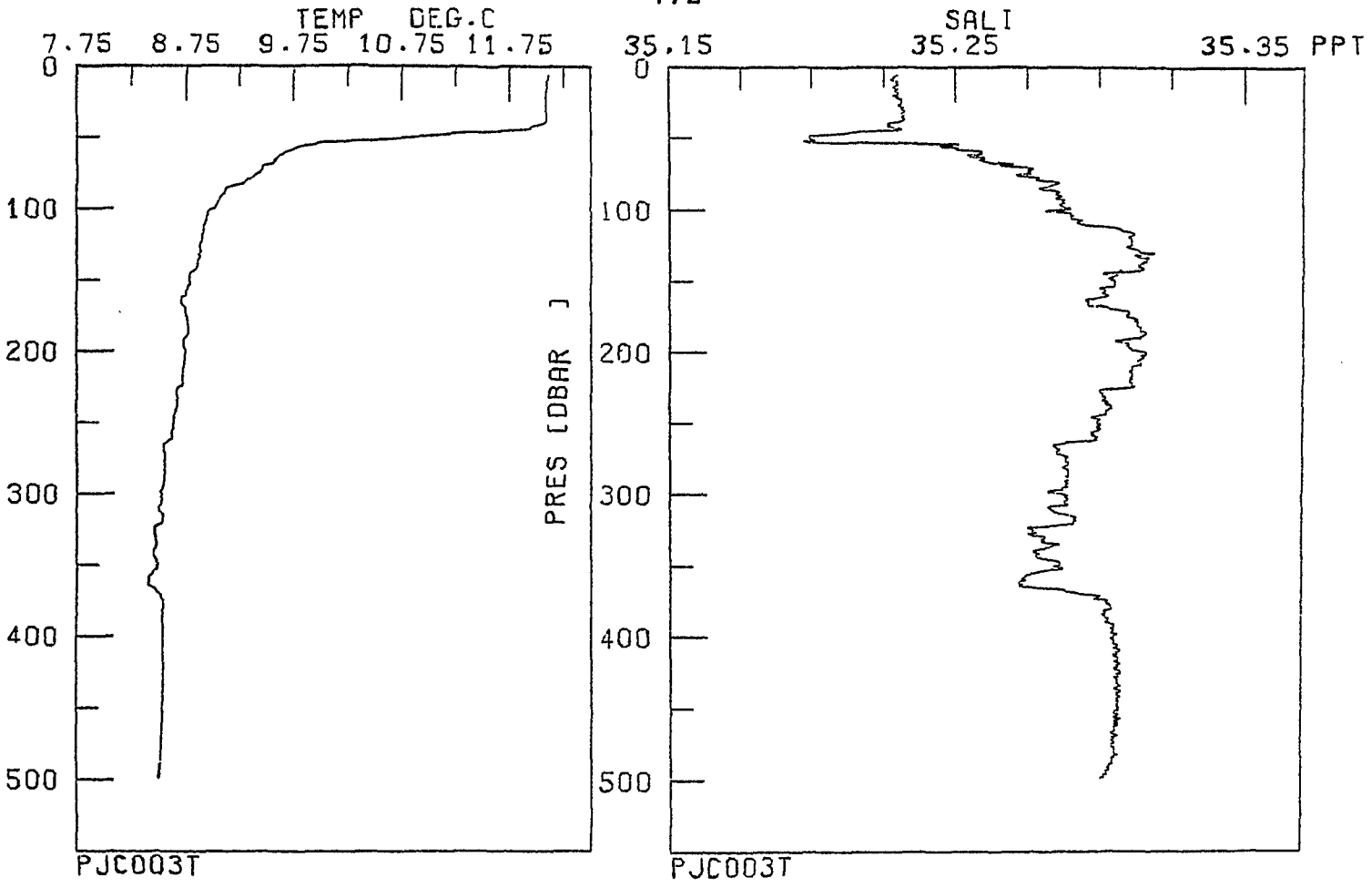

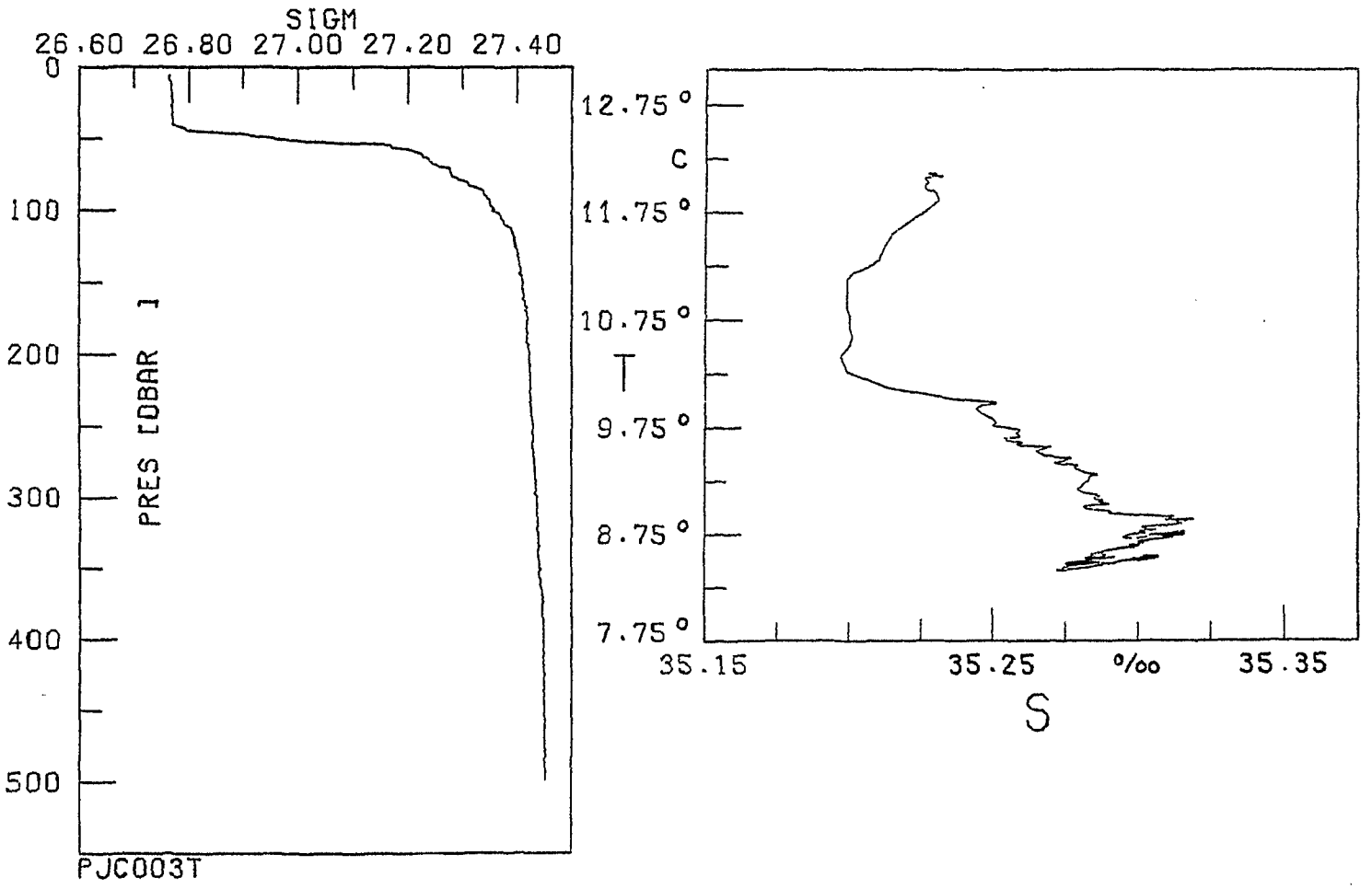

Fig. 149 Poseidon Box 1 South East Corner

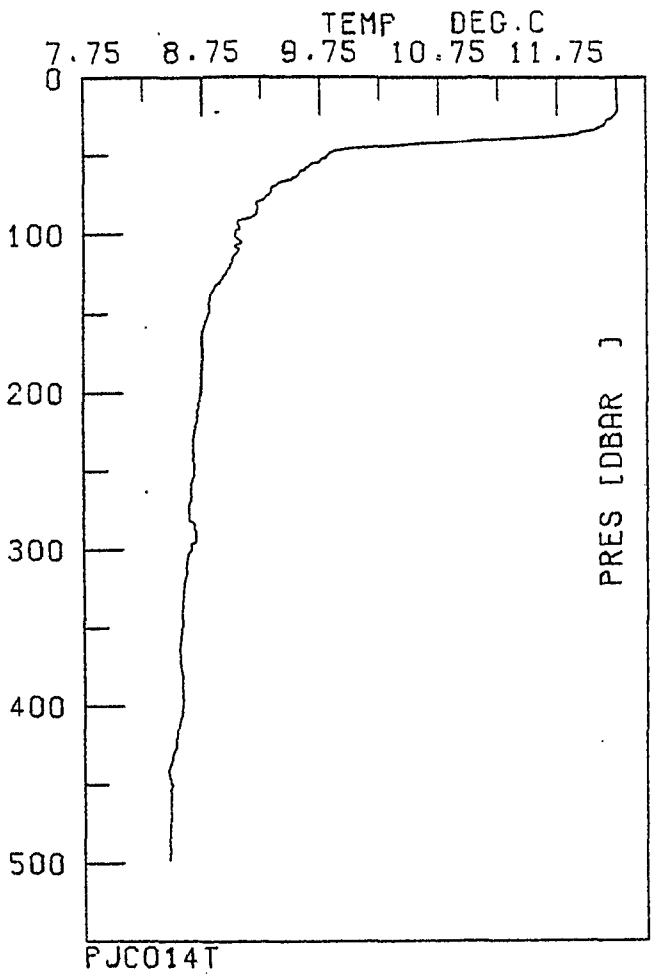

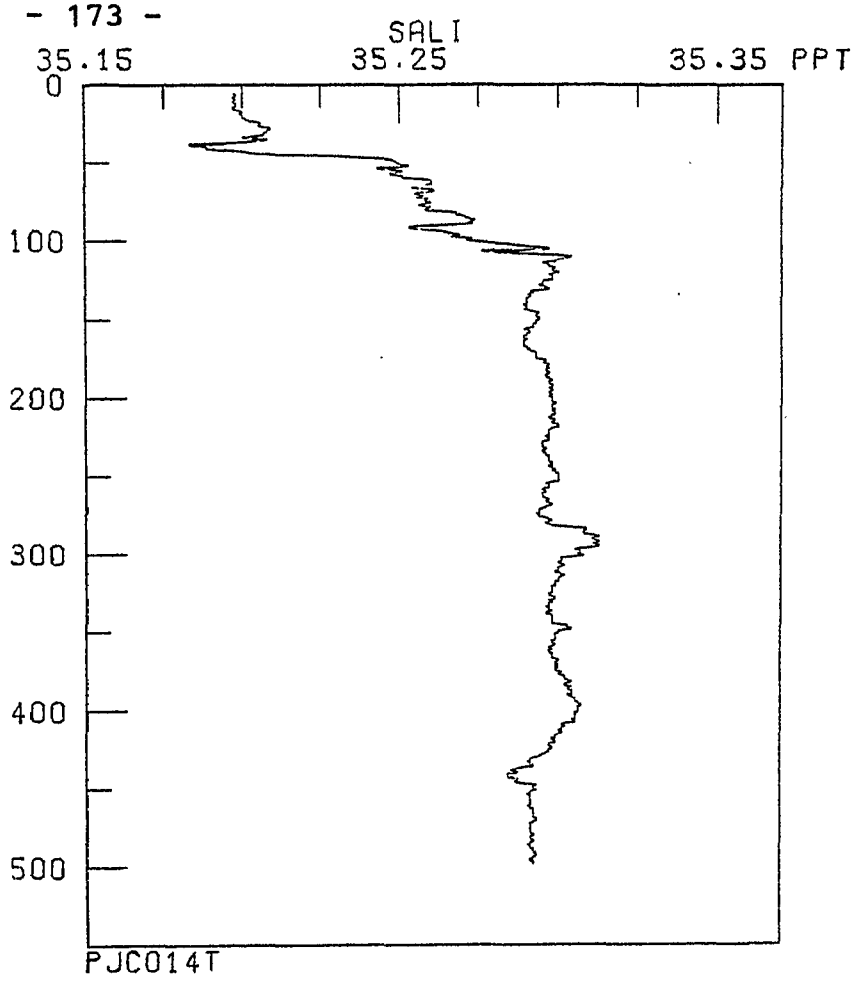

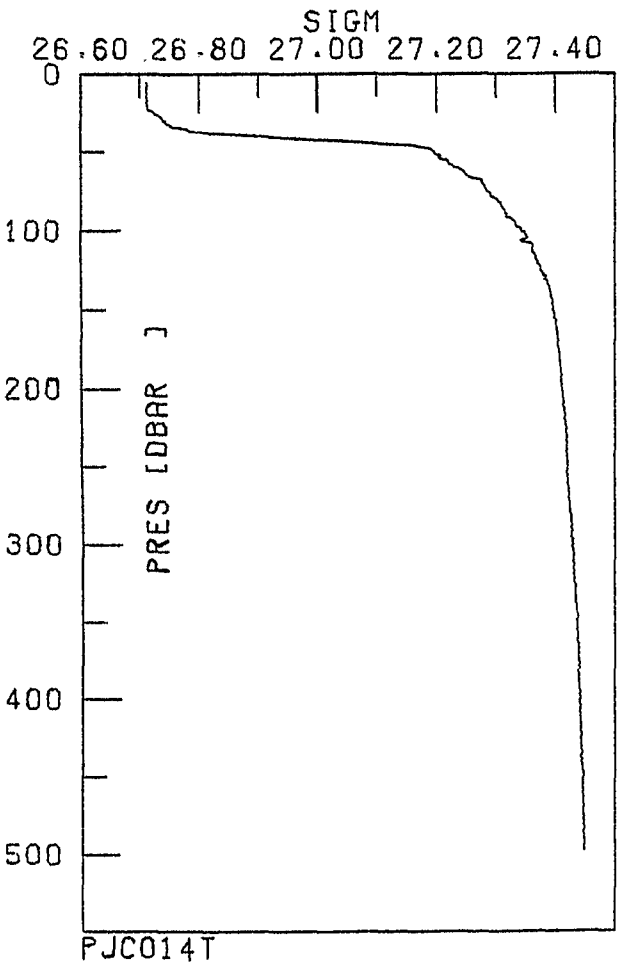

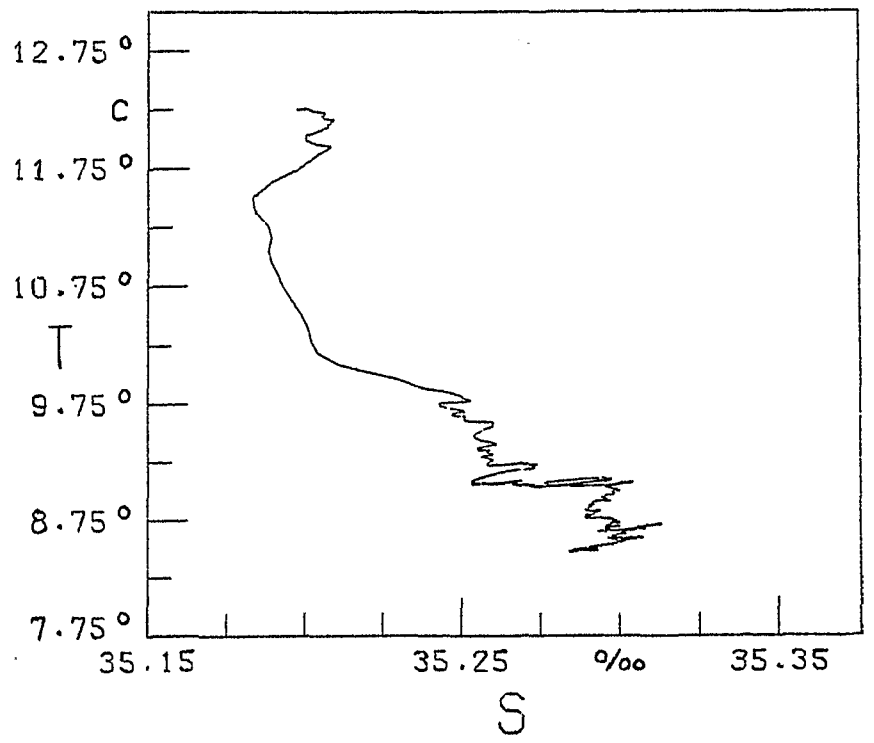

Fig. 150 Poseidon Box 1 North East Corner

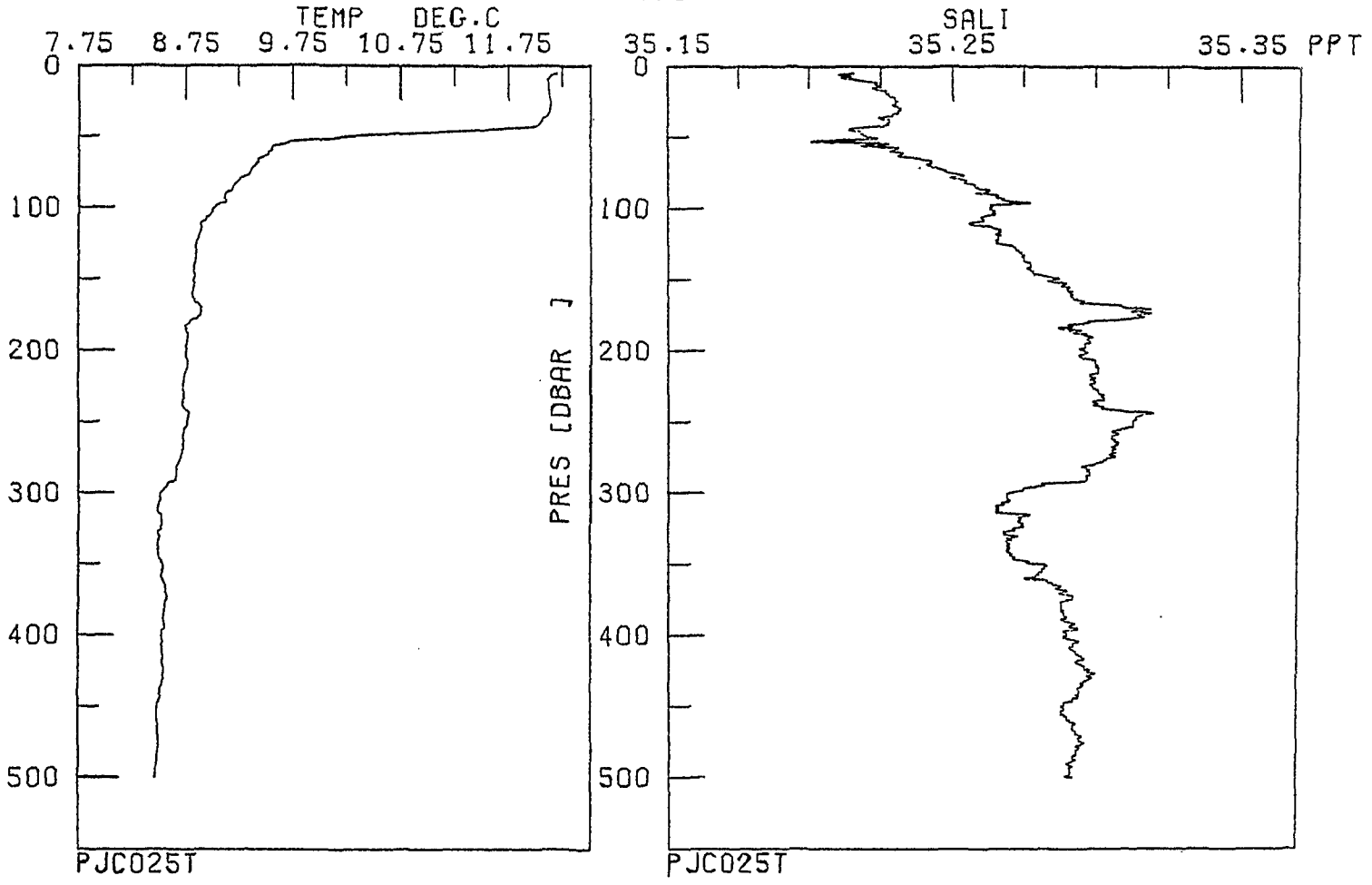

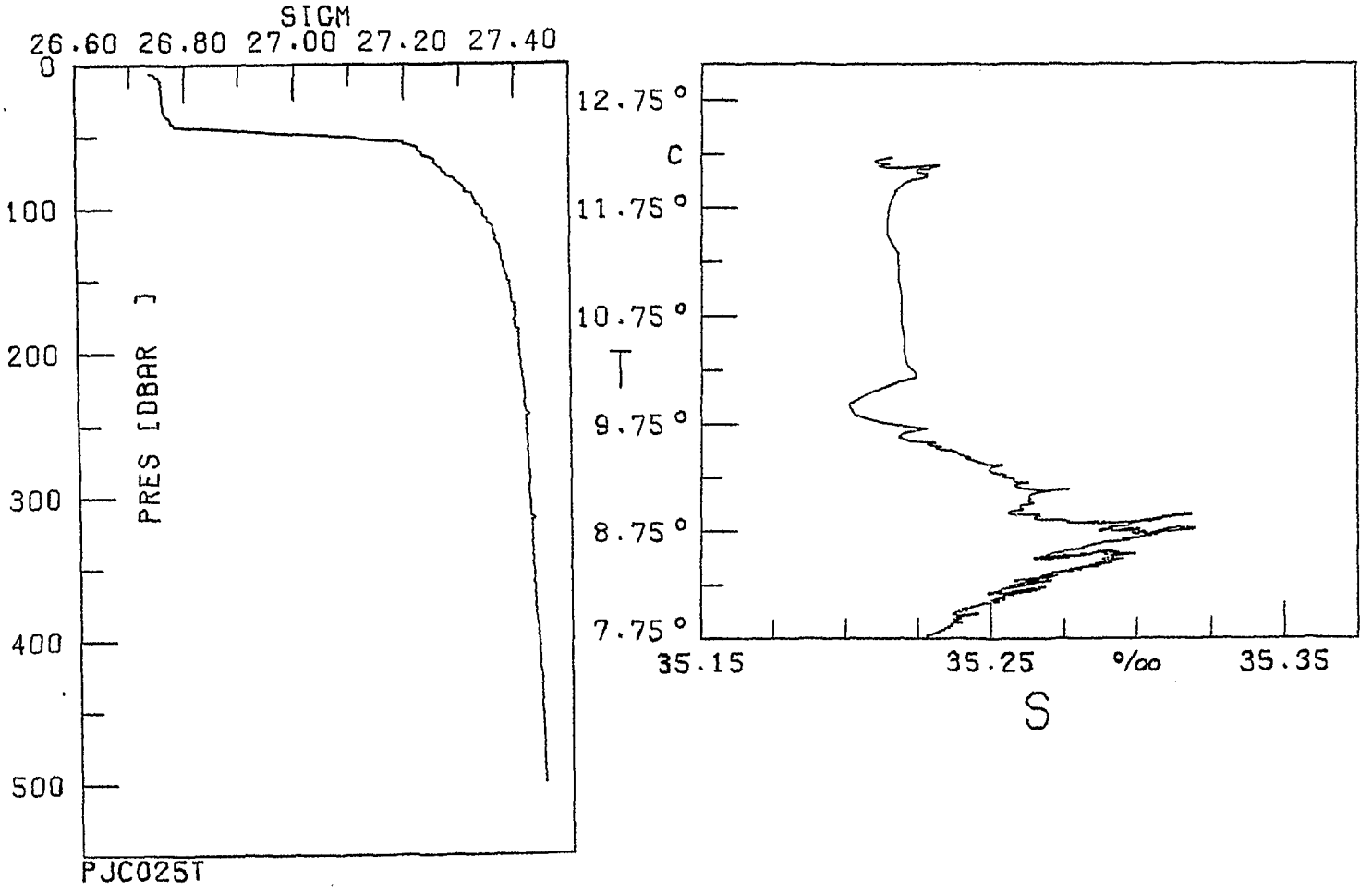

Fig. 151 Poseidon Box 1 North West Corner

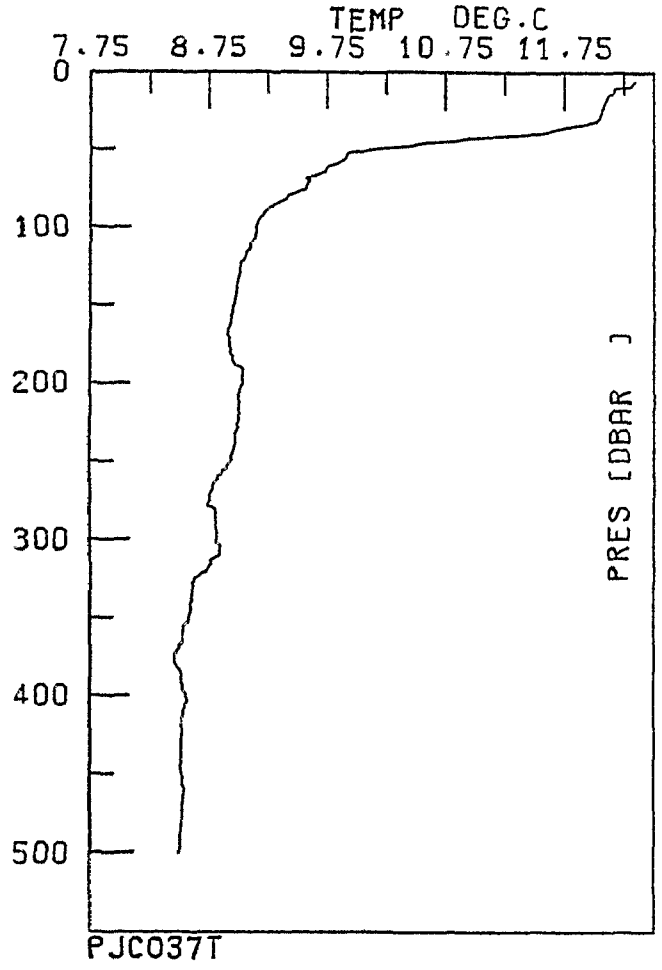

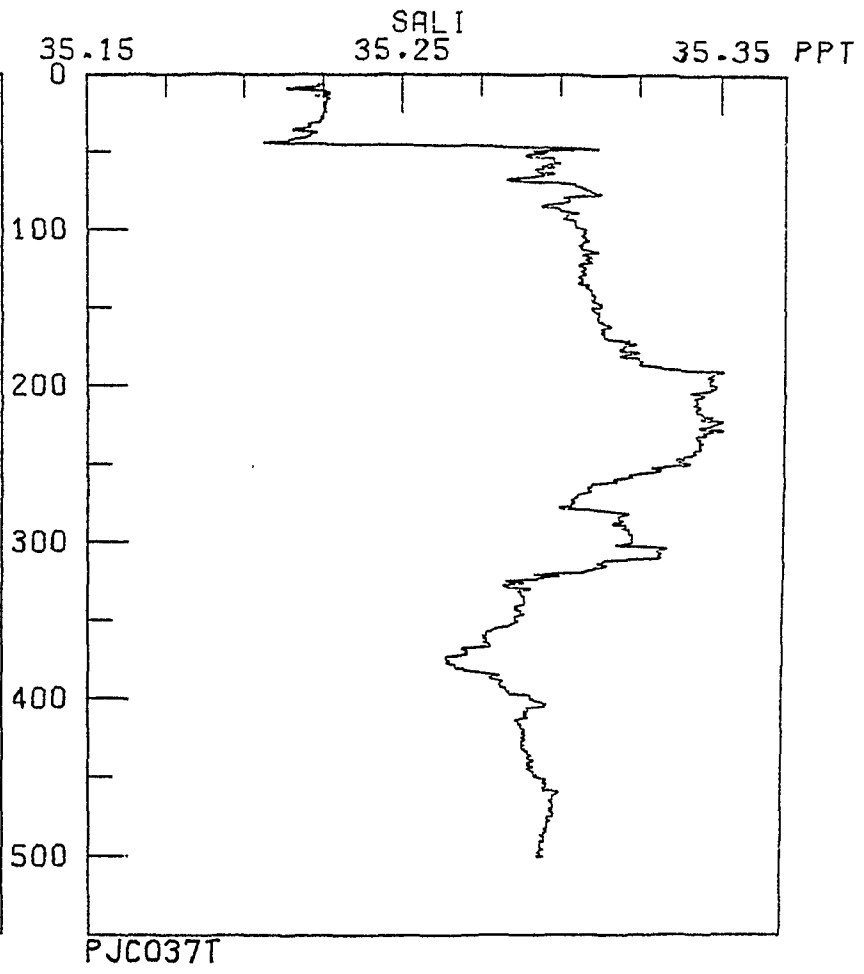

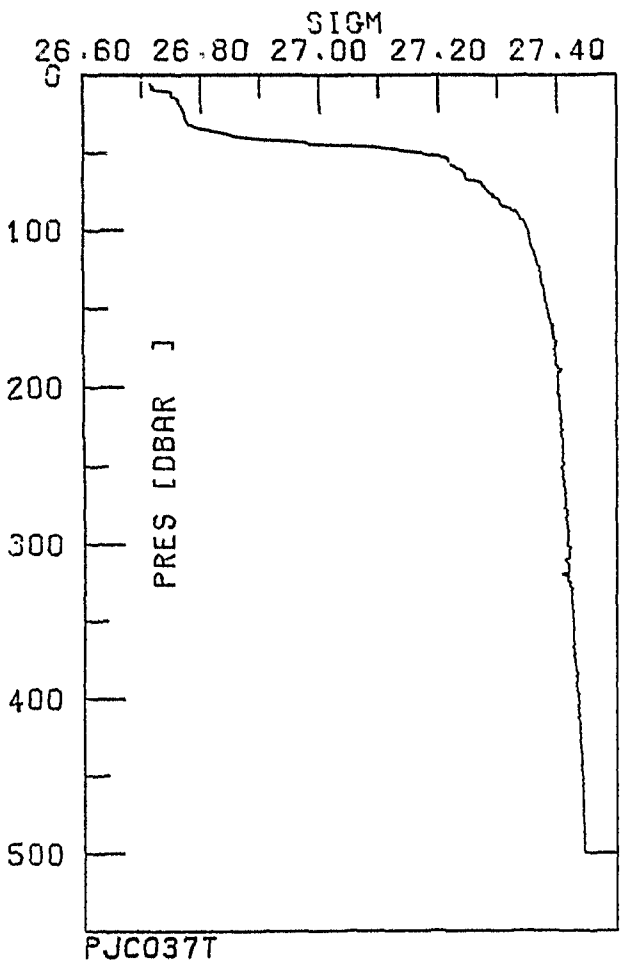

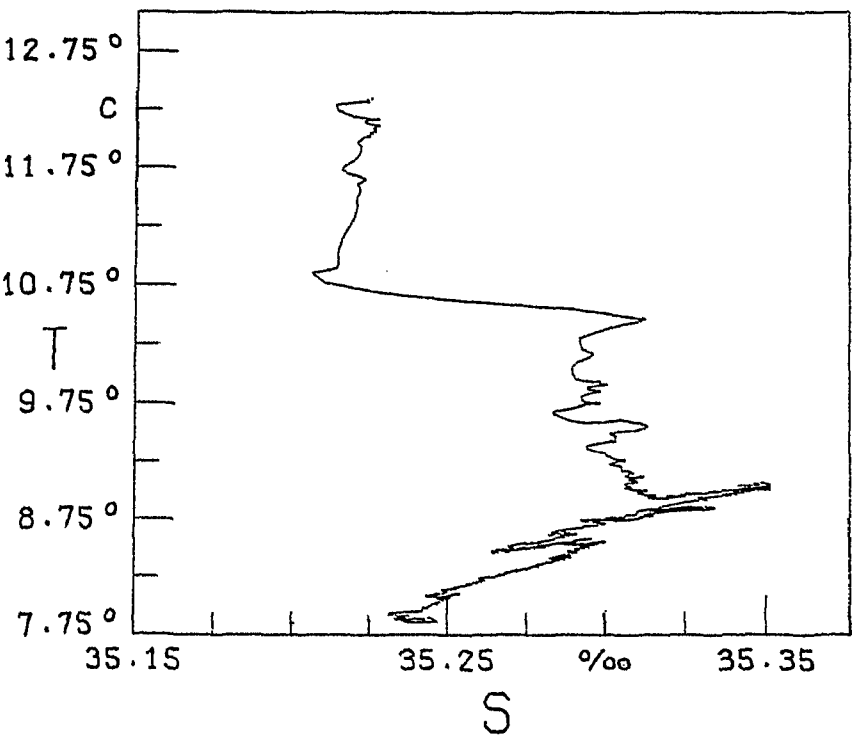

Fig. 152 Poseidon Box 1 South West Corner

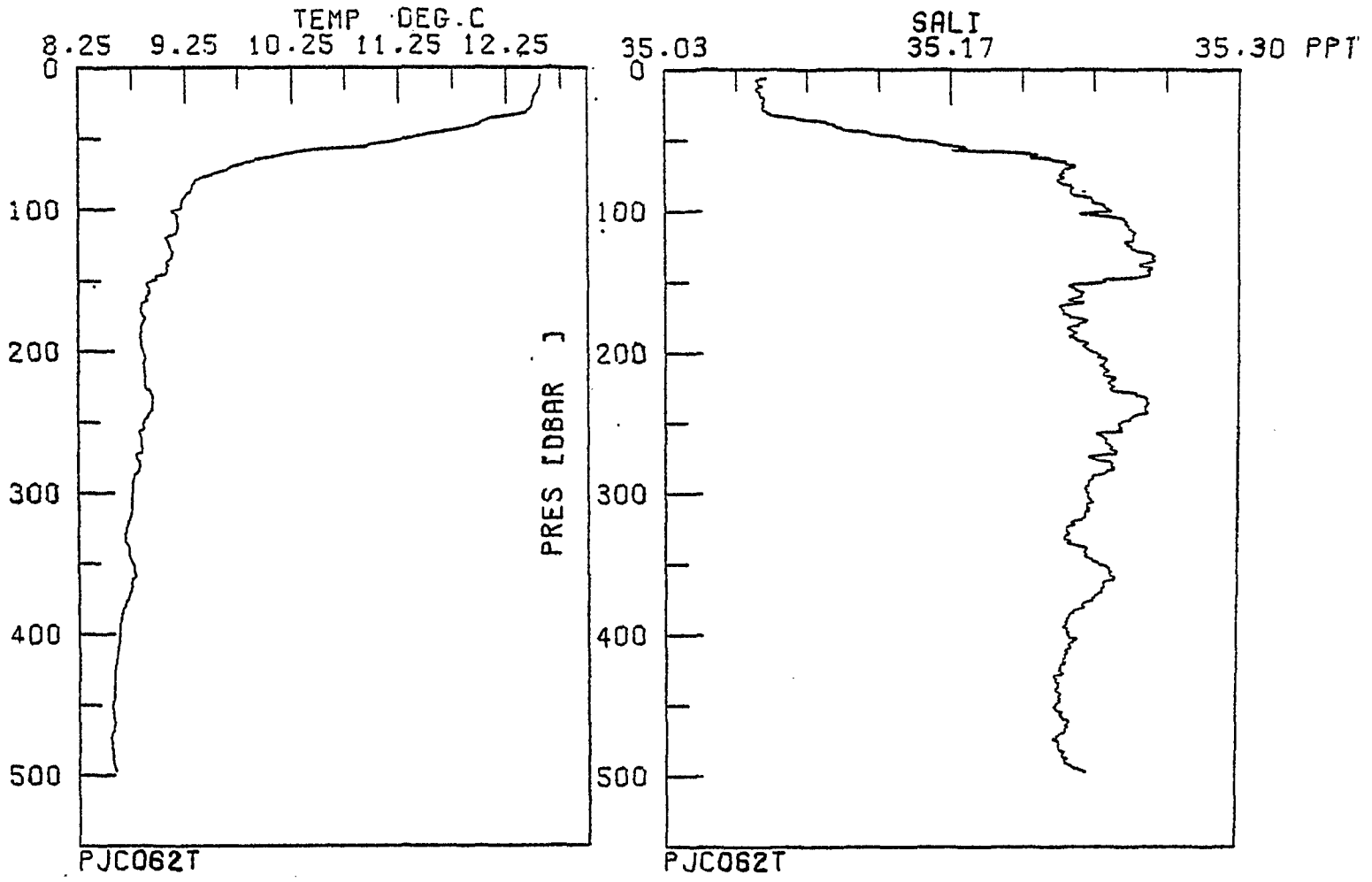

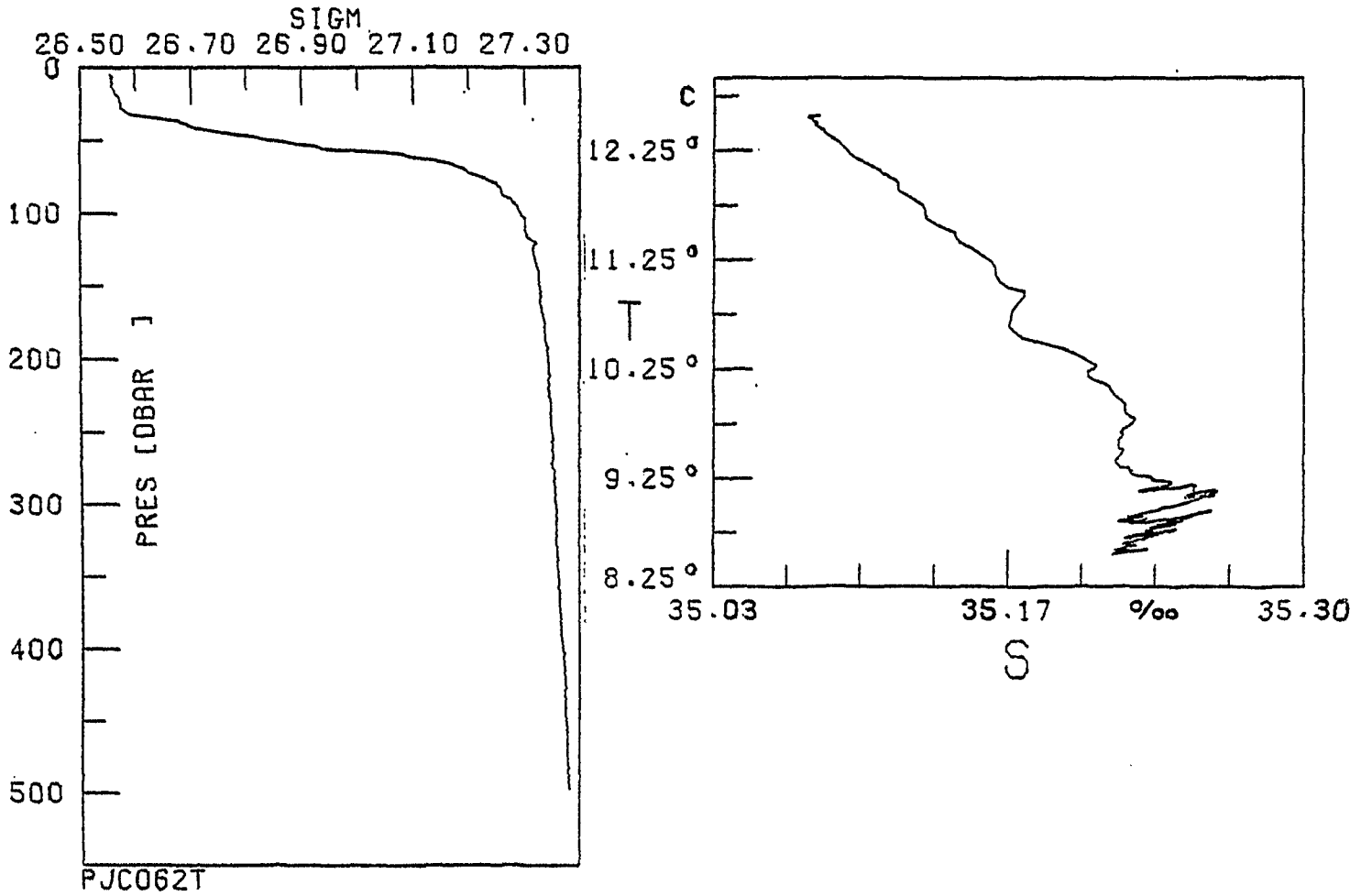

Fig. 153 Poseidon Box 2 North East Corner

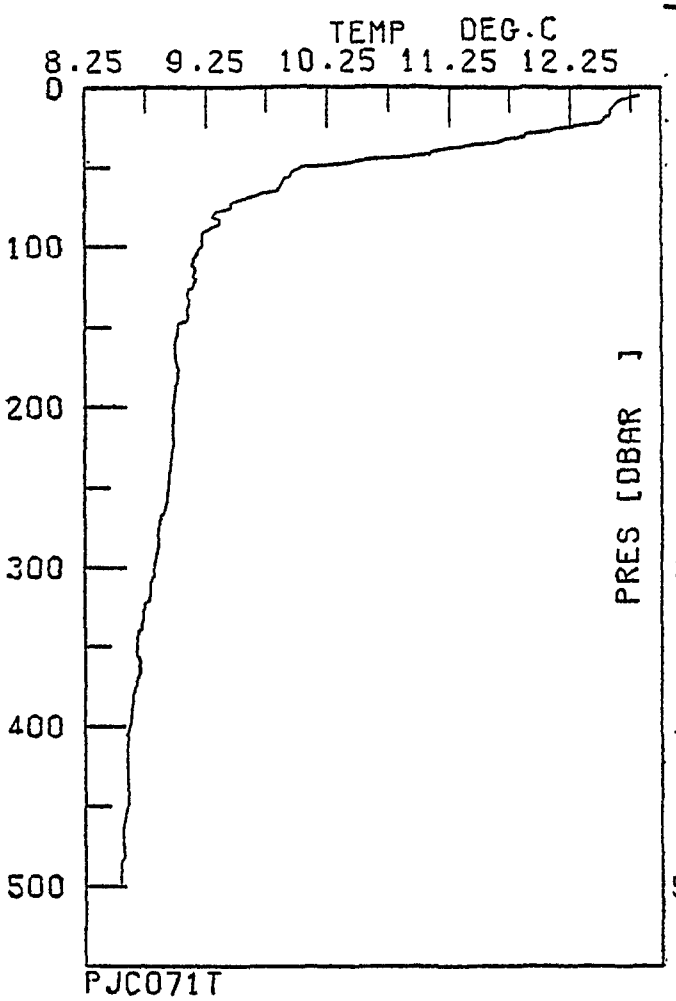

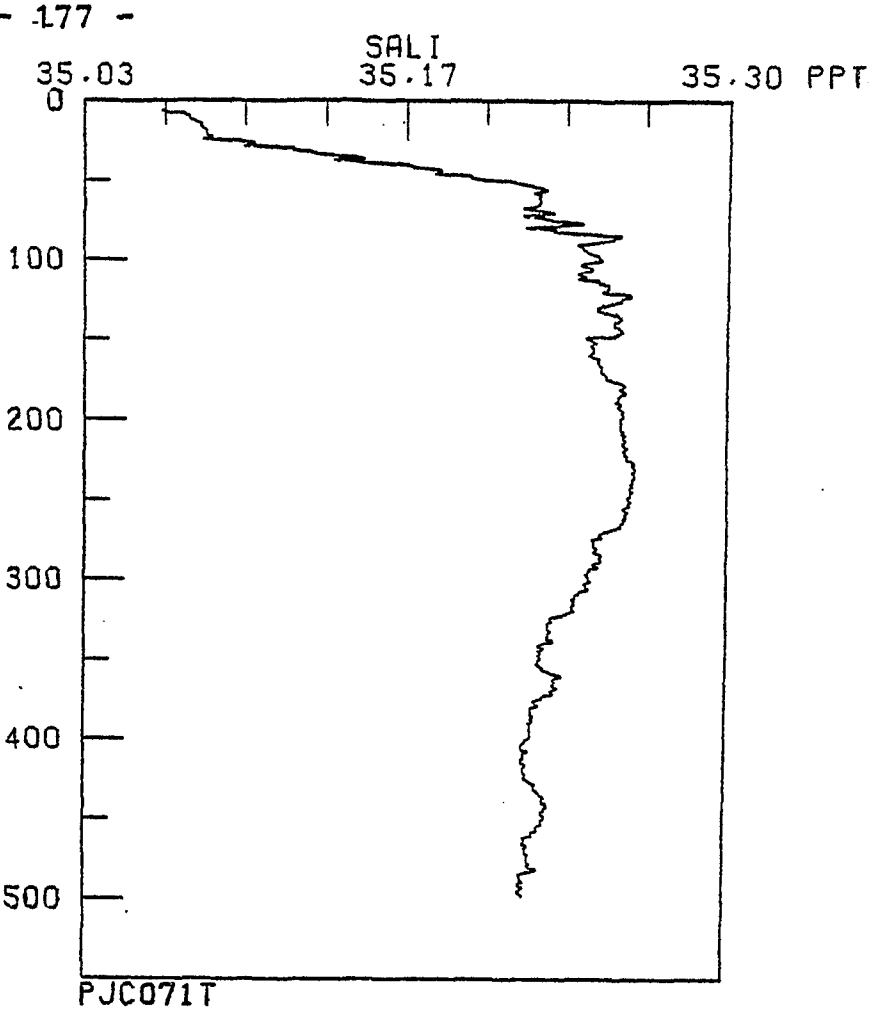

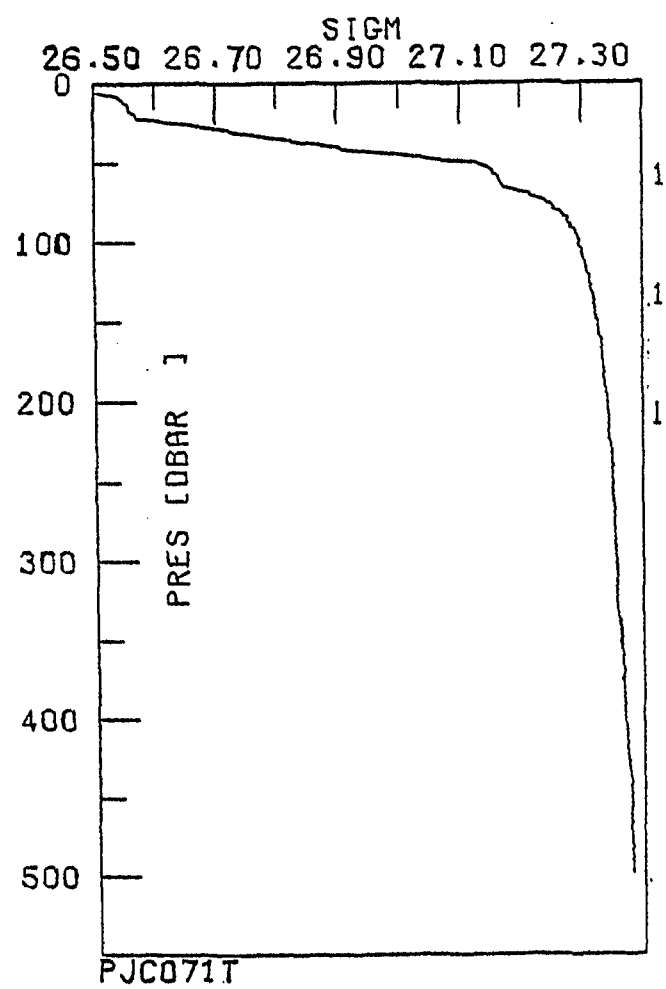

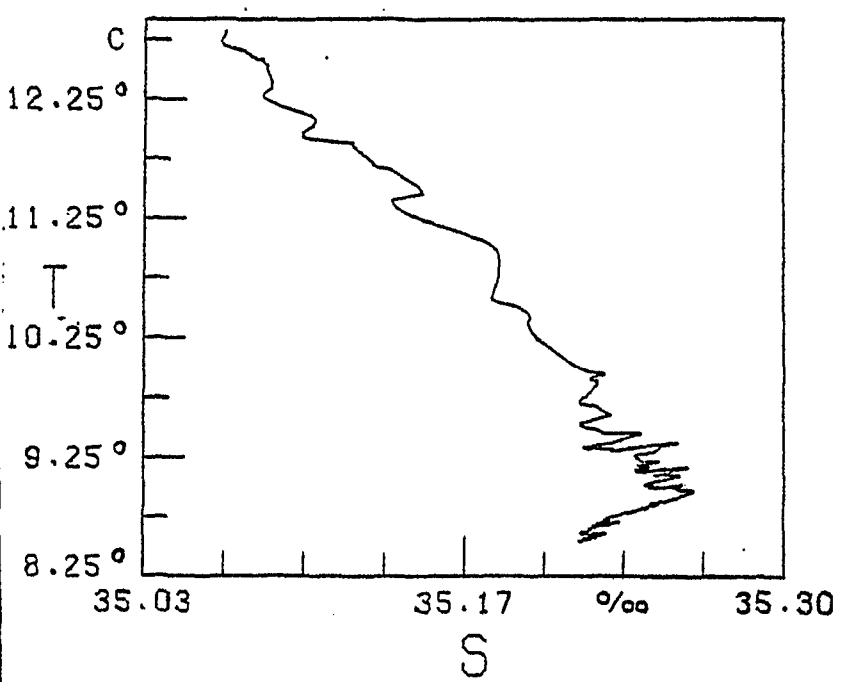

Fig. 154 Poseidon Box 2 South East Corner

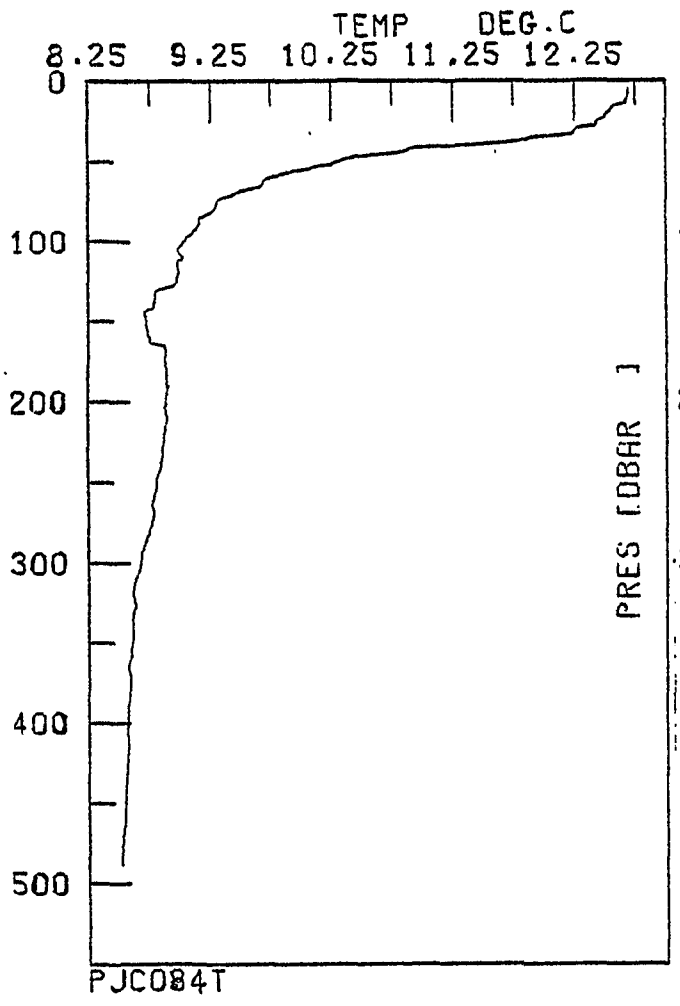

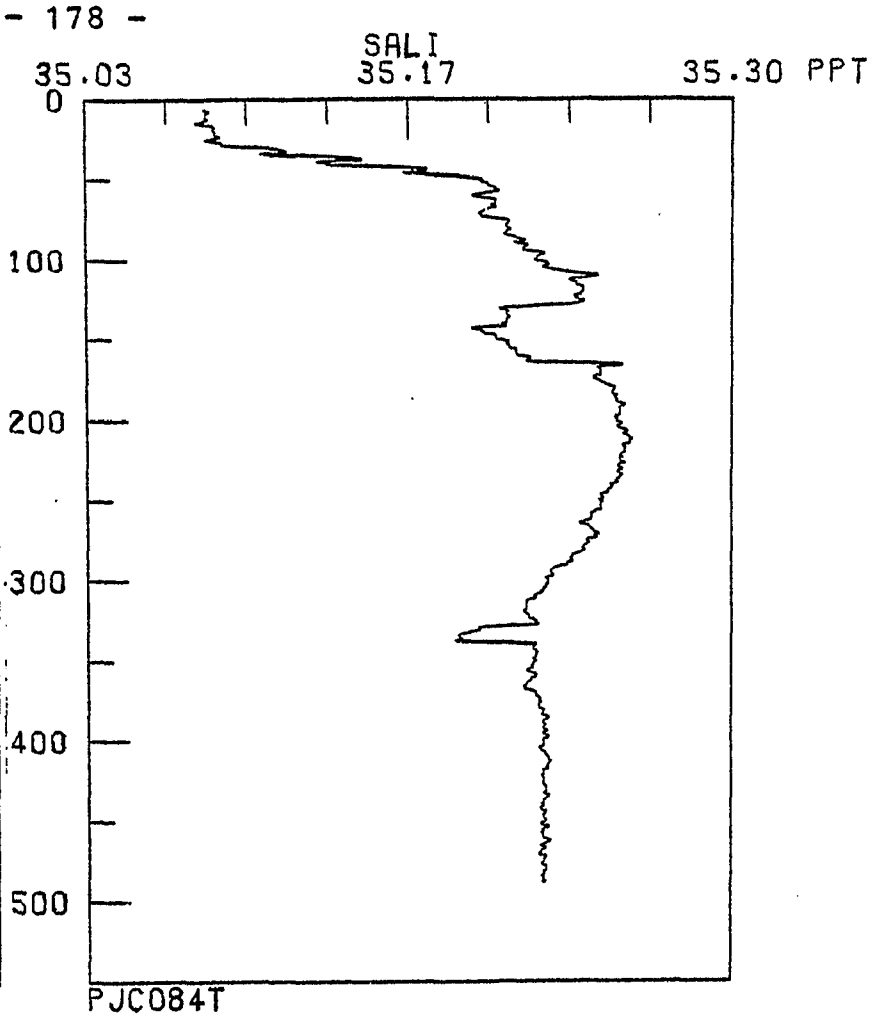

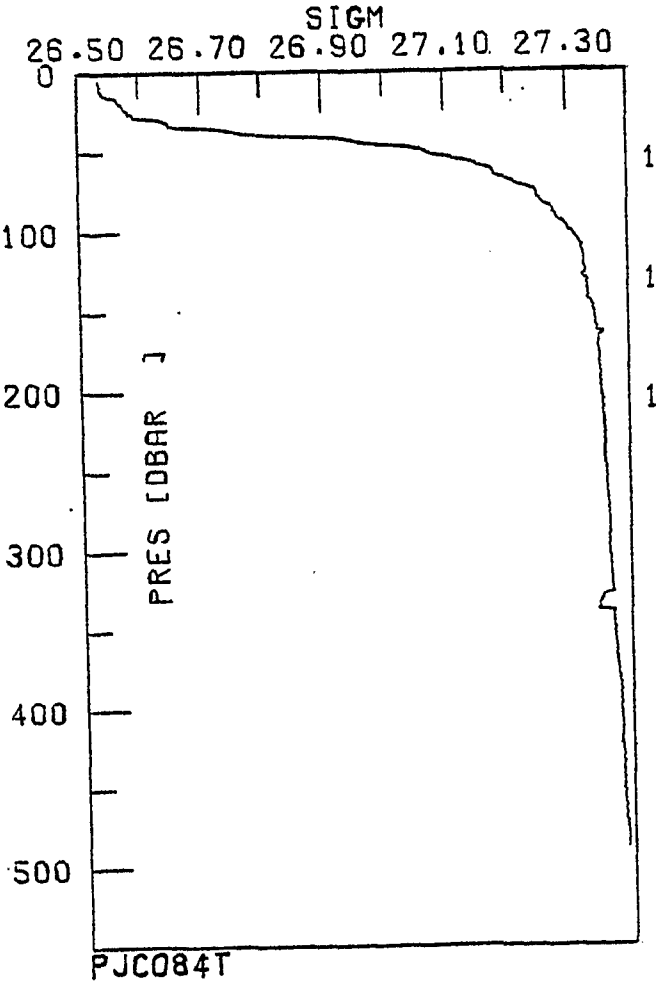

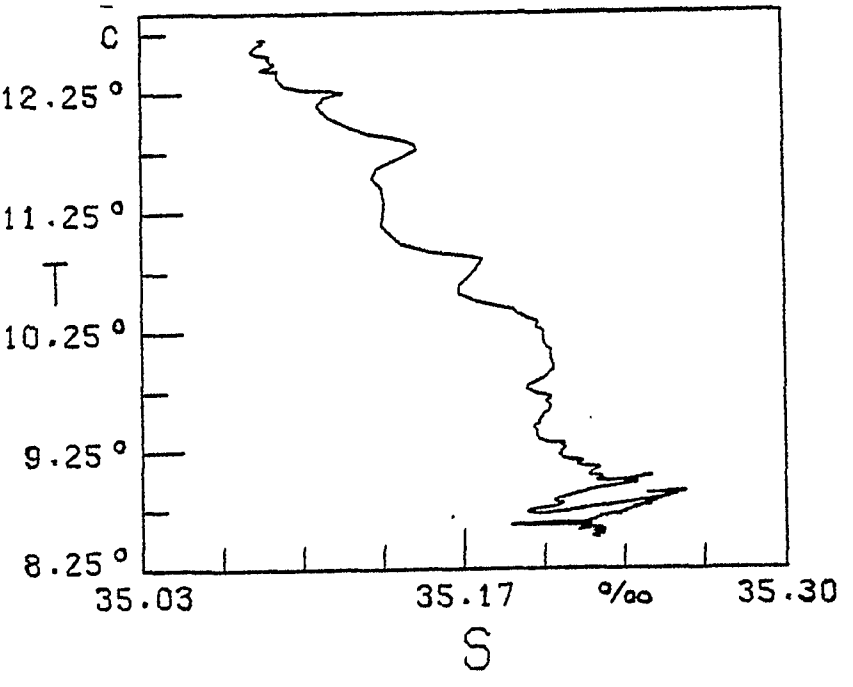

Fig. 155 Poseidon Box 2 South West Corner

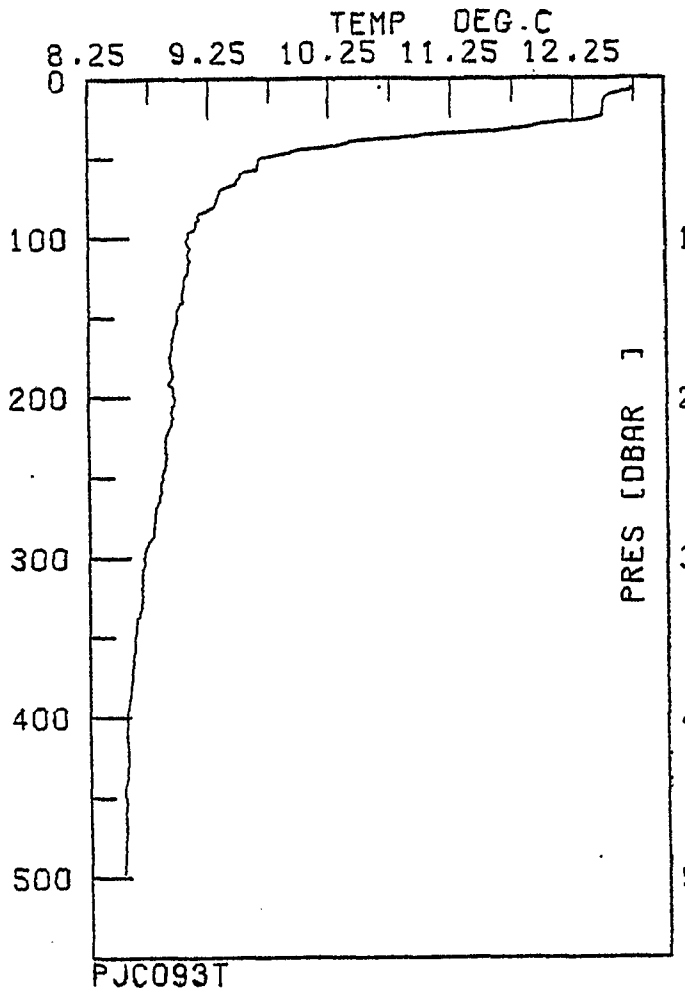

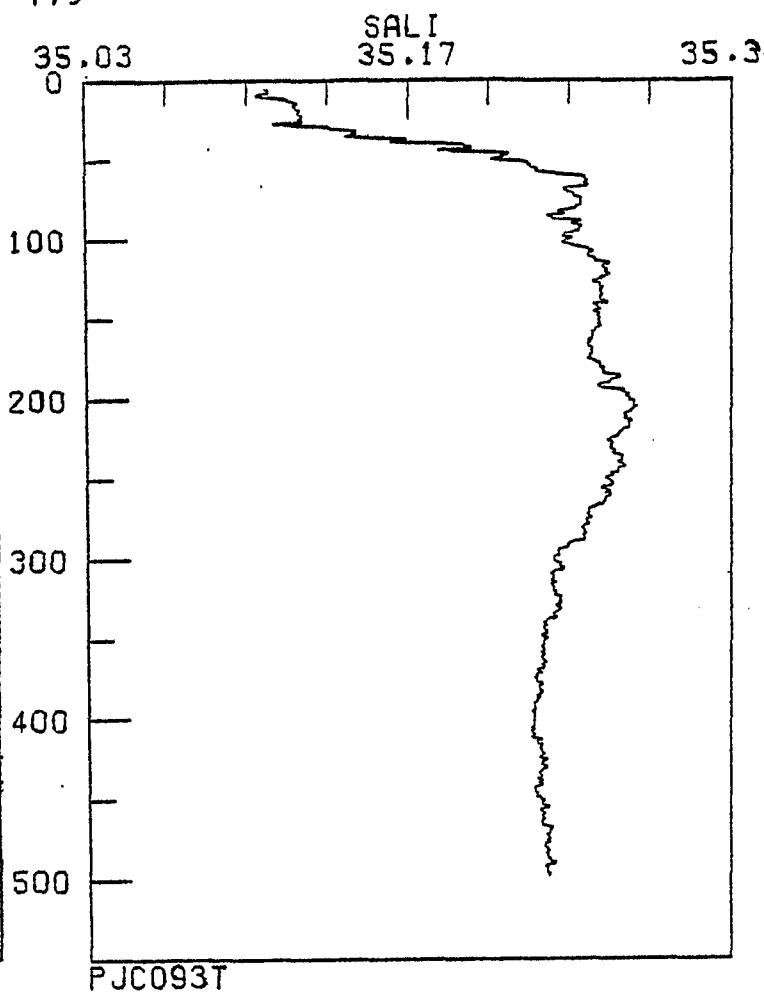

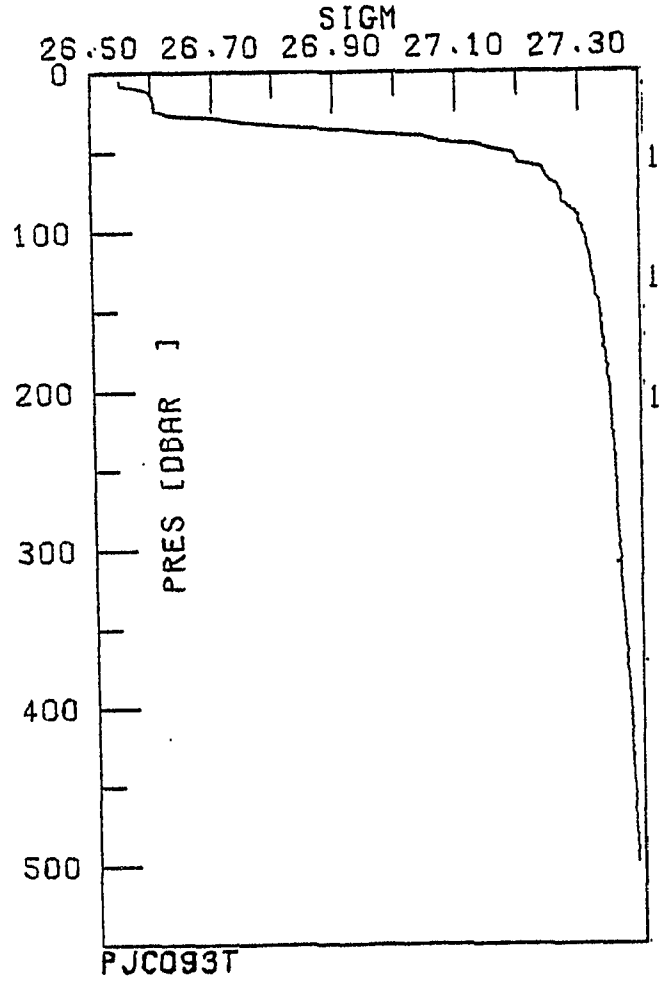

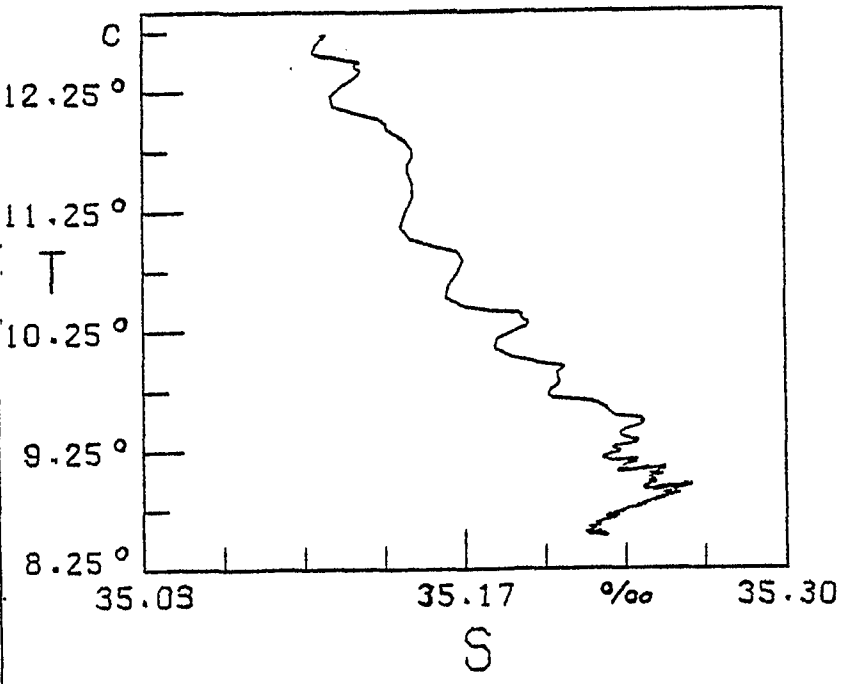

Fig. 156 Poseidon Box 2 North West Corner

References

Brown, N.L., 1974: A precision CTD microprofiler. Presented at IEEE International Conference on Engineering in the Ocean Environment. WHOI Contribution 3370.

Brown, N.L. and G.K. Morrison, 1978: WHOI/Brown conductivity temperature and depth microprofiler. WHOI Technical Report 78-23.

Fofonoff, N.P., S.P. Hayes and R.C. Millard, 1974: WHOI/Brown CTD microprofiler: methods of calibration and data handling. WHOI Technical Report 74-89.

Institut für Meereskunde, Kiel, 1979: Fahrtbericht-Poseidon 31: JASIN 1978. Unpublished Cruise Report.

Pollard, R.T., 1978; Bull. Amer. Meteor. Soc., 59, 1310-1318.

Royal Society, 1977: Air-Sea Interaction Project: Scientific plans for 1977 and 1978, London.

Royal Society, 1978: Air-Sea Interaction Project: Operational plans for 1978, London.

Royal Society, 1979: Air-Sea Interaction Project: Summary of the 1978 Field Experiment, London.

Siedler, G. and W. Zenk, 1980: JASIN 1978 - Field activities on the research vessels "Meteor", "Planet", "Poseidon", and the research aircraft D-CMET. "Meteor" Forschungsergebnisse, Reihe A, No. 21, 25-48.